On the Modeling of Dynamics and Operation of Reactive Distillation

Alma D. Estrada-Villagrana

A thesis submitted for the degree of
Doctor of Philosophy of the University of London

Department of Chemical Engineering
University College London
Torrington Place
London WC1E7JE, United Kingdom

March 2002

Abstract

The aim of the present project was to study the factors that affect gross scale reactive distillation behaviour and to set a useful framework for control system design of reactive distillation.

A modification of an equilibrium model based on using elementary quantities instead of molar quantities was used for different steady state and dynamic simulations of reactive distillation. Furthermore, a control system design method for reactive distillation was proposed and tested.

In the first part of the present study, the role of operating conditions in reactive distillation behaviour was investigated. It was found that the complex nature of reactive distillation make this kind of process susceptible to input and output multiplicity. Furthermore, it was found that such behaviour is triggered by operating conditions that create high internal flow rates, and it could be found for any column configuration for these examples.

The second part of the project was devoted to the dynamics and control system design of reactive distillation. A method, modified from other well known ones, was proposed to systematise the control system design of reactive distillation. The use of control tools on a linearised model gave the most convenient control configurations. It was found that the consideration of the possible disturbances was fundamental for correct discrimination between control schemes. The method was also able to recognise that for the case study, a high conversion point of an output multiplicity was relatively easy to control. Dynamic simulations which were used to corroborate the analysis results gave a good correspondence between them. Moreover, the dynamic simulations showed that the interaction between the important measurements controllers (such as temperature controllers) and the controllers of the column conditions (for instance, level controllers) may be important. Therefore, it is recommended to consider both of them during the control system design method.

It is considered that the findings of the present project will help in the understanding and design of reactive distillation processes.

Acknowledgements

I would like to thank to my first supervisor, Prof. David Bogle for all his help, encouragement, teaching and his always positive criticism during my project. I also owe much to my second supervisor, Dr. Eric Fraga for everything he taught me. His help to attack my constant numerical and programming disasters will never be forgotten.

I also want to thank Dr. Rafiqul Gani and Dr. Eduardo Pérez-Cisneros for their help at the early stage of my project.

Many thanks to all my colleagues at UCL, in particular to Johannes Hagemann, Haydn Furlonge, Myrian Schenck, Kian Low and Keming Ma for many constructive discussions on academic, deep and trivial issues.

As in every stage and aspect of my life, I received lots of love and confidence from my mother. Her support and encouragement were critical during these years.

I also want to thank the following people for their love, wisdom, encouragement and shelter: Omar Estrada, Laura Arellano, Irma Meléndez and family, Lucía Moncada, Felipe López, Rafael Maya, Araceli Martínez, Linda Baez, Elena Martínez, Rebeca Aguirre, Sabine Grundmann, Soumaya Ibrahim, Haydn Furlonge, Ezster Pozna, Lolita Campos, Verónica Rodríguez, César Ruíz, Eduardo Pretel, Christopher Klein, Yukiko Morita, "Bee" Ruedeekorn Wiwattanapatapee, Mr. Lane, Dr. Paul Walker, Lesley Black, Philip Vetter, "Pim" Boontarika Srithai, Antigone Lebessi, "Prim" Parimanan Cherntongchai, Tamae Yoshikawa and Helena Sanson.

Althought it may sound ludicrous, I want to thank Philip Glass, Ravi Shankar, Steve Reich, John Adams and Björk for their music. Listening their music during the writing-up was always a soothing remedy.

Financial support obtained from the mexican Council of Science and Technology (CONACyT) is gratefully acknowledged.

Dedication

A mi madre y a mi padre (*in memoriam*),
por su lucha por darnos una oportunidad.

Once, in a blue room, Ahmed Sinai improvised endings for fairy-tales whose original conclusions he had long ago forgotten; the Brass Monkey and I heard, down the years, all kinds of different versions of the journey of Sinbad, and the adventures of Hatim Tai . . . if I began again, would I, too, end in a different place?

— Salman Rushdie, *Midnight's children*

Each human being has the eternal duty of transforming what is hard and brutal into a subtle and tender offering, what is crude into refinement, what is ugly into beauty, ignorance into knowledge, confrontation into collaboration, thereby rediscovering the child's dream of a creative reality incessantly renewed by death, the servant of life, and by life the servant of love.

— Yehudi Menuhin

Contents

List of Figures

List of Tables

Chapter 1

Introduction and Literature Review

When in a distillation column reactions occur to produce specific products with certain specifications, the process is called reactive distillation.

In this chapter, the main research areas regarding reactive distillation are presented. In such contex, the main interest of the project, the study of the behaviour of reactive distillation and its relationship with operating conditions, is discussed. The chapter finishes with the discussion of the particular thesis objectives.

1.1 Introduction

In reactive distillation reactions occur to achieve specific goals, such as to get high conversions and high purity products, to minimise side reactions, etc. In addition, a chemical reaction can be used to eliminate azeotropes in a multicomponent separation.

Reactive distillation can be catalysed or not. When it is catalyzed, reaction may be homogeneous or heterogeneous. DeGarmo, Parulekar and Pinjala (1992) described different configurations in which a reactive distillation column can be heterogeneously catalyzed. The catalyst can be placed in a continuous medium (the chemical reactions and the separation occur in certain sections or in all the column). Alternatively, the catalyst can be laid on trays. It is possible to have rectifying. reaction and stripping sections.

Some of the industrial applications of reactive distillation are etherification, alkylation and hydrolysis processes (Tuchlenski *et al.*, 2001).

1.1.1 Reactive distillation history

Although reactive distillation has just recently become common for some chemical processes, such as esterification, the concept is not new. The earliest reference is a homogeneous esterification process patent to produce methyl acetate (Backhaus, 1921). However, the industrial implementation of that process was unsuccessful because of the presence of unknown azeotropes (Agreda, Partin and Heise, 1990).

Reactive distillation was again claimed as an alternative by Keyes in 1932 (esterification), Carney in 1937, Leyes and Othmer in 1945 (esterification), Hoffman in 1958 and Saito, Michishita and Maeda in 1971 (isomers mixture separation). Also in 1971 Sennewald, Gerhrmann and Schafer patented a heterogeneous reactive distillation for organic reactions.

The industrial use of reactive distillation was delayed due to its complexity. One of the first successful reactive distillation applications was the esterification of acetic acid to produce methyl acetate (Agreda and Partin 1984). Some of the current industrial applications of reactive distillation, reported by Stichlmair and Frey (1999) and Tuchlenski *et al.* (2001), are: etherification (methyl tert-butyl ether, ethyl tert-butyl ether), esterification (methyl acetate, ethyl acetate production), alkylation (cumene, ethyl benzene production) and hydrolysis (ethylene glycol, tert-amyl alcohol production).

1.1.2 Advantages

If a conventional process consists of one or more reactors followed by one or more distillation columns to separate reactants and products, that process could possibly be substituted by a reactive distillation column which could be followed by more distillation columns or some other separators for further purification. For instance, a conventional methyl acetate production process that consists of one reactor and nine distillation columns can be substituted by a distillation column in which the middle section is reactive (Taylor and Krishna, 2000).

Reactive distillation advantages were underlined by Doherty and Buzad (1992) and Sundmacher and Hoffmann (1993).

- Normally, excess of reactants is used to minimise side reactions and to overcome limitations imposed by chemical equilibrium. In reactive distillation, the continuous separation reduces the necessity for excess of reactants and it may be carried out closer to stoichiometric feed conditions.

- Reactive distillation may favour the elimination of azeotropes in the mixture.

- It can reduce the subsequent processing

- It can use the heat of reaction to heat the mixture and evaporate liquid and it may simplify the control of temperature

All these advantages bring lower capital and operating costs. Therefore, reactive distillation can be a very attractive option when it can be implemented.

1.1.3 Feasibility

The feasibility of the process is determined by the relative volatility of the reactants and products and the activity of the catalyst (if needed). When a catalyst is needed, it must be possible to achieve reasonable reaction rates at the relatively low temperatures and pressure normally encountered in distillation (DeGarmo *et al.*, 1992). If a solid catalyst is required, it should have a relatively long life of activity, to avoid frequent start-up and shut-down operations (Doherty and Buzad, 1992).

1.1.4 Applications

There are several examples of reactive distillation applications. Next, some of them are presented.

1. The production of methyl acetate is difficult because of the reaction equilibrium limitations and the formation of minimum boiling azeotropes between methyl acetate and methanol, and methyl acetate and water. In 1984, Agreda and Partin patented a reactive distillation process to produce methyl acetate. The former Eastman Chemical Co. process consisted of two reactors and eight distillation columns. Such a process was substituted by one reactive distillation column (Agreda, Partin and Heise, 1990). The middle section

of the column was the reaction section, the lower part separated water and methanol, while the top of the column refined the methyl acetate to obtain a high purity product. This technology has been applied in other esterification reactions such as the production of ethyl acetate and butyl acetate (Stichlmair and Frey, 1999).

2. Some ethers such as methyl tert-butyl ether (MTBE), tert-amyl methyl ether (TAME), and ethyl tert-butyl ether (ETBE) have been produced in reactive distillation columns. For instance, MTBE is produced with methanol and iso-butene by an exothermic reaction that is catalyzed by a strong proton donor (sulphuric acid or a strong acidic macro porous ion exchange resin). In 1981 Smith patented a reactive distillation process for the production of MTBE. The middle of the column has catalyst and the reaction takes places there (Doherty and Buzad, 1992).

3. A difficult separation that can be achieved by reactive distillation is the separation of the meta and para xylene isomers. It is possible to alkylate a mixture of meta and para- xylene with acetaldehyde in a reactive distillation column. The different alkylated products are separated in the column and later dealkylated (Sharma, 1985).

4. Some compounds can also be produced in a reactive distillation column via alkylation. An example is the production of cumene (Shoemaker and Jones, 1987). In this process benzene and propylene enter to a column that has a middle section filled with catalyst. The bottom stream of the column is distilled in a conventional column that separates the cumene from the reactants which are recirculated to the reactive column.

The examples might give the impression of reactive distillation being a straightforward implementing process. This idea is incorrect, because the reactive distillation implementation has offered multiple challenges to engineers. The next section addresses some of the complications that may be present in reactive distillation.

1.1.5 Reactive distillation problems

Reactive distillation presents some complications that restrict its practical use. In the following, there is a list of issues that have stimulated research in order to implement and improve reactive distillation.

- The presence of chemical reactions alters the expected vapour-liquid equilibrium. Issues such as reactive azeotropes requires investigation.

- The presence of a liquid catalyst will also affect the vapour-liquid equilibrium and have to be considered. Such a liquid catalyst has to be considered as well during design. For instance, its feed position need to be determined, and if it is an acidic catalyst, corrosion should be also considered.

- Increase of non-linearity due to the presence of reactions. For instance, reactions may complicate the relationship between molar and mass (or volume) internal and external flows.

- Side products or inert compounds can complicate the separation.

- When a solid catalyst is required and a reactive zone can be defined; it is necessary to decide its extension and characteristics. Thus, if a solid catalyst is needed, an efficient way to place it in the column must be found.

- In the same way, the feed location and its characteristics need to be considered regarding the reactants conversion and separation.

- There are modeling challenges due to the presence of reactions and the transport between phases.

- The presence of an exothermic reaction should be considered for heat integration issues.

The last list shows that there have been several questions to be answered along with the implementation of reactive distillation. Those points have stimulated different research areas.

1.1.6 Research areas on reactive distillation

Reactive distillation complexity has imposed new challenges for scientists and engineers. Hence, there have been many research areas that have contributed to the understanding and implementation of reactive distillation.

In this chapter, a general review of the different research studies regarding reactive distillation is given. This review is organised by topics starting with reactive distillation models. The review is not exhaustive. Moreover, there have been

some interesting reviews published in major circulation journals. The most important ones were written by Doherty and Buzad (1992), Stichlmair and Fair (1998). Stichlmair and Frey (1999) and Taylor and Krishna (2000).

1.2 Reactive distillation models

There have been two approaches to describe the reactive distillation behaviour. The first one is similar to the vapour-liquid equilibrium assumption commonly used for conventional distillation. The second one is more complex and considers no phase equilibrium but mass transport between phases.

Although non-equilibrium models can be more precise than equilibrium ones, we should consider their applicability to address different problems. In this fashion, an equilibrium model can be convenient for early in the design process and to get a first estimation of the column behaviour. On the other hand a non-equilibrium model is necessary to study the performance of the column packing or the catalyst behaviour.

In the present section both approaches are analysed. Moreover, some models and their use are presented. Furthermore, a rather non-exploited equilibrium model and its advantages is presented. The section concludes with a general discussion about the convenience of both approaches.

1.2.1 Equilibrium models

General Features

The main assumptions for the equilibrium models are:

1. The column is divided into a certain number of theoretical stages in which vapour and liquid phases are in chemical, thermal and mechanical equilibrium.

2. Each phase is perfectly mixed. Thus there are no composition, temperature or pressure gradients within a phase.

The main difference between the models is the way in which the equilibrium relationships are expressed. Some models can incorporate a reaction equilibrium

constant, while others make substitutions to avoid the inclusion of reaction rate terms.

Equilibrium models have advantages and disadvantages. The main advantage is their simplicity. Thus they can be easily solved or integrated. This sort of model is convenient when no point composition or temperature is required. The main disadvantage of this kind of model lies in its assumptions. Many of the practical processes operate far from equilibrium. Therefore, it is impractical when a detailed description of the process is required.

This kind of model has been used mainly for basic design and performance studies. In the next section, different examples and their uses are explained.

1.2.2 MESH equations models

Equilibrium models often consist of mass balances, equilibrium and summation equations; and energy balances. We refer to such system as MESH equations system. Figure 1.1 shows a scheme of a theoretical equilibrium stage p. If the hold-up of component i is represented by M_i, then the mass balance for such a component can be written as:

$$\frac{dM_{i,p}}{dt} = F_p z_i + V_{p+1} y_{i,p+1} + L_{p-1} x_{i,p-1} - \left\{ (V_p + S_p^V) y_{i,p} + (L_p + S_p^L) x_{i,p} \right\} + \sum_{m=1}^{r} \nu_{i,m} R_{m,p} \epsilon_p \tag{1.1}$$

where $\nu_{i,m}$ is the stoichiometric coefficient of component i in the reaction m, and ϵ_p is the reaction volume.

The vapour composition $y_{i,p}$ can be related to the liquid composition by a phase equilibrium relationship represented as follows:

$$y_{i,p} = K_{i,p} x_{i,p} \tag{1.2}$$

In addition, the component composition must comply with the summation equations:

$$\sum_{i=1}^{C} x_{i,p} = 1$$

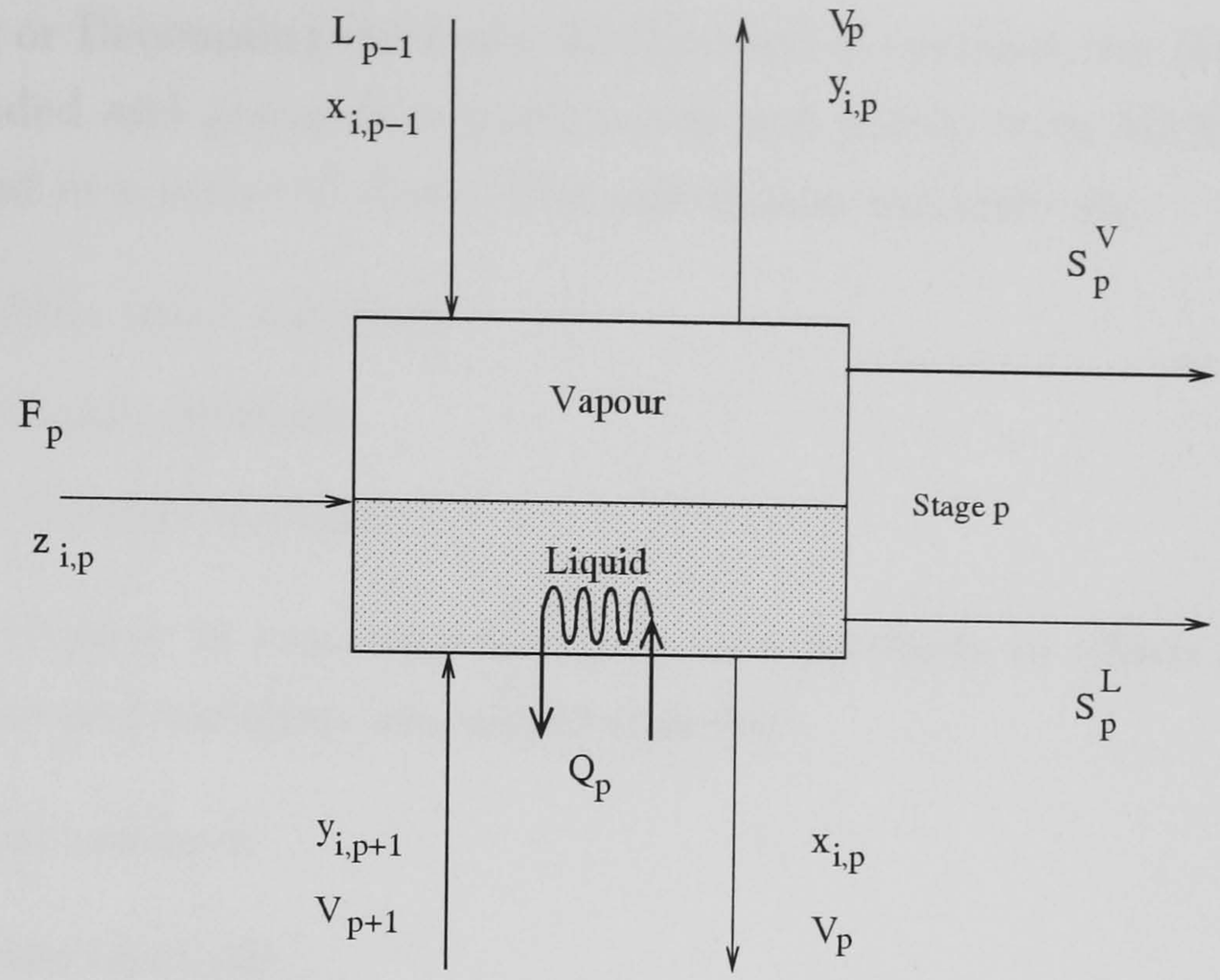

Figure 1.1: Scheme of a theoretical equilibrium stage of a distillation column

$$\sum_{i=1}^{C} y_{i,p} = 1 \tag{1.3}$$

The energy balances are written as follows:

$$\frac{dM_p H_p}{dt} = F_p H_p^F + V_{p+1} H_{p+1}^V + L_{p-1} H_{p-1}^L - \left\{ (V_p + S_p^V) H_p^V + (L_p + S_p^L) H_p^L \right\} + Q_p \tag{1.4}$$

If the enthalpies are referred to pure elements, then there are no reaction terms in the energy balances.

Depending on the final use of the model and the complexity desired, the model might include more equations such as hydraulics equations, control relationships, etc. If steady state simulations are needed, then the differential equations (1.1) and (1.4) are equalled to zero.

Solution of steady state MESH models

The solution of steady state reactive distillation problems can be done in a similar way to that used in conventional distillation. The rigorous computational methods used for conventional distillation problems are (Kister, 1992):

1. Tearing or Decoupling methods. In this kind of method, the MESH equations are divided and grouped or partitioned and paired with MESH variables to be solved in a series of steps. The calculation methods are:

   (a) Bubble point methods

   (b) Sum-rate methods

   (c) 2N Newton methods

2. Global Newton or simultaneous correction methods in which all the MESH equations and variables are solved together

3. Inside-out methods

4. Relaxation methods

5. Homotopy-continuation methods

The rest of the section includes a brief summary of the different methods that have been used to solve steady state reactive distillation equilibrium models.

Method 1.2.1 *Bubble point methods*

In this sort of method, the stage temperatures are calculated by solving the bubble point equation. Such an equation is obtained from the equilibrium equation, equation (1.2), and the summation equations, equations (1.3). The compositions and flow rates are recalculated with the mass and energy balances. Next the temperatures are recalculated. The process is continued until the variation of the variables between one calculation step and the last one are lower than a specified tolerance.

An improvement to this method was developed by Holland (1975). Here a convergence promoter named θ is used to correct the compositions calculated from the balances before using them in the temperature estimation.

The θ method was adapted to solve reactive distillation problems by Komatsu and Holland (1977) and by Izarraz, Bentzen, Anthony and Holland (1980) to solve acetic acid esterification distillation problems.

Method 1.2.2 *Newton and quasi-Newton methods.*

The MESH equations can be re-written as a system of nonlinear equations that can be solved by Newton or quasi-Newton methods.

Newton-Raphson or quasi-Newton methods were used to solve steady state reactive distillation problems by Isla and Irazoqui (1996) to solve the equilibrium model of a MTBE column for a sensitivity analysis. Another example is the work of Pilavachi, Schenk, Pérez-Cisneros (1997) who studied the parameter sensitivity of reactive distillation equilibrium models. Lee and Dudukovic (1998) used a Newton method to solve their equilibrium reactive distillation model to compare with a non-equilibrium one. They also compared the Newton solution with homotopy-continuation, finding the latter more efficient. In the three given examples, the method used was developed by Naphtali and Sandholm (1971) in which the equations are re-ordered to create a tridiagonal matrix of equations that is linearised and then solved by the Newton-Raphson technique.

Method 1.2.3 *Relaxation methods*

Relaxation methods are related to integration techniques. The basic idea is to integrate the dynamic MESH equations from an initialisation condition till the solution does not change with time (Kister, 1992).The problem is normally initialised with the liquid in every stage with the same composition (at bubble point) than the feed flow rate.

Since this sort of method is very demanding computationally, it has been rarely used in reactive distillation problems. An example of its use can be found in Komatsu (1977) whose results agreed with the experimental ones for the acetic acid esterification problem.

Method 1.2.4 *Homotopy-continuation methods*

The MESH equations can be difficult to solve when the column has a complex structure or when the relations for the component properties calculation are highly non-linear. When this happens homotopy-continuation can be used (Kister, 1992).

The homotopy-continuation method is based on the correction of a simple or different solution until the desired solution is reached. That is, given a certain solution of the system a path is followed to the desired solution (Kister, 1992).

There are two kinds of homotopy methods. In the first case, the continuation parameter is chosen without any relationship to the model, the method is called then a mathematical homotopy. In the second case, the continuation parameter is related to the characteristics of the problem and is called a physical or parametric

homotopy. To solve the MESH equations, the physical homotopy methods are recommended.

This method has been widely used to solve reactive distillation problems. Lee and Dudukovic (1998) used this method for the solution of reactive distillation problems to compare between equilibrium and non-equilibrium models. Ciric and Miao (1994) used different parameters to study the multiplicities in an ethylene glycol reactive distillation column. Sneesby, Tadé and Smith (1997b) used homotopy continuation to test the multiplicity of a MTBE reactive distillation column when different conditions were changed. Recently, Mohl *et al.* (1998 and 1999) used a simulator called *Diva*, based on homotopy continuation, to study the multiplicities of MTBE and tert-amyl methyl ether (TAME) reactive distillation columns.

Method 1.2.5 *Inside-out methods*

Inside-out algorithms consist of two loops, one external (outside loop) and one internal (inside loop). In the outside loop, the physical properties, such as activities, equilibrium constants and enthalpies, are calculated with simple models. The results from this outside loop are sent to the inside loop that uses the calculated properties for an iteration of the solution of the MESH equations algorithm (commonly a Newton method). The results of the internal loop are sent to the outside loop for the calculation of properties. The described cycle is repeated until the convergence criterion is met (Venkataraman, Chan and Boston, 1990).

Venkataraman *et al.* (1990) implemented the inside-out method in ASPEN PLUS to solve steady state reactive distillation problems and tested it with several systems. Such implementation is called RADFRAC. RADFRAC has been used by several authors to solve different reactive distillation problems. Nijhuis, Kerkhof and Mak (1993) and Hauan, Hertzberg and Lien (1995) used RADFRAC to study the multiplicities found in a MTBE reactive distillation column.

Dynamic simulations of reactive distillation equilibrium models

The study of reactive distillation has been also assisted with dynamic simulations. For instance, the integration of reactive distillation MESH equations was used to simulate the start-up operation of three reactive distillation columns by Scenna, Muñoz and Benz (1998a) and Scenna, Ruiz and Benz (1998b). The mentioned authors studied how start-up procedures can determine the final steady state reached.

The MESH equations were solved with a simulator previously developed by Ruiz. Basualdo and Scenna (1995) called READYS. Schrans, de Wolf and Baur (1996) used SPEED-UP to study the response of a MTBE reactive distillation column when changes in the feed composition or flow occur. The oscillatory behaviour that the mentioned authors found was reproduced by Hauan, Schrans and Lien (1997). SPEED-UP was also used by Sneesby *et al.* (1997a, 1998d) to study possible transitions between multiple steady states in a MTBE reactive distillation column. Six control alternatives for a hypothetical reactive distillation were tested with dynamic simulations by Al-Arfaj and Luyben (2000). The main conclusion is the same as that found by Sneesby *et al.* (1998d): early process control decisions should be regarded as crucial for later column performance.

1.2.3 A modification of the equilibrium model: the Doherty method

In 1987, Barbosa and Doherty proposed a set of composition variables to simplify the analysis of simultaneous phase and chemical equilibrium. Barbosa and Doherty (1987) used these variables to develop reactive phase equilibrium charts. How to obtain such variables is better understood with a simple distillation unit example (Barbosa and Doherty, 1988a). The system consists of a still with a certain liquid mixture and when this mixture is heated, reactions and separation occur.

The new composition variables (X_i and Y_i) and a new time variable τ were defined in terms of the c components mole fractions y_i and x_i and the reaction coefficients ν as follows:

$$\begin{aligned} X_i &= \frac{\left(\frac{x_i}{\nu_i} - \frac{x_k}{\nu_k}\right)}{(\nu_k - \nu_T x_k)} \\ Y_i &= \frac{\left(\frac{y_i}{\nu_i} - \frac{y_k}{\nu_k}\right)}{(\nu_k - \nu_T y_k)} \\ d\tau &= \left(\frac{V}{H}\right)\left(\frac{(\nu_k - \nu_T y_k)}{(\nu_k - \nu_T x_k)}\right) \end{aligned} \tag{1.5}$$

where $i = 1, \ldots, c$ and $i \neq k$.

For the simple distillation unit, these changes lead to a final set of c-2 linear, independent ODEs.

Barbosa and Doherty (1988a) extended the concept of residue curve maps to reactive distillation processes (1988a) with these variables. Furthermore, several authors have used these composition variables to model complex reactive distillation processes. For instance, Espinosa, Aguirre and Pérez (1995) used a similar set of variables to study the influence of inert compounds in the performance of a reactive distillation column, concluding that inert compounds play a key role in the column design. They also determined the thermodynamically feasible specification and the extent of the conventional minimum reflux calculation of reactive systems. In 1995, Ung and Doherty extended the method of new composition variables to systems with multiple reactions.

The main advantage of these composition variables is that direct correspondences can be made between reactive and conventional multicomponent distillation. Hence conventional design methods can be used for reactive distillation processes. However, since equations must be rewritten some complex problems can arise. For instance, for a simple reactive distillation column a new variable for time had to be added. This means that the application to dynamic problems is not simple, as it might not be possible to propose a new time variable to describe the process. In addition to this last problem, it is not easy to extend the new composition variables to a process with more than one reaction.

1.2.4 A modification of the equilibrium model: an element based model

In 1995, Michelsen proposed the use of chemical models for calculation of reactive phase equilibrium. A chemical model involves the equations of chemical equilibrium together with any appropriate physical model to determine the chemical potentials. The solution of the chemical model equations and the criteria of equilibrium, equality of chemical potentials for the coexisting phases, provide the phase compositions at equilibrium. Pérez-Cisneros, Gani and Michelsen (1997) developed an element model that was used to represent chemical and physical equilibrium of multicomponent and multi-reaction system. Thus, vapour-liquid phase equilibrium diagrams similar to the developed ones for physical equilibrium were constructed. In their method, an element is defined as a constituent part of the mixture components. For instance, a radical, a ion or a whole component if it is inert.

The use of elements instead of components offers benefits for reactive distillation modeling. Firstly, since there are either a less or equal number of elements than

components, this sort of model can reduce dimensionality of the reactive distillation modelling. Secondly, it can handle several reactions in a simple way. Thirdly, it leads to a simple representation of chemical and physical equilibrium that may lead to a reactive distillation column model simplification.

The element model was used to study the parameters that may affect the reactive distillation modelling (Pérez-Cisneros, Schenk, Gani and Pilavachi, 1996 and Pilavachi *et al.*, 1997). Chemical-physical equilibrium diagrams were constructed with the element model but with different thermodynamic models. Their results showed that appropriate thermodynamic models should be used to model a reactive distillation column since they can affect the column design.

Gani, Jepsen and Pérez-Cisneros (1998) presented a generalisation of a separation unit based on the element model. In such a model the MESH equations are used but the equilibrium was solved by the Gibbs energy minimisation proposed by Pérez-Cisneros *et al.* (1997). The kinetically controlled reactions approach and the chemical-physical equilibrium approach were compared for a ethylene glycol reactive distillation column.

Since the balances involved both elements and components, further use of the model besides simulation is complicated. Therefore, in the present work a modification of Gani *et al.* (1998) model was developed for the steady state and dynamic problems.

To improve the understanding of the model developed in the present work, the fundamentals of the element model developed by Pérez-Cisneros *et al.* (1997) are explained in the next chapter in Section 2.1.3.

1.2.5 Rate based models

In a rate based model, the equilibrium assumption is relaxed so that mass and energy transport between phases can be considered. Depending on the level of detail required, assumptions such as perfect mixing within a phase can be relaxed as well. Also, transport is commonly described by the use of mass and energy transport coefficients. Details about this kind of model and a generalised model can be found in Taylor and Krishna (2000).

This sort of model can be more precise than equilibrium models provided that the transport properties are properly determined. They have been used in the study of reactive distillation behaviour where an equilibrium model does not produce correct results.

The following is a section that shows some examples of the use of non-equilibrium models.

Examples

Sundmacher and Hoffman (1996) presented a steady state three-phase model to simulate a laboratory scale MTBE-column. The model included the transport of mass and energy from the liquid phase into the catalyst, the reaction on the catalyst, transport between the vapour and liquid phase and transport along the column. The influence of different operating conditions was tested. In particular, the feed location analysis suggested that larger conversion was obtained if the methanol and C_4 feed streams were arranged to be counter-current. The model was validated with experimental data.

Thiel, Sundmacher and Hoffmann (1997) presented a simpler model based on phase equilibrium between the liquid and vapour phase and a Langmuir-Hinshelwood approximation for the heterogeneously catalyzed reaction. Their results showed that the Damköler number and the pressure were the main influences on the process. The variation of these parameters determined the existence and position of stable nodes, saddles and separatrices in the residue curve maps.

Yu, Zhou and Tan (1997) developed a steady state model for a tray reactive distillation column that considered the transport between the liquid and vapour phases and the liquid and solid phases in which the reaction is assumed to occur at the catalyst surface. The model was solved using homotopy-continuation and was validated with experimental data. The authors found that for a bisphenol-A production example, this model performed better than one ignoring transport from the liquid to the solid phase.

Kreul, Górak, Dittrich and Barton (1998) developed a model that considered mass and energy transport between the liquid and vapour phases. However, the transport within the solid phase was ignored and the reaction was considered pseudo-homogeneous. Additionally, experiments were carried out to find the necessary transport coefficients. It was found that the correlations commonly used for non-reactive distillation to determine transport coefficients were still valid for reactive distillation.

In a similar way, Higler, Taylor and Krishna (1998) developed a model that included transport between liquid and vapour phases. It was assumed that the reaction took

place in the liquid phase. Their results showed that the reaction could affect the stage efficiency, suggesting that rate based models may be better for reactive distillation. Higler *et al.* (1999) used the developed model to compare the results between this model and an equilibrium model. Continuation analyses were done with the bottom flow rate used as continuation parameter. The authors found differences in the low conversion branch of the bifurcation diagram for a MTBE reactive distillation example between the equilibrium model and the non-equilibrium model.

Schenk, Gani, Bogle and Pistikopoulos (1999) presented a generalised hybrid model that could switch between non-equilibrium and equilibrium modes to accelerate calculations. The authors showed the importance of appropriate activity coefficient parameters and validated the model against reported experimental data.

Higler *et al.* (2000) presented another model (a "dusty model")that considered transport (diffusion) within the catalyst. It was found that the model produced different results for the MTBE example than when using a pseudo-homogeneous model. However, there were no differences for a TAME column example.

Conclusion

The examples reviewed showed that non-equilibrium models can be more precise for describing a reactive distillation column. However, the gross column behaviour can be reproduced with both kinds of models. Furthermore, detailed modelling requires more parameters that ideally should be found or corroborated with experiments.

1.3 Design

Different methods for design of reactive distillation columns have been developed. For instance, Barbosa and Doherty (1988b) used their set of composition variables (Section 1.2.3) to develop a method to find whether reactive distillation was feasible for a certain equilibrium reaction or not and to determine the minimum reflux for the column. In such methods, an equilibrium model is used to write mass balances above and below the column feed. Using the desired final composition, the balances are integrated to create composition trajectories for the rectifying and the stripping section. When the trajectories intercept the column is feasible.

The method was adapted to design columns in which kinetically controlled reactions take place (Doherty and Buzad, 1992). Furthermore, Okasinski and Doherty (1998) relaxed many of the original assumptions to make the method more general. Espinosa *et al.* (1995) used the Barbosa and Doherty method to design a reactive distillation column in which inert species were fed along with the reactants, finding that inert compounds should be considered during design.

Different methods were presented by Bessling, Schembecker and Simmrock (1997) and Giessler *et al.* (1998). Moreover, graphical methods were developed by Espinosa, Scenna and Pérez (1993) and Lee, Hauan and Westerberg (2000), among others.

Residue curve maps have been also used in reactive distillation column design. These curves link the liquid composition remaining for a simple distillation process and are related to the composition profiles in continuous distillation. They are useful to detect separation constraints. Furthermore, residue curve maps can help to analyse the effect of some design decisions such as feed composition, feed location, pressure, etc. (Jiménez, Wanhschafft and Julka, 2001). Barbosa and Doherty (1988a) used a model for a simple reactive distillation process expressed with transformed composition variables (Equations 1.6) to develop residue curve maps.

In all the cases mentioned above, the model usually includes the equilibrium between phases assumption. However, Taylor and Krishna (2000) suggested that industry may have already used non-equilibrium models for reactive distillation column design.

1.3.1 Reactive distillation column design and optimisation

There are many examples of optimisation applied to reactive distillation design. For instance, Grosser, Doherty and Malone (1987) found that when reactive entrainers are used to separate closely boiling mixtures, there is an optimum reflux ratio and an optimum entrainer feed rate. They concluded that there was little incentive to use reactive distillation when the relative volatility is greater than 1.06. Ciric and Gu (1994) used a mixed integer non-linear programming (MINLP) model to minimise the total annual cost of reactive distillation columns in which chemical reaction equilibrium cannot be ensured. Later, Cardoso, Salcedo, de Azevedo and Barbosa (2000) solve the same problem but with a non-equilibrium model. Pekkanen (1995) presented an algorithm based on directions in the concentration

space. Seferlis and Grievink (2001) minimised with collocation models the costs of a reactive distillation column that is subject to several constraints. Energy use for a reactive distillation column was optimised by Rojey (1994) with the exergy concept. Ismail, Proios and Pistikopoulos (2000) developed a method to optimise a general reaction-separation unit.

1.3.2 Design and column performance

As expected, basic design has important effects on the final column performance. For example, a MTBE reactive distillation column may display multiple steady states depending on the feed location (Schrans *et al.*, 1996 and Hauan *et al.*, 1995). Some other design decisions that can influence performance are: number of stages or total height of packing for the separation and reactive stages; feed features; and external and internal flow rates.

Since early design is fundamental for the column behaviour, we decided to study the factors relating to basic design that could influence a reactive distillation column performance. Such a study is presented in Chapter 4.

1.4 Reactive distillation detailed engineering

The practical use of catalytic reactive distillation has brought many challenges to engineers. There have been many investigations to improve: the catalyst used in some process, placement of such a catalyst, contact area, etc.

The most common commercial support for catalytic reactive distillation is bale packing in which catalyst pellets are placed between two layers of metallic mesh that can have a special pattern to form channels to improve flow. The packing is then rolled and placed in the distillation column. Brand names include Katapak, Katamax and Multipack which have been studied by several authors. Subawalla, Gonzalez, Seibert and Fair (1997) developed a model to predict the pressure drop and the height equivalent to a theoretical plate. It was found that the validation could be done in conditions without reaction. Ellenberger and Krishna (1999) experimentally determined the pressure drop, hold-up and mixing characteristics of Katapak-S. They found that the liquid phase may flow not only within the filled channels but also within the empty ones (designed for the vapour phase). van Baten, Ellenberger and Krishna (2001) presented simulations that were able

to describe the experimental results, suggesting that scale-up and design could be done also with simulations. Also for Katapak-S, Moritz and Hasse (1999) made a model to predict flow conditions for this packing. Kołodziej, Jaroszński, Hoffmann and Górak (2001) developed a model to describe the flow regime for Multipak. von Scala, Wehrli and Gaiser (1999) experimentally determined the overall heat transfer coefficient, the local wall heat transfer coefficient and the effective radial conductivity for Katapak-M.

Another kind of support that has been tested for catalytic reactive distillation are the internally finned monoliths. In this case the catalyst must be deposited on the structured monolith surface by impregnation or precipitation techniques. The monoliths can offer good contact area and good flow for the vapour and liquid phases. Lebens, Kaptein, Sie and Moulijn (1999) compared the performance of such monolithic packing with bale packing. Experimental results confirmed that the monoliths can offer more contact area, but the liquid hold-up is smaller.

Oudshoorn *et al.* (1999) used common structured distillation packing to develop a zeolite based catalyst on its surface. Compared with Amberlyst-15, the developed catalyst had similar or superior activity. The results suggested that the catalyst could offer good performance for the ETBE process.

1.5 Designing new processes: novel reactive distillation processes

Reactive distillation has been modified to solve new problems. Two examples are provided. The first one is an adaptation for photo-reactions done by Xu and Duduković (1999). They developed an equilibrium model to describe the toluene chlorination in a semi-batch reactive distillation in which photo-radiation was applied. The simulation and experimental results suggested that it is possible to achieve high selectivity and high conversion with this process.

The second example is a modified reactive distillation column proposed by Han, Jin and Yu (1997) in which the catalyst particles are placed in sieve trays that are covered with a metallic mesh. In the described compartment the particles can be fluidized by the liquid. Special vapour and liquid conduits were designed to allow good flow. The design was applied to the hydrolysis of methyl acetate. With the new design, the conversion can be increased from 20% (traditional process) to 50%.

1.6 Operation

The most important aspects investigated related to reactive distillation column operation are start-up, batch operation and multiple steady states.

1.6.1 Batch reactive distillation

Sørensen and Skogestad (1994) studied the controllability of a batch distillation column in which the reboiler acted as a reactor with an equilibrium model. They studied the column dynamic behaviour when different disturbances occurred. Also, Sørensen, Macchieto, Stuart and Skogestad (1996) optimised a reactive batch distillation column and studied its controllability properties. Furthermore, a one point control for the optimised column was implemented.

As mentioned before (Section 1.5), Xu and Duduković (1999) modelled a reactive batch distillation column in which photo-reactions took place.

Operation policies for a batch distillation column in which reactions took place in the still to produce butyl acetate were investigated by Venimadhavan, Malone and Doherty (1999) using a simplified equilibrium model. The solution was a non conventional policy that was related with the production rate.

Schneider, Noeres, Kreul and Górak (2001) developed a non-equilibrium model for a reactive batch distillation column. The simulations agreed with experimental results.

1.6.2 Start-up

It is common to startup reactive distillation columns in a similar way to conventional distillation columns. That is, the reboiler is charged with a certain amount of known composition liquid and evaporation starts. The column is operated at total reflux until a steady state has been reached. At that moment, the feed can start and the reflux ratio is decreased slowly (Alejski and Duprat, 1996).

The importance of correct start-up operation for a reactive distillation column that could display multiple steady states was studied by Scenna *et al.* (1998a and 1998b). They found that incorrect policies could send these columns to an undesirable steady state. This idea was also studied by Sneesby, Tadé and Smith

(1998d) who suggested that the multiple steady states that can be present in a reactive distillation column were more important for start-up operations than for control of a steady state since such a state can be very stable.

For a TAME production column, Mohl *et al.* (1998) experimentally found that a traditional start-up policy could produce only one of two steady states for certain conditions. The solution was to initiate the reboiler with a mixture with compositions similar to the final one. The composition at the desired steady state was almost flat and close to an azeotrope. Therefore, the reboiler was charged with a mixture close to the azeotrope.

Similar results were found by Bisowarno and Tadé (2000) for an ETBE reactive distillation column. Additionally, they suggested that if the desired operating condition cannot be stabilised, it should be stabilised during the separation only region.

1.6.3 Multiple steady states and transitions between them

It is common to reactive distillation columns to display input and output multiplicity. Sneesby *et al.* (1997b and 1998d) and Scenna *et al.* (1998a and b) among others pointed out the implications that such multiplicities could have in start-up operations and control.

The understanding of these multiplicities and the factors that motivate their existance can benefit the operation of reactive distillation columns. Hence, the explanations given till date are reviewed in Chapter 3 in which a new hypothesis is proposed.

1.7 Discussion

The behaviour of reactive distillation columns has been widely studied. Several authors have reported non-linear behaviour characterised by input and output multiplicity; and unexpected behaviour such as a decrease in the temperature of lower stages when the reboiler heat duty was increased. Although it is true that the multiplicities are inherently related to reaction-separation characteristics of the system, it is likely that they are prompted by the column conditions and operating policies.

specially those related to high internal flow rates. Hence, a study of reactive distillation steady state behaviour under different policies and design has been done here and is discussed in Chapter 3.

On the other hand, there are also contribution possibilities in the area of control system design of reactive distillation columns. Though there are several works related to the control system design of conventional distillation column, and although reactive distillation dynamics have been widely studied, the question of whether it is possible to develop a method or modify an existing one to improve control system design of reactive distillation is still open. Therefore, an investigation on such a possibility was undertaken. Additionally, it was desirable to know if it was possible to know prior to rigorous dynamic simulation if it was possible or not to control multiple steady states that are frequently found in reactive distillation but could result attractive. This aspect was also investigated in Chapter 4.

To perform the tasks, it was concluded that to work with an equilibrium model was enough, since it can represent the gross behaviour that is the main interest of the present work. It is reckoned that the profiles obtained through the study may not be precise, but if the calculation of properties is correctly done, the general behaviour should be appropriately represented. Moreover, to avoid working with reaction rates in the mass and energy balances, it was decided to develop a dynamic version of the Pérez-Cisneros *et al.* (1997) model. This is advantageous to reduce the number of states and allows the construction of a flexible model to be able to work with different configurations and reactions by just simple changes. This model is presented in Chapter 2. An additional interest of the present investigation is to analyse the model restrictions and difficulties both in the implementation and in performance.

The study of these particular contributions can lead to a better understanding of the operation and basic design of reactive distillation. Conclusions and suggested future work for further development in the area are presented in Chapter 5.

Chapter 2

Reactive Distillation equilibrium modeling

Equilibrium models have both disadvantages and advantages. The main disadvantage is that the simulation results represent a perfect system and this might not be close to reality. The profiles that result can be only qualitatively accurate. On the other hand, a major advantage is the simplicity of the model as a result of not dealing with the descriptions of transport phenomena.

For instance, since the problem is very complex there is no an exact way to represent the transport phenomena. Including relations that are intended to describe these phenomena require transport coefficients that are difficult to obtain unless they are found by experiment (Taylor and Krishna, 2000).

In this chapter the model developed to study the dynamics of reactive distillation is presented. Such a model was developed assuming vapour-liquid equilibrium. The equilibrium is modelled with an element model developed by Pérez-Cisneros, Gani and Michelsen (1997), which is also explained in this chapter.

When compared with another equilibrium model (Schrans *et al.*, 1996) the results were qualitative and quantitatively similar. However, when compared with pilot plant experimental results (Sundmacher and Hoffmann, 1994), the simulation results for the steady state problem failed to reproduce the composition profiles because transport resistances were ignored. When compared to dynamic experiments the model results are qualitatively similar.

2.1 Preliminaries

2.1.1 Equilibrium

Equilibrium is often expressed with the Gibbs free energy. The main advantage is that the Gibbs free energy can be written in terms of measurable variables such as temperature T, pressure P and composition.

$$nG = g\left(P, T, n_1, n_2, .., n_{NC}\right) \tag{2.1}$$

When an irreversible process takes place at constant pressure and temperature, there will be a decrease of the Gibbs free energy. Therefore a system is at equilibrium when the Gibbs free energy reaches a minimum for certain temperature and pressure (Smith and Van Ness, 1987):

$$\left(dG\right)_{T,P} = 0 \tag{2.2}$$

The total derivative of the Gibbs free energy, equation (2.1), for a single phase is written as follows:

$$d\left(nG\right) = \left(nV\right)dP - \left(nS\right)dT + \sum_i \mu_i dn_i \tag{2.3}$$

where $\mu_i \equiv \left[\frac{\partial(nG)}{\partial n_i}\right]_{P,T,n_j}$ is called the chemical potential of component i.

In addition, the first two members can be eliminated if we recall that it is assumed that the system is at thermal and mechanical equilibrium. Consequently, equation (2.3) is reduced to:

$$d\left(nG\right) = \sum_i \mu_i dn_i \tag{2.4}$$

The last equation can be written for a system that consists of NP phases as:

$$d\left(nG\right) = \sum_i \mu_i^1 dn_i^1 + \sum_i \mu_i^2 dn_i^2 + \ldots + \sum_i \mu_i^{NP} dn_i^{NP} \tag{2.5}$$

Equation (2.5) is minimised along with the mass transfer restrictions to find the compositions at equilibrium.

2.1.2 Chemical reaction equilibrium

The Gibbs free energy can be used to characterise the chemical reaction equilibrium. Such an equilibrium is represented again by equation (2.3). However, it is necessary to relate the change in the number of moles dn_i to the reactions that occur in the system. For instance, if there were a single reaction in the considered closed system, the change in the number of moles would be a result of such a reaction. This change can be expressed in terms of the extent of reaction, ε, and the stoichiometric coefficient, ν_i, as (Smith and Van Ness, 1987):

$$dn_i = \nu_i d\varepsilon$$

Thus, the chemical equilibrium for a closed system in which only one reaction takes place and in which there are no changes in temperature and pressure is reduced to:

$$\sum_i \nu_i \mu_i = 0 \tag{2.6}$$

Similarly to the physical equilibrium case, the chemical potential is defined as:

$$\sum_i \nu_i \mu_i = \left[\frac{\partial(nG)}{\partial \varepsilon}\right]_{T,P}$$

2.1.3 Element model

If reactions occur in a heterogeneous system, a usual approach is to assume that the reactions occur only in one phase, while there is material exchange between the phases to maintain the equilibrium (Smith and Van Ness, 1987).

In 1995, Michelsen proposed that the reactive phase equilibrium problem could be solved as a combination of a chemical model and a thermodynamic model. That is, the equality of chemical potentials for coexisting phases with the restrictions imposed by a chemical model can provide the composition at equilibrium. Pérez-Cisneros, Gani and Michelsen (1997), presented a method to represent equilibrium that uses the chemical model approach. In this method element balances are used as the chemical model along with the minimisation of the Gibbs free energy to find the compositions for a system at reactive and phase equilibrium.

In the Pérez-Cisneros *et al.* method, elements are not necessarily chemical elements, such as carbon, hydrogen etc., but rather basic units that form the different compounds of the considered mixture, for instance a CH_3 radical. Similarly to chemical elements, in spite of reaction, the total amount of an element in the system remains constant, while molar quantities can change.

There are two main advantages of using element models. The first one is that the solution of the problem resembles physical equilibrium calculations. For example, a reactive azeotrope is expressed as:

$$\omega_A^L = \omega_A^V$$

where ω_A^β is the element fraction of the element A in the phase β.

The second advantage of the element model is the reduction of the problem dimensions. For example, in the MTBE reaction there are three components: iso-butene, methanol and MTBE. Using the element model reduces the system to two elements, which for this case can be the reactants.

The conservation of element j in a system that consists of NP phases is expressed as follows:

$$b_{j,Total} = b_j^1 + b_j^2 \ldots + bj^{NP} \tag{2.7}$$

where b is the amount of element j in the mixture.

In addition, elements and components are related by the stoichiometry which is contained in matrix A_{ij} as follows:

$$b_j^\beta = \sum_{i=1}^{NC} A_{ji} n_i^\beta \tag{2.8}$$

The formula matrix A_{ji} relates the elements and components of the system. For example, to produce MTBE, matrix A_{ji} is expressed in Table 2.1. This table shows that element A is present both in iso-butene and MTBE, but it is not contained in MeOH. If there were an inert component, it would have linearly independent rows and columns. The reader can find a more specific explanation on how to get the formula matrix in Appendix B.

Substituting equation (2.8) in equation (2.7) and rearranging, the final equation that express the conservation of element j in the system is:

Table 2.1: Formula matrix for the MTBE reaction

	iso-butene	MeOH	MTBE
Element A	1	0	1
Element B	0	1	1

$$\sum_{\beta=1}^{NP}\sum_{i=1}^{NC} A_{ji} n_i^{\beta} - b_j = 0 \tag{2.9}$$

where NP is the total number of phases, NC is the total number of components and $j = 1, \ldots, M$ elements.

If one wants to determine the composition at equilibrium one needs to minimise equation (2.5) subject to the M constrains expressed in equation (2.9). A way to solve this problem is with the Lagrange multiplier formulation:

$$\hat{L} = \sum_{\beta=1}^{NP}\sum_{i=1}^{NC} \mu_i n_i^{\beta} - \sum_{j=1}^{M} \lambda_j \left(\sum_{\beta=1}^{NP}\sum_{i=1}^{NC} A_{ji} n_i^{\beta} - b_j \right) \tag{2.10}$$

Equation (2.10) is derived to find the conditions for a stationary point. Note that at equilibrium μ_i is constant and equal for every phase that conforms the system. Thus, the conditions for a stationary point are:

1.
$$\frac{\partial \hat{L}}{\partial n_i^{\beta}} = \mu_i - \sum_{j=1}^{M} A_{ji} \lambda_j = 0 \tag{2.11}$$

2.
$$\frac{\partial \hat{L}}{\partial \lambda_j} = -\sum_{\beta=1}^{NP}\sum_{i=1}^{NC} A_{ji} n_i^{\beta} + bj = 0 \tag{2.12}$$

Equations (2.11 and 2.12) are the equations to solve in order to find the composition of the mixture at equilibrium.

There are two important things to notice. First, in the Lagrange equation, equation (2.10), there is one Lagrange multiplier λ_j for each element and such a multiplier is independent of any phase. That is because such multipliers are related to the restrictions imposed by the conservation of elements, equation (2.9). Second, equation (2.11) defines the element chemical potentials λ_j, that are valid only at

equilibrium. Hence, the equilibrium has been reached if the chemical potentials of element j are equal in every phase:

$$\lambda_j^{(1)}(b_j^{(1)}) = \lambda_j^{(2)}(b_j^{(2)}) = \ldots = \lambda_j^{(NP)}(b_j^{(NP)}) \tag{2.13}$$

and the total amount of elements in the system is conserved:

$$\sum_{\beta=1}^{NP} b_j^{\beta} = b_j^f \tag{2.14}$$

where b^f is the total amount of element j in the system.

2.1.4 Reactive phase equilibrium solution

The minimisation of Gibbs free energy for a system with only one reaction was outlined with equation (2.6). In that case, the extent of reaction was used to express mass restriction. However, with the element method, the mass restriction is given by the conservation of elements (equation 2.12). A way to generalise to NR independent reactions is with the formula matrix A_{ji}. That is, instead of using an extent of reaction for each reaction, a matrix that contains the information of the independent reactions is used.

Pérez-Cisneros *et al.* used an optimisation method presented by Fletcher (1981) to solve the Gibbs free energy minimisation problem. Let's assume that matrix A_{ji} consists of two matrices:

$$\mathbf{A} = [\mathbf{A_I} : \mathbf{A_{II}}]$$

where $\mathbf{A}_I$ is non-singular and preferably an identity matrix. Matrix $\mathbf{A}_I$ does not need to be an identity matrix. However, if such a matrix corresponds to an identity matrix this benefits the visualisation of the problem because in this way there would be an exact equivalence between the elements and certain components.

In addition, the equilibrium condition is given by equation (2.4). The derivatives of n_i with respect to n_j can be written in terms of $\mathbf{A}_I$ and $\mathbf{A}_{II}$. Therefore, there is an stationary point when:

$$\mathbf{Z}^T \mu = 0 \tag{2.15}$$

where matrix $\mathbf{Z}$ is:

$$\mathbf{Z} = \begin{bmatrix} -\mathbf{A}_I^{-1}\mathbf{A}_{II} \\ \mathbf{I} \end{bmatrix}$$

The condition for a local minimum is that the second derivative of the Gibbs free energy with respect to the number of moles of components is positive definite:

$$d^2G = \mathbf{Z}^T\mathbf{U}\mathbf{Z} \tag{2.16}$$

where $\mathbf{U}$ is defined as:

$$U_{ij} \equiv \left(\frac{\partial \mu_i}{\partial n_j}\right)_{T,P} \tag{2.17}$$

Equation (2.15) depends on the composition of the system. Moreover, the composition cannot take any values but is related to the moles of elements as established by equation (2.12). Thus, to find the composition of the system at equilibrium, it is necessary to solve equation (2.15) subject to restriction (2.13). If a Newton or quasi-Newton method is used, equation (2.16) defines the Jacobian matrix of equation (2.15).

2.1.5 Solution of the isothermal reactive flash problem

Flash calculations are the base of the solution for the distillation problem at steady state. In this sort of calculation the composition at equilibrium of the vapour and liquid phases at a given pressure, P, and temperature, T, is determined.

Pérez-Cisneros *et al.* (1997) developed an algorithm to find the compositions at equilibrium of the isothermal reactive flash problem. Their solution of the reactive flash problem consists of finding the composition that assures that the chemical potential of element j is the same for all phases (equation 2.13) and the conservation of elements (equation 2.14). If only liquid and vapour phases coexist in the system, the equations to be solved are:

$$f_j = \lambda_j^L - \lambda_j^V = 0 \tag{2.18}$$

$$f_{j+M} = b_j^V - b_j^L - b_j^f = 0 \tag{2.19}$$

Their solution of the reactive flash problem is based on the solution of two sub-problems. The first one is to find the component composition of each phase that minimises the Gibbs free energy (equation 2.15), but comply with the conservation of elements (equation 2.12). The second sub-problem is to find the element composition that ensures the equality of the chemical potential of element j in all phases and the conservation of elements (equations 2.18 and 2.19). The problems are not independent of each other. The second set of equations needs to be solved for every time the first one is to be solved. Furthermore, the first set of equations needs to be solved for each phase.

2.2 Dynamic Reactive Flash

Developing this model was important since it is the base for the reactive distillation column model. The study of this unit can also be used to get more insight on more complex reactive separation units.

The model assumes that vapour liquid equilibrium exists. In addition to the energy and mass balances, the equilibrium is modelled with the element model.

2.2.1 Description of a Reactive Flash Unit

Figure 2.1 shows a diagram of a flash tank. The tank is at lower pressure than the feed. The feed stream changes its pressure instantaneously when it passes through a flash valve. This change of pressure causes the separation of the stream into liquid and vapour phases.

The amount of vapour leaving the tank controls the pressure. On the other hand, the liquid flow rate can be used to control the liquid level. Along with the phase change, there may be reactions. These reactions can be boosted by the separation. If the reaction is exothermic, the heat of reaction can be used for the separation. Therefore, this unit can achieve good conversion from the benefit of combining reaction and separation.

Despite the apparent simplicity of the unit, several phenomena take place: for instance, the expansion through the flash valve, transport phenomena between phases, the formation of a possible second liquid phase and reactions with complex stoichiometry.

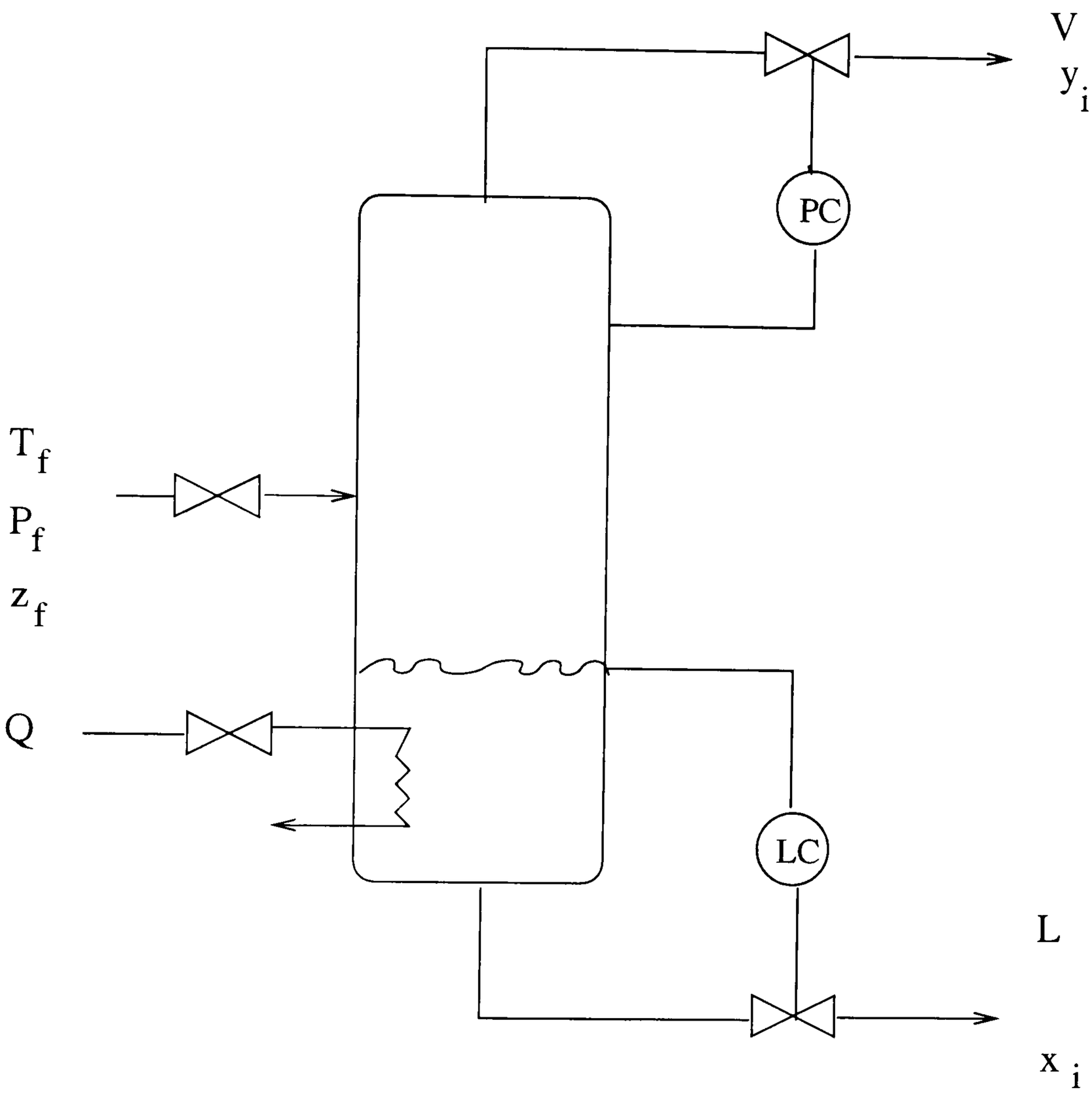

Figure 2.1: Diagram of a flash unit

2.2.2 Dynamic Flash Model

A model has been developed which is intended to describe the gross scale events that have a major influence on the dynamics of the flash unit and to be the foundation for the mathematical model of a reactive distillation column.

The model includes only the dynamics of the liquid phase. Moreover, it was assumed that both liquid and vapour phase are in equilibrium. Therefore, the model does not include a description of the transport phenomena between phases.

Assumptions

Next the main assumptions to develop the model are described. The validity and implications of the assumptions are also explained.

- Vapour and liquid phases are in equilibrium.

- Phases are perfectly mixed. This assumption implies that both temperature and pressure are the same for liquid and vapour phases. Moreover, there are no temperature or composition gradients within a phase. Consequently the composition in the outlet streams is the same as in the bulk of the liquid and vapour phases.

- Vapour dynamics are neglected. When the hold-up of the liquid phase is much larger than the vapour hold-up, it is possible to neglect the vapour dynamics.
  Vapour hold-up can be important,for instance, at high pressures. When this is the case, vapour dynamics should be considered.

- Reactions are homogeneous and take place just in the liquid phase. This means that no interaction between catalyst and liquid phase is considered.
  This assumption may be possible when the liquid-solid transport and the transport within the catalyst is faster than the reaction and the external phenomena. Indeed, there is a potential source of error for the dynamics if liquid-catalyst transport is the dominant step.

The main consequence of the assumptions is a compromise between accuracy and simplicity. The existing references for the reactive flash problem, (Gumuz and Ciric, 1997 and Perez-Cisneros *et* al., 1997), do not not include transport phenomena. However it has been demonstrated that the pattern of dynamic behaviour of a RDC can be described with either non-equilibrium or equilibrium models (Krishna et al. 1999, Kreul, 1999 and Schrans *et al.* 1996)

Mathematical model

The material balance for the hold-up, B, of element j is

$$\frac{dB_j}{dt} = \mathcal{F}\omega_j^F - (\mathcal{V}\omega_j^{*V} + \mathcal{L}\omega_j^L) \tag{2.20}$$

where B_j is the hold up of element j in the flash, $j = 1, \ldots, M$ and $\omega_j^\beta = B_j^\beta / \sum_{j=1}^{M} B_j^\beta$.

The balance for the hold up of energy, H, is also written in terms of elements:

$$\frac{dH}{dt} = \mathcal{F}\check{H}^F - (\mathcal{V}\check{H}^V + \mathcal{L}\check{H}^V) + Q \tag{2.21}$$

where $\check{H}^\beta$ is the specific enthalpy of phase β with respect to the elements. Q is the heat exchanged between the flash and the surroundings. The feed flow rate, $\mathcal{F}$, its composition and its specific enthalpy are known.

When the liquid hold-up of each element is known, the element fraction in the liquid phase, ω_j^L, can be calculated directly. However, the vapour element fraction, ω_j^V, needs to be calculated considering that liquid and vapour are in equilibrium. The equilibrium calculation will provide the composition in the vapour phase, ω_j^V; the specific enthalpy of the liquid phase $\check{H}^V$ and the temperature and pressure within the flash unit.

Equilibrium. For each integration, the composition and temperature that satisfy the equilibrium must be found. There are two requirements for phase equilibrium: the Gibbs free energy is at a minimum value and the element model requires that the elements are conserved (Section 2.1.3):

$$G_{eq} = \sum_{i=1}^{NC} n_i\mu_i = \sum_{i=1}^{NC} n_i(\sum_{j=1}^{M} Aji\lambda_j) = \sum_{j=1}^{M} B_j\lambda_j \tag{2.22}$$

while

$$B_j - \sum_{j=1}^{M} A_{ji}n_i = 0 \tag{2.23}$$

The convergence criterion is that the specific liquid enthalpy (based on elements) calculated must be the same as that which comes from the integration. This is an iterative calculation that will be explained in more detail in Section 2.4.1.

Once the liquid phase mole fractions, x_i, are known, the vapour composition and the pressure can be found with a pressure-bubble point calculation from the equilibrium relationship:

$$P\phi_i y_i^* = x_i P_i^{sat}\gamma_i \tag{2.24}$$

The element mole fractions for the vapour phase can be calculated as follows:

$$\omega_j^{*V} = \frac{\sum_{i=1}^{NC} A_{ji} y_i^{*V}}{\sum_{j=1}^{M} \sum_{i=1}^{NC} A_{ji} y_i^{*V}} \tag{2.25}$$

Properties. Once the temperature, pressure and composition in the liquid and vapour phase are known, it is possible to calculate properties such as average molecular weight, densities and the enthalpy in the vapour phase. The calculation of properties can be found in Appendix C.

Degrees of freedom of the dynamic flash model

To find the total number of the degrees of freedom the number of equations and variables are counted. Table 2.2 shows that the total number of equations is $6M + 5NC + 10$. In Table 2.3 the total number of variables is $6M + 6NC + 15$. Therefore the total number of unknown variables is: $NC + 5$. Since the feed and its conditions (T_f and P_f) are specified by the user, there are $NC + 2$ fixed variables. Hence there are then three degrees of freedom: the liquid flow rate, the vapour flow rate and the heat given or subtracted to the flash.

Exit flows. To calculate the exit flow rates two equations are necessary. The first one is for a proportional controller that relates the total element hold-up B_T in the tank and the liquid flow rate $\mathcal{L}$:

$$\mathcal{L} = \mathrm{k}(N_T - N_{T0}) + \mathcal{L}_0 \tag{2.26}$$

The vapour flow rate depends on the pressure drop between the tank and the surroundings:

$$\mathcal{V} = \mathrm{C_v}\sqrt{P - P_{ext}} \tag{2.27}$$

Heat exchanged. This is calculated with Newton's cooling law:

$$Q = U_H A(T - T_{ext}) \tag{2.28}$$

where U is the overall heat transfer coefficient and A is the area for heat exchanging.

Table 2.2: Equations for the dynamic model of a reactive flash

Equations		Total
Dynamic equations	2.20 and 2.21	$M+1$
Definition of ω_j^β		$3(M-1)$
Summation equation for element mole fraction		3
Conservation of elements	2.23	M
Equilibrium	2.22	1
Definition of element chemical potential	2.13	M
Vapour liquid equilibrium		NC
Criterion $H_{calculated} - H_{intergration} = 0$		1
Raoult law (T)		1
Definition of liquid mole fraction		$NC-1$
Definition of feed mole fraction		$NC-1$
Summation equations for component mole fraction		2
Calculation of component chemical potential		$2NC$
Calculation of specific enthalpy (components)	Section C.5	3
Calculation of specific enthalpy (elements)	Section C.5	3
Total number of equations		$6M+5NC+10$

Table 2.3: Variables of the dynamic model of a reactive flash

Variable	Total
P_f	1
T_f	1
$\mathcal{V}$	1
$\mathcal{L}$	1
$\mathcal{F}$	1
Q	1
T	1
P	1
$\check{H}$	3
H	3
z	NC
y	NC
x	NC
n_i	NC
μ_i^β	$2NC$
B_j	M
H	1
ω_j^F	M
ω_j^{*V}	M
ω_j^L	M
λ_j	2M
Total number of unknowns	$6M + 6NC + 15$

2.3 Dynamic Distillation Column

As was mentioned before, the main purpose of the model is to study the gross scale dynamics of reactive distillation. In this section, the assumptions and models for the dynamic and steady state are presented.

A general diagram of the unit modelled can be seen in Figure 2.2. The column has a total condenser and a reflux drum at the top. At the bottom it has a partial reboiler. It is possible to withdraw liquid or vapour through side streams. Moreover, sections of the column can be considered either as reactive or non-reactive.

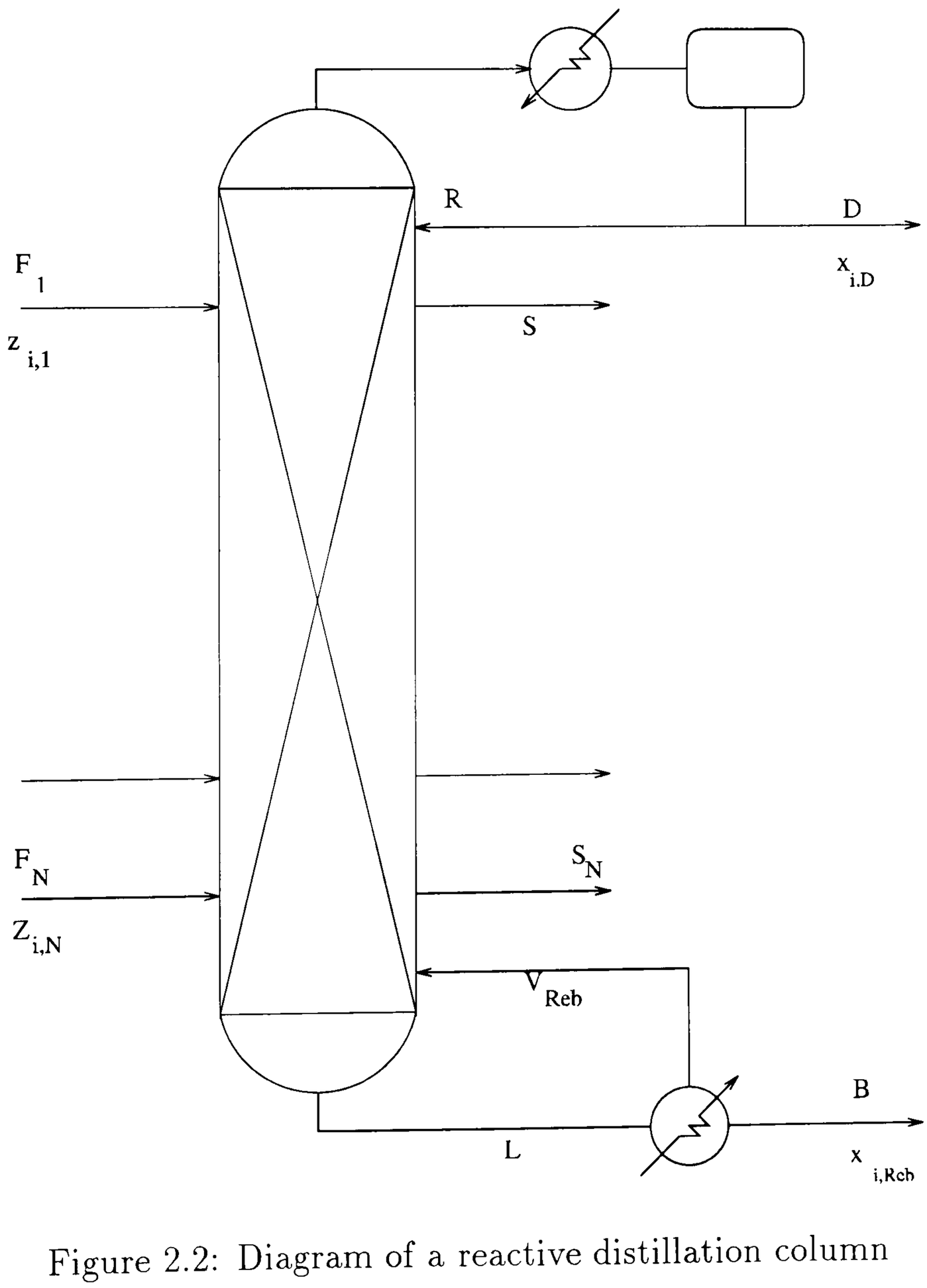

Figure 2.2: Diagram of a reactive distillation column

2.3.1 Dynamic Reactive Distillation Model

The following assumptions and simplifications were made to develop the current model. The first four assumptions are the same as for the flash unit and therefore will not be explained. The model developed was presented in Estrada-Villagrana *et al.* (1999b)

- Vapour and liquid phases are in equilibrium.
- Phases are perfectly mixed.
- Vapour dynamics are neglected.
- Reactions are homogeneous and take place just in the liquid phase.
- The efficiency of the distillation column is considered constant. The efficiency has been set as constant because according to the fourth assumption there are no composition gradients within a phase and it is not possible to calculate a local efficiency. The use of a non complete efficiency reduces the effect of the liquid vapour equilibrium assumption. Note that the calculation of the actual vapour phase composition using an efficiency factor is independent of the equilibrium calculation established in Section 2.1.3.
- The pressure in the total condenser is constant. This assumption allows the direct calculation of vapour flow rates. If this assumption were not made, then an iterative calculation would be required.
- There is no accumulation in the total condenser. However, accumulation is allowed in a reflux drum that follows the condenser. Thus, the composition of the liquid that abandons the condenser has the same composition than the vapour that abandons the column. To know the specific enthalpy of this liquid flow, the liquid is considered as saturated liquid and a dew-T calculation is done to know the temperature of the outlet stream for later calculate its liquid enthalpy.
- Entrainments are negligible.
- The dynamics of the downcomer are not considered. This and the previous two assumptions allow a simplification of the hydraulic equations.

- The distillation stage is considered to be a sieve plate. This assumption allows working with known relationships between the pressure drop and the hold up.

Mathematical model

As in the case of the dynamic flash unit, the model for a RDC uses the element model approach (Section 2.1.3). Figure 2.3 shows the characteristics of the modelled column.

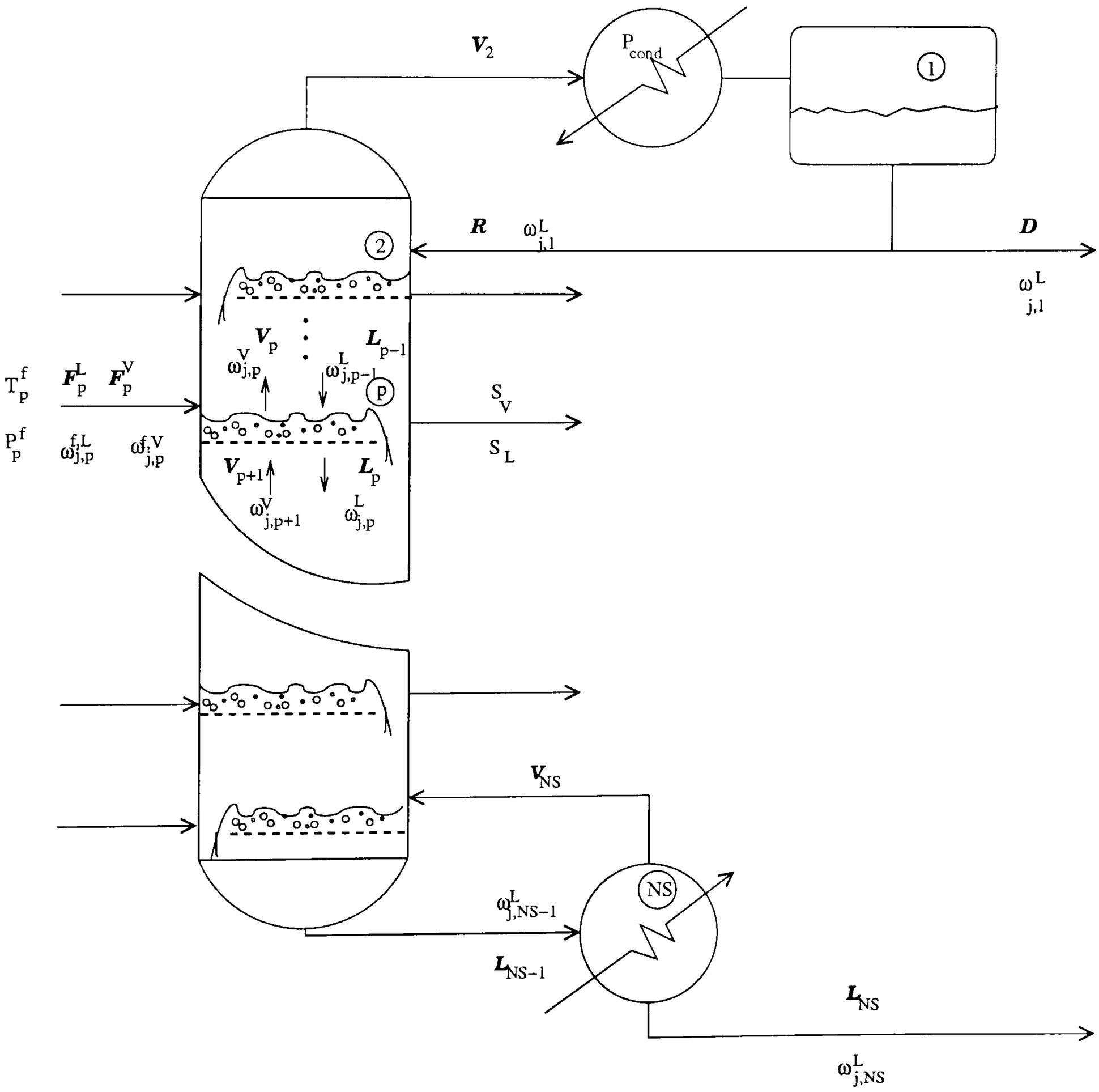

Figure 2.3: Modelled distillation column

The material balance for the hold-up, B, of element j at the stage p is

$$\frac{dB_{j,p}}{dt} = \mathcal{F}_p^V \omega_{j,p}^{F,V} + \mathcal{F}_p^L \omega_{j,p}^{F,L} + \mathcal{V}_{p+1}\omega_{jp+1}^{V} + \mathcal{L}_{p-1}\omega_{jp-1}^{L} - [(\mathcal{V}_p + \mathcal{S}_p^V)\omega_{j,p}^{V} + (\mathcal{L}_p + \mathcal{S}_p^L)\omega_{j,p}^{L}] \tag{2.29}$$

where $j = 1, \ldots, M$ and $p = 1, \ldots, NS$

The definition for the element mole fractions is:

$$\omega_{j,p}^{L} = \frac{B_{j,p}}{\sum_{j=1}^{M} B_{j,p}} \tag{2.30}$$

The energy balance for the hold-up of energy, H_p is also written in terms of elements:

$$\frac{dH_p}{dt} = \mathcal{F}_p^V \check{H}_p^{F,V} + \mathcal{F}_p^L \check{H}_p^{F,L} + \mathcal{V}_{p+1}\check{H}_{p+1}^{V} + \mathcal{L}_{p-1}\check{H}_{p-1}^{L} - [(\mathcal{V}_p + \mathcal{S}_p^V)\check{H}_p^{V} + (\mathcal{L}_p + \mathcal{S}_p^L)\check{H}_p^{L}] + Q_p \tag{2.31}$$

where $\check{H}_p^{\beta}$ is the specific enthalpy of phase β with respect to the elements at stage p. Q_p is the heat added or subtracted to stage p.

The model is complemented with a series of algebraic equations. These equations define equilibrium, properties and hydraulics for each stage.

Equilibrium. The equilibrium for each stage means that the free energy is to be minimal as described by equations (2.22), (2.23). In the same way as for the flash, once the component fractions in the liquid phase are known, P-bubble point calculations are done to find the stage pressure and vapour composition from equation (2.24).

Efficiency. As explained above, in order to represent the imperfect mass transfer between phases, a fixed efficiency would be used. Hence, there are equations to relate the vapour composition at equilibrium with the actual composition.

Properties. There are a number of properties that need to be calculated for each stage: the specific enthalpy of the vapour phase, the average vapour and liquid densities and the average molecular weight. These calculations can be seen in Appendix C.

Hydraulics. The liquid flow rates are calculated considering the hold-up and the pressure drop between stages. Details can be found in Appendix D.

Control There were two kinds of controllers:

Table 2.4: Equations for the dynamic model of a reactive distillation column

Equations		Total
Dynamic equations	2.29, 2.31	$NP(M+1)$
Definition of ω_j^β	2.30	$3NP(M-1)$
Summation (element mole fraction)		$3NP$
Conservation of elements		$NP(M)$
Element chemical potential	2.13	$NP(M)$
Equilibrium		NP
Vapor liquid equilibrium		$NP(NC)$
Criterion $H_{calculated} - H_integrated = 0$		NP
Raoult law (T)		NP
liquid mole fraction		$NP(NC-1)$
Feed mole fraction		$NP(NC-1)$
Summation (component mole fraction)		$2NP$
Component chemical potential		$NP(2NC)$
Specific enthalpy (components)	Sec. C.5	$3NP$
Specific enthalpy (elements)	Sec. C.5	$3NP$
Hydraulic equations (liquid flows)	App. D	$NP-2$
Hydraulic equations (vapour flows)	App. D	$NP-1$
Total number of equations		$NP(6M+5NC+12)-3$

1. Proportional level controllers for the reflux drum and the reboiler.

2. Proportional integral controllers for two temperatures. These controllers are explain with more detail in Chapter 4.

2.3.2 Dynamic degrees of freedom for the dynamic reactive distillation model

The model of a column of NP stages consists of $NP(6M+5NC+12)-3$ equations (see Table 2.4). On the other hand, there are $NP(6M+6NC+17)+1$ variables (See Table 2.5). Therefore, there are $NP(NC+5)+4$ unknowns. There are $NP(NC+2)$ variables that are fixed. These are the feed flow rate, the temperature and pressure of the feed and the component mole fractions. Hence, there are $3NP+4$ degrees of freedom, that correspond to the liquid and vapour side streams and the heat added or subtracted to the stage. The four remaining degrees of freedom correspond to the external flow rates and the reflux and the pressure at the condenser which is fixed.

Table 2.5: Variables of the dynamic model of a reactive distillation column

Variable	Total
P_{fp}	NP
T_{fp}	NP
S_p^L	NP
S_p^V	NP
$\mathcal{V}_p$	NP
$\mathcal{L}_p$	$NP+1$
$\mathcal{F}_p$	NP
Q_p	NP
T_p	NP
P_p	NP
$\check{H}_p$	$3NP$
$\hat{H}$	$3NP$
z_{ip}	$NP(NC)$
y_{ip}	$NP(NC)$
x_{ip}	$NP(NC)$
μ_{ip}^{β}	$2NP(NC)$
B_{jp}	$NP(M)$
H_p	NP
n_{ip}	$NP(NC)$
ω_{jp}^{F}	$NP(M)$
ω_{jp}^{*V}	$NP(M)$
ω_{jp}^{L}	$NP(M)$
λ_{jp}	$2NP(M)$
Total number of unknowns	$NP(6M+6NC+17)+1$

2.3.3 Steady state model

The model includes the mass and energy balances and the equations to ensure that the chemical potential λ_j for element j is the same for all phases. An additional assumption for this model is that the pressure is known on all the stages. The pressure in the column can be the same for the whole column or it can be a pressure profile.

The material balance for the element j at the stage p is:

$$g = b_{j,p}^{F,V} + b_{j,p}^{F,L} + b_{j,p+1}^{V} + b_{j,p-1}^{L} - [b_{j,p}^{V} + b_{j,p}^{S,V} + b_{j,p}^{L} + b_{j,p}^{S,L}] = 0 \tag{2.32}$$

where $j = 1, \ldots, M$ and $p = 2, \ldots, NS$

The energy balance is also written in terms of elements:

$$\begin{aligned} g = {} & \mathcal{F}_p^V \check{H}_p^{F,V} + \mathcal{F}_p^L \check{H}_p^{F,L} + \mathcal{V}_{p+1} \check{H}_{p+1}^{V} + \mathcal{L}_{p-1} \check{H}_{p-1}^{L} \\ & -[(\mathcal{V}_p + \mathcal{S}_p^V)\check{H}_p^V + (\mathcal{L}_p + \mathcal{S}_p^L)\check{H}_p^L] + Q_p = 0 \end{aligned} \tag{2.33}$$

where $p = 2, \ldots, NS - 1$ and the flows $\mathcal{F}, \mathcal{V}$ and $\mathcal{L}$ are defined as:

$$\mathcal{F}_p^\beta = \sum_{j=1}^{M} b_{j,p}^{\beta}$$

$$\mathcal{V}_p = \sum_{j=1}^{M} b_{j,p}^{V}$$

$$\mathcal{L} = \sum_{j=1}^{M} b_{j,p}^{L}$$

The reboiler energy balance can be substituted by a total mass balance for the column:

$$g = \sum_{k=2}^{NS} b_k^F - \mathcal{D} - \sum_{j=1}^{M} b_{j,NS}^{L} = 0 \tag{2.34}$$

The energy balance for the reboiler can be used, once the solution is found, to determine the reboiler heat duty.

The equilibrium is expressed by the element chemical potential balances:

$$g = \lambda_{j,p}^{L} - \lambda_{j,p}^{V} = 0 \tag{2.35}$$

Note that in the last balances it is assumed that the side streams $\mathcal{S}_p$ known. This is also the case for the heat exchanged Q_p except in the reboiler. Furthermore, the solution requires a T-bubble point calculation for each stage to find the composition in the vapour phase and the temperature.

In addition to the balances, there are some other necessary equations to describe the model. For instance, to calculate activity coefficients, fugacity coefficients, ideal gas enthalpy, excess properties, etc. All these calculations can be seen in Appendix C.

Degrees of freedom for the steady state model

There are $2(NS-1)M+(NS-1)$ elements for the function g. The model has $NS-1$ element balances (equations 2.32), $NS-2$ energy balances (equations 2.33), one global mass balance (equation 2.34) and $(NS-1)M$ element chemical potential balances (equations 2.35).

On the other hand, there are $2(NS-1)M+(NS-1)+2$ unknowns. The unknowns are $(NS-1)M$ element vapour flow rates ,b_j^V; $(NS-1)M$ element liquid flow rates b_j^L; (NS-1) temperatures, T_p and two of the following set: distillate flow rate, $\mathcal{D}$; reflux ratio, R; reflux flow rate, $\mathcal{L}_1$; bottom flow rate, $\mathcal{B}$; reboiler heat duty, Q_{NS} and vapour flow rate in the reboiler $\mathcal{V}_p$.

Therefore there are two degrees of freedom.

2.4 Solution algorithms

2.4.1 Integration method

To integrate the differential equations for the flash and the distillation column, an explicit 5th order Runge-Kutta-Fehlberg method with adaptive step was used (Press, Teukolsky, Vetterling and Flannery, 1996). The algorithm is similar for both problems. Hence, the methodology will be explained for the reactive distillation problem only.

Algorithm

Since the method is explicit, it uses the information of the initial state to update the value of the dependent variables at the next time step. The new right hand side function for these values is evaluated. This information is then used to find the value of the variables at the next time step. This procedure continues until the final time is reached.

A schematic representation of the algorithm can be seen in Figures 2.4 and 2.5. The steps of the method are:

1. The first step of the solution method is to acquire the information that defines the problem: the characteristics of the column and the mixture problem, the parameters and finally the operating and initial conditions:

   - The configuration of the column: number of stages, nature of each (reactive or non-reactive) and location of feed streams.
   - The chemistry and properties of the mixture of interest: number of components, number of elements and formula matrices for the reactive and non reactive mixtures, critical properties, Antoine constants, etc.
   - Operating and initial conditions: set points, feed composition and flow rate, composition and temperature of the initial hold up.

2. The next step of the method is the calculation of the matrices that the element method needs. These matrices, like the formula matrix A, are different for the reactive and non reactive cases. Details are found in Section 2.1.3.

3. Next, the equilibrium composition and enthalpy of the feed are found. It is assumed that the feed cannot react until it is inside the column. The feed composition is also re-expressed in terms of elements. It is necessary to determine whether the feed is a mixture or a stable liquid or vapour. The solution is based on the idea that the Gibbs free energy is at its minimum at equilibrium:

   (a) Assume that the feed mixture is a liquid. Find the corresponding Gibbs free energy.

   (b) Assume now that the feed mixture is a vapour. Again find the corresponding Gibbs free energy.

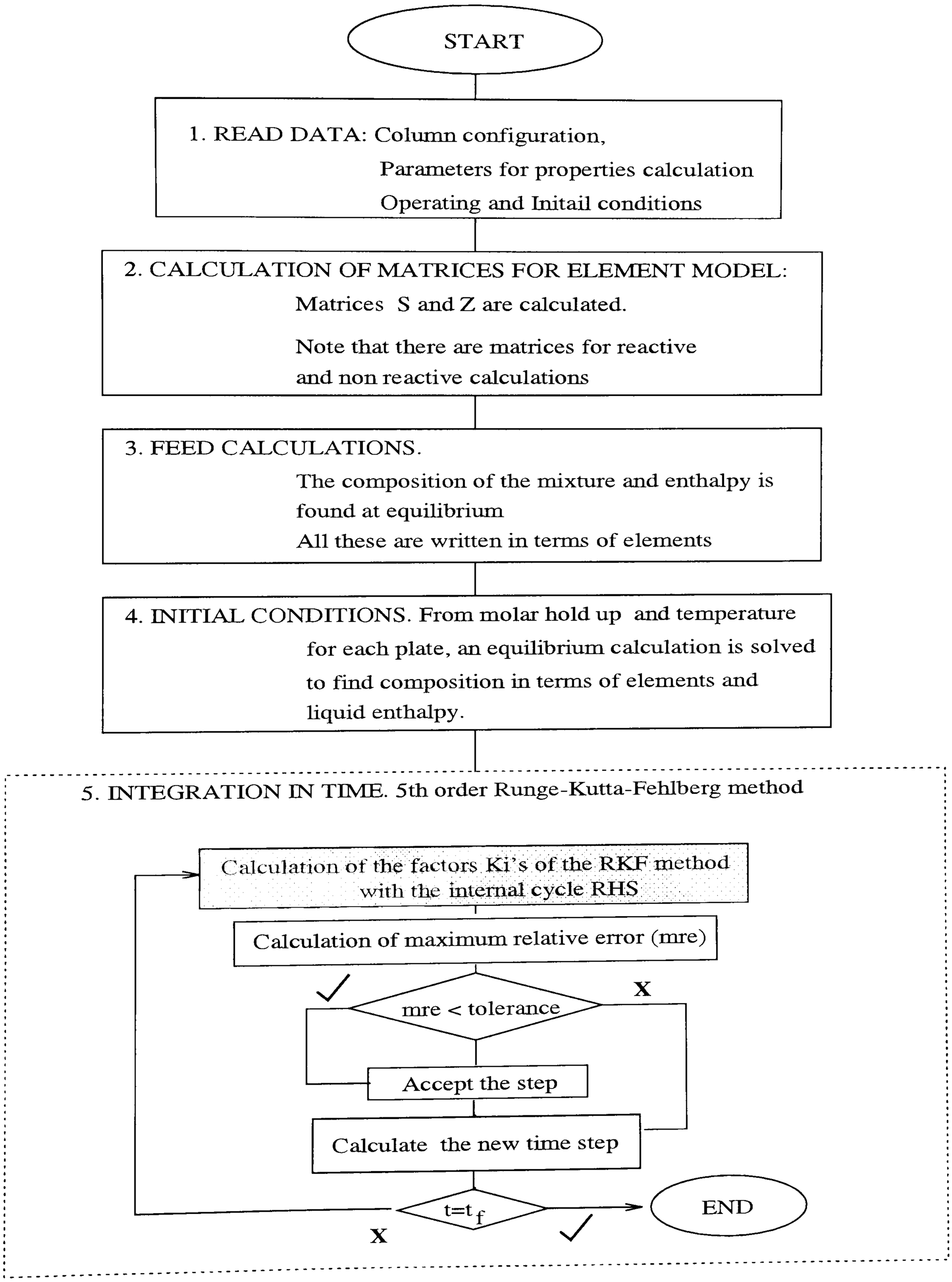

Figure 2.4: External cycle of the dynamic simulation algorithm

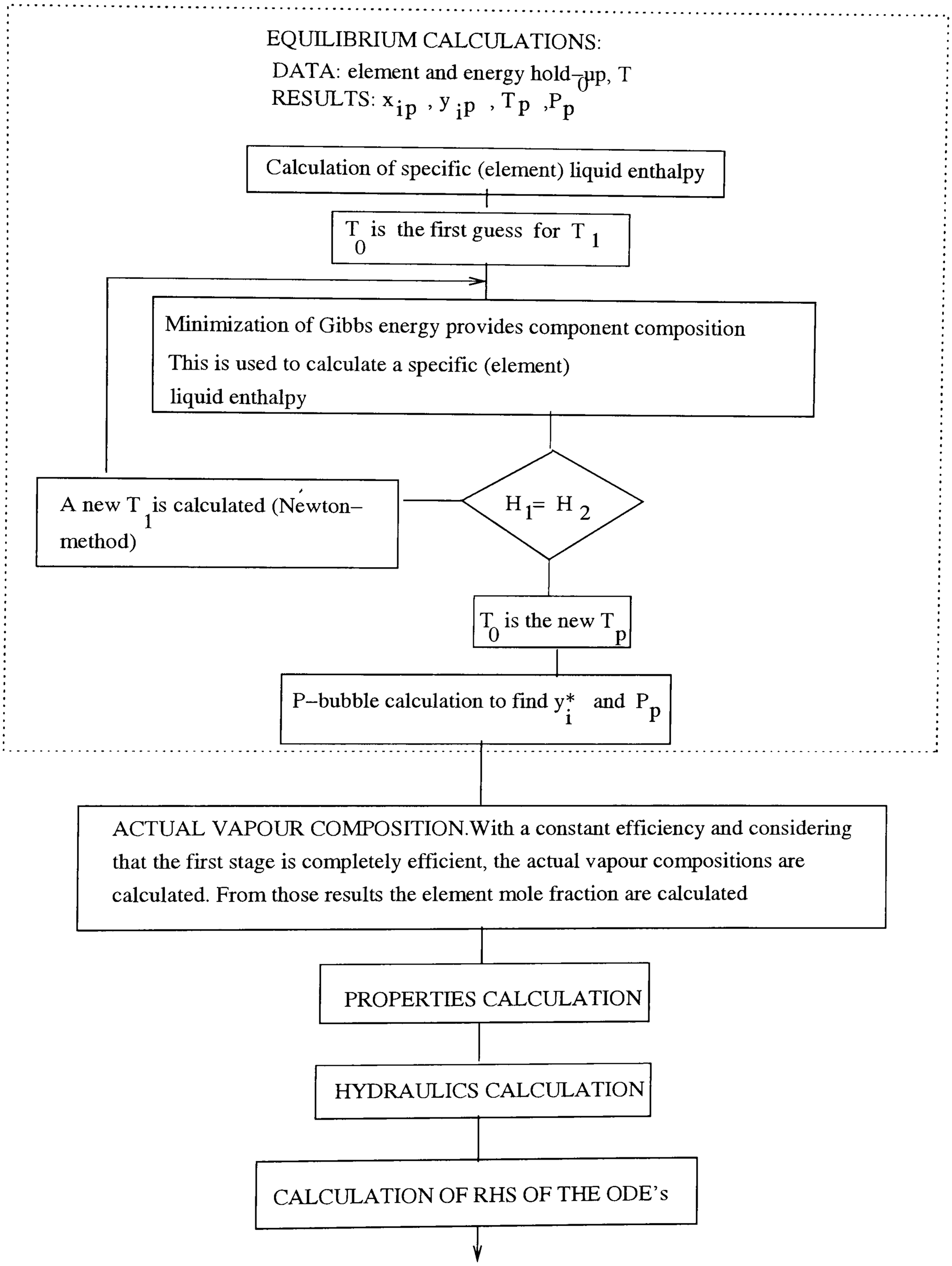

Figure 2.5: Internal cycle of the dynamic simulation algorithm

(c) Compare the calculated Gibbs free energies. Check if the phase with the smallest Gibbs free energy is stable (Section 2.1.3).

(d) If the phase is not stable, then a flash calculation is done to find the composition of the liquid and the vapour phases and the amount of each (Section 2.1.3)

4. Find the initial condition of the column. The set of initial data includes the different component hold-ups and initial temperatures for each stage. Therefore, it is necessary to determine the composition of the mixture in term of elements and the initial hold up of energy. The calculation of the initial state is done considering that the mixture is Initially at equilibrium. Moreover, the reaction is considered to start at this time. Hence, the equilibrium for each stage is calculated considering whether the stage is reactive or not.

   The hold-up of element j at stage p is calculated according to equation (2.23). Note that when one stage is reactive, a matrix A that contains the stoichiometry is used for the calculation of the elements hold-up. In contrast, for a non-reactive stage, the unit matrix is used.

   Once the amount of each element is known, calculations of equilibrium are done to find the component compositions when equilibrium is reached. This calculation will also yield vapour enthalpy. The equilibrium calculation consists of the minimisation of the Gibbs free energy for the liquid phase (Section 2.1.3).

   When the component compositions at equilibrium are known, the specific enthalpy (based on elements) can be calculated (Appendix C).

5. Integration in time. As mentioned before, the integration is made by using an explicit 5th order Runge-Kutta-Fehlberg method. The method requires the calculation of the right hand sides of the ODEs:

   (a) Equilibrium calculation. From the integration the hold-up of elements and energy for each stage are determined. To find the component composition, it is necessary to minimise the Gibbs free energy, equation (2.22), maintaining constant the hold-up of each element, equation (2.23). The solution criterion is different from the steady state problem. In the steady state problem, the convergence criterion is the equality of chemical potentials for the different phases. However, in the dynamic simulation, the criterion of convergence is that the calculated specific enthalpy

(with respect to elements) must be equal to that calculated from the hold-up data:

$$\check{H}_p^L = H_p^L / \sum_{j=1}^{M} B_{j,p} \tag{2.36}$$

The last equation shows the calculation of the "actual" specific enthalpy. On the other hand, the next equation shows the "iterated" specific enthalpy:

$$\check{H}_p^L = H_{p,Eq}^L / \sum_{j=1}^{M} A_{j,i} x_i \tag{2.37}$$

Figure 2.5 shows the equilibrium solution algorithm. Note that once the temperature and liquid phase mole fractions, $x_{L,p}$, are known a pressure-bubble point calculation is performed to find both the pressure and the vapour phase mole fractions. The element mole fractions at equilibrium, $\omega_{j,p}^{*V}$, for the vapour phase are calculated now. These calculations are made for all the equilibrium stages.

(b) Actual vapour compositions. When the element mole fractions at equilibrium for the vapour phase are known, the actual values are found using an efficiency factor, η. This factor is considered as constant and known for the process:

$$\eta = \frac{y_{i,p} - y_{i,p-1}}{y_{i,p}^{*} - y_{i,p-1}} \tag{2.38}$$

The actual composition is calculated from equation (2.38) assuming that the efficiency in the first equilibrium stage is equal to one. This is assumed to allow a direct calculation of the remaining actual vapour phase compositions.

The actual element mole fractions are calculated by using equation (2.25) and the actual vapour phase mole fractions, $y_{i,p}^{V}$

(c) Properties calculation. The properties calculated at each stage are: the density of the liquid and vapour phase, ρ_p^L, ρ_p^V; the molecular weight for both phases and the vapour specific enthalpy (with respect to elements). These calculations are detailed in Appendix C.

(d) Hydraulic calculations. These calculations are based on correlations for sieve plates assuming that the downcomer dynamics are insignificant. This leads to explicit calculations for the molar flow rates that are later converted into the element basis. A detailed description of these calculations is found in Appendix D.

(e) Total condenser calculations. The temperature and liquid specific enthalpy are calculated assuming that the pressure is constant and known; the liquid composition is known and equal to the composition of the vapour entering the condenser. An additional assumption makes the liquid leaving the total condenser a saturated liquid. Therefore, a temperature bubble point calculation can be done to find the temperature and the enthalpy can be then calculated.

(f) Function calculation. The calculation of the RHS of the ODEs, equations (2.29) and (2.31) needs an additional consideration. Since the balances for the pth stage involve flows from adjacent stages that can be of a different nature (reactive or non-reactive) to stage p, a conversion to the element basis of the pth stage is needed. When the necessary conversions have been made, the calculation of the RHS of the ODEs can be done.

6. The next steps of the algorithm are related to the Runge-Kutta-Fehlberg method. The method requires six different evaluations of the RHS functions. Once this is completed, the error for the integration is calculated. If the maximum relative error is lower than the tolerance the time step is accepted and the value of the dependent variables calculated. When the decision is made, a new time step is calculated. This new step is either equal or bigger than the previous step if the step was accepted or smaller if the step was rejected.

7. With the new time step the iteration is repeated. The procedure continues until the final time is reached.

2.4.2 Solution Algorithm for the steady state problem

The solution algorithm is similar to the solution for the reactive flash at steady state and can be seen in Figure 2.6. There is an external loop to solve equations (2.32), (2.33), (2.35) with a Broyden method (Press *et al.* 1996) and an internal cycle that uses a Newton-Raphson method to find the component mole fractions in the equilibrium stages.

As for the dynamic problem, it is necessary to re-express the element flow rates when the stage has a different nature (reactive or non-reactive).

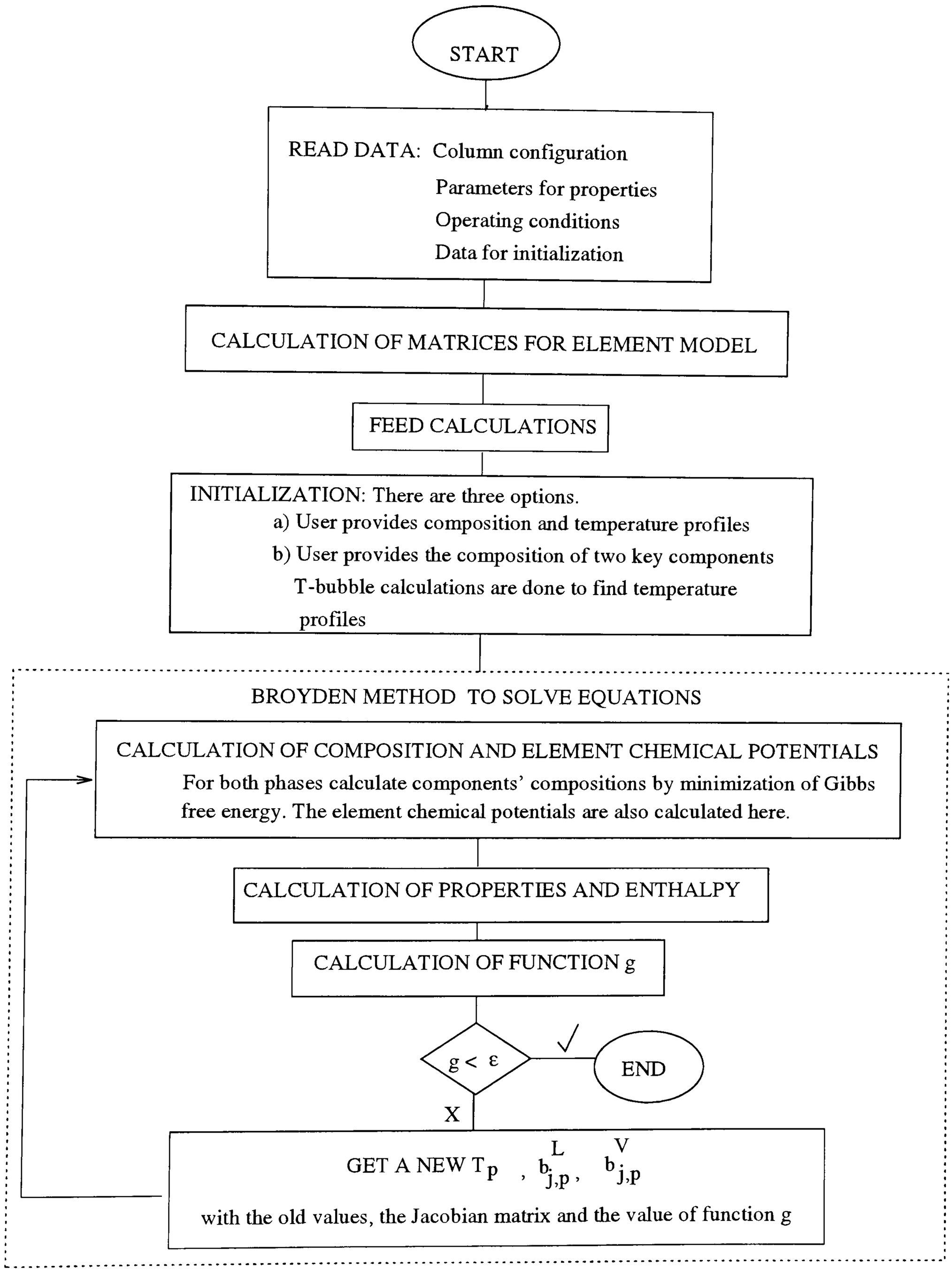

Figure 2.6: Diagram of the steady state solution method for a reactive distillation column

2.5 Important thermodynamic parameters

As mentioned before, to calculate the equilibrium of a system with reactions by the use of a chemical model approach, it is necessary to couple the chemical model with an appropriate thermodynamic model. Such a thermodynamic model and its parameters may have a major impact in the simulation results.

The most influential parameter was the standard Gibbs free energy of formation for ideal gas, $\Delta G^{o,ig}_{f298}$. In this section the influence of such a parameter is discussed. For a case study, three data options are considered and one is selected based on the analysis results.

2.5.1 Importance of Gibbs free energy of formation

Section 2.1.4 shows that in order to solve the system equilibrium, the component chemical potentials, μ, and their derivatives need to be calculated. The calculation of chemical potentials and their derivatives requires the value of the standard Gibbs free energy of formation (ideal gas) for each component of the mixture (Appendix C).

The case study was the MTBE reaction. Three sets of enthalpy and Gibbs free energy of formation have been reported. The first set of data (Table 2.6) was reported by Reid, Prausnitz and Poling (1987). The second set (Table 2.7) is taken from the DIPPR data base. The last set (Table 2.8) was presented by Rehfinger and Hoffmann (1990), but comes originally from Colombo *et al.* (1983), Reid *et al.* (1977) and Fenwick *et al.* (1975). In the present work, this set will be labelled as Rehfinger data. The selection of these data proved to be of particular importance. In fact, the results for the steady state solutions can be completely different depending on the set of data used.

Table 2.6: $\Delta G^{o,ig}_{f298}$, $\Delta H^{o,ig}_{f298}$, Reid *et al.*, 1987

	iso-butene	MeOH	n-butane	MTBE
$\Delta H^{o,ig}_{f298}$	-1.691×10^{4}	-2.013×10^{5}	-1.262×10^{5}	-2.931×10^{5}
$\Delta G^{o,ig}_{f298}$	5.811×10^{4}	-1.626×10^{5}	-1.610×10^{4}	-1.255×10^{5}

For example, consider an eight stages MTBE column whose characteristics are shown in Table 2.9. In this column all the stages, except the total condenser, are

Table 2.7: $\Delta H^{\circ,ig}_{f298}$, $\Delta G^{\circ,ig}_{f298}$, DIPPR data base

	iso-butene	MeOH	n-butane	MTBE
$\Delta H^{\circ,ig}_{f298}$	-1.6903×10^4	-2.0108×10^5	-1.262×10^5	-2.9288×10^5
$\Delta G^{\circ,ig}_{f298}$	5.8073×10^4	-1.6238×10^5	-1.610×10^4	-1.1732×10^5

Table 2.8: $\Delta H^{\circ,ig}_{f298}$, $\Delta G^{\circ,ig}_{f298}$, Rehfinger and Hoffmann (1980)

	iso-butene	MeOH	n-butane	MTBE
$\Delta H^{\circ,ig}_{f298}$	-1.691×10^4	-2.013×10^5	-1.262×10^5	-2.8366×10^5
$\Delta G^{\circ,ig}_{f298}$	5.811×10^4	-1.626×10^5	-1.610×10^4	-1.1731×10^5

reactive and at equilibrium. Figures 2.7 and 2.8 show the temperature profiles and the MTBE liquid mole fraction profiles when Reid and Rehfinger sets of $\Delta H^{\circ,ig}_{f298}$ and $\Delta G^{\circ,ig}_{f298}$ are used. The solution for the problem with DIPPR data is not presented because it is similar to the solution with Rehfinger data.

Table 2.9: Settings for the MTBE eight stages column

P	11 atm
D	3 mole/s
R	5
F (stage 4)	10 mole/s
$z_{iso-butene}$	0.5
z_{MeOH}	0.5
P_f	11 atm
T_f	350 K

Figure 2.8 shows that the concentration of MTBE through the column is much higher when the Reid data are used. This means that the reaction equilibrium constant is larger when the Reid data are used.

The almost isothermal profiles observed in the lower part of the column when the Reid data are used can be explained with the element equilibrium curve, shown in Figure 2.9. The high MTBE concentration from stages 4 to 8 for the Reid problem, correspond to $\omega_A \simeq 0.5$; this is at the top of the large loop of the equilibrium curve.

On the other hand, the equilibrium curve for the system when the Rehfinger data are used (Figure 2.10) is very different. In this case no reactive azeotrope is observed

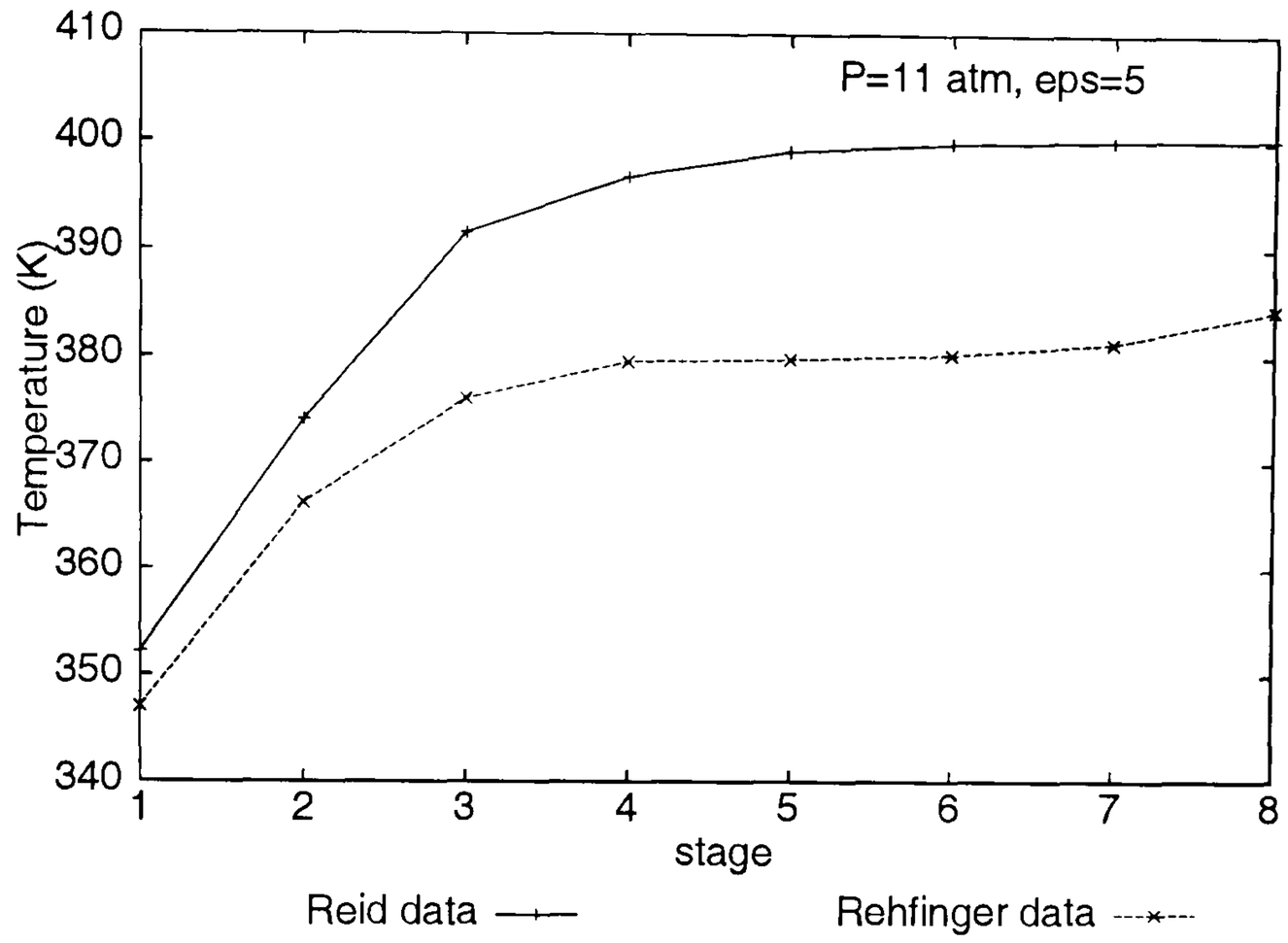

Figure 2.7: Comparison of temperature profiles for two different sets of $\Delta G^{\circ,ig}_{f298}$

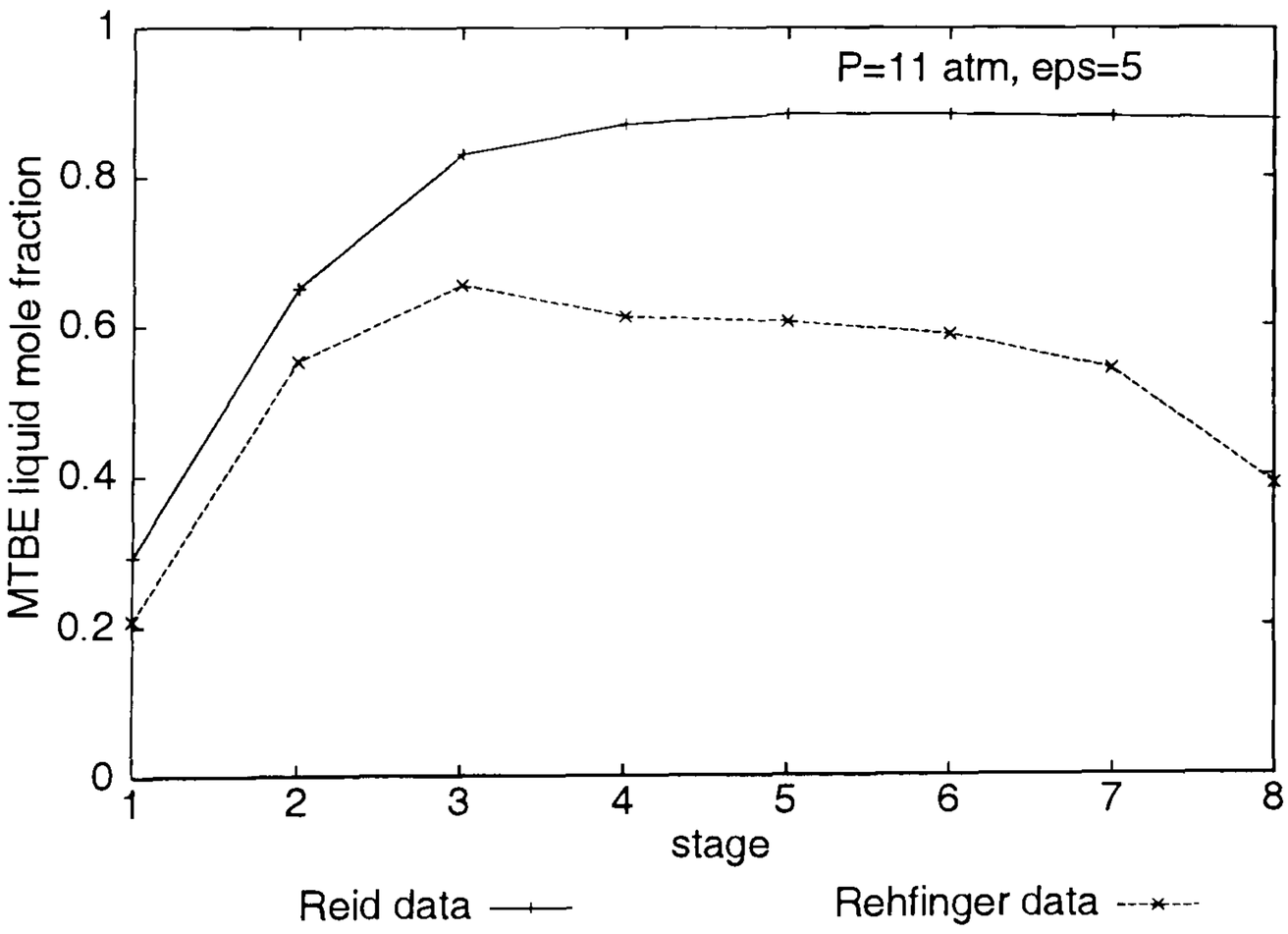

Figure 2.8: Comparison of MTBE liquid phase profiles for two different sets of $\Delta G^{\circ,ig}_{f298}$

and the distribution of element A correspond to a broader area for stages 4 to 8 (mole fractions between 0.33 and 0.47).

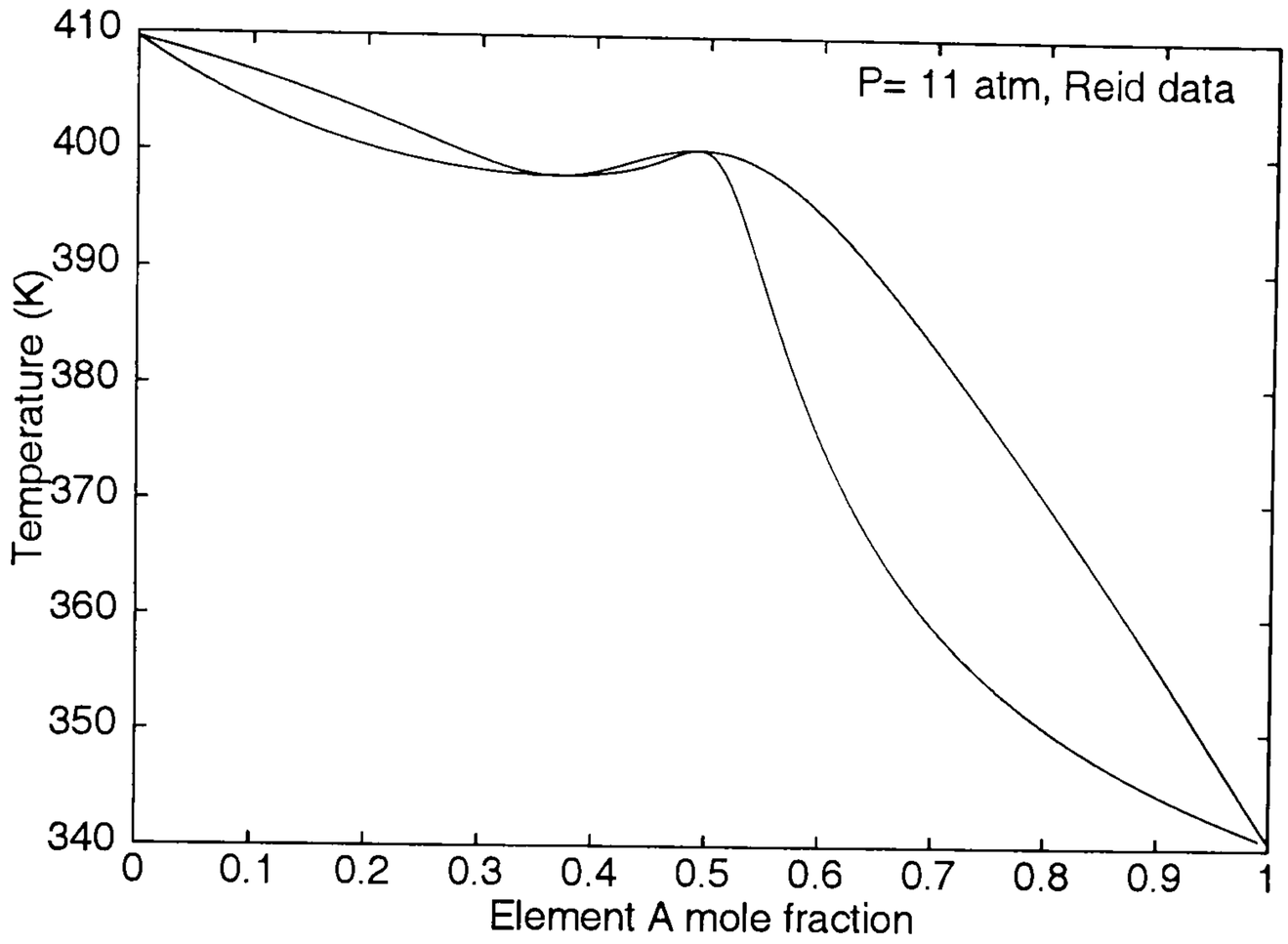

Figure 2.9: Reactive element equilibrium curves for the system, iso-butene, MeOH and MTBE. Reid *et al.* (1987) data ($\Delta G^{\circ,ig}_{f298}$, $\Delta H^{\circ,ig}_{f298}$). Source: $CPE^{(CR)}$

This example shows the importance of the $\Delta G^{\circ,ig}_{f298}$ selection. To decide with which set of data the results could be more reliable, the three sets were tested for three calculations. Firstly, the calculation of equilibrium curves was made. Secondly, the reproduction of known equilibrium constants were made. Finally, the calculation of reactive azeotropes was tested.

Reproduction of equilibrium curves

Sundmacher and Hoffmann (1996) presented residue curve maps for the heterogeneous MTBE process. They presented a curve that corresponds to a pure chemical equilibrium curve (Damkhöler number equal to one), with which the current model is compared.

The mentioned curve was reproduced with the $CPE^{(CR)}$ program, developed by Pérez-Cisneros and Gani (1997), with the three sets of data presented in Tables 2.6. 2.7 and 2.8. Results are presented in Figure 2.11. None of the three curves fits perfectly the one reproduced in Sundmacher and Hoffmann paper. However, the curve corresponding to the DIPPR data gives the best result.

The results corresponding to the Reid data are far from the equilibrium curve reported by Sundmacher and Hoffmann using the Rehfinger data. Furthermore,

when the Reid data were used, two reactive azeotropes appear. This contrasts Sundmacher and Hoffmann results because they reported no azeotrope for the system under the same conditions.

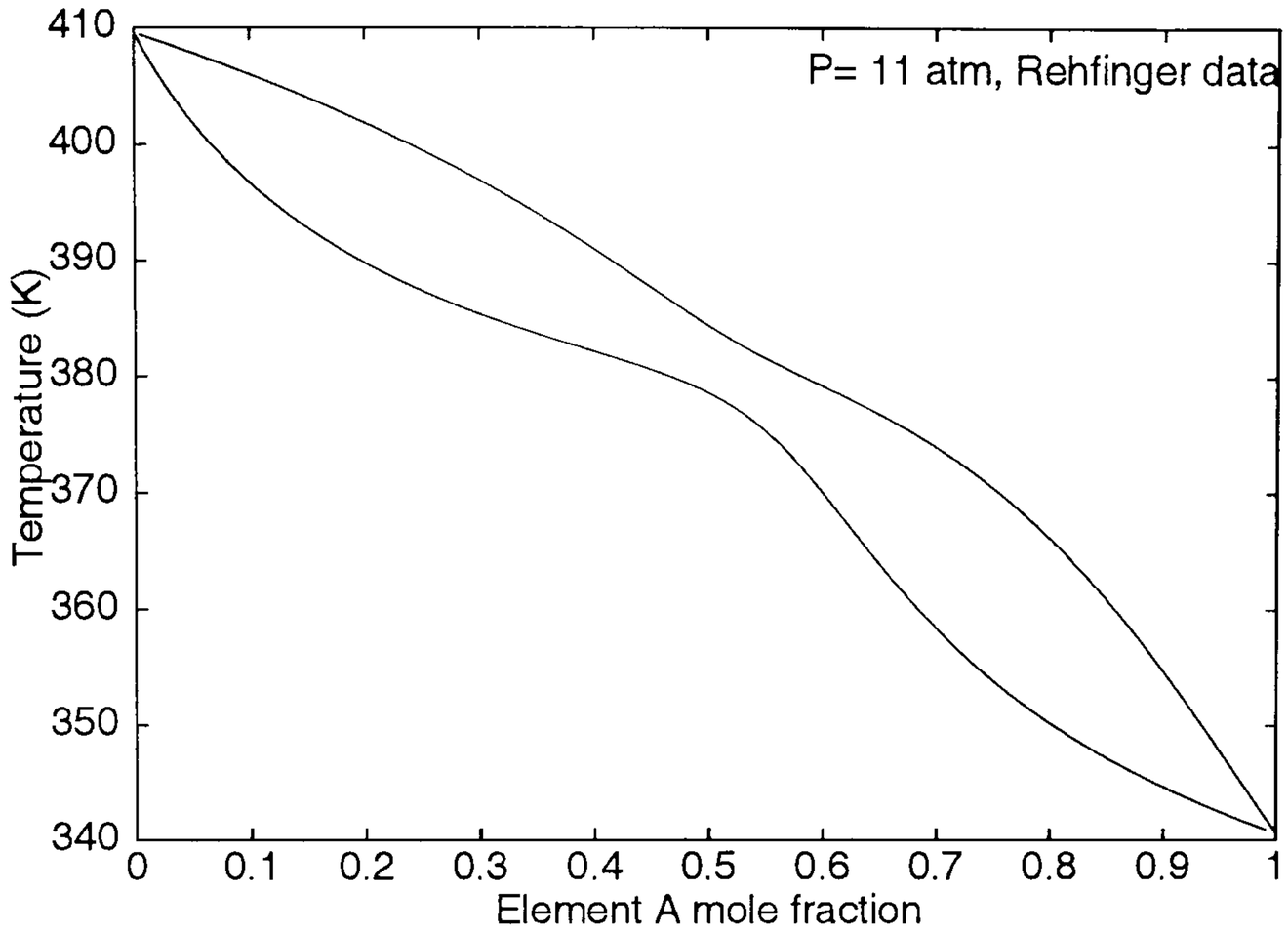

Figure 2.10: Reactive element equilibrium curves for the system, iso-butene, MeOH and MTBE. Rehfinger and Hoffmann (1980) data ($\Delta G^{o,ig}_{f298}$, $\Delta H^{o,ig}_{f298}$). Source: $CPE^{(CR)}$

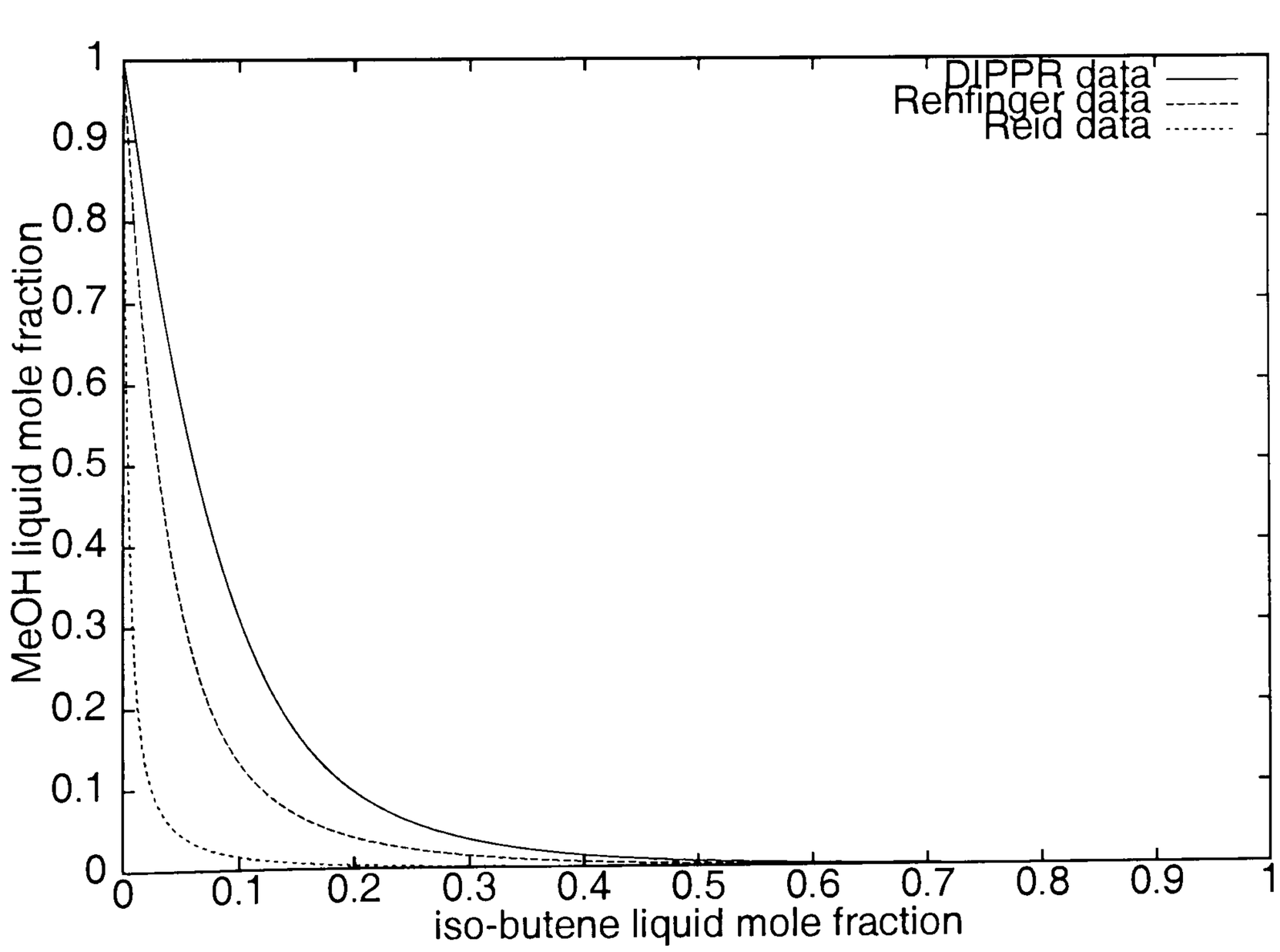

Figure 2.11: Reactive element equilibrium curves for the system, iso-butene, MeOH and MTBE for the three sets of $\Delta G^{o,ig}_{f298}$, $\Delta H^{o,ig}_{f298}$ available. P=8 atm. Source: $CPE^{(CR)}$

Equilibrium constant prediction

There are two studies of the kinetics of the MTBE reaction. Firstly, Colombo *et al.* (1983) studied the homogeneous MTBE production reaction. There was good agreement between experimental and predicted compositions. Later, Rehfinger and Hoffmann (1990) presented a kinetic expression for the heterogeneous reaction. Such an expression was obtained from experimental data and written in terms of activity coefficients.

The predicted values of the constant of equilibrium, K_{eq}, at 350 K were compared with the values predicted with the element model with the different sets of data available. K_{eq} was approximated as:

$$K_{eq} = \frac{\gamma_{MTBE} x_{MTBE}}{\gamma_{iso-butene} x_{iso-butene} \gamma_{MeOH} x_{MeOH}}$$

The results are presented in Table 2.10. The value of K_{eq} predicted with the Reid data is extremely high. This confirms the high conversion results for the 8 stages column presented above. On the other hand, the Rehfinger data yields a result similar to that reported by Colombo *et al.* (1983) and the DIPPR data yields a value close to the Rehfinger and Hoffmann (1990) one. Recalling that the element model works with the homogeneous reaction assumption, it may be sensible to choose the data set that better approximates the Colombo *et al.* result.

Table 2.10: K_{eq} for MTBE reaction at 350 K

Source	K_{eq}
Rehfinger and Hoffmann (1990)	28.5
Colombo *et al.* (1983)	37.3
Reid data	503.6
DIPPR data	19.9
Rehfinger data	42.6

Reactive azeotrope prediction

The relationship between K_{eq} and the occurrence or not of reactive azeotropes was studied by Okasinsky and Doherty (1998) for the MTBE reaction system. They found that there was a K_{eq} limit after which reactive azeotropes appeared. This limit value, at 8 atm, was equal to 31.9. They showed that the equilibrium constant

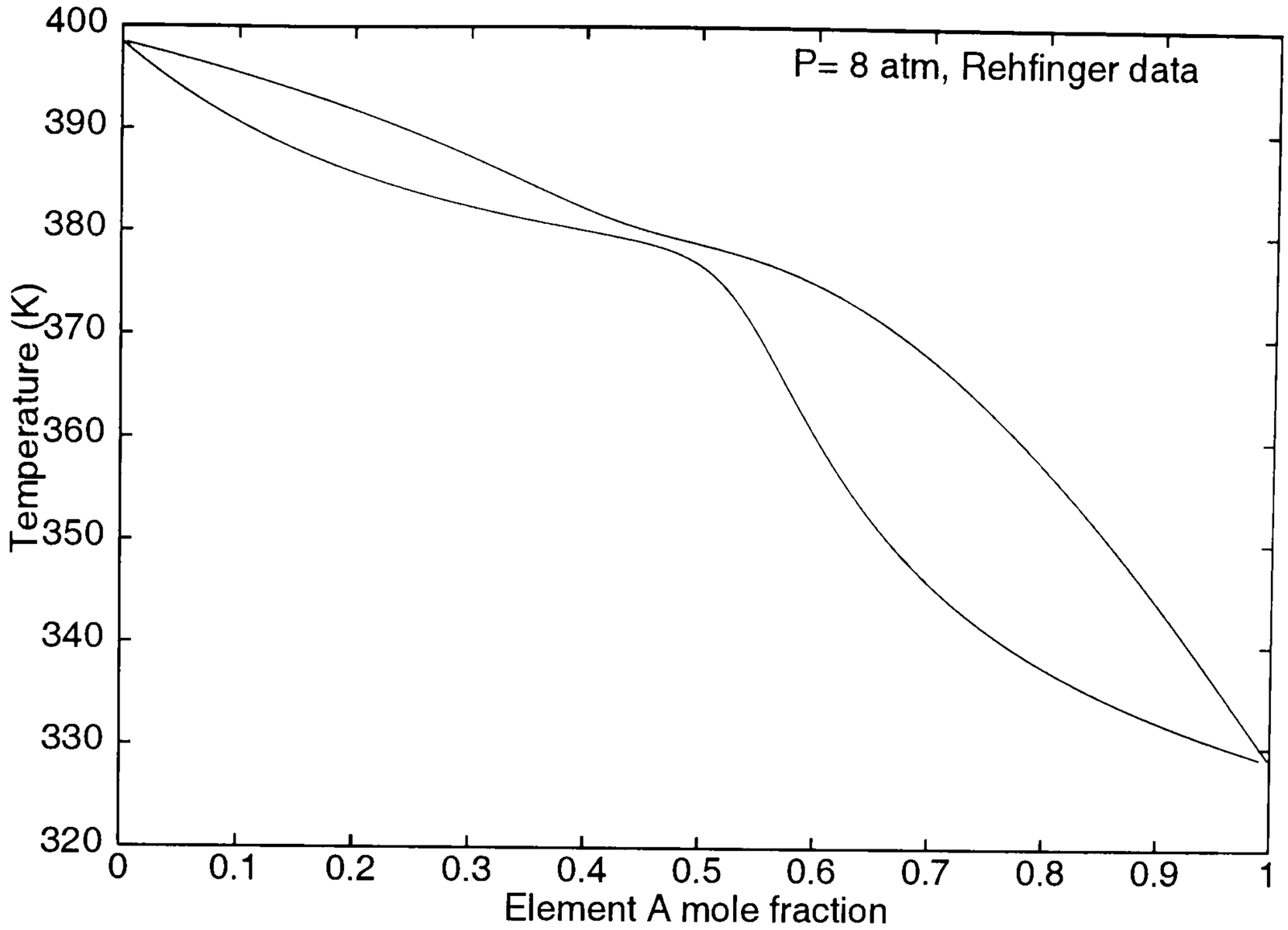

Figure 2.12: Reactive element equilibrium curves for the system, iso-butene, MeOH and MTBE at P=8 atm. Rehfinger data. Source: $CPE^{(CR)}$

value reported by Rehfinger and Hoffmann (1990) was below $K_{eq,limit}$ and yielded no reactive azeotropes. Moreover, they showed that the equilibrium constant reported by Colombo *et al.* (1983) was higher than $K_{eq,limit}$, in this case two azeotropes were found.

Table 2.10 shows the reported and calculated equilibrium constant. Since the Reid data produced $K_{eq} = 500$, this set of data yields two azeotropes at $P = 8atm$. In contrast, neither the Rehfinger data nor the DIPPR data yields azeotropes at $P = 8atm$. However, with the element model and Rehfinger data the results are closer to those reported by Okasinsky and Doherty (Figure 2.12). Note that no reactive azeotrope was reported by Sundmacher and Hoffmann (1996) for the MTBE system at 8 atm. This behaviour was confirmed by Harding and Floudas (2000) for the MTBE system at 1 atm.

Final decision

The Reid data set was eliminated because it produced a value for K_{eq} which was too high. Both Colombo *et al.* (1983) and the present work, consider that the reaction is homogeneous. Rehfinger's data set produced a K_{eq} closer to Colombo's

predictions. Hence this data set was preferred. Furthermore, this set of data could predict more precisely the reactive azeotrope formation.

2.6 Validation of the column model

To validate a model it is always better to compare the simulations with experimental results. Unfortunately, experimental work was not considered during the present project. Therefore, the model is compared with previous simulation reports and experimental results reported in literature.

2.6.1 Comparison with another equilibrium model

Since the model developed in the present work is an equilibrium model, its results should be comparable with the results of some other equilibrium models.

Schrans *et al.* (1996) presented steady state and dynamic simulations of a 17 equilibrium stages (plus total condenser) MTBE production column. Such a column consists of a total condenser, two rectification, eight reactive, and five stripping trays, plus a partial reboiler. The assumptions are similar to the corresponding to the present work (Section 2.3.1). With such a model, Schrans *et al.* (1996) were able to find the previously reported low and high conversion steady states for MTBE column (Jacobs and Krishna (1993), Nijhuis *et al.* (1993) and Hauan *et al.* (1995)). Moreover, Schrans' dynamic simulations showed that there were additional unstable steady states (medium conversion) for the reported configuration (Table 2.11).

The main objective of this section is to compare the present model with that developed by Schrans. It was expected that the element model would reproduce qualitatively and quantitatively the reported results.

Steady state simulations

The numerical experiments have similar characteristics to the base case problem reported by Schrans *et al.* (1996). The characteristics of the column are found in Table 2.11.

The configuration BR (bottoms flow rate and reflux ratio) for the MTBE column is reported to present multiple solutions depending on the position of the MeOH

Table 2.11: Base case data (Schrans, 1996) for a 17 stages MTBE reactive distillation column.

MeOH feed (l)		
Flow rate	215.5	mole/s
Temperature	320.0	K
Pressure	11.0	atm
C_4 feed (v), stage 11		
Flow rate	549.0	mole/s
Temperature	350.0	K
Pressure	11.0	atm
iso-butene	0.3568	mole fraction
n-butane	0.6432	mole fraction
Bottom flow rate	197	mole/s
Reflux ratio, R	7	
Reactive stages	[4,11]	
Column pressure	10	atm

feed. The reproduction of this behaviour was chosen to validate the element model developed in this work.

In Figure 2.13 the conversion of iso-butene versus the MeOH feed position is presented. Although the model presented in Section 2.3.1 solved with the algorithm presented in Section 2.4.2 was able to find the multiple steady states when methanol was fed in stages 10, 11 and 12, it was not possible to find a solution when the methanol was fed in the stripping section.

The problem was of numerical nature. When the mole fractions of the C_4 compounds were almost zero, the calculation of the chemical potentials was inaccurate and it was impossible that the equations relative to the equilibrium converged. Therefore, a change in the model was necessary. The equilibrium function for the non-reactive stages was rearranged.

The element chemical potentials and the component chemical potentials are identical when the stage is non-reactive. The chemical potentials are written as follows:

$$\mu_i^L = \mu_i^\circ + \ln(x_i\gamma_i) + \ln(P_i^s) \tag{2.39}$$

and

$$\mu_i^V = \mu_i^\circ + \ln(y_i\phi_i) + \ln(P) \tag{2.40}$$

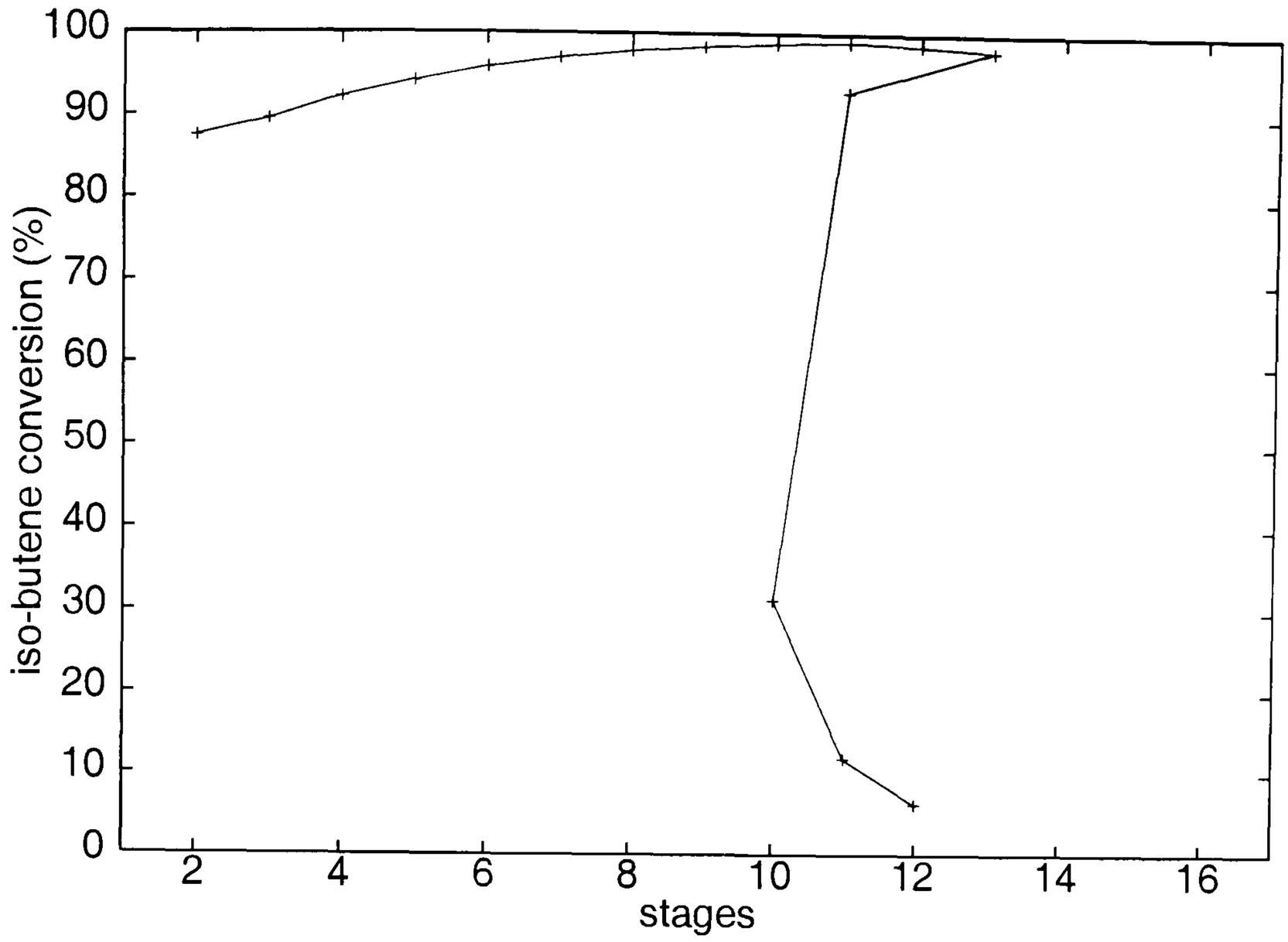

Figure 2.13: Change of iso-butene conversion with respect to MeOH feed location.

and the equilibrium condition is:

$$\mu_i^L - \mu_i^V = 0 \tag{2.41}$$

Substituting equations (2.39) and (2.40) in equation (2.41) and considering that the quantities in the logarithms are greater than zero, the equilibrium condition is written as:

$$x_i \gamma_i P_i^s - y_i \phi_i P = 0 \tag{2.42}$$

To avoid major changes in the solution algorithm, the terms in equation (2.42) were defined as "false" element chemical potentials, λ_j^L and λ_j^V, only for the non-reactive stages.

With this new version, all the reported solutions were found (Figure 2.14). Note that in addition to the high and low conversion states, medium conversion states were found when methanol was fed in stages 10 and 11. These solutions were found by Schrans *et al* (1996), but with dynamic simulations. and were reported as unstable states.

Characteristics of the profiles

In Figure 2.15 it is possible to see that although the medium conversion is high (88 %), the temperature profile is more similar to that corresponding to the low conversion steady state. That medium conversion state must correspond to the unstable steady state reported by Schrans *et al.* (1996). The stability of the multiple steady states will be analysed in the next chapter.

Indeed the main difference between the high conversion and the low conversion states is the split of feed. At the low conversion state, most of the methanol feed does not reach the upper parts of the reactive section, but it drops towards the stripping section. This is better visualised in Figure 2.17. The same figure shows that there is an almost constant flow rate for the MTBE in the reactive section that is actually higher than the rest of the flows in that zone. Consequently, the direction of the reaction does not occur towards products, but towards reactants. This phenomenon must be increased in the lower part of the reactive section, this would explain the MTBE profiles in Figure 2.16.

Figure 2.17 shows that when the column is at the low conversion steady state, the methanol and MTBE internal flow rates in the stripping section are nearly 15 times higher than their external flow rates in the bottom. That means that most of the liquid that arrives to the reboiler is evaporated. Hence, there is a recirculation of methanol and MTBE in the stripping section when the low conversion state is established. This is related to the possible formation of a low boiling azeotrope between them. Since the concentration of C_4 compounds is very low in the stripping section, the azeotrope between MeOH and MTBE is rather favoured. This azeotrope is shown in the vapour-liquid equilibrium diagram for methanol-MTBE, Figure 2.18. The mixture methanol-MTBE that occurs in the stripping section is actually in the second loop of the diagram and is not at the azeotrope point.

There is another difference between the low and high conversion steady states. The reboiler heat duty is higher for the low conversion steady state. These duties are reported in Table 2.12. Since most of the methanol is dropping towards the stripping section and the MTBE flow rate is high, in order to keep the bottom flow rate, the reboiler heat duty is increased.

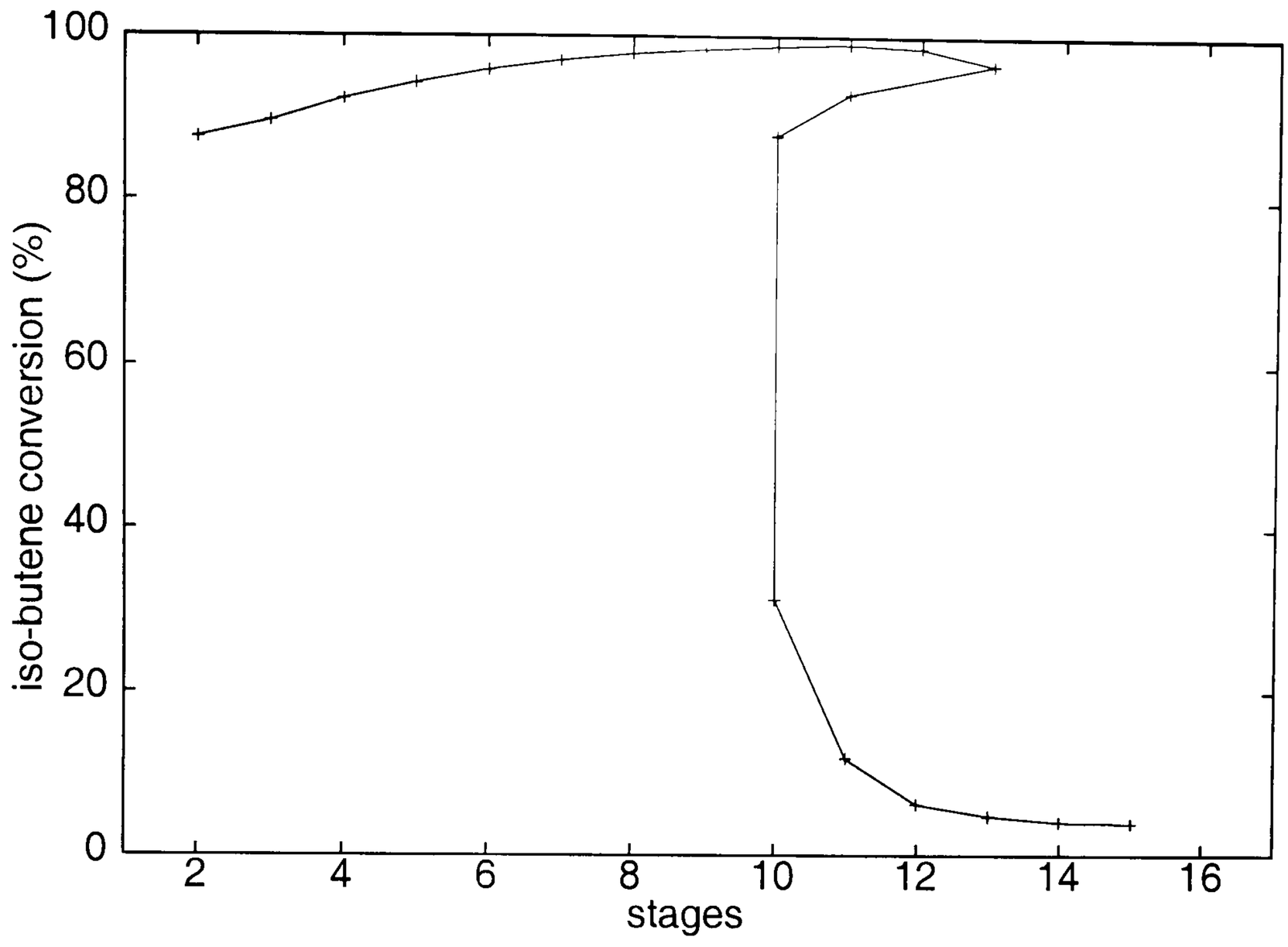

Figure 2.14: Change of iso-butene conversion with respect to MeOH feed location. Improved algorithm solution

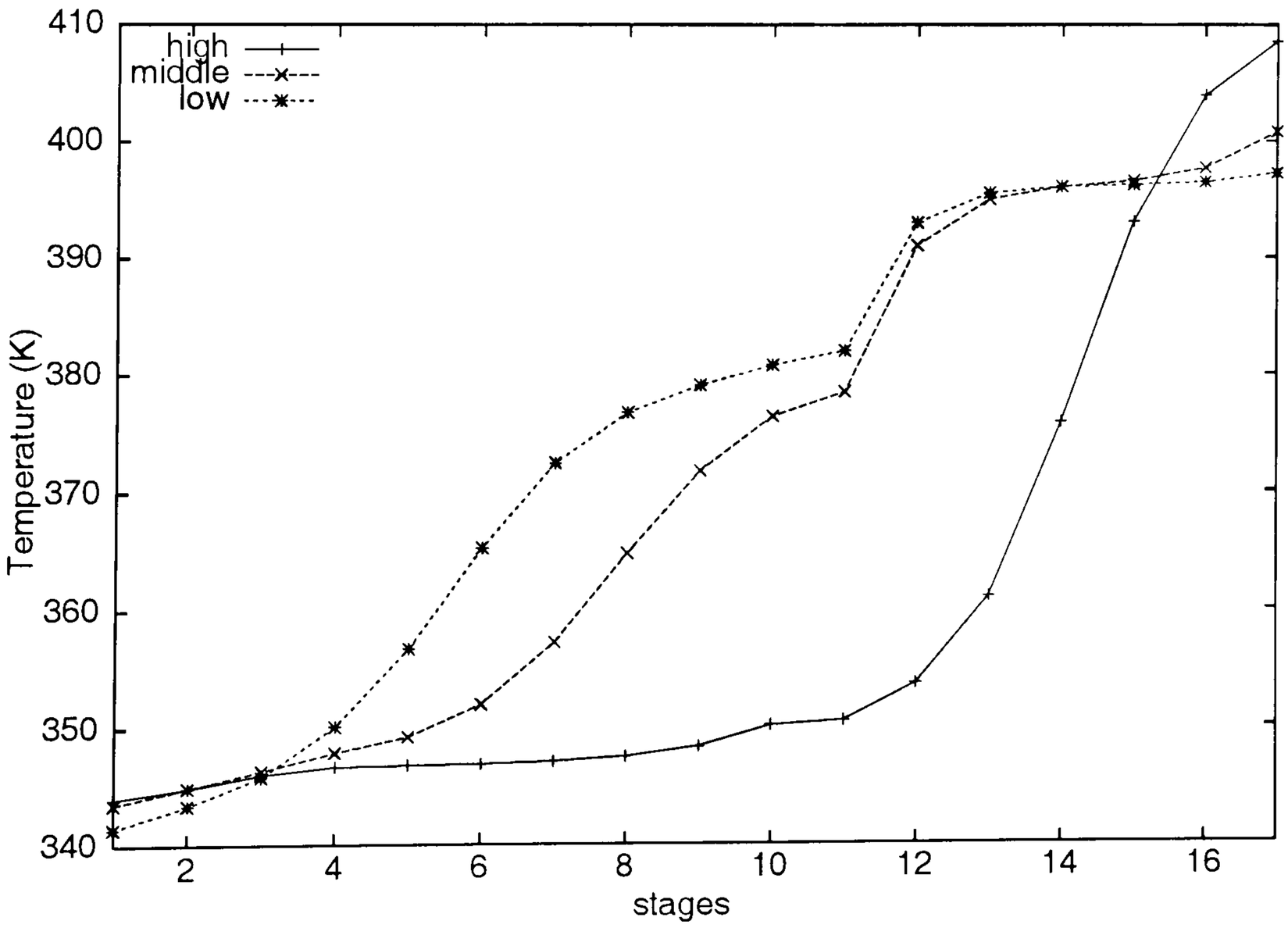

Figure 2.15: Temperature profiles for the 17 stages distillation column, methanol feed at stage 10.

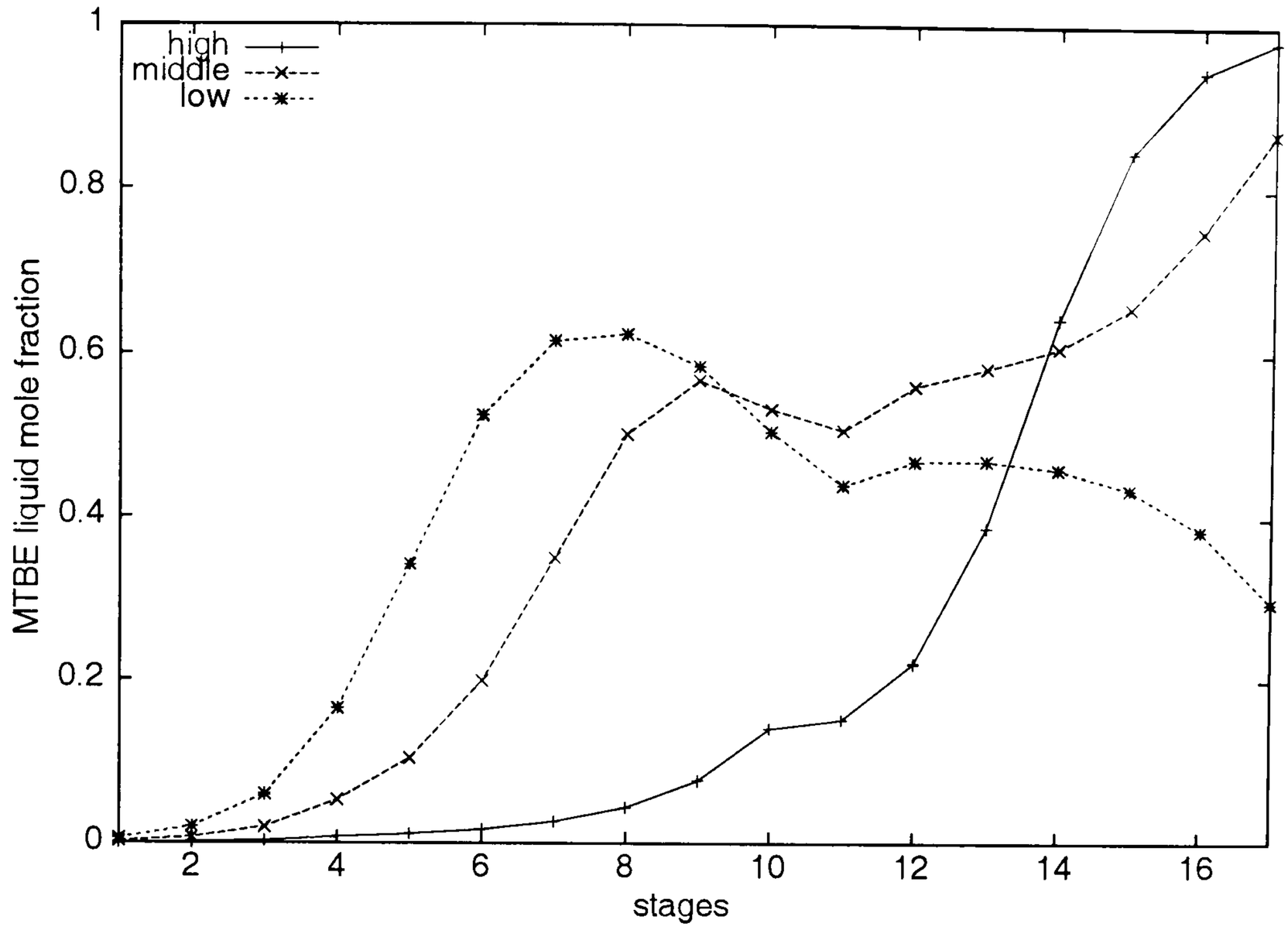

Figure 2.16: MTBE liquid mole fraction for the 17 stages distillation column, methanol feed at stage 10.

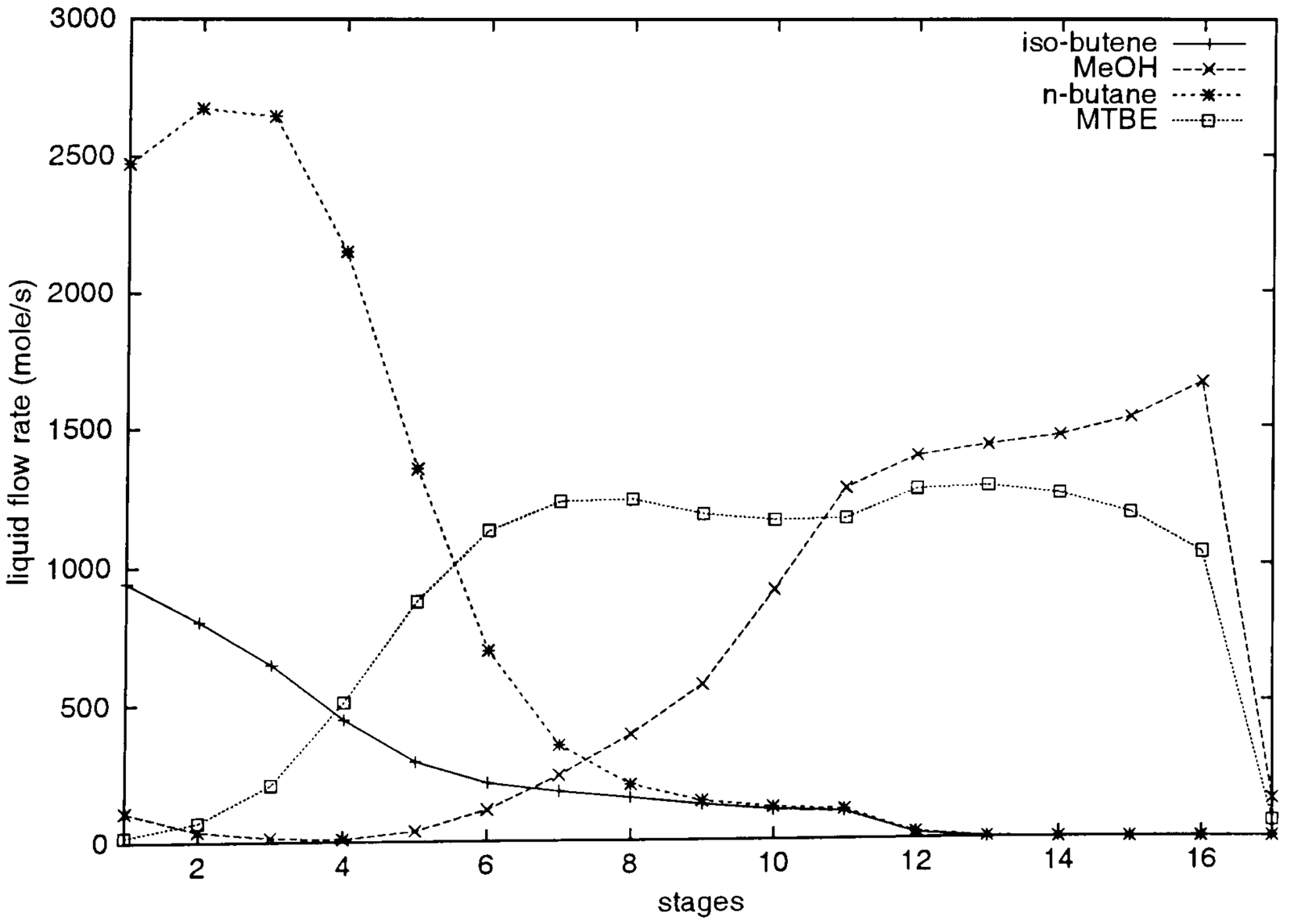

Figure 2.17: Internal liquid flow rates for the 17 stages distillation column, methanol feed at stage 10. Low conversion

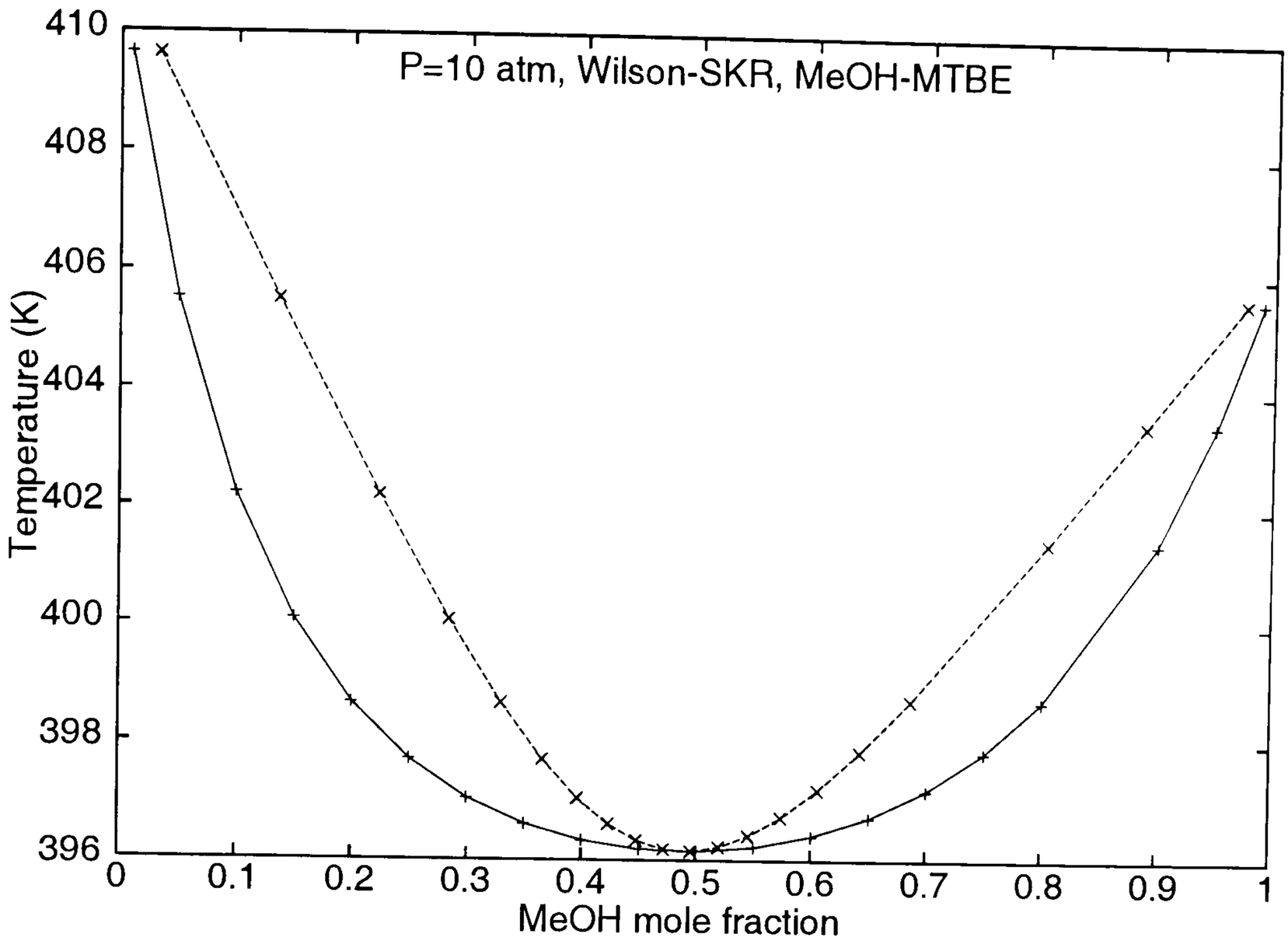

Figure 2.18: Vapour-liquid equilibrium diagram for mixture MeOH-MTBE at 10 atm

Table 2.12: Reboiler heat duty for the base case, methanol feed at stage 10

	Low	Medium	high
Q_{reb} (MW)	75.1	52.9	48.8

2.6.2 Comparison with experimental results

The critical test for the developed model was the comparison between simulation and experimental results. Sundmacher and Hoffmann (1995, 1996) presented experimental results for both dynamic and steady state operation of an MTBE reactive distillation column. Their pilot plant column was used to test two different kinds of catalyst supports and to validate their non-equilibrium model.

Experimental configuration

Sundmacher and Hoffmann (1995, 1996) column is depicted in Figure 2.19. The operating conditions for the case study are presented in Table 2.13.

Table 2.13 shows that some important feed data conditions, such as temperature and pressure conditions are missing. Furthermore, the base is volumetric. To

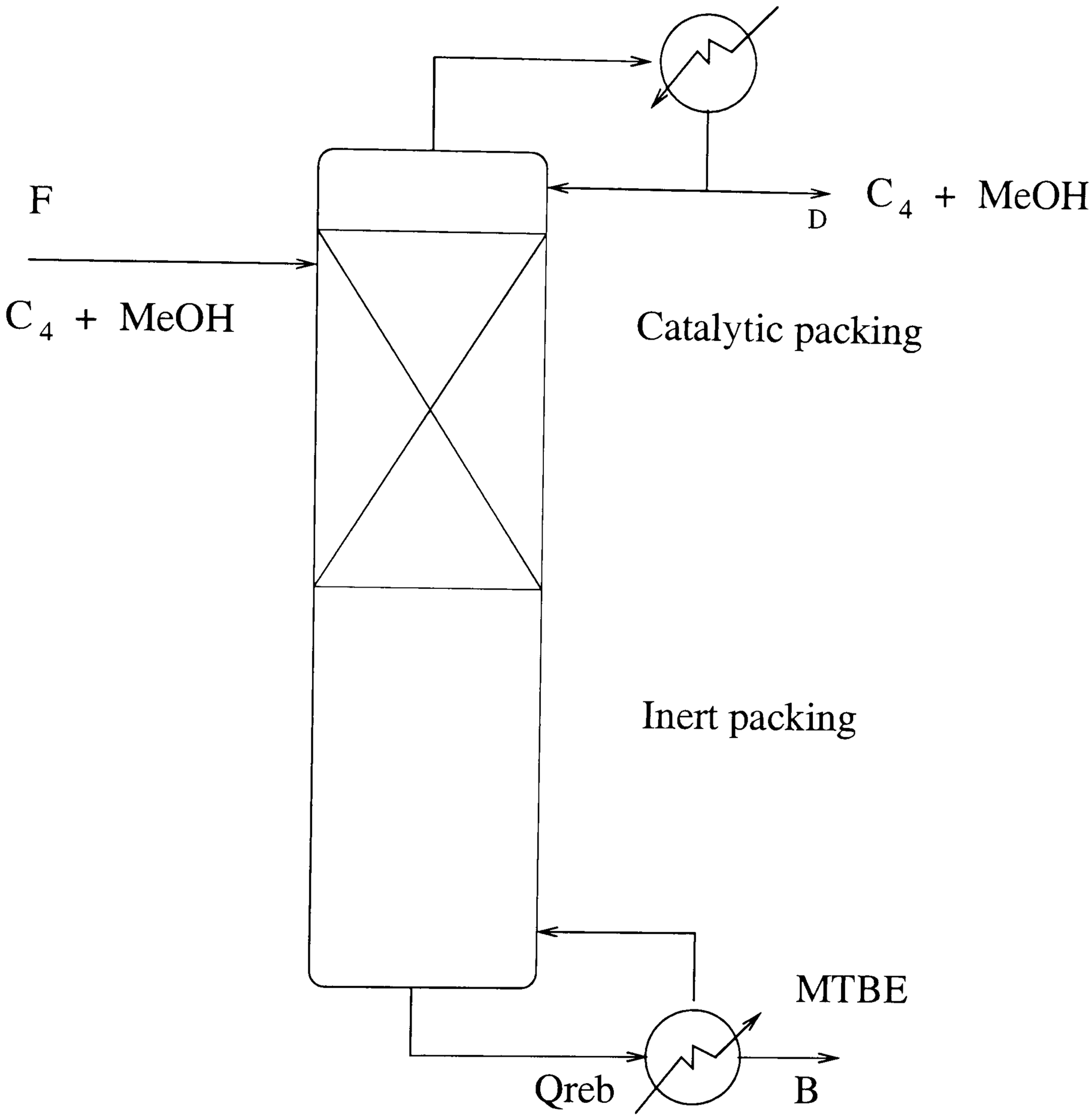

Figure 2.19: Pilot plant column used by Sundmacher and Hoffmann, 1996

calculate the molar flow rate, the data relative to a column filled with glass rings reported in Sundmacher and Hoffmann (1995) were used.

To perform the steady state simulations, some assumptions were made:

- The feed pressure was assumed to be 1 atm larger than the column pressure (7.4 atm). On the other hand, the temperature of the feed was assumed as $330K$. This lead to a cooled liquid.

- To simulate the column, each section was divided into 5 equilibrium stages.

To get a solution it was necessary to solve a problem with lower heat duty ($Q_{reb} = 300$). Then the solution of that problem was used for a problem with higher heat

Table 2.13: Pilot plant column operating conditions (Sundmacher and Hoffmann, 1995, 1996)

reflux ratio	6.7	
Feed (l), top		
Flow rate	25	ml/min
	4.3 E-3	mol/s
z_{i-b}	0.127	
z_{MeOH}	0.153	
z_{n-b}	0.720	
Column Pressure	6.4	atm
Reboiler heat duty	560	W

duty. This iterative process was repeated until the problem was $Q_{reb} = 590$.

Results

The comparison between the simulation results and experiments, can be seen in Figure 2.20. The profiles shown in Figure 2.20 are qualitatively similar to the experimental points. However, there is a great difference for between the middle point of the results. The differences at the top and the bottom of the column can be explained by the selection of the thermodynamic models used for the simulation (Wilson equation and SRK). The difference in the reactive section and consequently in the middle of the column shows that in the experiments the conversion of iso-butene is lower. Furthermore, in the simulations the heat duty leads to a greater evaporation of C_4 compounds than in the experiments. This means that the resistances between the liquid phase and the catalyst and the resistance of energy are greater in the experimental case and the equilibrium model can not reproduce exactly the profiles. This was expected due to the limitations of the model. However, it is consider that the model reproduces qualitatively the experimental results.

In Table 2.14 the conditions of a second experiment presented by Sundmacher and Hoffmann (1996) are shown. In this case, the reflux ratio is greater. As a result of a greater reflux, the conversion of the iso-butene is greater.

For a problem with larger reflux ratio (Table 2.14), the simulation results are better. The simulation and experimental results are presented in Figure 2.21. These results also confirm the differences between the element model and the experimental results, though the trend is qualitatively closer in this case.

Table 2.14: Second experiment conditions (Sundmacher and Hoffmann, 1996)

Reflux ratio	12.7
Feed (l), top	
z_{i-b}	0.3125
z_{MeOH}	0.3750
z_{n-b}	0.3125

Dynamic simulations

Sundmacher and Hoffmann (1994) presented experimental results of an MTBE column not at steady state. Nevertheless, their results are difficult to reproduce because many conditions are missing. However an attempt was made to reproduce one of the experiments. The operating conditions of the column are presented in Table 2.15. The feed flow rates were approximated since those reported are based on volume. Nothing was said about control issues. For the current work, simulations were carried out assuming that the reboiler heat duty was kept constant and the distillate and bottoms flow rates were used to control mass (liquid) level for the reflux tank and the reboiler respectively.

For illustration purposes only, a case with a change in the feed flow rate is presented. At t=0, a pulse in the C_4 fraction feed was introduced. This pulse was simulated as 10% increment of the C_4 feed that lasted 1800 s. The results are presented in Figures 2.22 and 2.23. The results show that the configuration is able to come back to the initial steady state. As expected, the increment of iso-butene benefits the system and there is an increment in the MTBE purity. Sundmacher and Hoffmann (1984) results have a similar trend, though the middle temperature, in this case T_5 was stable in the simulations, while in the experiments it dropped to a new value. A possible explanation is that Sundmacher and Hoffmann might have used a different sort of disturbance.

Table 2.15: Pilot plant operating conditions (Sundmacher and Hoffmann, 1994)

Reflux ratio	6.7	
Feed (l), stage 2		
Flow rate	3.13	mole/s
z_{MeOH}	1.0	
Feed (v), stage 6		
Flow rate	5.21	mole/s
z_{i-b}	0.5	
z_{n-b}	0.5	
Condenser Pressure	6.4	atm
Reboiler heat duty	540	kW
Distillate flow rate	used to control reflux tank level	
Bottoms flow rate	used to control reboiler level	

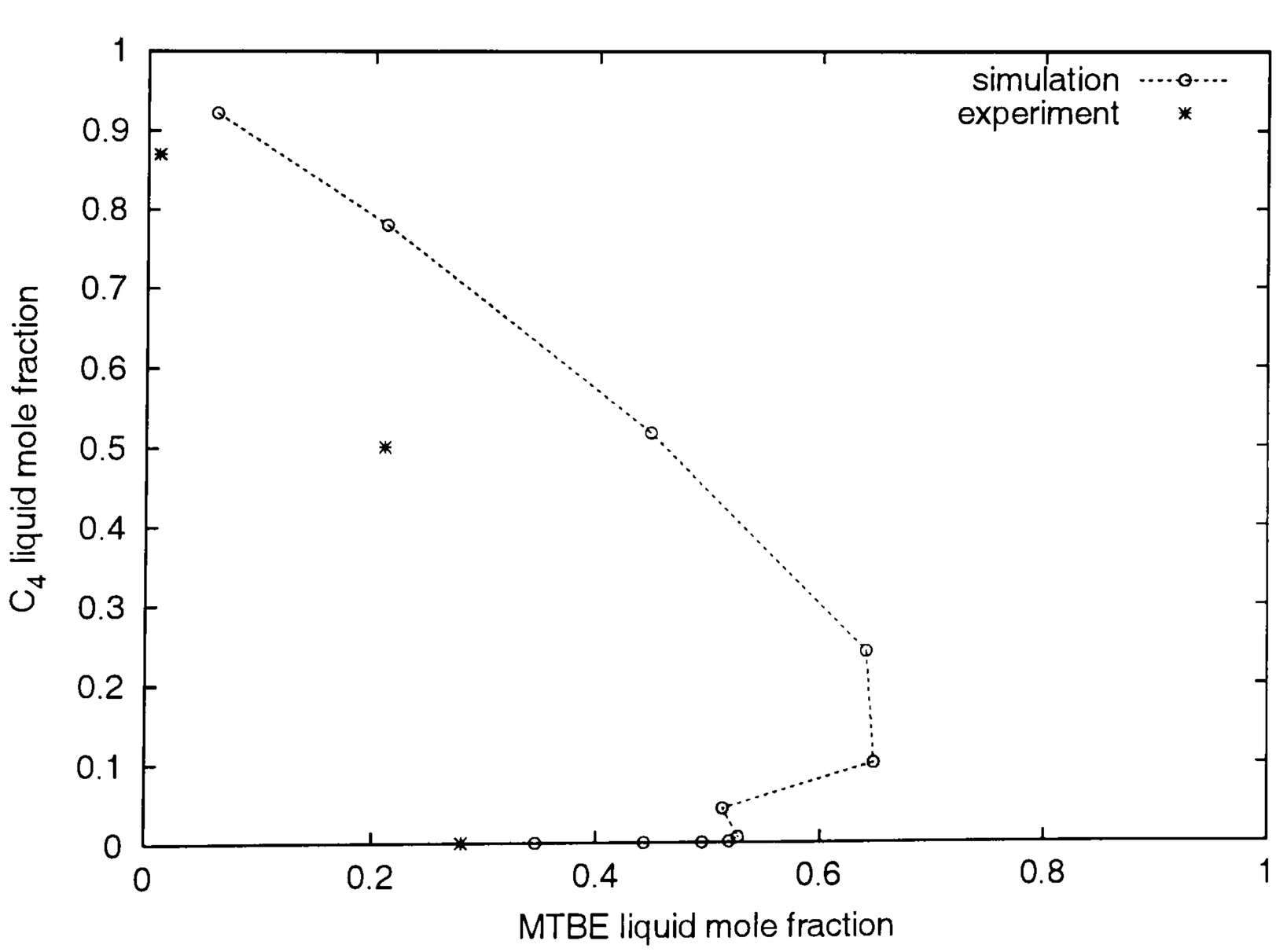

Figure 2.20: Comparison between experimental results (Sundmacher and Hoffmann, 1996) and element model prediction. $P = 6.4atm$, $R = 6.7$ and $Q_{reb} = 590W$

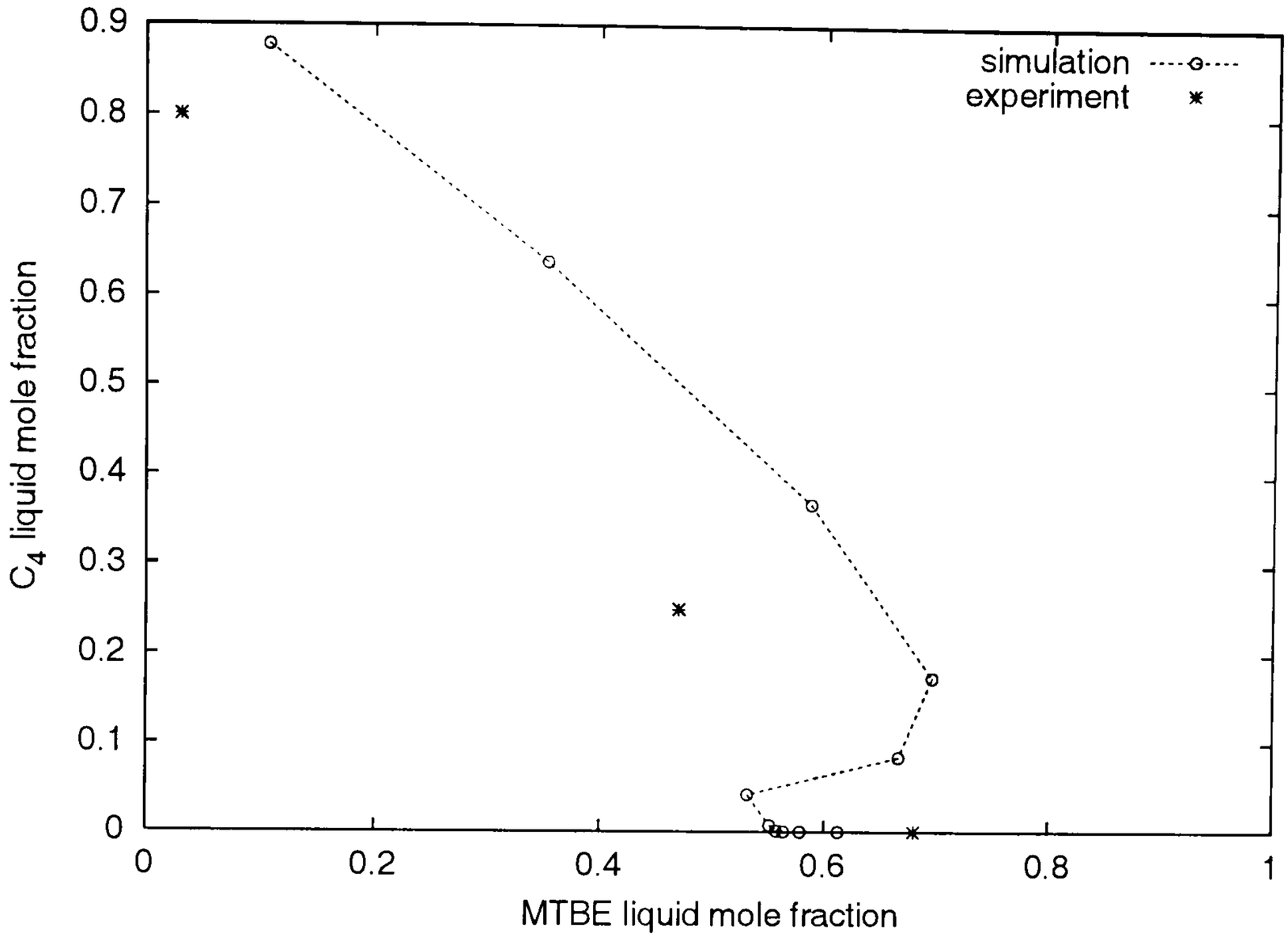

Figure 2.21: Predicted composition profiles for the second experiment reported in Sundmacher and Hoffmann, 1996. $P = 6.4atm$, $R = 12.7$ and $Q_{reb} = 560W$

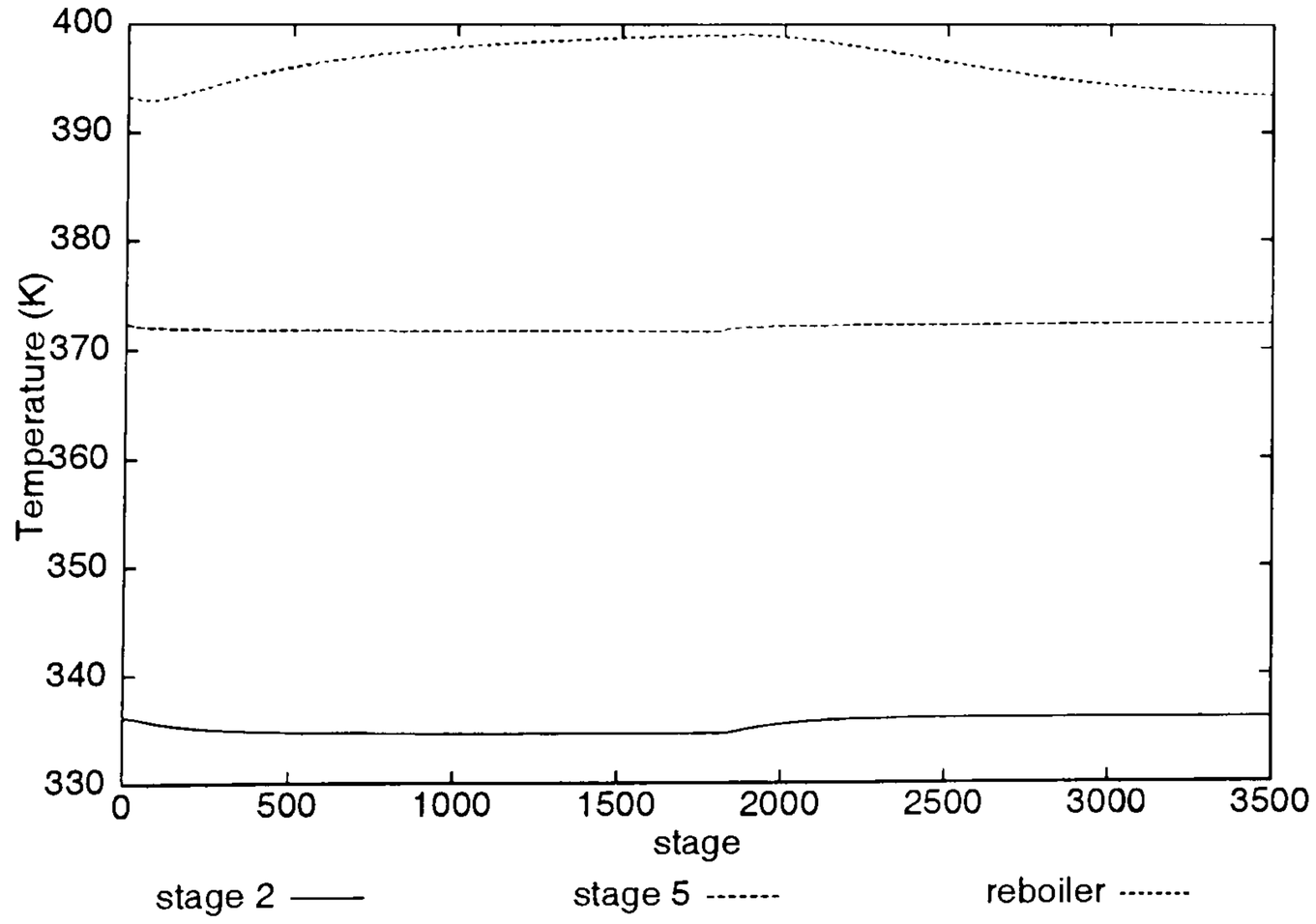

Figure 2.22: Response to a pulse of the C_4 feed flow data from Sundmacher and Hoffmann (1994) example

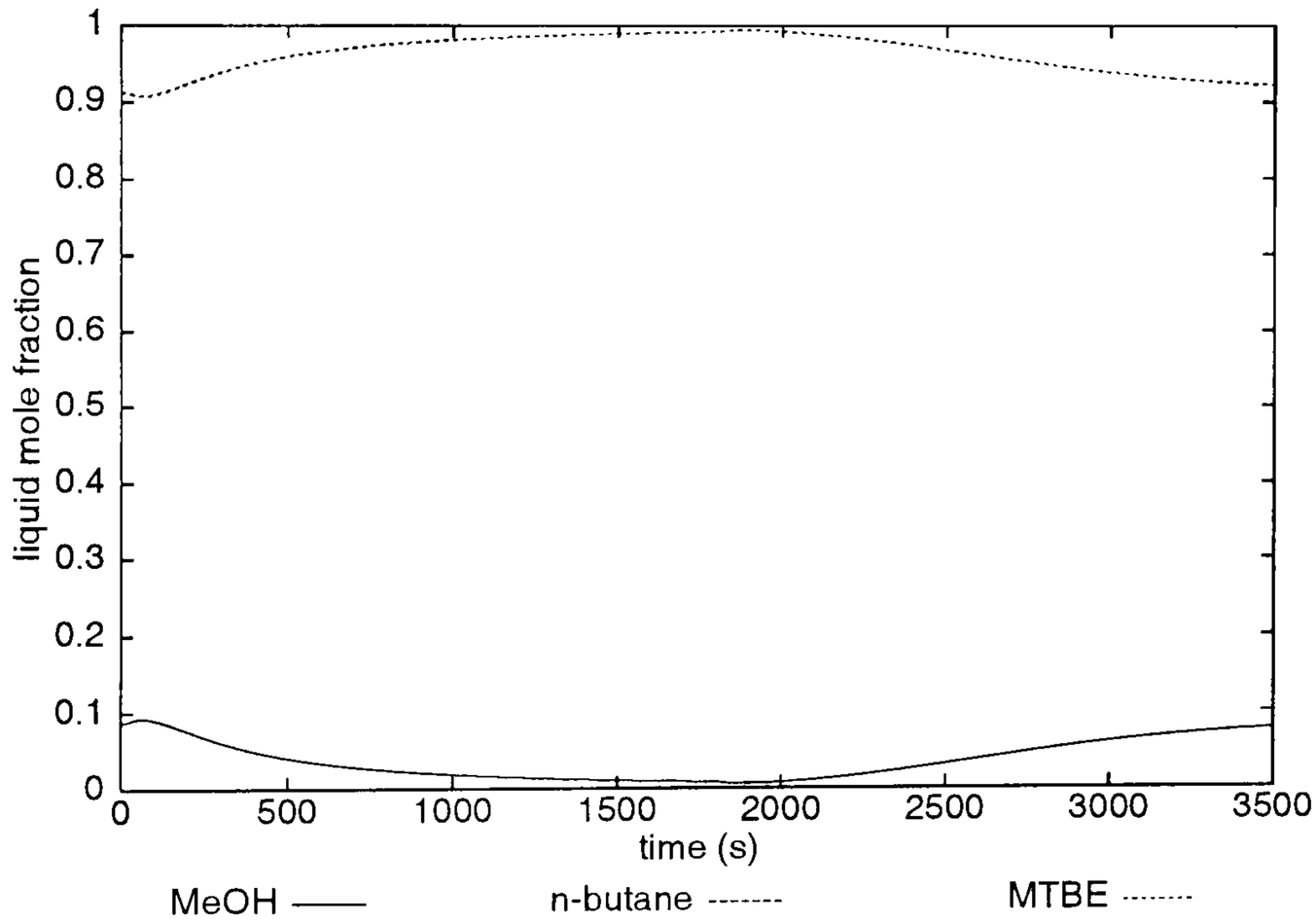

Figure 2.23: Response to a pulse of the C_4 feed flow data from Sundmacher and Hoffmann (1994) example

2.7 Conclusions

One of the purposes of this part of the project was to develop a mathematical model for reactive distillation processes by the use of an element model. Though simple because of the equilibrium assumption, the model should be able to reproduce the gross behaviour of reactive distillation columns. It was important also, to test the model performance under different situations since it would be used to analyse the dynamic behaviour of reactive distillation columns. During the validation process, some changes to the model were necessary due to numerical problems. However, the general algorithm was not changed.

It was found that the model is sensitive to the value of ΔG^{oig}_{f298}. The model predicts well both qualitatively and quantitatively when tested against another equilibrium model. For the experimental validation the best possible solution was found. This is explained by the lack of consideration of mass transfer between phases. However the model can reproduce qualitatively the column behaviour.

Indeed, the last issue is a limitation of the model. Therefore, it could produce incorrect results for cases where the mass transfer is important. One possible way to overcome this problem is the introduction of an efficiency in the calculations.

High and low conversion solutions are reproducible by the model developed. Therefore, the model should be appropriate to evaluate the controllability and dynamic behaviour issues of reactive distillation which is the main issue of the present work.

Chapter 3

Influence of operating conditions and column configuration on reactive distillation

In this chapter some of the reactive distillation characteristics, such as multiplicity, are analysed.

A literature review was made to find the different theories that has been proposed to explain the presence of output multiple steady states (OMSS) in reactive distillation. From this review, it was concluded that the non-linearity of the reaction, separation and the combination of both was responsible of such multiplicity. In addition, the present investigation proposed that OMSS is developed from the input multiple steady states IMSS present in the process due to the inherent non-linearities. In addition it was proposed that such OMSS were more likely to appear when the internal flow rates were high. Simulations of the MTBE reactive distillation process which were made to prove the hypothesis are presented. Such simulations were done with the steady state model of a reactive distillation column developed in Chapter 2.

The chapter finishes with a discussion of the results.

3.1 Introduction

3.1.1 Generalities

The performance of a chemical process is determined by the equipment characteristics and the operating conditions. Both kinds of features are decided during the design process. For distillation the decisions related to operating conditions are for example: the column pressure, the feed properties and location and input variable values such as reboiler heat duty or external flow rates. The final combination of inputs can lead to an unstable column, a column with a stable steady state or a column with various stable and unstable steady states (Jacobsen and Skogestad, 1994).

In the next sections the most relevant studies related to reactive distillation performance and design decisions are discussed.

3.1.2 Characteristics of the reactive distillation operation

In 1995, Sundmacher and Hoffmann presented a series of experiments with a packed reactive distillation column pilot plant for the production of MTBE. The open loop operation of such a column was complex. The column could operate at steady state after start-up without major fluctuations. However, if the column was operated with doubled feed, there were pressure, reflux rate, temperature and composition oscillations. These oscillation phenomena show the effect of operating conditions on the reactive distillation performance. Interestingly, oscillations could also appear for the column operating as a non-reactive column.

Modeling the non-reactive distillation of methanol and iso-butene, the authors found that using the distillate flow rate and the reboiler heat duty, DQ_{reb}, as input pairs produced no output multiple steady states (OMSS). The relationship between the distillate flow rate and the reflux rate stopped being unique at a certain reflux rate, L'. When the reflux rate and the reboiler heat duty, LQ_{reb} were used as inputs, OMSS appeared for reflux rates larger than the L' reflux rate. The stability of the states was analysed using the relationship between the distillate flow rate D and the reflux rate L in a similar way to Jacobsen and Skogestad (1994). Possibly the oscillations presented were related to the steady state characteristics found with the simulations. These experiments are important since they show the possible complexity of reactive distillation operation.

Output multiplicities

When for a system a certain arrangement of input variables can produce two or more values for the output variables, we say that the system displays output multiplicity (Sneesby, Tadé and Smith, 1997b). Jacobsen and Skogestad (1991) showed that output multiplicity was possible even for the simplest distillation problem: the binary ideal distillation.

They presented arguments that proved that there were two multiplicity sources (Jacobsen and Skogestad, 1991 and 1994). The first source is the transformation from mass or volume base to molar base (Type Ia). This kind of transformation creates non-linearities because the internal flows are molar based while the external flows are mass or volume based. The second source of multiplicity is the interaction between compositions and flows (Type Ib). The multiplicity originating due to the last phenomenon can be predicted only if the energy balances are included.

Jacobsen and Skogestad (1994) found with open-loop simulation that not all the multiple steady states of their column were stable. They derived stability conditions for the simple case to prove the effect of the two mentioned multiplicity sources. For example:

$$\left(\frac{\partial L_w}{\partial L}\right)_V < 0$$

is a condition of instability for the problem. However, the authors recognised that such a proof cannot be used to test whether one point that is stable is unique. They suggested that to assess the last point it was easier to perform steady state simulations than to perform a mathematical analysis.

Several researchers have simulated both with equilibrium and non-equilibrium model reactive distillation processes that presented output multiplicity among others: Nijhuis, Kerkhof and Mak (1993); Schrans, Wolf and Baur (1996); Hauan, Hertberg and Lien (1995); Sneesby, Tadé and Smith (1998d and 1998c); Highler, Taylor and Krishna (1999) and Monroy-Loperena and Alvarez-Calderon (1999). Mohl *et al.* (1999) presented experimental evidence of the output multiplicity existence for a TAME reactive distillation column.

Input multiplicities

When a certain output value can be generated by two or more input values, we say that the process possesses input multiplicity. This situation can create con-

trol problems for reactive distillation (Sneesby *et al.* 1998d). Input multiplicity in reactive distillation has not received as much attention as output multiplicity. However, Sneesby *et al.* (1998d) pointed out that it was possible that the major problems relative to reactive distillation control were related to input multiplicity. The importance of this phenomenon was also emphasised by Monroy-Loperena *et al.* (1999).

Reactive distillation steady state behaviour

The first major factor that determine a column performance is the column configuration. Such an influence for reactive distillation was studied by Nijhuis *et al.* (1993) and Hauan *et al.* (1995). These authors used an equilibrium model for the study of a 17 stage MTBE production distillation column. While keeping constant the bottom flow rate and the reflux ratio, the methanol feed location was varied from the second to the penultimate equilibrium stage. The authors found a single steady state when the feed was introduced from the second to the ninth stage. While they found multiple steady states (a high and a low conversion state) when the feed was placed from the tenth to the twelfth stage.

Hauan *et al.* (1995) repeated the experiment changing the inert amount fed to the column. The results showed that the multiplicity region was extended when the inert feed flow rate increased. The case with the minimum amount of inert presents no multiplicity region and the case with the maximum inert feed flow rate was extended for all the methanol feed locations. They explained that the dilution of MTBE in the lower stages favoured the high conversion steady state. However, this did not address the multiplicity origin.

Schrans, Wolf and Baur (1996) studied the same system with an equilibrium model. With dynamic simulations they found a third state. With dynamic simulations this third state was proved to be unstable.

Another factor that determines reactive distillation columns behaviour is the input selection. For example, it was already mentioned how for the conventional distillation of methanol and iso-butene Sundmacher and Hoffmann (1995) avoided OMSS if the distillate flow rate and the reboiler heat duty, DQ_{reb}, were used as inputs.

Another example of the relationship of inputs to performance for a reactive distillation column was presented by Sneesby *et al.* (1998c). For a 10 stages MTBE column with a unique feed location, they found with steady state simulation OMSS

when the inputs where the reflux flow rate L and the boilup flow rate V. However OMSS did not occur when the reflux flow rate L and the reboiler heat duty Q_{reb} were used as inputs. The mentioned authors also worked with an ETBE column with the same characteristics for the MTBE column. In this case they found only input multiple steady states (IMSS). Also, Sneesby *et al.* (1998a), presented steady state simulations for a 28 stages ETBE column. In this case OMSS was found for the problem reboiler temperature-reflux ratio.

The next section contains a review of the explanations found in literature for the the origin of OMSS in reactive distillation.

OMSS explanation

One of the most peculiar facts related with the reactive distillation output multiplicity steady states, is that it can be found with simple and complex models. In the first list of references given in the present section, some used equilibrium models, some others non-equilibrium models. Therefore, the explanation can not rely entirely on the column model. Furthermore, the OMSS existence has been found experimentally for a TAME distillation column (Mohl *et al.*, 1999).

The OMSS explanation for conventional distillation offered by Jacobsen and Skogestad (1991 and 1994) can not explain all OMSS cases present in reactive distillation. For instance, Nijhuis *et al.* (1993) MTBE reactive distillation column presented multiplicity despite using reflux ratio R and molar based bottom flow rate B. It is more difficult to discern whether OMSS are caused or not by interaction of compositions and flow rates through the energy balance (multiplicity type Ib). Usually, energy balances are included in reactive distillation models.

Jacobsen and Skogestad (1994) proved that instabilities were unlikely to occur for the case defined by molar reflux rate L and reboiler heat duty Q_{reb} if the change of vapour enthalpy with respect to composition, dH^V/dy, was negative and there were no influences due molar-mass transformation. However, to arrive to that conclusion, they assumed that the enthalpy of the liquid was independent of composition. They recognised that it was possible that OMSS occurred if this assumption was removed.

Mohl *et al.* (1999) simulated a TAME process using reflux ratio R and reboiler heat duty Q_{reb} as inputs. This was made to avoid type Ib multiplicity according to the Jacobsen and Skogestad (1994) proof. They found OMSS and suggested that

the origin of this multiplicity could not be due the interactions of compositions and flows through the energy balances. Mohl *et al.* and some other authors consider that the OMSS in reactive distillation is introduced due to the reactions taking place in the process. This is not simple to distinguish due to the presence of several phenomena occurring within a reactive distillation column. Moreover, some authors do not think reactions alone can explain the OMSS in reactive distillation.

Ciric and Miao (1994) did a homotopy continuation study for an optimal ethylene glycol column (Ciric and Gu, 1994). In their study, the liquid holdup volume in the reactive stages was used as homotopy parameter. For the base case nine steady state solutions were found. In that process there are two parallel reactions that are expressed as bilinear functions of the reactants (water and ethylene oxide).

The base case was modified to find the origin of the multiple steady states. The modification of the volatility relationship between the reactants produced a significant change of the homotopy curve. When the differences of volatility disappeared, the multiple steady states vanished. On the other hand, when the column was non-reactive, only one steady state was found. With the obtained results, Ciric and Miao (1994) conclude that the multiplicities for the ethylene glycol column arise as a result of the combination of two factors: the great volatility difference between the reactants and the presence of reactions.

Ciric and Miao (1994) suggested that this difference between the reactants volatilities combined with reactions could explain the OMSS presence in MTBE process since the reactants, iso-butene and methanol, have very different normal boiling points, $266K$ and $337.7K$ respectively. On the other hand, a process like the production of ethyl acetate from ethanol and acetic acid which normal boiling points are $351K$ and $391K$, not distant boiling points, did not present multiplicity when Chang and Seader (1988) did a homotopy continuation study of the process. The lack of multiplicities was also found by Vora and Daotidis (2001) with a bifurcation study.

Güttinger and Morari (1999 a,b) arrived to the conclusion that OMSS in reactive distillation was caused by the reactions present in the system. The mentioned authors extended the ∞/∞ method developed by Bekiaris, Meski and Morari (1996) for conventional distillation. Roughly speaking,the ∞/∞ method is a graphical method which approximates a distillation column as a column with infinite number of equilibrium stages and infinite reflux ratio. Furthermore, the reaction is considered at equilibrium. The method was applied first for a MTBE column with reactive stages only. It can predict what feed conditions can produce OMSS.

In a second paper, Güttinger and Morari (1999b) worked with reactive distillation columns with reactive and non-reactive stages, a hybrid reactive distillation column. The mentioned authors suggested two additional sorts of OMSS, both caused by the thermodynamic equilibria. The first one, type IIa, occurs because of the simultaneous vapour-liquid and chemical equilibria. This kind of multiplicity can occur in non-hybrid columns (a column without non-reactive sections). However, they could also appear in hybrid reactive distillation columns (columns with reactive and non-reactive sections). The second kind, type IIb, arises due the interaction of reactive and non-reactive stages.

Güttinger and Morari (1999a) found that the feed condition of Nijhuis *et al.* (1993) MTBE column is outside the region that causes OMSS in a non-hybrid distillation column (∞/∞). Furthermore, no OMSS were found for the non-reactive distillation (Güttinger and Morari, 1999a). Hence, Güttinger and Morari concluded that the multiplicities for the Nijhuis problem must be of type IIb. That is, OMSS were caused by the interaction of reactive and non-reactive stages. This could explain why they have been found with equilibrium and non equilibrium models.

Blagov, Bessling, Schoemakers and Hasse (2000) used Güttinger and Morari's (1999a) ∞/∞ method to study a reactive distillation column with two competing hypothetical reactions. The reactions resemble the ethylene-glycol production reactions. The reaction rates were expressed as bilinear functions of liquid mole fractions. They found that there were two conditions for multiplicity in this system. The first condition was that two or more mathematical solution sections with different separation regions had to overlap. The second condition was the combination of linearity of both reaction rates.

The first condition of multiplicity found by Blagov *et al.* (2000) is comparable to the great differences of reactant volatilities requirement proposed by Ciric and Miao (1994). The large differences of volatility can create different separation regions that overlap because of the reactions. Unfortunately, not enough physical data was provided in order to compare the exact reactants volatility difference.

The second condition is comparable to multiplicity IIa (Güttinger and Morari, 1999a): a combination of vapour phase equilibrium and reactions, though Blagov *et al.* consider irreversible reactions.

Mohl *et al.* (1999) studied TAME and MTBE production with a model in which resistances within the solid phase were not considered. They studied the OMSS of TAME considering the possibility that OMSS could arise from kinetic instabilities

as may happen in a continuous stirred tank reactor. When the process was modeled as approaching equilibrium, by increasing the activity of the catalyst. the OMSS zone decreased. OMSS was found when the reaction was far from equilibrium. The multiplicity regions had similar shapes for the CSTR and the one stage reactive distillation column. However, the multiplicity region for the single stage column was bigger, possibly due to separation effects. The authors increased stages until the final configuration was achieved. The shape of the multiplicity region grew. Furthermore, for the 8 and 12 stage (condenser, reboiler and the rest half reactive and half non-reactive) columns OMSS multiplicity appeared even for chemical equilibrium.

The results agree with the Güttinger and Morari classification. Apparently there are two sources of multiplicity appearing in the problem. The first one can be labelled as a IIa multiplicity type. This type would be produced by kinetic instabilities alone. The second multiplicity appeared because of the combination of reactive and non reactive equilibrium stages, this is multiplicity IIb that occurs for the 8 and 12 stages column.

Another important finding of Mohl *et al.* was that TAME and MTBE simulations with reflux ratio R and reboiler heat duty Q_{reb} as inputs showed that the multiplicity region is small and appeared at high reflux ratios and reboiler heat duties. This result is similar to Jacobsen and Skogestad (1994) results for the ideal binary distillation problem.

There are also examples showing that kinetic expression simplification can dismiss multiplicity from the process. The first example was shown by Sneesby *et al.* (1998b). When the authors simulated a MTBE column with an equilibrium constant fixed (composition and temperature independent), the OMSS disappeared. The second example was shown by Schenk (1999) who showed that a simplified kinetic expression from the DIPPR data bank lead to no multiplicities for the Nijhuis *et al.* (1993) MTBE column.

3.1.3 Conclusions from the literature review

From the last literature review two main causes of non-linearity can be distinguished: The first one is the effect of reactions (kinetically controlled or at equilibrium). The second one is the effect of the reaction-separation interaction. The last has been noticed when the volatilities differences between reactants are significant.

It is important to notice that a column may present inherently those non-linearity sources. However, it is the input decision that can yield OMSS, just in the same way that happens in conventional distillation (see for instance, Jacobsen and Skogestad, 1994).

Is it possible to find a general trend for multiplicity to occur and therefore design a reactive distillation of column in which output multiplicity is not present? Evidence suggests that it is possible (Jacobsen and Skogestad, 1994; Mohl *et al.*, 1999).

The main objective of this chapter is to show that input multiplicity can become output multiplicity when the internal flows are high, though it is not trivial to address a minimal internal flow rate that will produce output multiplicity.

A secondary aim of this chapter is to show that any combination of inputs is likely to produce OMSS provided that the internal flow rates are high enough.

Although much has been said of the OMSS and reactive distillation, a better understanding of the relationship between the operating conditions and its occurrence is necessary.

3.2 Multiplicity analysis method

To prove that if a column has input multiplicity, it will develop output multiplicity, a series of steady state simulation experiments was designed. In the experiments a system that can have output multiplicity is used to show the evolution from input multiplicity to output multiplicity. The experiments start with the non-reactive distillation of the system. The second part of the experiments consists of simulations of the reactive distillation column firstly with small internal flow rates and then with larger internal flow rates that produce output multiplicity. During the experiments, many configurations were tested to study the influence of different inputs on the system

For the steady state simulations experiments the model developed in the preceding chapter was used.

3.2.1 Case study

The example chosen was the MTBE reactive distillation column. The case study column is similar to the reported by Nijhuis (1993). The column consists of a total

condenser, 15 stages and a partial reboiler. It is advantageous to work with this system since there are several reports to compare with the results got in the present investigation.

3.2.2 Simulation experiments

The experiments done can be divided into two groups. The first group of experiments was aimed to study the inputs effect. The second group of experiments was aimed to study the configuration effect. Following there is a description of the realized experiments:

1. The first experiment was made to study whether non-reactive MTBE distillation yielded either IMSS or OMSS. Two feeds were studied. The first one had a significant amount of MTBE. The second feed had a small amount of MTBE.

2. The second experiment dealt with reactive distillation and was aimed to see an expected transformation from IMSS leading to OMSS by increasing internal flow rates.

3. The aim of the third experiment was to investigate if it was possible to find a methanol feed location that produced no OMSS. The aim of this experiment was to study the influence of the column configuration.

4. The aim of the fourth experiment was to show the effect of a different internal configuration (number of reactive and non-reactive stages).

5. The last experiment aimed to show that any of the common configurations used in conventional distillation could result in OMSS if the internal flows were high enough.

3.3 Results and discussion

3.3.1 n-butane, MeOH, MTBE non-reactive distillation

As mentioned before, the objective of this experiment was to search for input or output multiplicity for the n-butane, MeOH, MTBE conventional distillation. The inputs selected were the reflux ratio R and the reboiler heat duty Q_{reb}.

Table 3.1: Characteristics of the reactor preceding the non-reactive MTBE distillation column. Case 1

Feed (l)		Product (l)	
Flow rate	764.5 mol/s	Flow rate	587.53 mol/s
$z_{iso-butene}$	0.2561	$x_{iso-butene}$	0.03204
z_{MeOH}	0.2819	x_{MeOH}	0.06574
$z_{n-butane}$	0.4620	$x_{n-butane}$	0.60115
z_{MTBE}	0.0000	x_{MTBE}	0.30107

P=11 atm, T=358.5 K

Table 3.2: Non-reactive MTBE column feed. Case 1

Feed flow rate (l)	587.53 mol/s
z_{MeOH}	0.06574
$z_{n-butane}$	0.63319
z_{MTBE}	0.30107

P=11 atm, T=358.5 K

Case 1. The feed to the 17 stage non-reactive column comes from a isothermal homogeneous reactor in which methanol and iso-butene react (with 90% iso-butene conversion). Table 3.1 shows the feed to the reactor and the product characteristics. Both streams are at $358.5K$ and $11atm$.

To simplify the problem, the iso-butene in the reactor product was lumped with the n-butane. Thus, the feed to the non-reactive column has only three components: methanol, n-butane and MTBE (Table 3.2).

Three different reflux ratios were tested while the reboiler heat duty was varied. Figure 3.1 shows the main results for this experiment. All the attempts to find IMSS or OMSS failed for the three reflux ratios tested. Moreover, simulations were not successful for higher reboiler heat duties than the maximum ones that appear in the graph.

Case 2 The same experiments were done with a feed that came from a reactor with only 10% iso-butene conversion. Table 3.3 shows the feed and product features of such a reactor. The homogeneous reactor temperature is fixed at $345K$.

Again the iso-butene and the n-butane were lumped as n-butane. The characteristics of the feed to the non-reactive distillation feed are presented in Table 3.4.

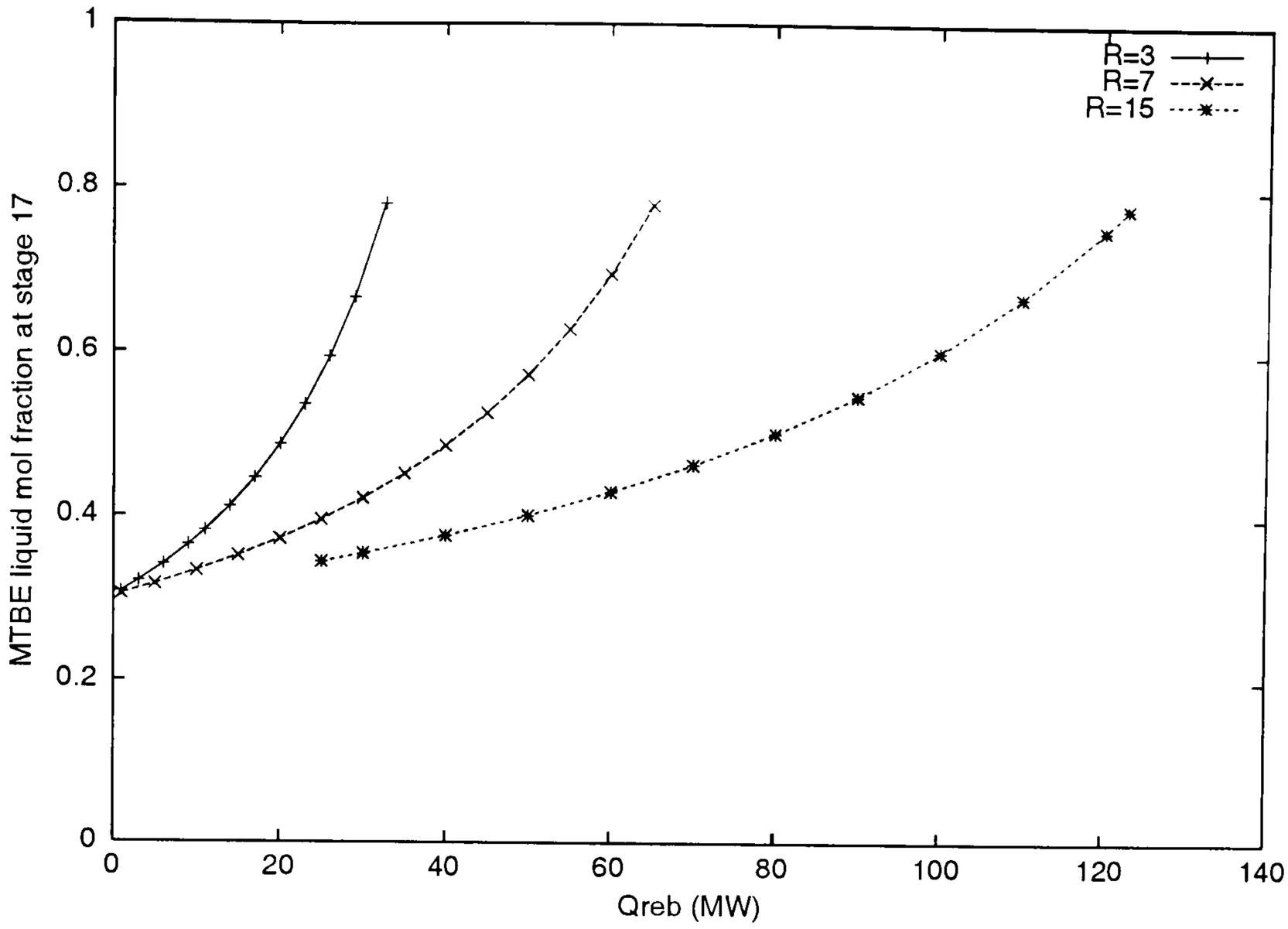

Figure 3.1: MTBE Liquid mol fraction at stage 17. Non-reactive distillation. Case 1

The results are shown in Figure 3.2. Similar to case one, it was not possible to find solutions that showed that the system had multiplicity. Furthermore, it was not possible to get solutions once a maximum heat duty was reached.

Once the conventional MTBE distillation was proved of presenting neither IMSS nor OMSS for the RQ_{reb} analysed, the next step was to study the MTBE reactive distillation with the same inputs. This leads us to the second experiment.

3.3.2 MTBE reactive distillation, from IMSS to OMSS

In the second experiment, a reactive distillation column with similar characteristics to the ones reported by Nijhuis *et al.* (1993) was used. Such a column consisted of 17 stages. The first stage was a total condenser. The rest of the stages were equilibrium stages and were arranged as follows: 3 non-reactive stages (rectifying section), 8 reactive stages, 5 non-reactive stages (stripping section) and a partial reboiler. MeOH feed was located at stage 10 and C_4 feed at stage 11. The characteristics of the column are given in Table 3.5 Similarly to the previous experiments. the inputs were the reflux ratio R and the reboiler heat duty Q_{reb}.

Case 3. The problem described constitute Case 3. For this case, three different reflux ratios were tested. The results are shown in Figure 3.3. The column with

Table 3.3: Characteristics of the reactor preceding the non-reactive MTBE distillation column. Case 2

Feed (l)		Product (l)	
Flow rate	764.5mol/s	Flow rate	744.92mol/s
$z_{iso-butene}$	0.2561	$x_{iso-butene}$	0.23655
z_{MeOH}	0.2819	x_{MeOH}	0.26303
$z_{n-butane}$	0.4620	$x_{n-butane}$	0.47414
z_{MTBE}	0.0000	x_{MTBE}	0.02628

P=11 atm, T=345 K

Table 3.4: Non-reactive MTBE column feed. Case 2

Feed flow rate (l)	744.92 mol/s
z_{MeOH}	0.26303
$z_{n-butane}$	0.71069
z_{MTBE}	0.02628

P=11 atm, T=345 K

Table 3.5: Data for the 17 stages MTBE reactive distillation column (Nijhuis *et al.*, 1993).

MeOH feed (l), stage 10		
Flow rate	215.5	mole/s
Temperature	320.0	K
Pressure	11.0	atm
C_4 feed (v), stage 11		
Flow rate	549.0	mole/s
Temperature	350.0	K
Pressure	11.0	atm
iso-butene	0.3568	mole fraction
n-butane	0.6432	mole fraction
Column pressure	10	atm

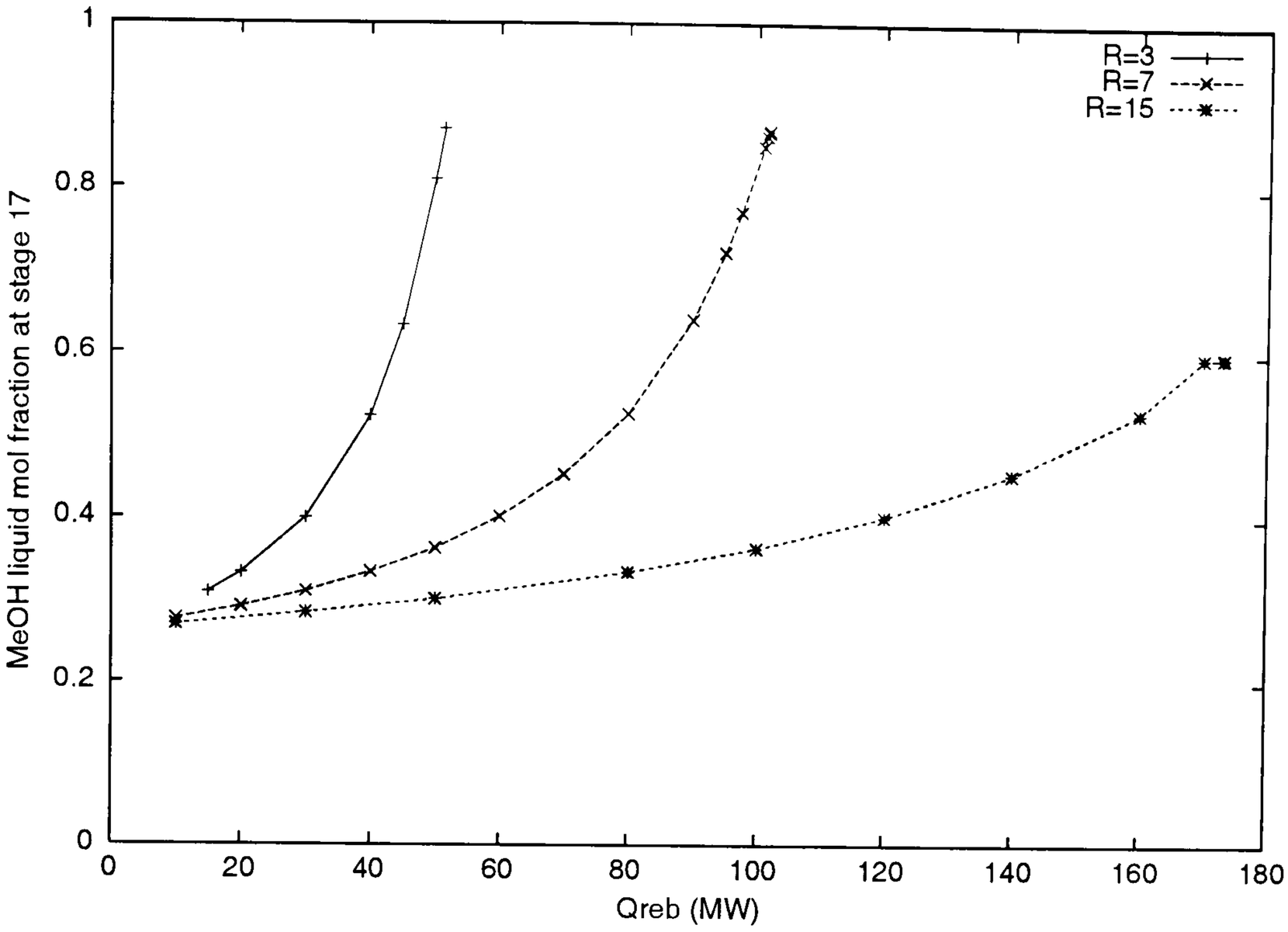

Figure 3.2: MeOH liquid mol fraction at stage 17. Non-reactive distillation. Case 2

the lowest reflux ratio exhibits only IMSS. For the columns with higher reflux ratio the IMSS is less evident. Moreover, those cases present OMSS. Note, that there is a maximum conversion for each column. Once this maximum has been reached, the conversion plunges. Another important feature of Figure 3.3 is that the high conversion steady state is rather constant and higher when the reflux ratio is also higher. Furthermore, when the reflux ratio is increased, the high conversion steady state can be maintained for an extended range of reboiler heat duties, possibly because the mixing is better. However, the distance from the high conversion to the low conversion in the multiple steady state point for $R = 15$ is greater than for the $R = 7$ column.

The results in Figure 3.3 suggest that increasing the internal flow rates increases the probability of OMSS. Note that even for low flow rates ($R = 3$) the system is non-linear and possesses IMSS. The results suggest that the non-linearities present in the system increase when the flows are higher.

Let's examine closely what happens for the lowest reflux ratio. This will show us the effect of the reboiler heat duty increment. When the reboiler heat duty is equal to $10MW$ there is a unique solution with a relatively high iso-butene conversion (see Figure 3.3). For this case, the temperature gradients in the stripping section are moderate, though the effect of the reaction in the temperature profile is already

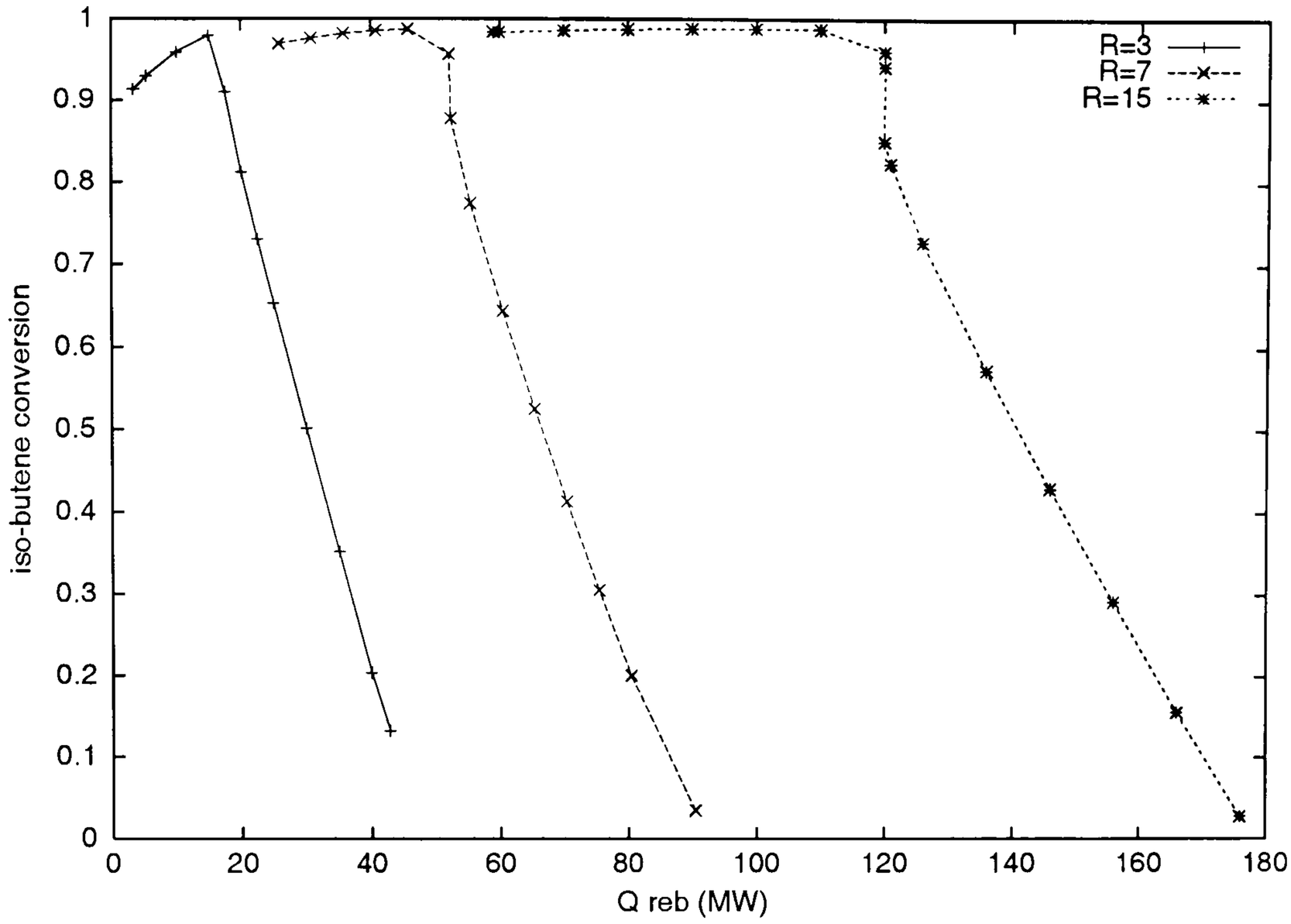

Figure 3.3: Iso-butene conversion for a MTBE column. Case 3

established (Figure 3.4).

A further increment of the reboiler heat duty ($Q_{reb} = 15MW$) has a significant effect on the separation and conversion. The extra heat duty leads to a purer bottom stream and to a higher iso-butene conversion (Table 3.6). The temperature in the stripping sections (Figure 3.4) increases. Note that the temperature profile for the rectification and reactive section are almost equal to the lower Q_{reb} solution. The improvement is explained due to the further evaporation of the C_4 components of the stripping section. There is higher conversion because more iso-butene arrives to the reactive section. Further C_4 evaporation also implies a bottom flow rate richer in MTBE. Compare Figures 3.5 and 3.6.

Summarising, a high conversion is obtained when reaction and separation are balanced.

Table 3.6: Iso-butene conversion for the 17 stages MTBE column. R=3.

Q_{reb} (MW)	iso-butene conversion
10	0.9594
15	0.9798
17.5	0.9102

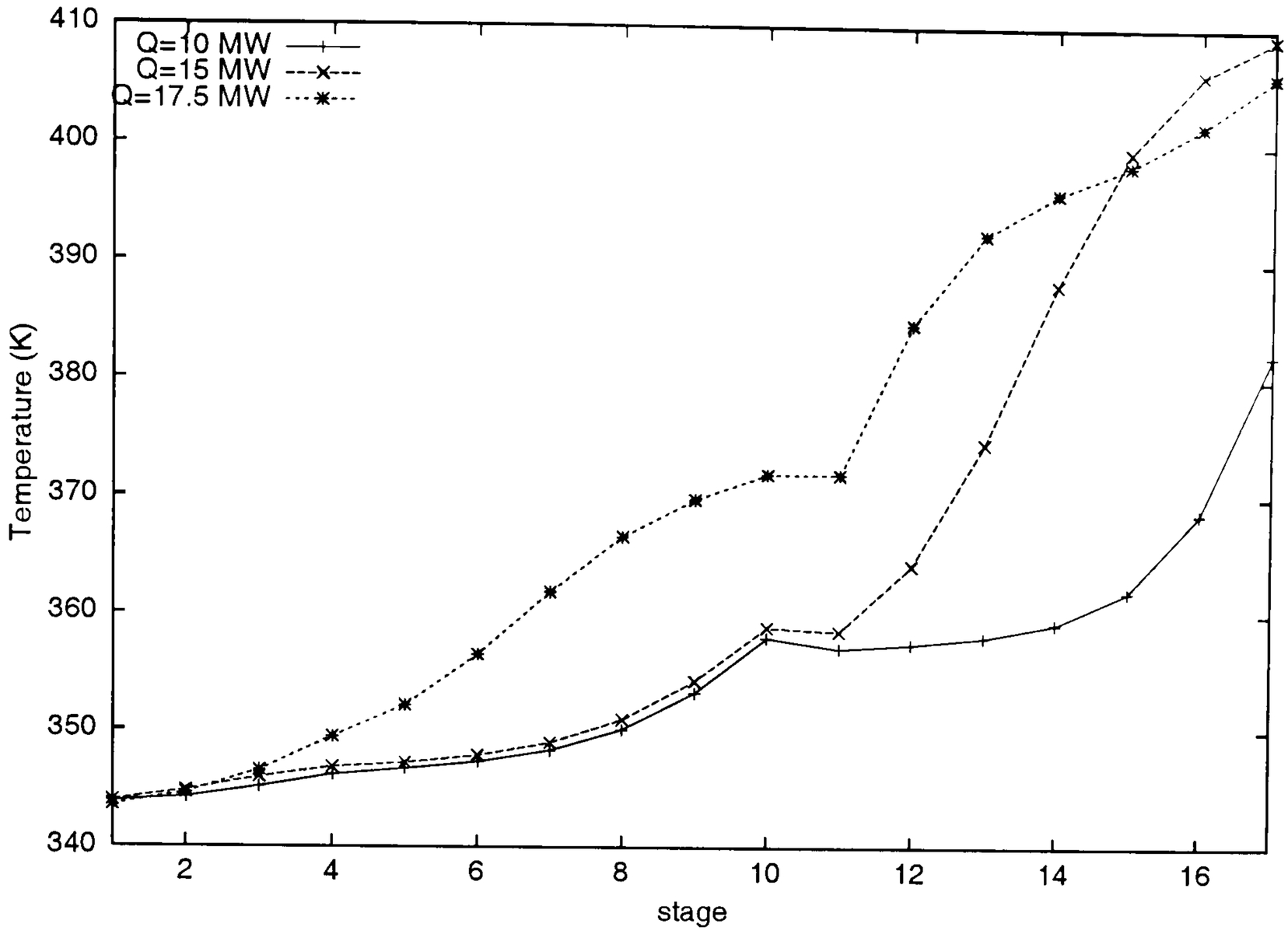

Figure 3.4: Temperature for a MTBE reactive distillation column. $R = 3$.

A further reboiler heat duty increment (Q_{reb}=17.5 MW) has disastrous effects for the column. The temperature profile of the column changes drastically (Figure 3.4). The extra heat duty leads to smoother temperature gradients for the stripping section (compare Q_{reb}=15 MW and Q_{reb}=17.5 MW). Moreover, since the lightest components were not present in large quantities in the stripping section, the further reboiler heat duty increment evaporates MTBE which arrives to the reactive section where it decomposes. The methanol formed due to this decomposition plunges towards the stripping section. Since the lower part of the reactive section is used in the MTBE decomposition, part of the methanol and iso-butene reacts in the upper stages of the reactive section. All these factors provide the temperature increment observed for the reactive section (Figure 3.4, stages 4-11).

Further reboiler heat duty increment worsens all the phenomena explained before, decreasing substantially the iso-butene conversion. The results for the problem with Q_{reb} equal to 42.8 MW are shown in Figures 3.7 and 3.8. We can observe, that the extra reboiler heat duty leads to a reduction of the temperature gradients in the stripping section. Simultaneously, more MTBE is evaporated to the reactive zone with its consequent decomposition. We observe how the temperature in the reactive zone is increased even in the top, this being a signal of the MTBE formation in that zone.

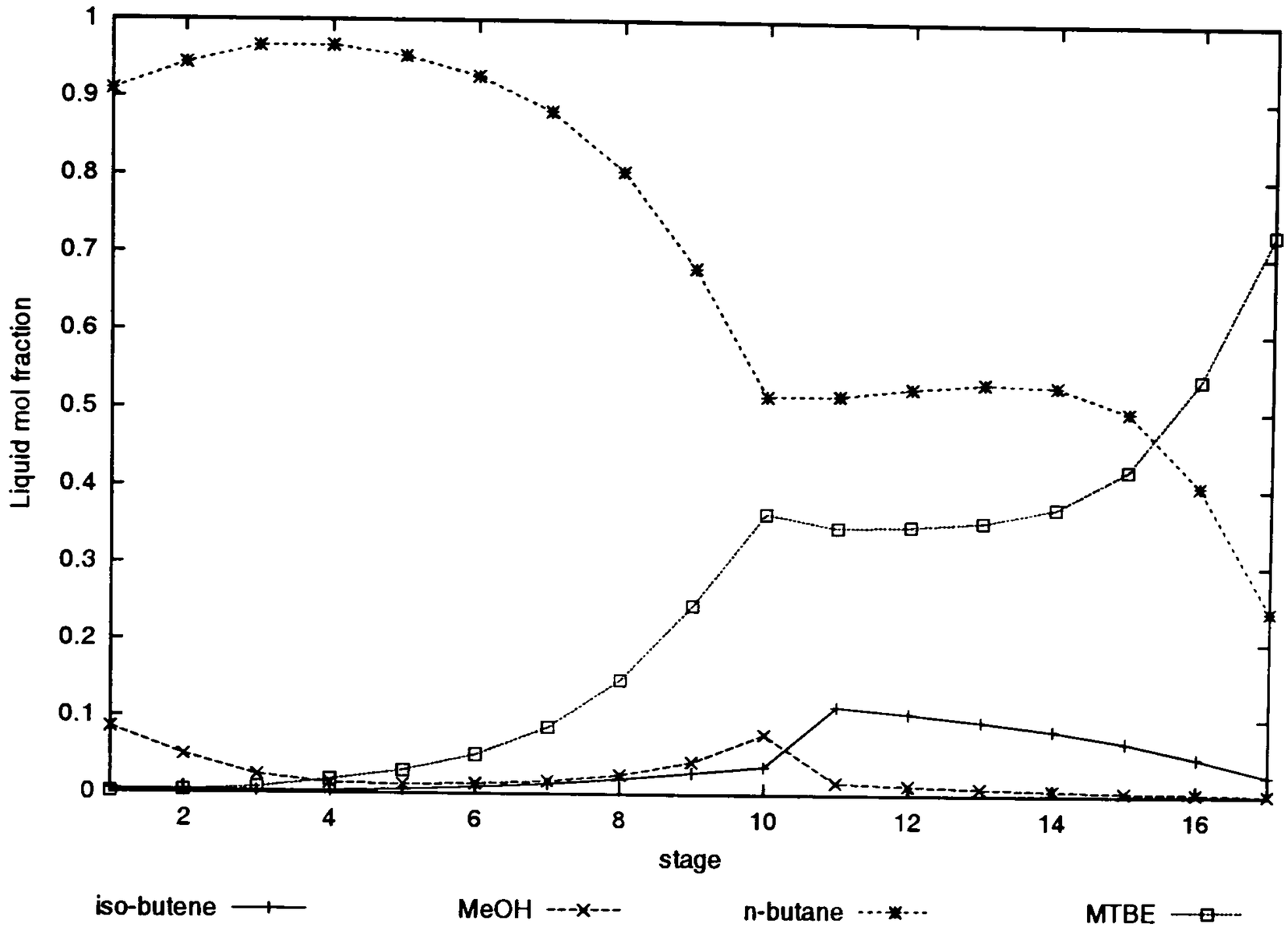

Figure 3.5: Liquid mol fraction profiles for an MTBE reactive distillation column. Reflux ratio= 3, $Q_{reb} = 10MW$.

All the discussed characteristics of the problem with reflux ratio $R = 3$ are related to the non-linearity of the process. Although there are no sudden changes due to the variation of the reboiler heat duty, the nonlinearity is observed with a maximum possible conversion and a steady drop of the conversion beyond this point.

The phenomena that occur when the reflux ratio was kept as $R = 3$ while the reboiler heat duty was changed are the same that would occur for the system with higher reflux ratios. The example shows that depending on the input values, the reaction and separation effects can be balanced and the column can achieve maximum conversion and separation. On the contrary, the input values can break the balance, affect the separation (lifting heavy components towards the middle column section) and consequently affect the reaction.

Those non-linear effects are increased when the reflux ratio and therefore the reflux flow rate is increased. A possible explanation is internal flows have strong effect on the the column composition, if these are increased the interaction between reaction and separation is more complex and OMSS appear. But it should be noticed that the system has a complex behaviour even at low internal flow rates.

All these characteristics must be pondered during design. Figure 3.3 shows that the lowest reflux ratio produces no OMSS. But, it also shows that further increment

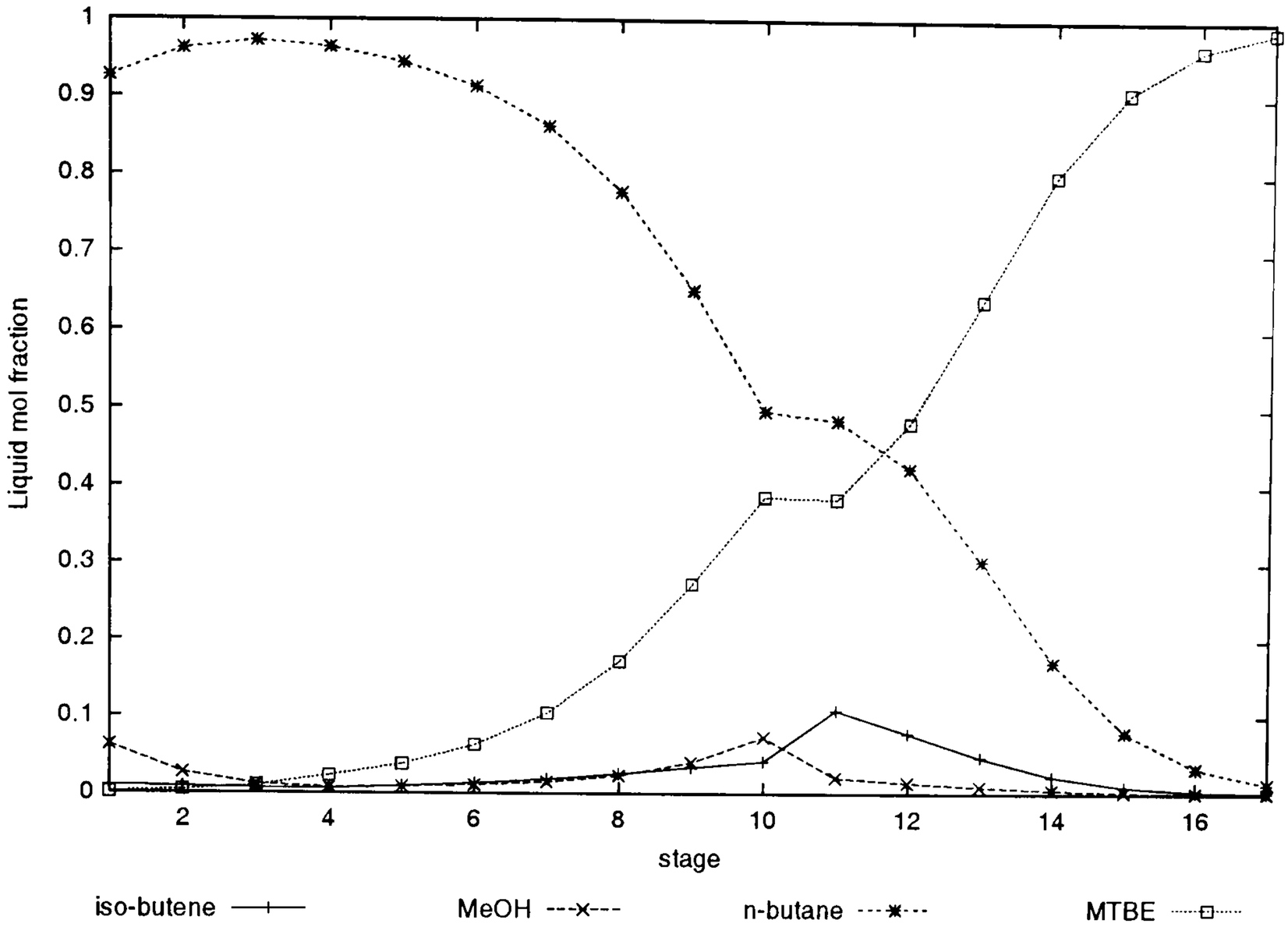

Figure 3.6: Liquid mol fraction for a MTBE column. R= 3, $Q_{reb} = 15MW$.

of the reboiler heat duty once the maximum conversion has been reached, would result in a lower conversion. On the other hand, a higher reflux ratio can lead to OMSS, but a good iso-butene conversion rate can be maintained for a broader, but higher, reboiler heat duty range. The risk is that the conversion can plunge about 20% if the reboiler heat duty is increased beyond the maximum conversion state. The major OMSS drawback for the process is that it might not be easy to restore the column to high conversion state once it has plunged to a low conversion state through a OMSS

3.3.3 Column configuration and steady state behaviour

Feed location effect on operation

There are some publications relative to MTBE reactive distillation that show that certain methanol feed locations are more susceptible to OMSS. (Nijhuis *et al.*, 1993; Hauan *et al.*, 1995 and Schrans *et al.* 1996). A common feature of these publications is that the inputs were the bottom flow rate B and the reflux ratio R and both inputs were kept constant.

The objective of the next MTBE reactive distillation simulation is to show that

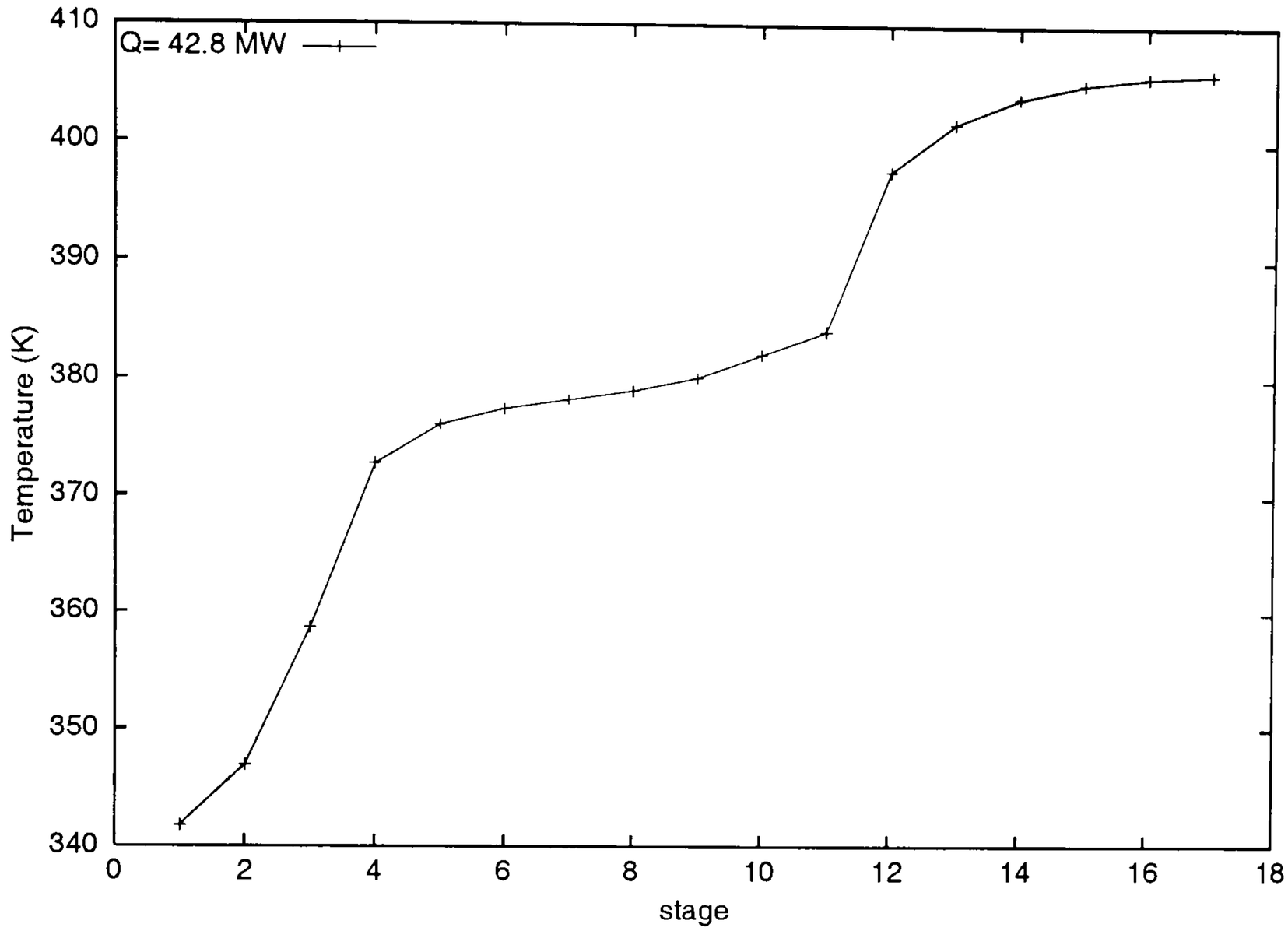

Figure 3.7: Temperature for a MTBE column. R= 3, $Q_{reb} = 42.8MW$.

Figure 3.8: Liquid mol fraction. MTBE column. $R = 3$, $Q_{reb} = 42.8MW$.

any methanol feed location can lead to OMSS with certain inputs. To perform this experiment the same configuration used by the above authors was here used. The bottom flow rate was fixed at 197 mol/s while varying the reflux ratio.

Three different methanol feed locations were used for the steady state simulations: the first one was at the top of the reactive zone (stage 4); the second one was at the same place chosen by the authors, the penultimate stage of the reactive zone (stage 10); the third methanol feed location studied was at the middle of the stripping section (stage 14).

As expected, the three chosen feed locations presented OMSS. However, the minimum reflux ratio at which OMSS appeared depended on the methanol feed location.

Figures 3.9, 3.10 and 3.11 show the iso-butene conversion versus reflux ratio for the three problems. The figures show that at low internal flow rates (low reflux ratio) there is is only one possible conversion. However, for higher internal flows (high reflux ratio) there are three possible iso-butene conversion for the same reflux ratio.

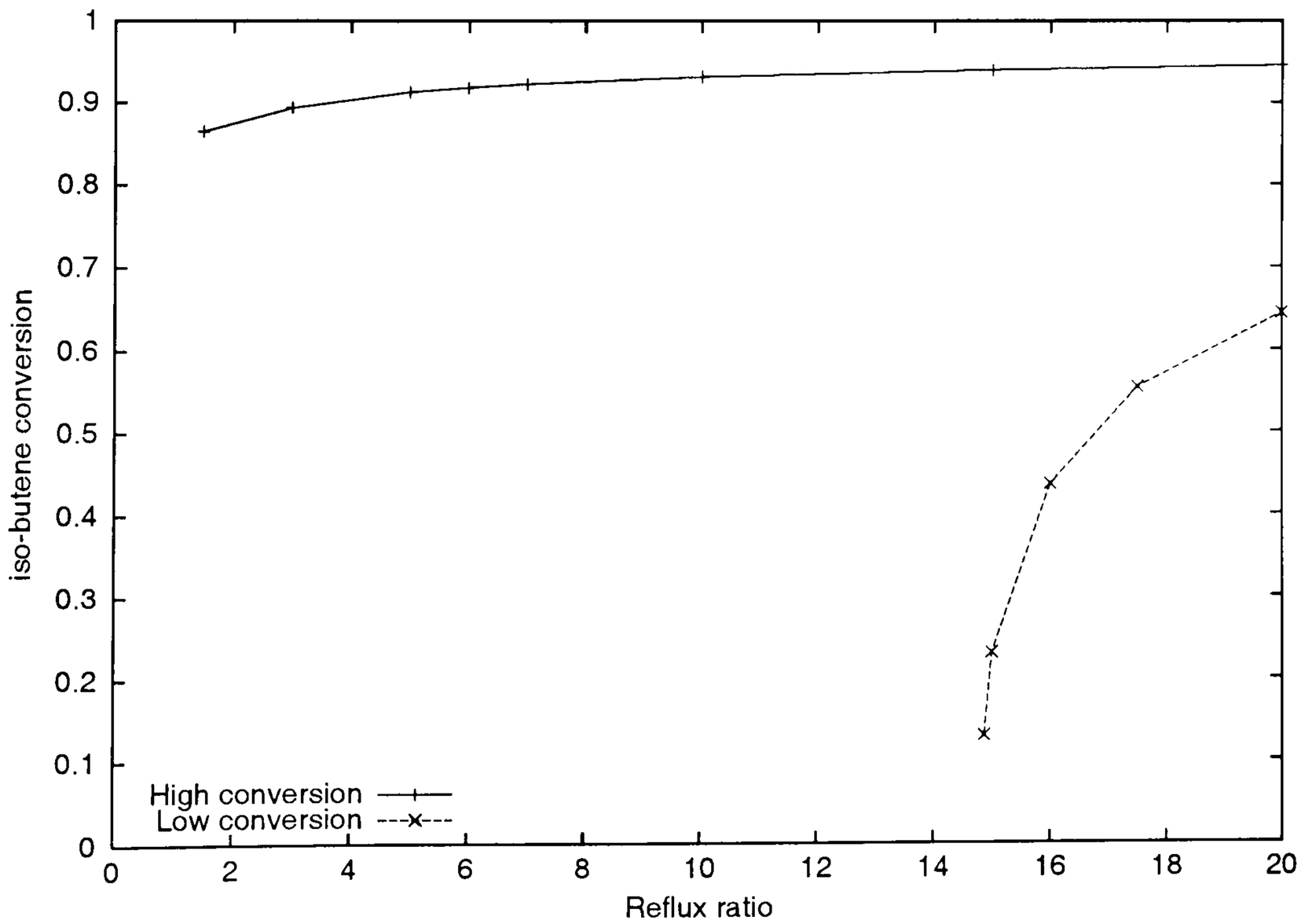

Figure 3.9: Conversion for a MTBE column. $B = 197 mol/s$. MeOH feed at stage 4.

The experiment suggested, that when the methanol and the iso-butene are fed in the reactive zone, the more distant these feeds are, the greater reflux ratio needed for multiplicity to appear. When the methanol and iso-butene feeds are distant the

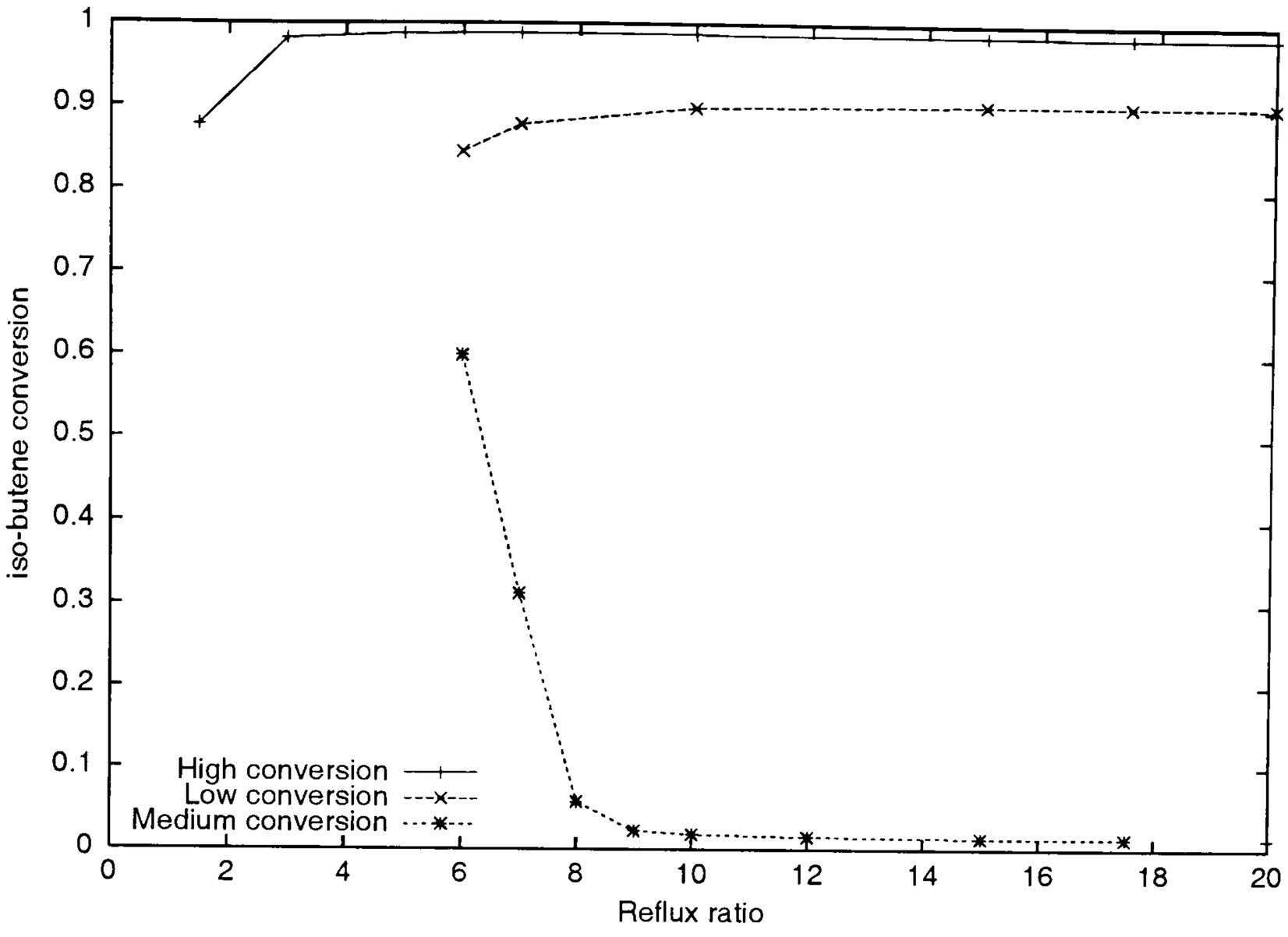

Figure 3.10: Conversion for a MTBE column. $B = 197mol/s$. MeOH feed at stage 10.

effect the separation and the reaction effects are more balanced. If the reflux is high enough, the differences in reactant composition through the reactive section become lower favouring reaction. Consequently, OMSS can appear. On the other hand, when the feeds are close the reaction effect becomes more important easily and OMSS appears for lower reflux ratios. Thus, the results suggest that multiplicities appear when the reaction effects are more important.

For the methanol feed location at stage 14, OMSS also appears. However, it would be expected that the high conversion states were difficult to achieve. Furthermore, the difference between the high conversion and low conversion states is large. The solution says that it is possible to get either 98% or almost zero conversion with the same input values. This process could be difficult to operate and control.

Figures 3.9, 3.10 and 3.11 showed very different shapes for the three methanol feed locations analysed. Therefore, the effect of the methanol feed location on the reactive distillation column will be analysed.

Although operating the column with the methanol feed at stage 10 increases the possibility of OMSS at lower reflux ratios, it is advantageous compared with the system with the methanol feed at stage 4 because it can achieve better conversion. Note that when the methanol is fed at stage 10, it is possible to achieve high

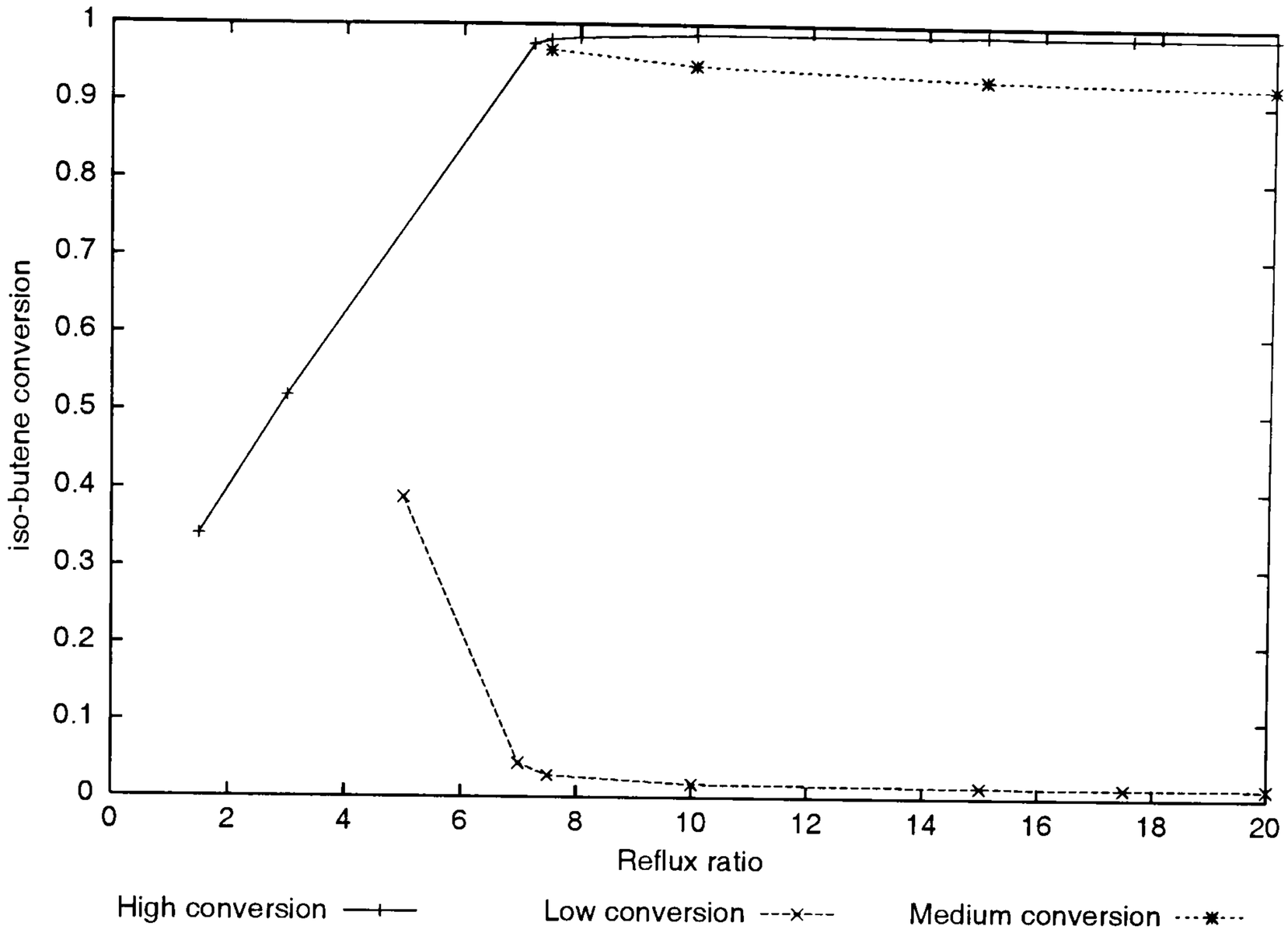

Figure 3.11: Conversion for a MTBE column. $B = 197mol/s$. MeOH feed at stage 14.

conversions with relatively low reboiler heat duty (Figure 3.12). On the contrary, when the methanol is fed at stage 4, and the reactant feeds are far from each other, it requires high reflux ratio and high reboiler heat duty to get the maximum conversion (Figure 3.13).

For the column in which the methanol is fed at stage 10, at relatively low reflux ratios OMSS appears. We notice that the reflux ratio equal to six is a delicate operating condition since the reboiler heat duty gradient between the high and medium conversion steady states is relatively low, about 3 MW (Figure 3.12). The figure shows that if a disturbance occurs and the heat is increased, the column could arrive to the low conversion steady state. An actual column operation with the present settings might use the reboiler heat duty to control the reboiler level, so a scenario like that described is possible.

It is important to note that both in the methanol feed at stage 4 case and methanol feed at stage 10 case, the low conversion steady state solution results in a higher reboiler heat duty. These results agree with the results for the MTBE column with RQ_{reb} inputs. At constant reflux ratio, the increment of the reboiler heat duty can improve the process until a maximum conversion is found. A further increment of the reboiler heat duty may result in lower conversions.

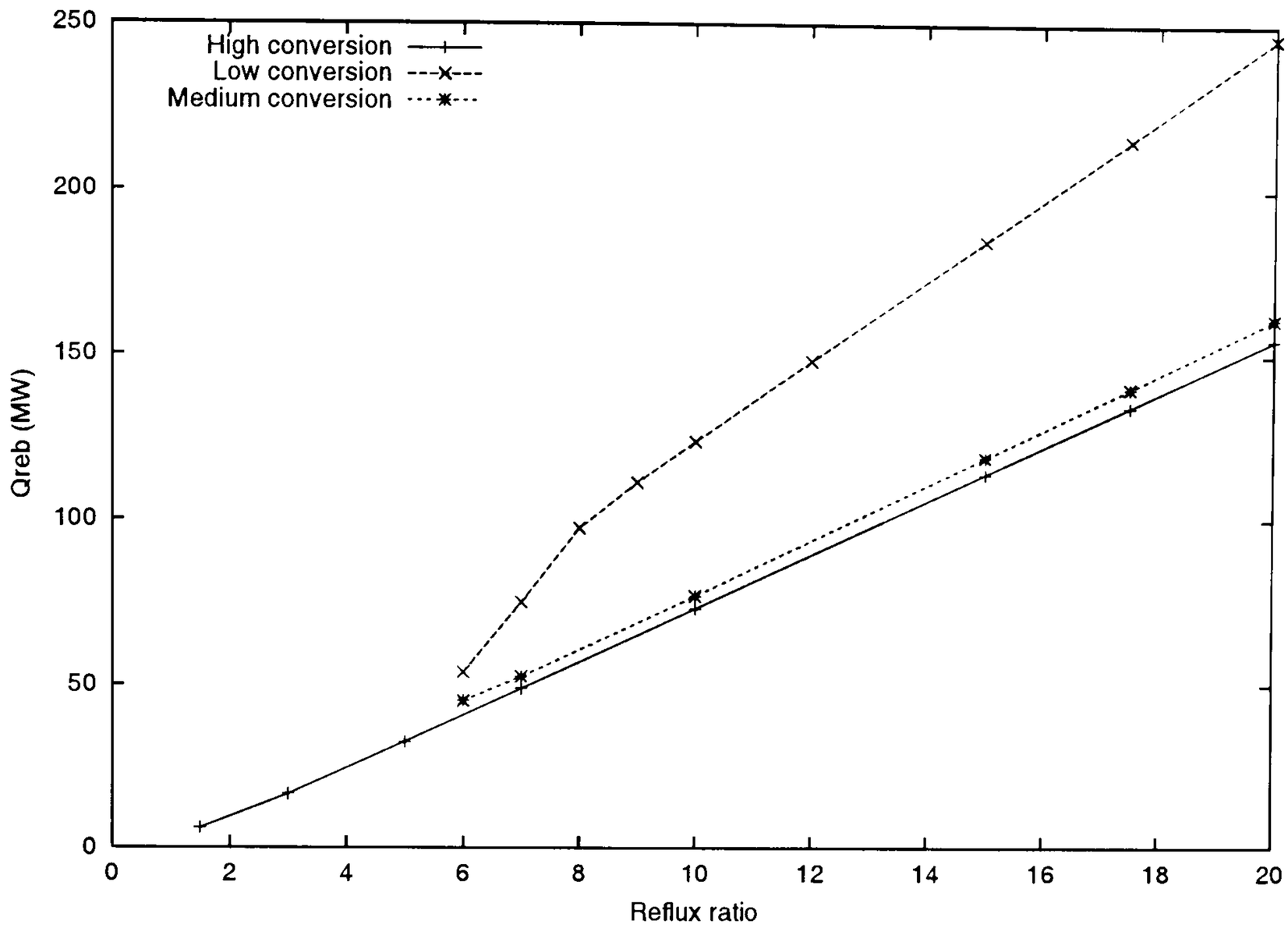

Figure 3.12: Q_{reb} for a MTBE column. $B = 197mol/s$. MeOH feed at stage 10.

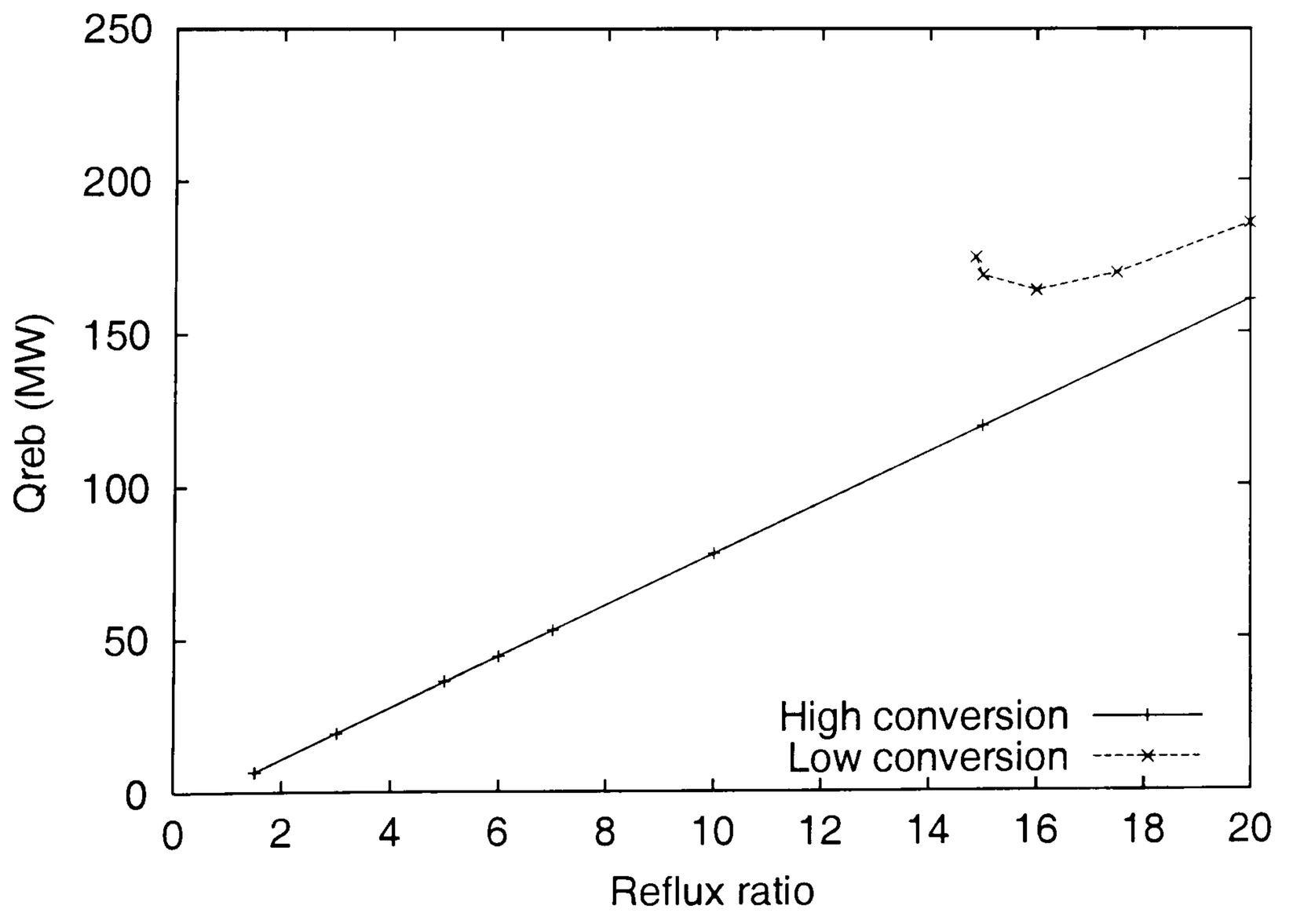

Figure 3.13: Q_{reb} for a MTBE column. $B = 197mol/s$. MeOH feed at stage 4.

Change on the plates number

The results found from the analysis on feed location suggested that this can be a crucial factor for the column operation. The experiment also suggested that it is when the reaction becomes more important that OMSS appears. This suggests that increasing separation would balance the reaction effect and it would be more difficult to find OMSS.

Since the iso-butene conversion can be affected by the separation in the stripping section,it was decided to add 4 stages in such a section. The input pair used was RB to compare with Case 3. The bottom flow rate was made constant and equal to 197 mol/s. The reflux ratio was varied from 1.5 to 20.

However, the results were very different to those expected and were similar to the results for the column with 17 stages (Case 3). In fact, the minimum reflux ratio at which OMSS occurs is almost the same. The results are presented in Figure 3.14. The results suggest that the stages number in the separation sections is not as important as the feed location.

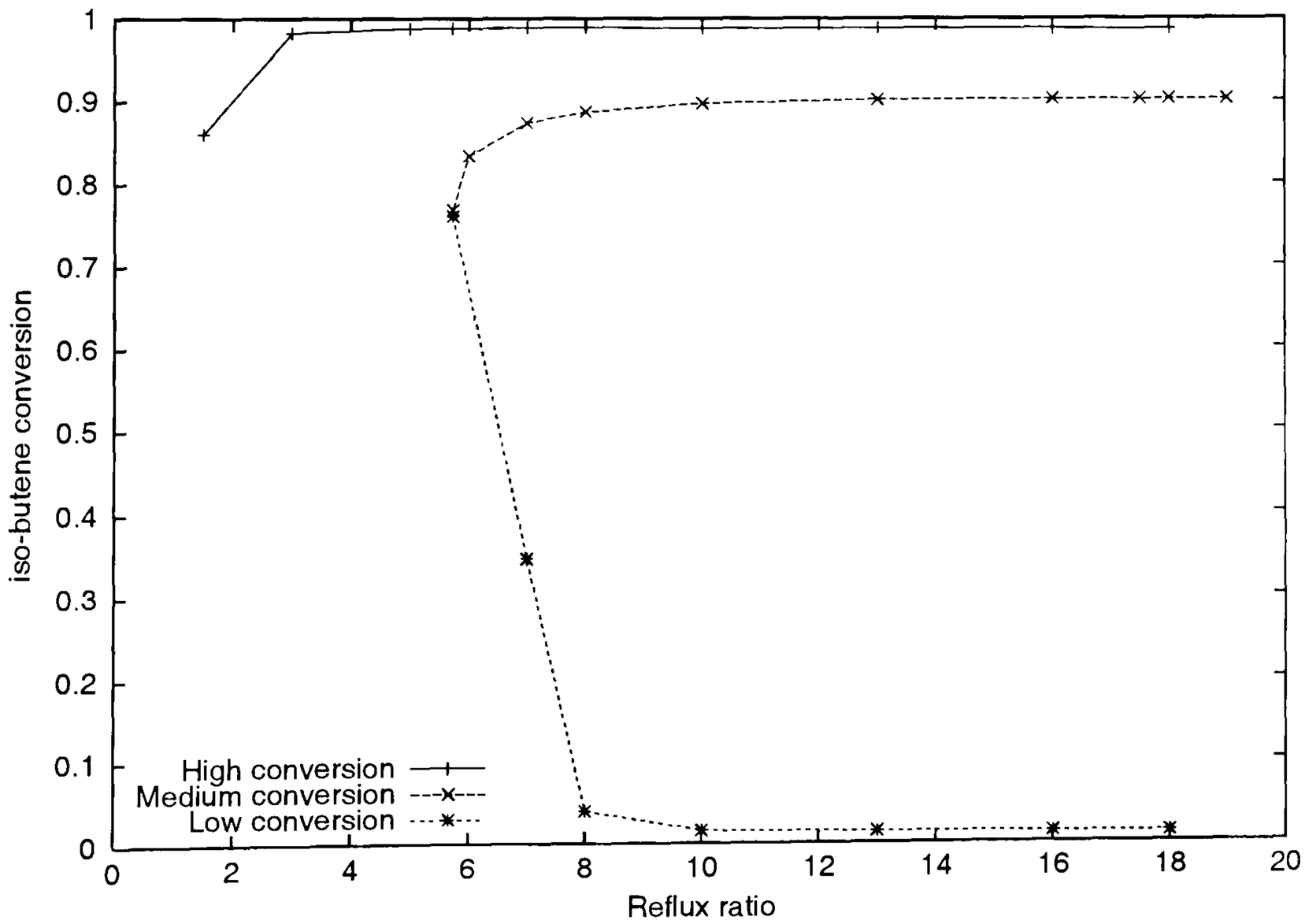

Figure 3.14: Iso-butene conversion for a 21 stages MTBE distillation column. B = 197 mol/s.

3.3.4 OMSS in MTBE reactive distillation and some other input pairs

The results shown in the two preceding sections suggested that OMSS for the MTBE process was perhaps possible for most of the commonly used input pairs in distillation.

Instead of repeating the process followed for the RQ_{reb} and RB input pairs shown above, the problem with fixed reflux ratio and methanol liquid mol fraction for the reboiler, $x_{17,MeOH}$, was solved. The solution of this problem allows to find steady state solutions for further input pair and OMSS relationship analysis. The MTBE column was described in Section 3.3.2. The methanol feed is located at stage 10 and the C_4 feed at stage 11.

A solution *grid* was created by solving problems defined between the following input ranges:

$$x_{17,MeOH} \in [0.01, 0.98]$$

and

$$R \in [1.5, 18]$$

The initialisation to find the different solutions was a solution for the same column that had a reflux ratio equal to 7 and $x_{17,MeOH}$ equal to 0.5. Problems to find the solutions were found for the extreme pairs. Solutions close to these points were necessary to initialise the simulation. In some cases no solution was found.

In the following section the results are presented as input pair combinations.

Reflux ratio as input

Most of the input pairs containing reflux ratio presented OMSS. Next are presented the results for possible configurations for the 17 stages MTBE reactive distillation problem previously described.

The pair reflux ratio and boilup flow, RV resulted in OMSS for large internal flow rates. Results are shown in Figure 3.15. In this case, the output multiplicity appears when the low reflux ratio equals 5. The same figure shows us that the multiplicity zone is magnified as the boilup increases.

When the reflux ratio is paired with the reboiler reflux ratio, R_B, defined as the ratio between the reboiler boilup and the bottom flow rate, the results are similar

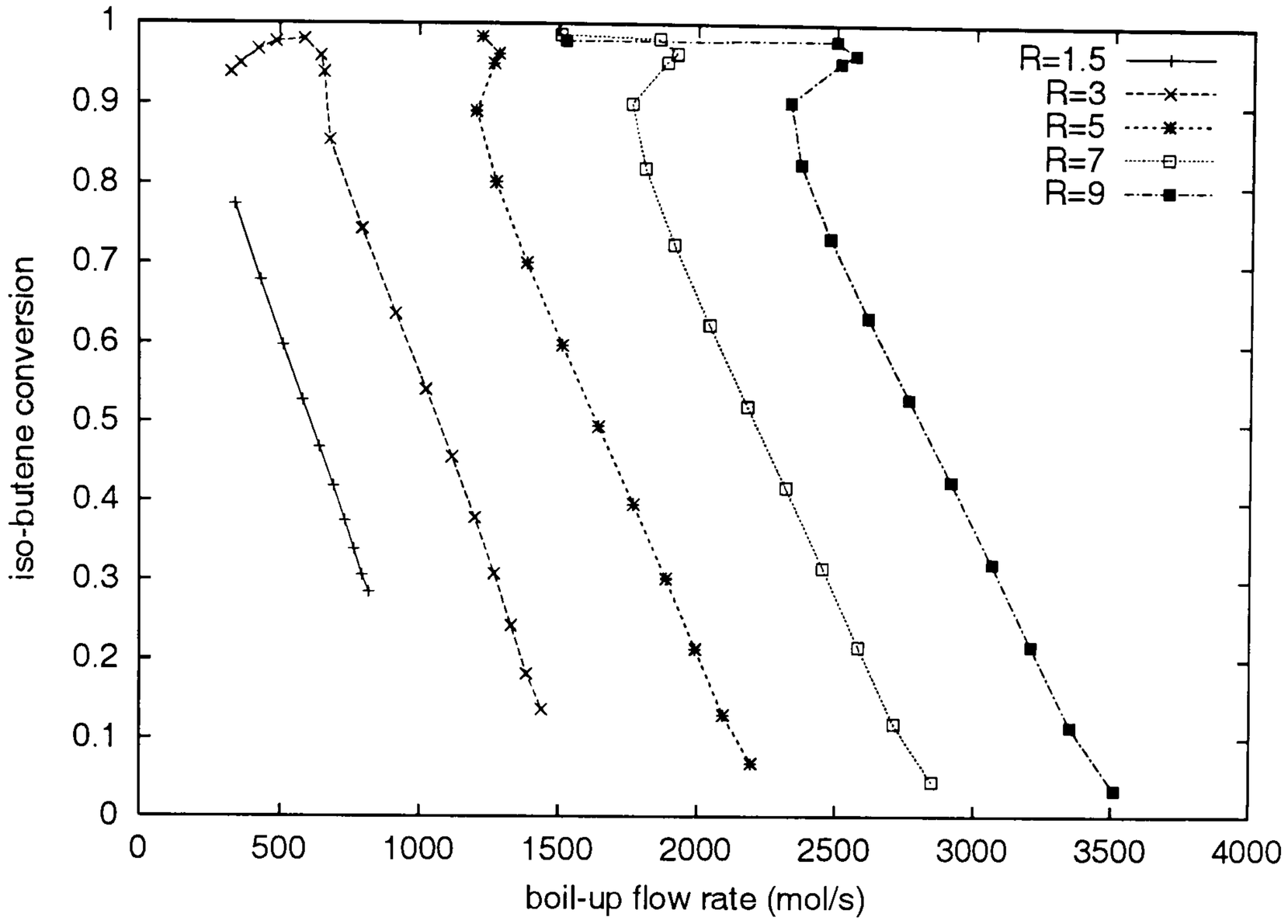

Figure 3.15: Iso-butene conversion for a MTBE column. Methanol feed location at stage 10. RV configuration.

to the previous case. The system produces OMSS when the internal flow rates are high (Figure 3.16). This result is important because this configuration eliminates any possibility of multiplicity due to transformation between molar internal flow rates and mass external flow rates commonly found in distillation. This means that multiplicity Ia could be ruled out as the possible multiplicity type in the studied column.

It was shown before that the combination reflux ratio R and reboiler bottom flow rate B may result in OMSS. This was also found with the present experiment. Figure 3.17 confirms that a bottom flow rate equal to 197 mol/s produce OMSS if the reflux ratio is greater than seven. These results show that in this case, the combination of high internal flow rates, represented by high reflux ratios, are likely to yield OMSS for the MTBE problem.

Reflux rate as input

One input pair commonly used in distillation is the pair reflux rate and reboiler boilup, LV. This configuration may produce also OMSS for the MTBE column. Figure 3.18 shows how three different conversions can be achieved by the same

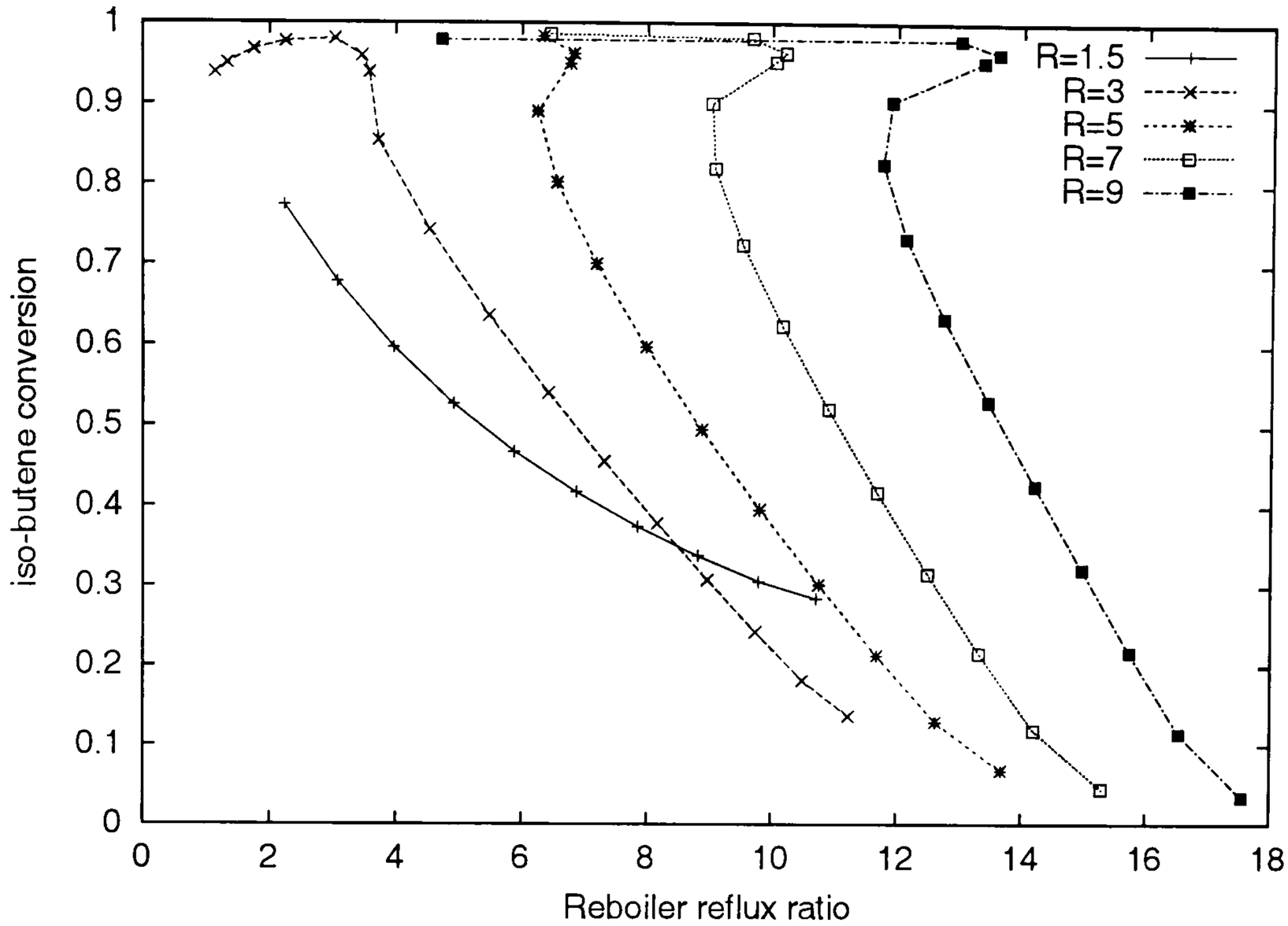

Figure 3.16: Conversion for a MTBE column. RR_B inputs.

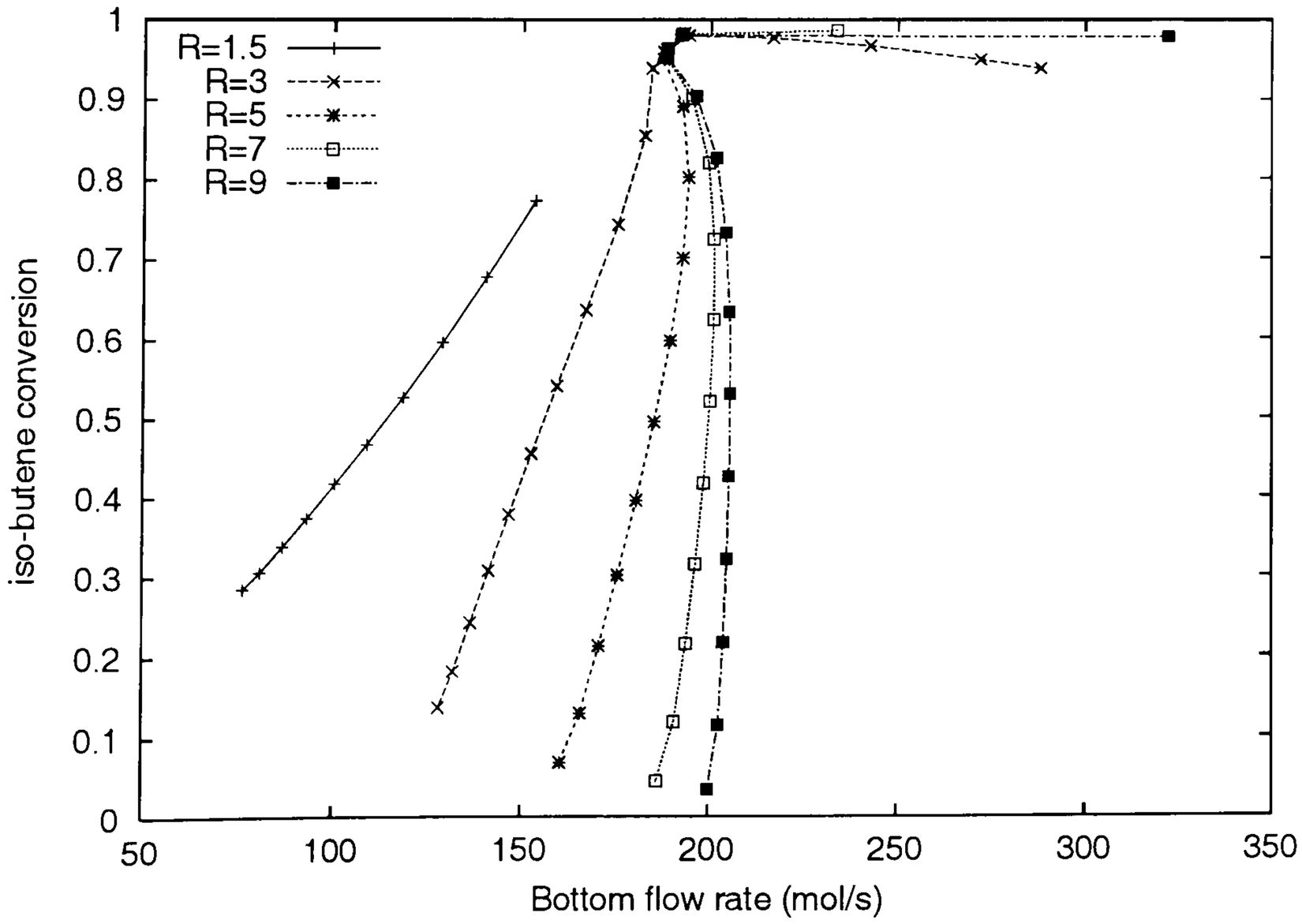

Figure 3.17: Conversion for a MTBE column. RB inputs.

reflux rate and boilup values.

More illustrative is to plot the iso-butene conversion in terms of the reflux rate and the boilup. This three dimensional plot is seen in Figure 3.19. This figure shows that this configuration can be extremely inconvenient since low and high conversions can be produced with the same LV values.

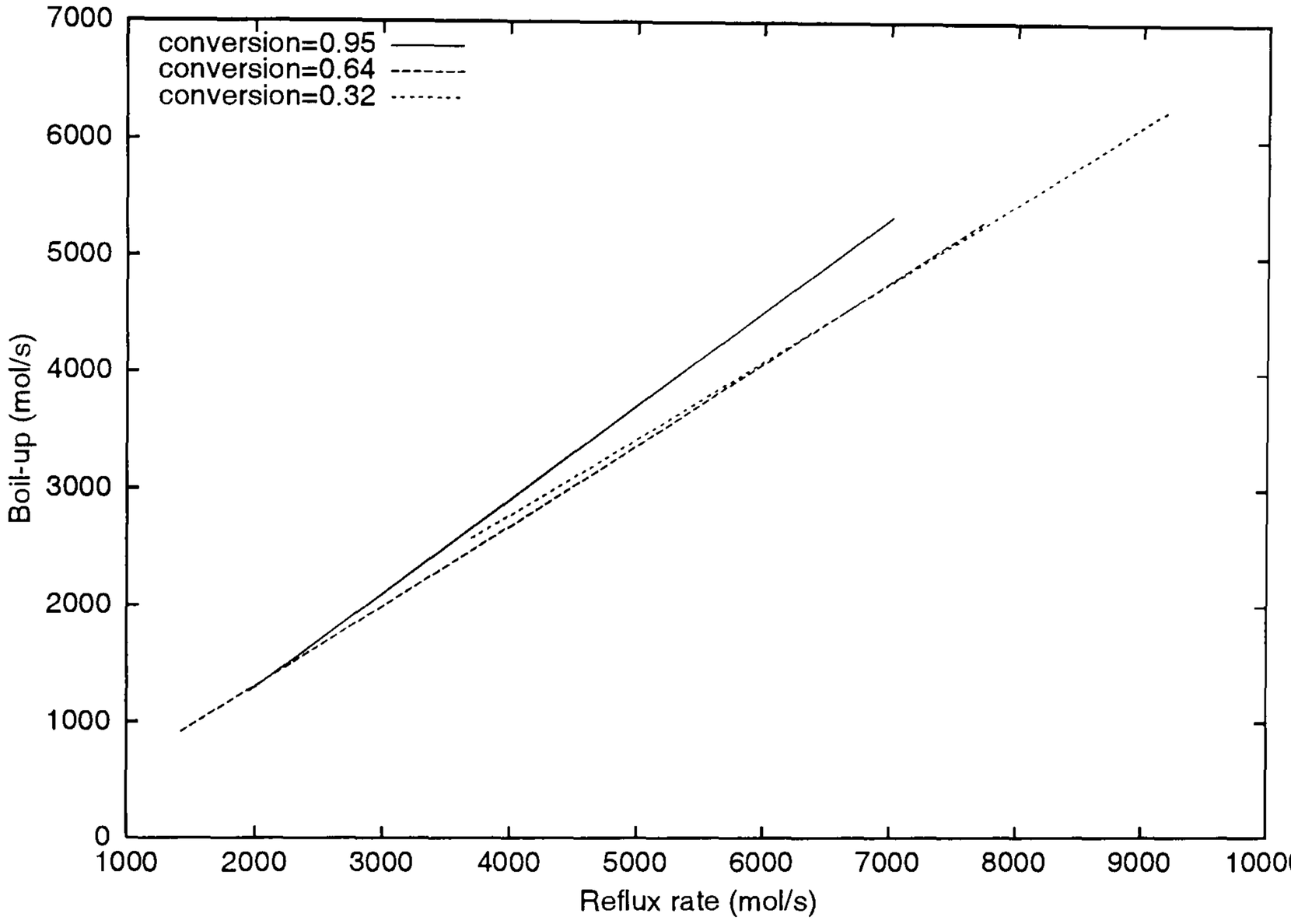

Figure 3.18: Iso-butene conversion and its relationship with the input pair LV. MTBE column, methanol feed location at stage 10.

Another possible pair is the reflux rate and the bottom flow rate LB. This pair can also produce OMSS. Figure 3.20 shows the relation between the input pair LB and the iso-butene conversion. The projections of the conversion on the plane LB (Figure 3.21) show that OMSS occurs when the reflux rate is greater than 2000 mol/s. This value coincide with the obtained for the LV configuration.

Distillate flow rate as input

Figure 3.22 shows the pair reflux ratio and distillate flow rate, RD. When the multiplicity appears it can result in an iso-butene conversion decrease lower than 5%. Higher reflux ratios lay very close to the reflux equal to 9 curve. Observing Figure 3.22 we found that the OMSS may appear when the distillate flow rate is small and high reflux ratios. That is, at high internal flow rates.

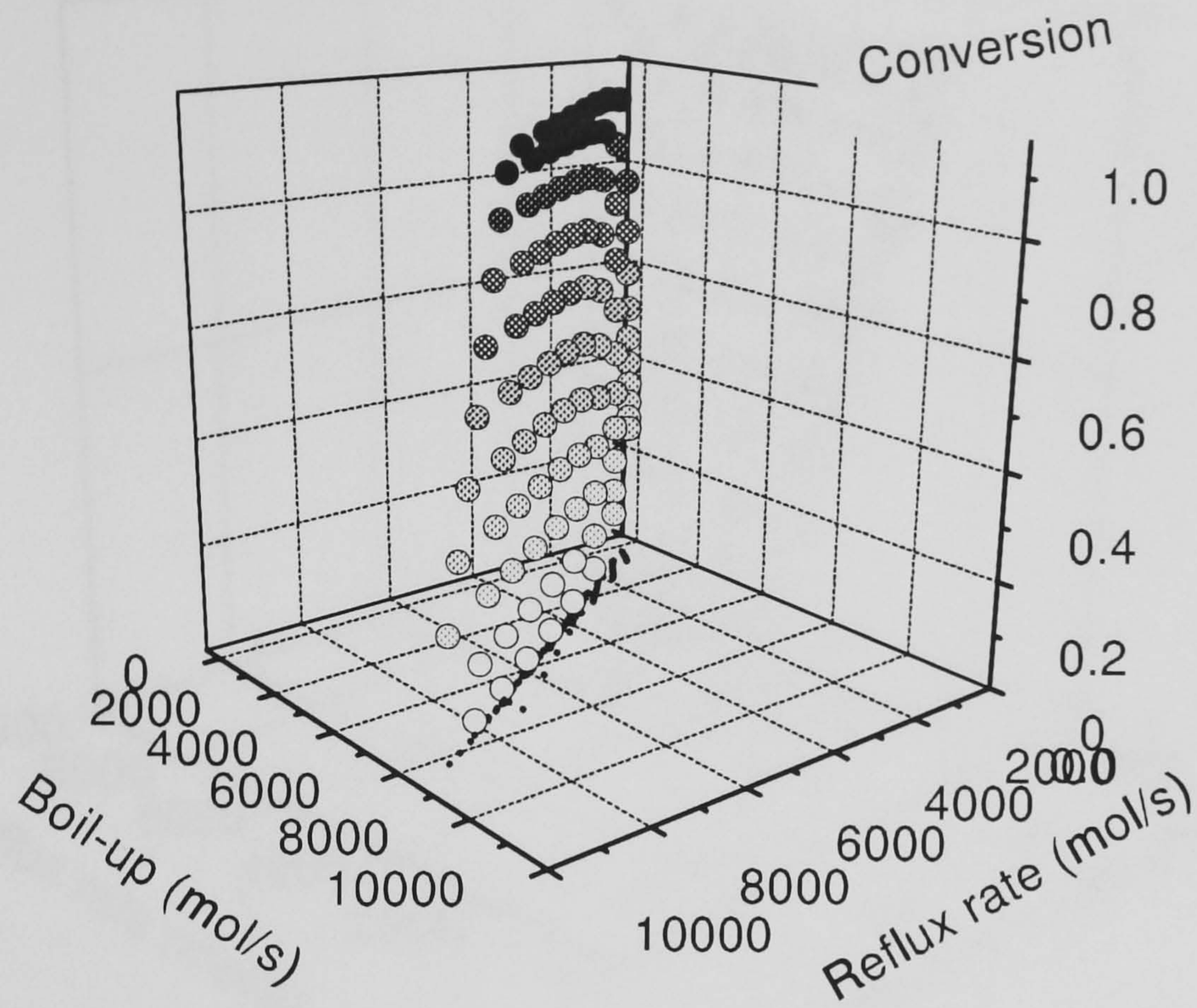

Figure 3.19: Iso-butene conversion and its relationship with the input pair LV. MTBE column, methanol feed location at stage 10. The darkest points represent highest conversion.

Another possible combination is the pair distillate flow rate and bottoms flow rate, DB. Figure 3.23 shows that higher conversion is obtained when the bottoms flow rate is higher. A conversion projection on the plane DB (Figure 3.24) shows that when the distillate and bottom flow rates are relatively high, the conversion reaches its maximum. Moreover, the results presented in this figure suggest that there might not be OMSS for this configuration.

On the other hand, the input pair distillate flow rate and reboiler heat duty, DQ, seems not to present OMSS (Figure 3.25). The conversion projection on the plane DQ (Figure 3.26) shows that higher conversion is found when the distillate flow rate is low. A possible explanation for this result is that low distillate flow rates allow more iso-butene back to the reactive zone.

Mass pair inputs

The importance of the mass flow rates presentation rests on the fact that in actual distillation operation this is the sort of flow that would be used.

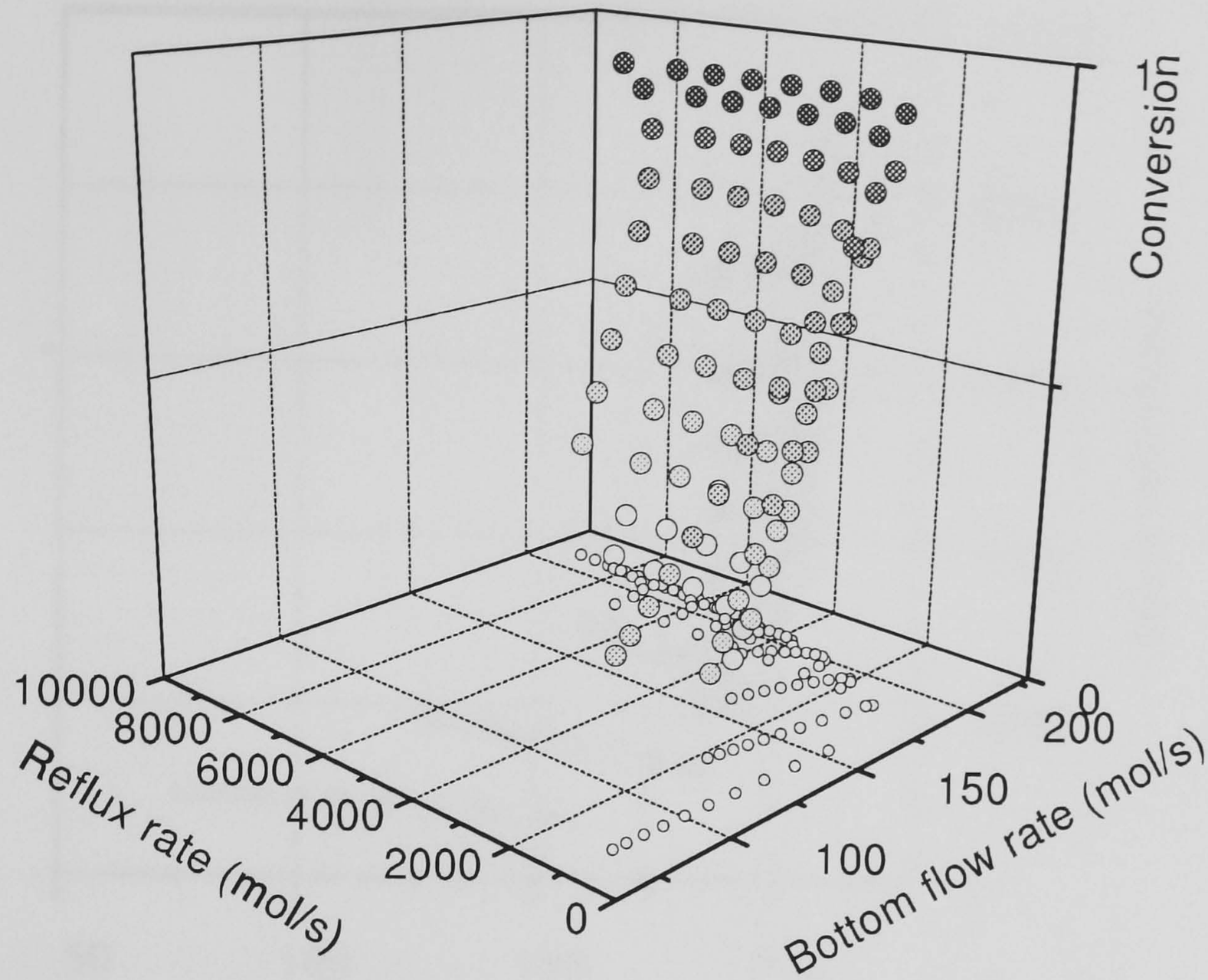

Figure 3.20: Iso-butene conversion and its relationship with the input pair LB. MTBE column, methanol feed location at stage 10. The darkest points represent highest conversion.

The first input pair analysed is the pair mass distillate, mass bottoms flow rates, $D_m B_m$. Figure 3.27 shows that OMSS can appear. This sort of multiplicity belongs to the type Ia proposed by Jacobsen and Skogestad (1991, 1994). These multiplicities appear for non-linearity that results from transformation of molar internal flow rates and mass external flow rates.

Although it is unlikely to use this configuration for practical purposes, it is important to see that OMSS can also result from transforming from molar to mass flows. This fact is important for reactive distillation since the reactions can change the number of moles.

The second input pair analysed is the pair formed by the mass distillate flow rate and the mass bottom flow rate, $D_m Q$. This pair also presented OMSS (Figure 3.28). In this case the OMSS is present only when the distillate flow rate is high. The shape of the conversion projection on the plane $D_m Q$ (Figure 3.28) suggests that this input pair could be more easily manipulated to produce high conversion. OMSS emerges due the mass-molar transformation for the internal and flow rates.

Summarising, different input pairs have been tested for the MTBE reactive distil-

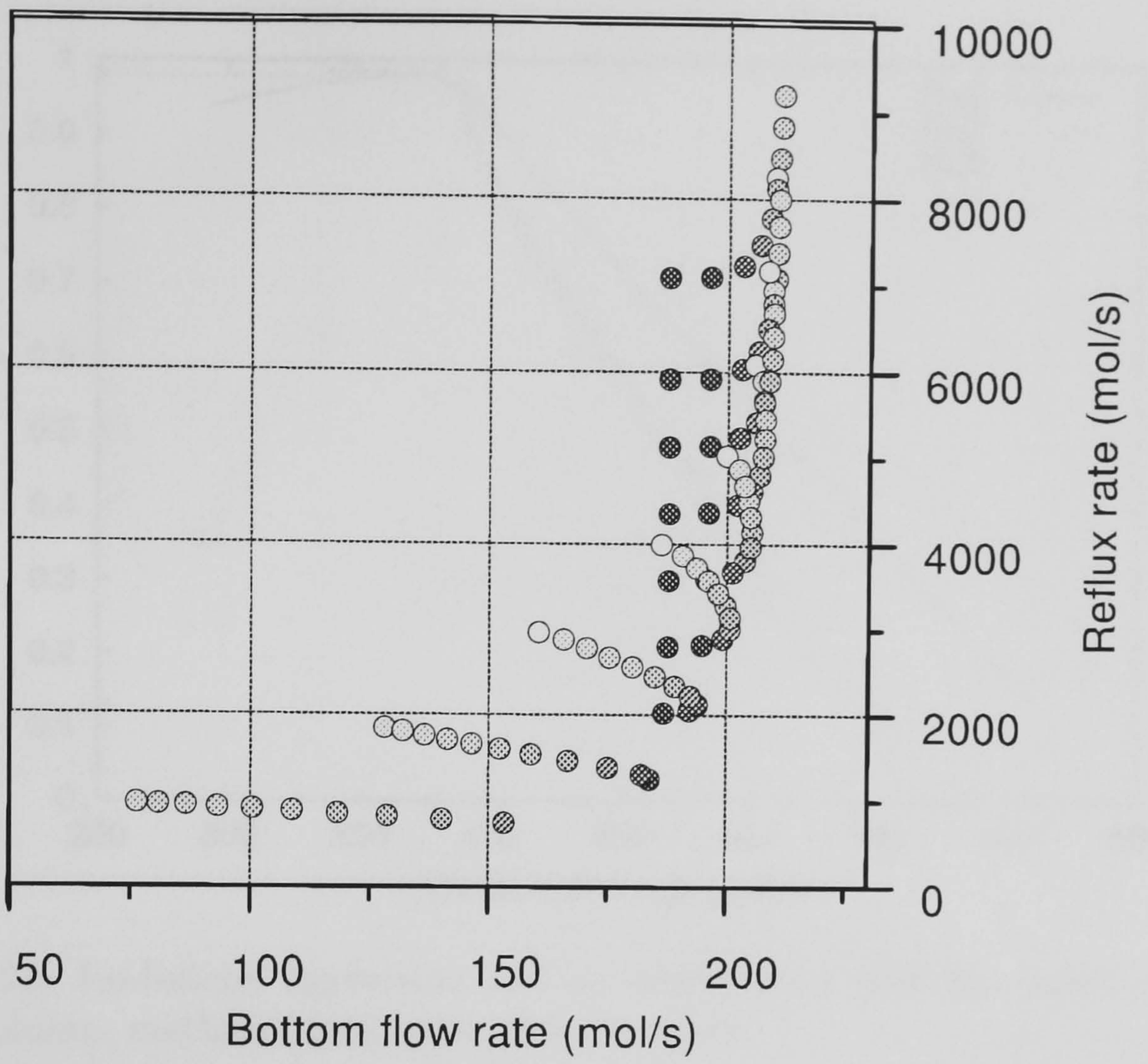

Figure 3.21: Iso-butene conversion projection on the plane LB. MTBE column, methanol feed location at stage 10. The darkest points represent highest conversion.

lation column example. With the exception of the schemes directly related with external flow rates, most of the schemes presented OMSS when the internal flow rates were high. It is difficult to see in 3D diagrams and their projections in the input plane the transitions between IMSS and OMSS. However, for all the diagrams related to the reflux rate, it is possible to see that if for low internal flow rates there is IMSS, for high internal flow rates there is OMSS.

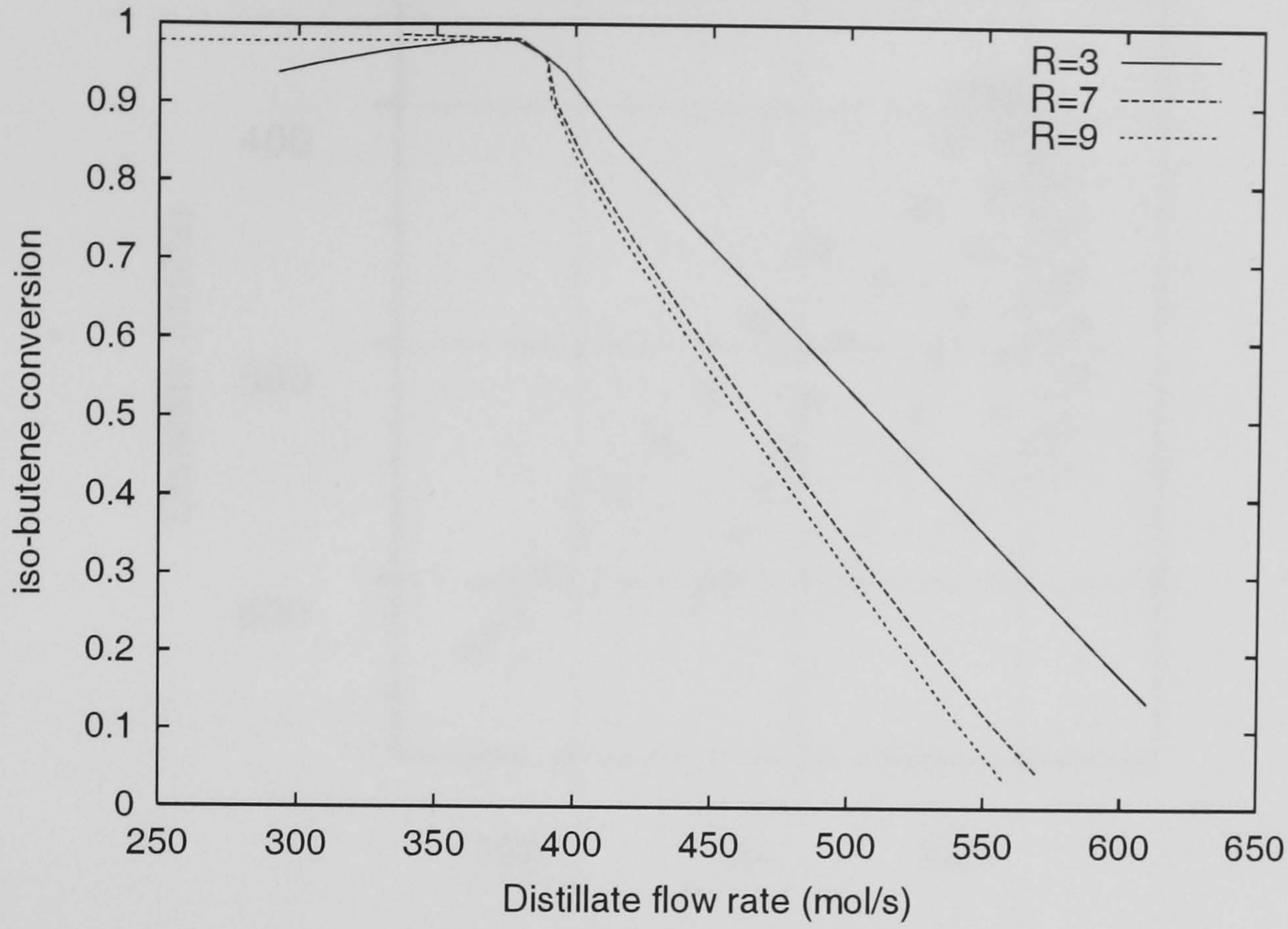

Figure 3.22: Iso-butene conversion and its relationship with the input pair *RD*. MTBE column, methanol feed location at stage 10.

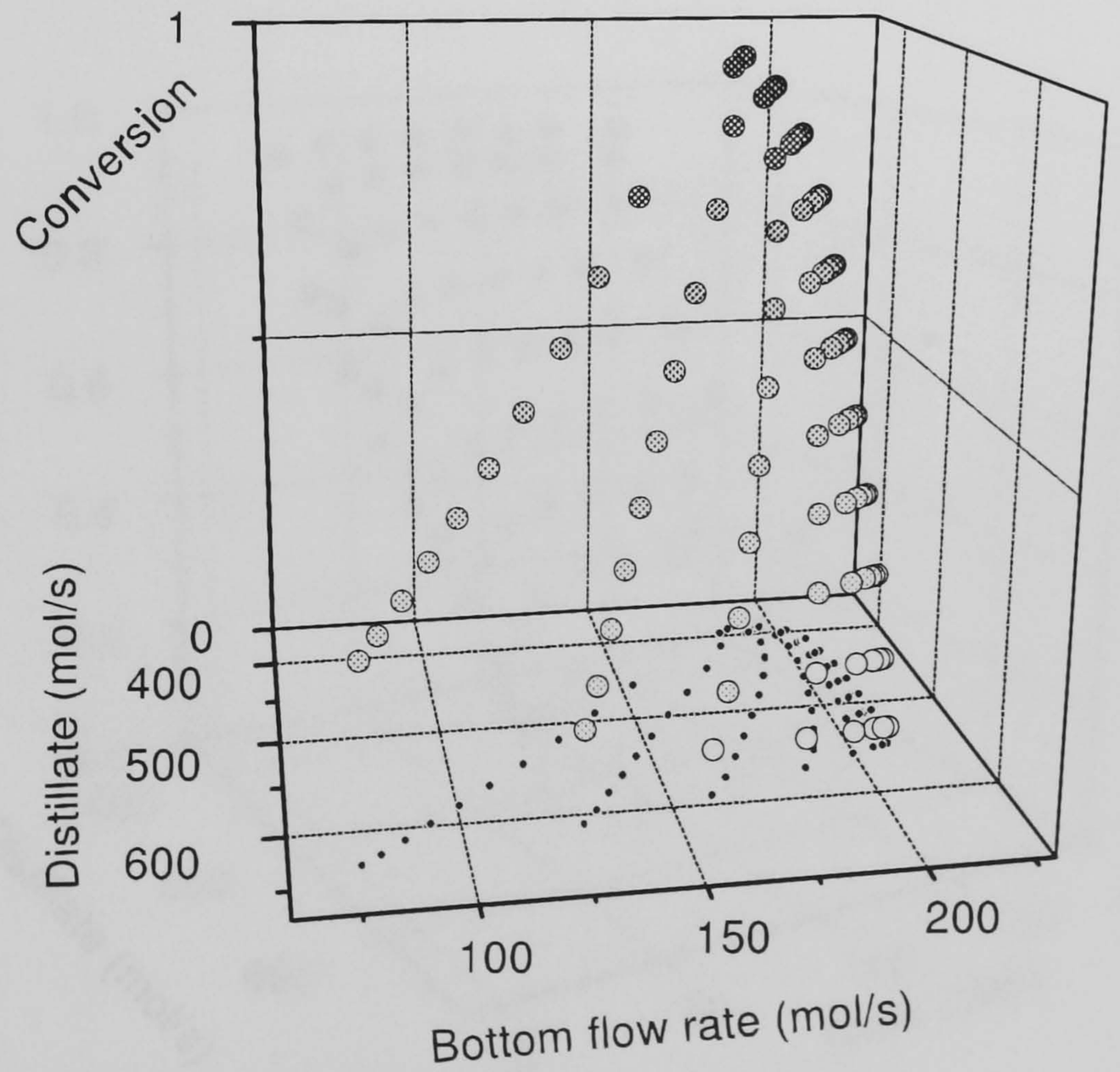

Figure 3.23: Iso-butene conversion and its relationship with the input pair *DB*. MTBE column, methanol feed location at stage 10. The darkest points represent highest conversion.

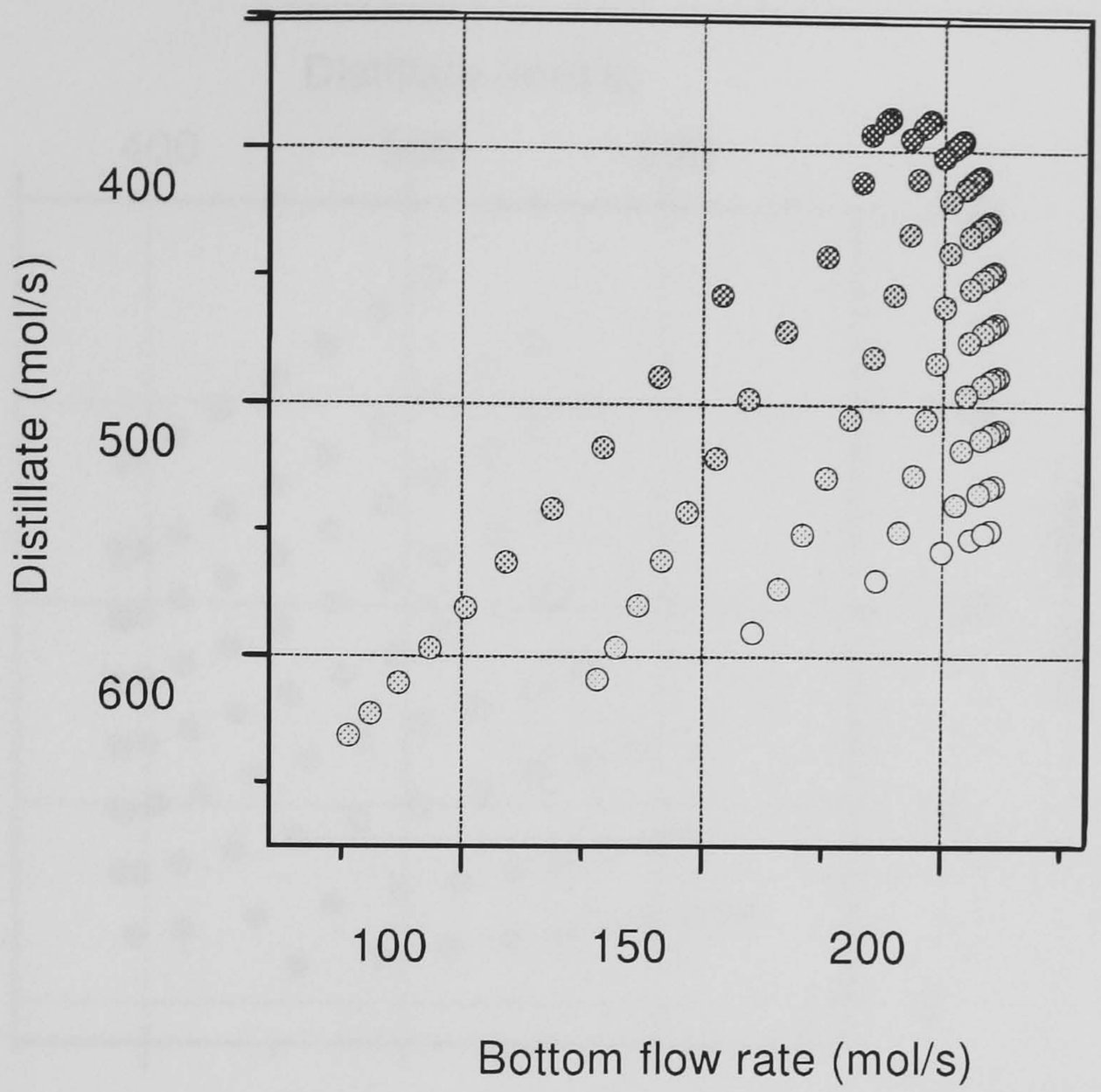

Figure 3.24: Iso-butene conversion projection on the plane DB. MTBE column, methanol feed location at stage 10. The darkest points represent highest conversion.

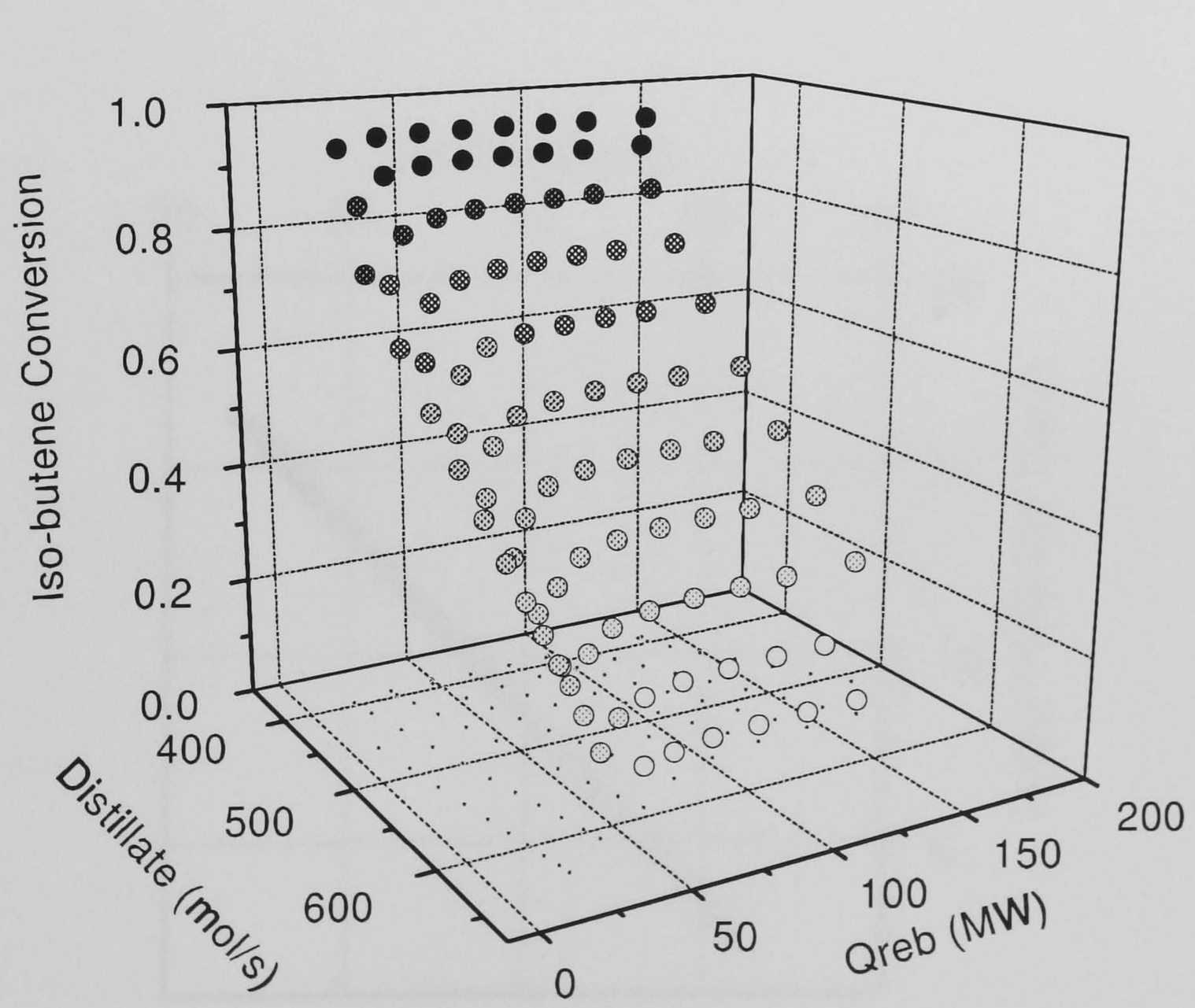

Figure 3.25: Iso-butene conversion and its relationship with the input pair DQ. MTBE column, methanol feed location at stage 10. The darkest points represent highest conversion.

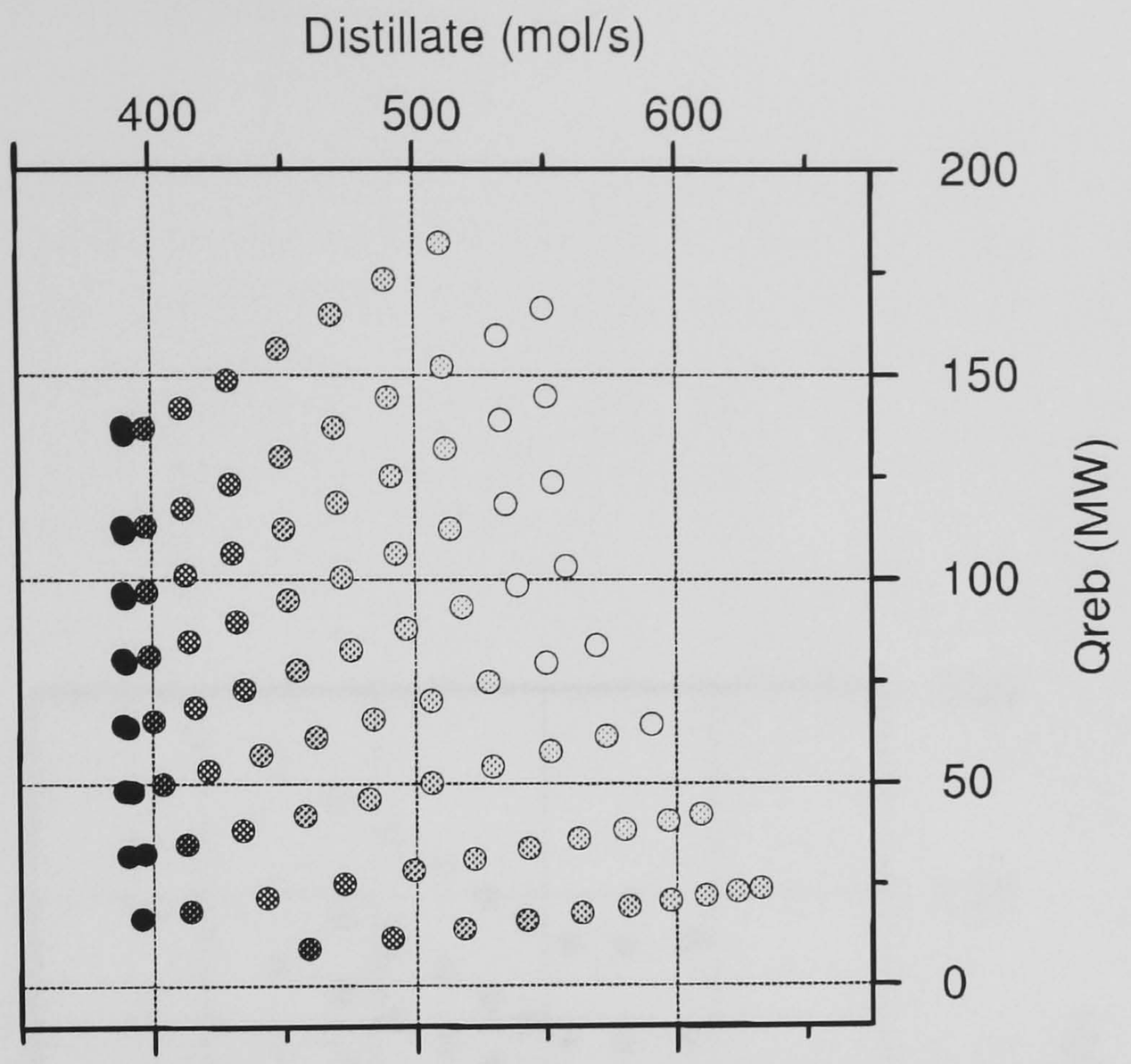

Figure 3.26: Iso-butene conversion projection on the plane DQ. MTBE column, methanol feed location at stage 10. The darkest points represent highest conversion.

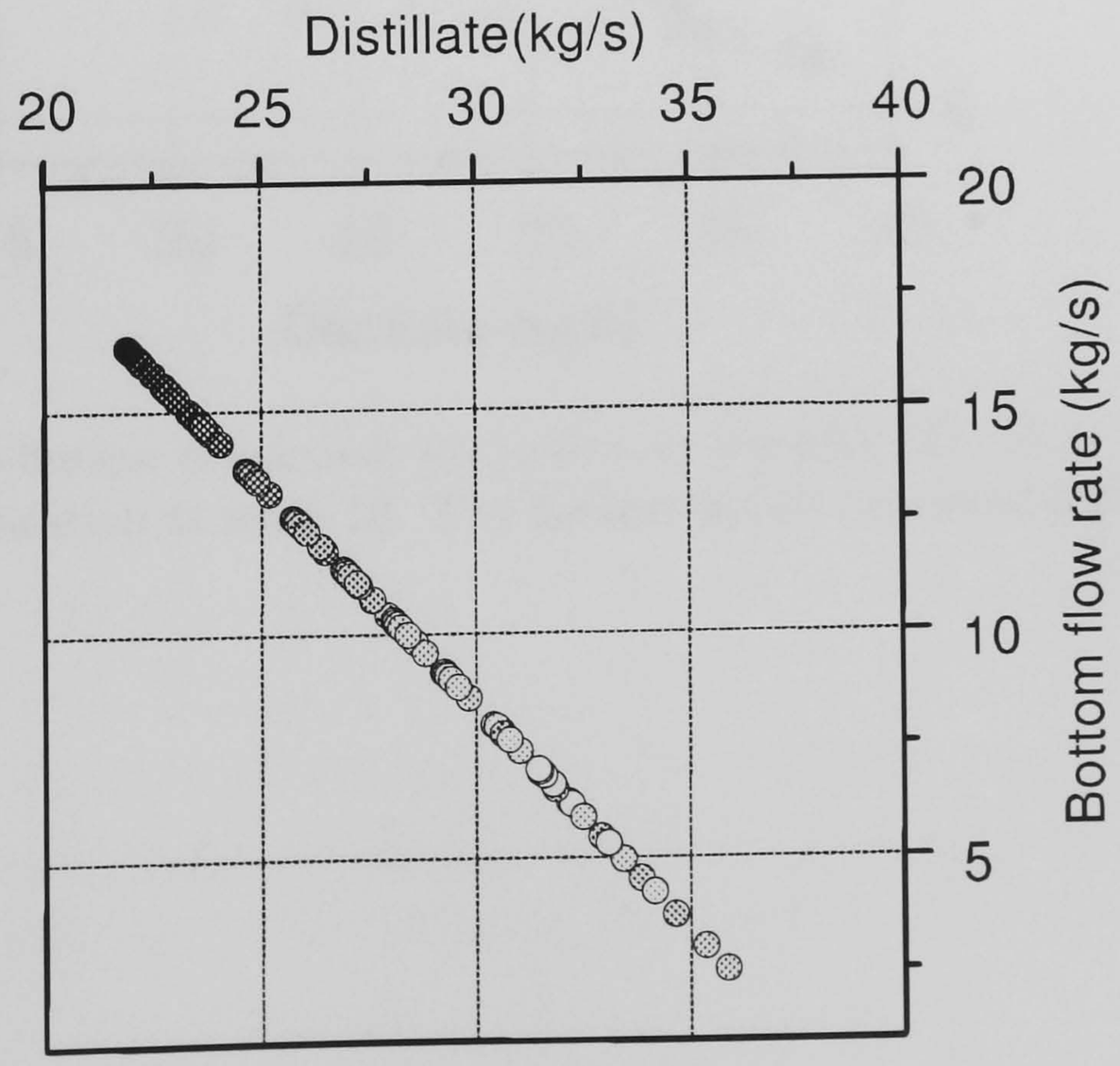

Figure 3.27: Iso-butene conversion projection on the plane $D_m B_m$. MTBE column, methanol feed location at stage 10. The darkest points represent highest conversion.

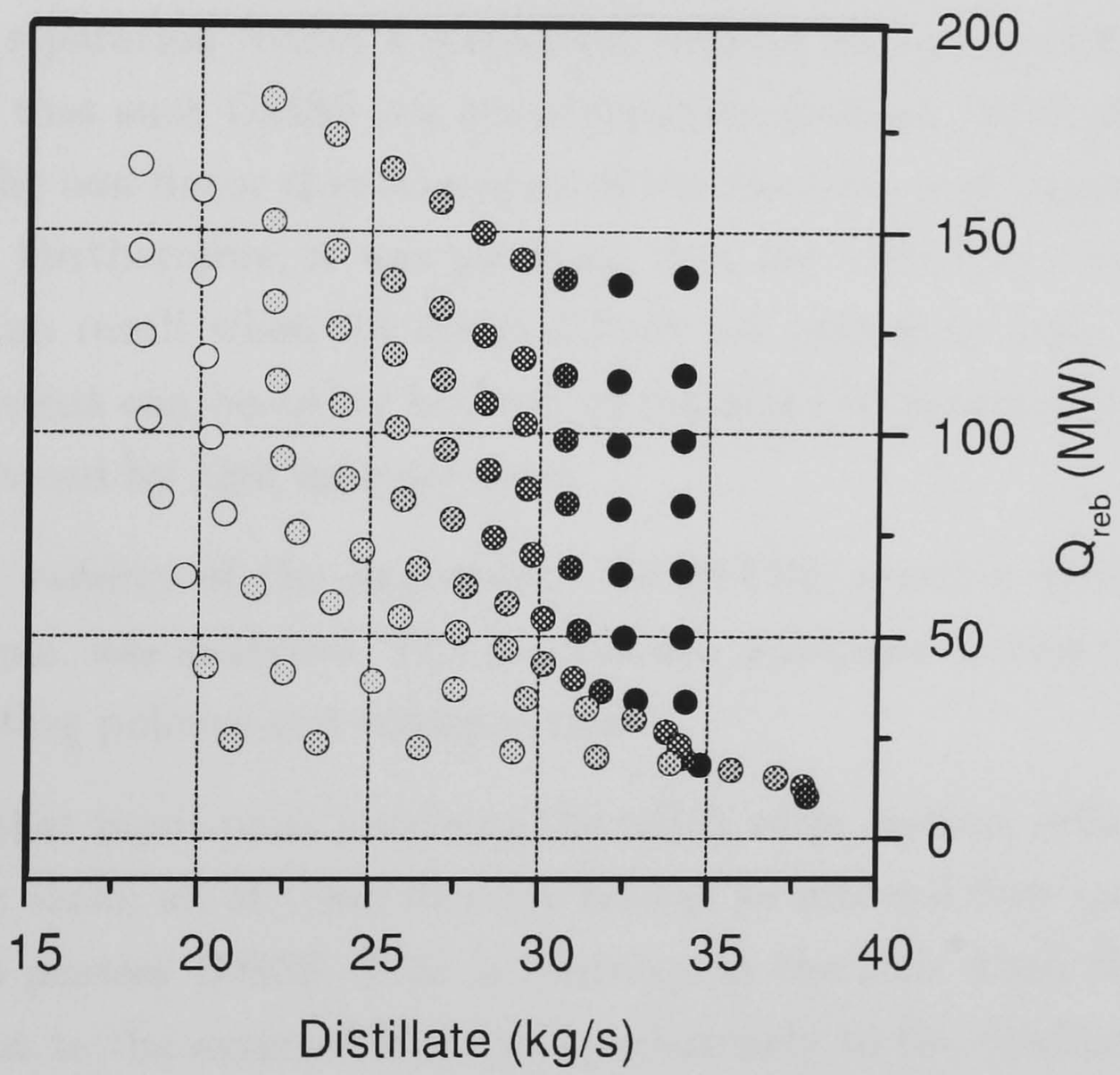

Figure 3.28: Iso-butene conversion projection on the plane $D_m Q_{reb}$. MTBE column, methanol feed location at stage 10. The darkest points represent highest conversion.

3.4 Conclusions

The literature review provided some possible explanations for the OMSS that can occur in reactive distillation. It was suggested that OMSS can emerge when the volatility difference between reactants and products is large (Ciric and Miao, 1993). It has also been suggested that OMSS can appear as a result of the interaction between chemical and physical equilibria or be the interaction between reactive and non-reactive zones within the column.

The hypothesis of this chapter was that it is possible to generalise that the relationship reaction-separation within a distillation column may yield OMSS. However it was proposed that such OMSS is a transformation from an IMSS phenomena that results from the non-linear characteristics of the reactions and separation and their combination. Furthermore, it was proposed that the OMSS in a reactive distillation column can result when the internal flows are extremely high. Moreover, the OMSS phenomena can be either boosted or inhibited with certain input combinations characterised by high internal flows.

To study the validity of the hypothesis, the MTBE reactive distillation, a well studied example, was analysed. The process was simulated testing the influence of process operating policies and configuration.

It was found that input pairs involving the reflux ratio, boilup, reflux rate and the reboiler reflux ratio, all of them directly related to internal flow rates, were more susceptible to possess OMSS. This is contrary to the case when the inputs were directly related to the external flow rate, particularly to the distillate flow rate.

The use of mass input pairs revealed that the multiplicity type Ia related with the transformation between internal molar flow rates and the external mass flow rates (Jacobsen and Skogestad, 1991 and 1994) is very likely to appear in the process.

Although the process was deeply analysed, no *measure* of OMSS susceptibility was found from the simulations. Nor was a minimum internal flow rate for the OMSS occurrence found, mainly because such a minimum depends on the input pair and the column configuration. For instance, when the methanol feed was located at stage 10, the minimum reflux rate at which OMSS would emerge was about three times the feed. However, when the methanol feed was introduced at stage 4, the mininum reflux rate at which output multiplicity appears, is eight. The results allow to generalise that if for a reactive distillation column there is IMSS at low internal flow rates, there are high possibilities that the same system will posses

OMSS at high internal flow rates. However, the results do not allow to find a general minimum flow rate in which OMSS will occur.

On the other hand, the results suggested that the feed location can influence more the column behaviour than the number of separation stages. The relationship between reaction and separation was well illustrated with the differences between a column with close reactants feeds and a column with distant feeds. Both cases present OMSS once the internal flows are high enough. However, in the first case, the minimum reflux ratio necessary for the occurrence of OMSS is lower. When the feeds are distant the conversion and the possibility of OMSS decreases.

A possible explanation for the findings is that when the internal flow rates were very high the effects of reaction become more important than the effects of separation. That is because, all the reactants are better distributed through the column. Thus, the reaction is favoured.

The results suggest that for reactive distillation system with very different volatilities, inputs directly relative to internal flow rates can result in OMSS if the internal flow rates are high enough.

The results also suggest that since OMSS should be avoided, this issue must be considered during design. A possible way of avoiding it is by limiting high internal flow rates by correct design of input configuration and parameter values, for example reflux ratio.

Here only steady state operation has been studied. Although OMSS is an issue to consider during design, the controllability of the state should also been addressed. Perhaps, an input that is more susceptible to produce OMSS could be more easily manipulated for control purposes.

Chapter 4

Control System Design for Reactive Distillation

The use of control in reactive distillation columns is important to keep the product at constant production rate at the specifications required. Nevertheless, an inadequate controller can destabilise the system. Therefore, a critical part of design is control system design.

In this chapter a method for the control system design of reactive distillation columns is presented and tested with dynamic simulations. Such a method is based on process knowledge and linear control tools. In spite of its simplicity, the method produces good results.

4.1 Preliminaries

4.1.1 Control System Design

During the operation of a process, keeping control is fundamental. The reasons to use a controller are disturbance rejection and change of set points. The basic idea is to keep the system working at desired specifications in spite of anticipated changes (Stephanopoulos, 1987).

On the other hand, an inefficient or an inappropriate controller can create instabilities in the system. For example, in a distillation column, the condenser level could be controlled by the distillate flow rate. If the distillate flow rate is small compared

with the feed flow rate the resulting controller would have a limited action range and it may not cope with flow fluctuations.

In addition, problems may arise because of uncertainty in the model, complex nonlinear relationships between the inputs and outputs, or interactions involuntarily created by manipulating certain inputs. Hence controller design should be undertaken carefully.

The design of the necessary controllers for a determined system is often called *Control System Design.* Although the procedure is not simply a sequence of steps, the following six steps can be distinguished (Boyd and Barratt, 1991):

1. definition of control objectives
2. development of a model for the system
3. design of control structure
4. controller design
5. control system evaluation and tuning
6. controller implementation.

It is expected that this process is not sequential. While designing the controller, for instance, the model assumptions can be inadequate and the model would need to be changed.

The focus of this chapter is on definition of control objective, control structure design and the controller design for reactive distillation. It has been shown that the decisions made during those stages can affect widely the reactive distillation performance (Sneesby *et al.*, 1997a).

The next section discusses the definition of control objectives and control structure design. The chapter continues with controller design.

4.1.2 Control Structure Design

Control Structure Design is that part in control system design in which the engineer decides what variables (*manipulated* or *input* variables) can be used to control certain important variables (*controlled* or *output* variables). That is, control structure design is the design stage when the engineer has to express general control objectives into specific and physically achievable control objectives. For instance.

let's suppose that a CSTR for an exothermic reaction needs to be designed. The general control objective is to keep the production rate at a certain value. Since the conversion is related to the mixture temperature, a specific control objective can be expressed as "to keep the reactor temperature at a certain temperature T_s". To control this temperature the flow in the reactor cooling jacket can be used. This sort of decision constitutes control structure design: Once a control objective has been defined, select the "best" variables for achieving such an objective.

Control structure design decisions affect the final design. For example, those decisions determine the selection and location of valves, sensors etc. Moreover the decisions affect the process performance.

In our CSTR example, if the reaction is very exothermic, the use of the flow in the cooling jacket may not be enough for controlling the production rate. Perhaps controlling the feed flow would give better results.

Interconnections within a process increase the need for careful control structure design decisions. This is the case of distillation. For example, if the reboiler and reflux drum levels are not controlled the column may present flow fluctuations and the column become unstable (Jacobsen and Skogestad, 1994). Thus, even though our main interest is to control product composition, decisions relative to the level and pressure controllers should not be view as secondary or unimportant.

In reactive distillation the general control objectives are:

- to keep the column stable
- to keep the product composition at the set value

all this in spite of external temperature changes, flow and feed fluctuations, set point changes, etc.

For reactive distillation control structure design decisions are equally important. The next sections summarise how control structure design has been done for reactive and conventional distillation. This review will allow the formulation of the main chapter objective.

4.1.3 Control system design for reactive distillation

Since studies on reactive distillation dynamics are relatively new (Ruiz *et al.*, 1995; Schrans *et al.*, 1996), control system design for reactive distillation has not been

deeply studied. However, there is enough material to distinguish four different kinds of control studies for reactive distillation.

A first branch of control studies corresponds to controller design. In this kind of research a certain control configuration is assumed as the best and a controller is then designed. These kinds of studies may incorporate model uncertainty to design robust controllers (Monroy-Loperena *et al.*, 1999, 2000); or the final controller may be nonlinear (Kumar and Daoutidis,1999; Grüner *et al.*, 2001). In such studies the control quality is evaluated with closed loop simulation. The mentioned studies could have benefited by the study of the controllability of the proposed schemes before completion of the design. That is, some simulation would have been unnecessary. Moreover, some good alternatives for inputs and outputs may be rejected without a good reason.

Secondly, there are a number of investigations in which the control of a certain distillation column was designed and analysed by closed-loop dynamic simulation. For instance, Schrans and de Wolf (1996) studied the performance of three different control schemes for a MTBE reactive distillation column. The input for their column is the reboiler heat duty, and three possible outputs were analysed: Their conclusions were that the selection of the outputs could significantly affect the dynamics of the column. More complex controllers have been designed and analysed with closed-loop simulation. For instance, Al-Arfaj and Luyben (2000) analysed with closed loop simulation, six uncommon control structures for an ideal reactive distillation column. The column has pressure, base level and reactive concentration controllers for the lowest reactive stages. Six control structures are proposed to keep the purity of one of the products in spite of set point changes and variation of the second reactive feed flow. The main result is that some of the control schemes tested cannot cope with the mentioned disturbances, while others help to keep an almost stoichiometric feed. These examples show that although closed loop simulation allows direct observation of the control performance, the use of it may lead to early rejection of many control schemes and that it can be time consuming.

In the third kind of study of reactive distillation control, control structure decisions are made according to specific reactive distillation behaviour. For instance, Sneesby *et al.* (1997a) selected a control structure selection for an ETBE column to avoid input multiplicity. The outputs selected were the temperature beneath the reactive section, which was a nonlinear function of composition, and the top temperature. The input selection was based on testing different inputs by closed-loop simulation. Sneesby *et al.* stressed the relationship between column behaviour and

control system design. Their research also confirms that inappropriate decisions in control input-output selection and controller design can result in instability and poor control performance.

Finally, some authors have considered that it should be possible and positive to use a systematic approach to investigate the different control structure possibilities for a reactive distillation column. After all, for the conventional distillation problem, this kind of decision has benefited from control tools. In (Estrada-Villagrana, Bogle, Fraga and Gani, 1999), we presented a simple study of the use of linear control tools for the selection of inputs and outputs for a MTBE reactive distillation column. The analysis was based on positive zeros and poles analysis, singular value decomposition and relative gain array (RGA). The results suggested that control tools could be used in decision of control structure for reactive distillation. In this chapter, a modification of such a study is used to analyse different control structures for a given example to conclude which one is better. Vora and Daoutidis (2001) designed single input and single output (SISO) controllers for an ethyl acetate reactive distillation column. The pairing between a limited number of inputs and outputs was decided with RGA analysis. Fernholz *et al.* (2001), selected appropriate inputs for an industrial column based on the column behaviour and RGA analysis. The three mentioned studies showed that, in the same fashion as for conventional distillation, control tools can assist the engineer to make better control system design decisions.

The examples presented demonstrate that control system design of reactive distillation should be assisted by process knowledge and simulations. However, it could be assisted as well by different tools. In the next section, a review on the application of control measures for control system design of conventional distillation is presented. The main interest is to show that the use of control tools can help to design the most appropriate controller for conventional distillation.

4.1.4 Control system design for conventional distillation

Distillation is one of the most studied systems in Chemical Engineering. Hence, the following review does not intend to be exhaustive, rather presents examples of the application of tools for the design of distillation columns controllers.

For a simple distillation column that presents only two phases and which reboiler and condenser or reflux drum can accumulate liquid, there are 5 degrees of freedom.

The variables selected can be the feed flow rate, the feed composition, the feed temperature, the distillate flow rate, the reflux ratio, the reflux flow, the condenser heat duty, the vapour that enters to the condenser, the reboiler heat duty, the boil-up, the bottom flow rate and side stream flows.

Distillation control system design can partitioned. The controller can be divided into two: control of the operating conditions (pressure and levels) and control of one or two important compositions (or temperatures). Alternatively, the control system is not divided and a 5×5 controller is designed.

Although it is desirable to control the operating conditions and the products purity, for many years the only variables that were controlled were the column pressure and the condenser (or reflux drum) and the reboiler levels, because without these controllers the column can become unstable. If the levels are not controlled, the major effect is not a composition change, but a flow fluctuation. Such a fluctuation can lead to instability. Frequently, column control consisted of using distillate and bottoms flow rates to control level controllers and the vapour flow entering to the condenser to control the pressure of the column. This would leave the reflux rate L and the boil-up V to control products purity (Rademaker, Rijnsdorp and Maarleveld, 1975).

Shinskey (1984) proposed the use of the steady state RGA as a tool for control variable selection. Shinskey's proposal was to use control configurations which at steady state had the first RGA element λ_{11} value between 0.9 and 4.

Skogestad and Morari (1987) and Skogestad, Lundström and Jacobsen (1990a) suggested that a more rigorous method for selecting control configurations was necessary. They analysed several control configurations for a binary distillation column with RGA not only at the steady state, but also at high frequencies up to the closed-loop bandwidth frequency. Their conclusion was that a system well conditioned at higher frequencies would constitute a better selection. For instance, for the DB (distillate and bottom flow rates) configuration, the RGA analysis extended to the limit of the closed-loop bandwidth of interest, quickly approaches to one. Thus, this suggests that DB configuration could be used for their example. On the other hand, for the LV configuration the analysis suggested that such a scheme was convenient for one-point control (use of the reflux rate to control the distillate composition). This shows that control tools can reveal control characteristics that could take many simulations to find.

Agamennoni, Figueroa, Barton and Romagnoli (1994) determined the best control

configuration for a three component distillation column. Although the inputs and outputs were already selected, control tools were used to discriminate between three kinds of controllers. The analysis included the use of open and closed loop measures such as disturbance condition number, a measure of the control action needed to reject the disturbance (open and close loop), an interaction measure and a robustness measure. The use of such tools allowed avoidance of a model predictive controller since the job could be done by a simpler correctly-tuned multi-loop controller. This research is a good example of how controller system design can benefit from the use of control measures.

RGA and singular valued decomposition (SVD) were used to study the control of a binary (methanol-water) high-purity distillation column by Sågfors and Waller (1998). The analysis suggested that the LV configuration was ill-conditioned and that the directionality of the system favoured one-point composition control.

Optimisation techniques and control tools have been use together to improve distillation column design. An example of this treatment was presented by Luyben and Floudas (1994) who optimised design parameters of the column such as column diameter and number of plates to minimise cost. The control configuration using reflux ratio and boil-up (RV) was fixed during the optimisation. The controllability of each solution was analysed with the RGA at the steady state to reduce the optimisation region. With the solution region restricted the optimisation was done again. The final solution was a compromise between cost and controllability.

An example showing how to select the best control configuration for a distillation column as an optimisation problem, was presented by Hansen, Jørgensen, Heath and Perkins (1998). who designed the controller of an energy integrated column. The control of the heat pump section was already established. The task was to design a controller for the bottom and top composition and the pressure at the bottom of the column. The main disturbances to be rejected were feed composition fluctuations. The method assumed perfect control up to a certain frequency ω_d to minimise the largest time domain deviation of the uncontrolled outputs. Moreover, there was a restriction on the maximum allowed input deviation. The resultant configurations were then analysed with RGA, relative disturbance gain (RDG), positive zeros and condition number.

This concludes the review of control system design assisted with control tools for distillation. We have seen that although control tools are not essential for control system design of conventional distillation, they have been helpful to assess the

effectiveness of control structures before those are implemented, saving time and improving design. Since the examples show that control tools can be effective, even in complex cases, it is expected that they can also be useful for the reactive distillation problem.

4.2 Aim of this chapter

In the preceding section some applications and the importance of control system design for conventional distillation were reviewed. In particular, it was found that many convenient schemes for conventional distillation that could be rejected based only in heuristics would not be rejected by a mathematical method based on control tools. Moreover a systematic method for control system design can be convenient when the distillation system is more complex, for example, the distillation column with the integrated heat pump.

On the other hand, the literature review showed that although some attempts to formalise control system design decisions for reactive distillation have been done, there is still room for improvement.

Since the application of control tools has been successful for control system design of conventional distillation, the aim of this chapter is to generate an appropriate method for control system design decisions for reactive distillation columns. Such a method can not be entirely based on control measures but it would need considerations related to the phenomena occurring within the process.

In particular, is important to answer the following questions:

- Is it possible to create a method for the control system design of reactive distillation?
- What would be the limitations of such a method? Would this process alone be enough? If not, how can it be complemented?
- How can the process knowledge be related to control system design decisions? What is the relationship between the process knowledge and a method that uses control tools to design a controller for reactive distillation?
- Are control system design methods for conventional distillation applicable to reactive distillation?

- What are the most important considerations when selecting the " best" control structure for a reactive distillation column?

- Are the most appropriate structures for conventional distillation convenient for reactive distillation?

- What is the relationship between control system design decisions and column design decisions?

- Are the normal control objectives enough? That is, would temperature control be enough to control reactant conversion and product purity?

4.3 Methodology

This section contains a suggested method for control system design of reactive distillation. The method is based on different sources such as Stephanopoulos (1984), Seborg, Edgar and Mellicamp (1989) and Skogestad and Postlethwaite (1996).

1. Development and validation of a model that properly describe the system.

2. Control objective definition and selection of possible inputs and outputs. At this stage candidates to be outputs and inputs are chosen. However, no final decision should be made here. Rather, some tentative outputs are chosen.

   In the particular case of reactive distillation, two primary control objectives are to keep a reactant conversion at a certain level and product purity at a certain value. This control objective can be expressed as to keep the output concentration of the reactant and product at a certain values. Thus, the primary control objectives would be expressed in terms of possible outputs. Secondary control objectives include the relative to operating conditions, such as pressure of the column, level controllers, etc.

   In this pre-selection of inputs and outputs the characteristics of the process must be taken account. For example, if the conversion displays an output multiplicity with the reactive stages temperature, it may be better to select temperatures of sections of the column in which such an output multiplicity is not found (Sneesby *et al.*, 1997a). Another option could be to operate the column at different conditions in which multiplicity does not appear.

3. The model is linearised and scaled at the steady state of interest. Moreover, the linear model is rewritten using Laplace transformations. The results are the system transfer function $G(s)$ and the disturbance transfer function $G_d(s)$ (Appendix E.1 and E.1.1).

4. Preceding the analysis of the different possible schemes, an analysis of the risk that expected disturbances offer is done. Such a judgement is based on the disturbance transfer, disturbance condition number (Appendix E.1.1) that expresses the direct relationship between outputs and inputs, and the outputs and the disturbances.

5. Another aspect that must be analysed is that there should not be hidden states, so that the results got represent only the states that determine the system. Thus, the model is a *minimal realization* of the system. This is complied if the system is s-controllable and s-observable (Appendix E.2).

6. Control structure design. The objective is to find a control structure that is measurably efficient and robust (so that the system is stable is spite of uncertainty and modeling errors). At this step, decisions with respect to number, location, actuators (manipulated variables) and sensors (measurements) are made. Moreover, the relationship or connection between measure and manipulated variables is considered. (Stephanopoulos, 1984). Such decisions should be based both in Engineering knowledge and a method that can "measure" the possible performance of a certain structure (Seborg, 1982).

   The following list includes the linear control indices used during the present work to discriminate between control structures. For each index, a short description and explanation about its usefulness is included. Some of the control tools should not be checked just at the steady state, but for a frequency range or bandwidth of interest, that will be called Ω, Since reactive distillation problems are non-linear, frequency range Ω should not be far from the linearisation steady state.

   (a) The first index to be addressed is the functional controllability. This index shows whether or not the inputs can influence the outputs. This measure is addressed firstly by requiring that in the control structure there are at least as many inputs as outputs. The second requirement is that the rank of the transfer function must be equal to the number of inputs (Appendix E.3). This property is checked both at the steady state and for the frequency range Ω.

(b) The next step is to check whether the system can achieve perfect control in spite of the disturbances presence. If $||G^{-1}g_d||_{max} \leq 1$ is met for each considered disturbance for a frequency range, then the system can achieve perfect control (Appendix E.1.1). We would prefer schemes that comply the requirement for a large frequency range.

(c) The next step is to find the poles and zeros of the system. RHP-poles are related with instability and RHP-zeros are associated with no perfect control (Appendix E.4 and E.5). Therefore, control schemes without RHP-zeros or RHP-poles would be prefered. In addition, when there are paired positive poles and positive zeros, it is necessary to check their directions to see if they are coupled.

(d) If positive zeros were present in the system, then the direction of the outputs must be compared with the direction of the disturbance at such points. When both directions coincide, the probabilities of control problems are high (Appendix E.5.1). Because the disturbance is aligned to the system and at that point perfect control is no possible. Hence, the range of application may be limited.

(e) The next test to be applied is singular value decomposition (Appendix E.7) both at the steady state and at frequency range Ω. Inputs of schemes in which the minimum singular value is lower than one do not have great influence on the outputs. Furthermore, the condition number should be calculated since it can indicate whether a system is bad conditioned.

(f) Input saturation must be checked as well since in most cases there is an input limit (either an operating or safety restriction). In Appendix E.6 there is a criterion to measure whether a configuration can achieve acceptable control or not without breaking the limit of the inputs. Such a measure is related to direction of the disturbances that may occur in the system and the system direction (that can be got from the singular value decomposition). Configurations that can achieve acceptable control at the steady state within the operation bandwidth Ω are preferable.

(g) The next step of the analysis is frequency response. Bode diagrams are got for the open-loop transfer function. The main objective at this point is to investigate the relationships between inputs and outputs, and to find if there is a critical frequency. When at frequency ω the magnitude is larger than one and the phase is equal to $-180°$, the system is unstable and that frequency is called critical frequency or ω_{180}. Furthermore, if

the system is open-loop unstable, the closed-loop will be also unstable.

(h) Relative gain array (RGA) is calculated for a range of frequencies that include the critical frequency (if it exist). When for a configuration the RGA elements are larger than one, the configuration has strong interaction between the different input-output pairs. Furthermore, large RGA elements indicate that the system is sensitive to input uncertainty. This property should not be attained just at the steady state but for frequency range Ω that includes, if it exists, the critical frequency. Thus, schemes with elements close to zero or one are preferred (Appendix E.8 and Skogestad, Lundström and Jacobsen, 1990).

(i) The analysis is repeated for all the proposed schemes and the "best" control schemes are selected.

(j) The RGA at the steady state can be used to select the best interconnection between inputs and outputs for the selected scheme. If the RGA elements are negative, the present interconnection is incorrect, the relationships between inputs and outputs must to be re-assigned and the RGA calculated again. Alternatively, the RGA of the RGA can be calculated. This process is repeated until the elements are equal to ones and zeros. If the element $\lambda_{ij} = 1$ that means that the pair output i and input j is recommended.

7. The next step is the controller design. This design process can be assisted by different tools such as frequency response.

8. The controller is implemented, tuned and tested by closed-loop simulations that include the expected disturbances.

4.4 Case study

To exemplify the methodology proposed in the preceding section, it is applied to design the controllers of a 17 theoretical stages MTBE production column that is fed in the 10th and 11th stages. The feed characteristics are shown in Table 4.1.

The primary control is to maintain the desired conversion in spite of feed flow and composition fluctuations. Additional control objectives are defined to help in the maintenance of the column stability. There are three operating conditions that must be kept as constant as possible: column pressure, reflux drum level

and reboiler level. The column pressure is considered perfectly controlled by the condenser heat duty. Furthermore, to simplify the problem, level controllers are implemented as mass controllers.

The dynamic model developed in Chapter 2 for a reactive distillation column with heat exchange only in reboiler and no side streams had four degrees of freedom. However, for the case study, the control objectives analysed are the main control objectives, which are the product compositions. The control of the reboiler and reflux drum levels are considered perfect. Therefore, during the analysis there were only two inputs and two outputs.

Two problems are analysed. The difference between them is that in the first one the reflux ratio is equal to 3; while in the second one the reflux ratio is equal to 7. In the preceding chapter, it was shown that the MTBE column was more susceptible of output multiplicity when the internal flows were high. The aim is to find it is possible to find control differences between the two problems with the linear control tools and to determine which one is easier to control. The second problem presents output multiplicity with most of the inputs. Hence it is expected that such a problem is more difficult to control.

Table 4.1: Feed conditions for the MTBE column

	MeOH feed (l)	C_4 feed (v)
Flow (mol/s)	215.5	549.0
$z_{iso-butene}$	0.0	0.3568
z_{MeOH}	1.0	0.0
z_{butane}	0.0	0.6432
T (K)	320.0	350.0

$P_f = 11atm$

Problem 1

This first problem considers a steady state of the column in which the system present no output multiplicity for the iso-butene conversion for most of the inputs. At the selected steady state, the iso-butene conversion is equal to 97.99%. The operating conditions for this problem are presented in Table 4.2.

Table 4.2: Steady state characteristics. Problem 1

	Stage 1	Stage 17			
T (K)	343.9089	409.3488	D	377.673	mol/s
P (atm)	10.0000	10.1797	B	194.955	mol/s
$x_{iso-butene}$	0.00995	0.00130	L	1133.0184	mol/s
x_{MeOH}	0.06240	0.00317	Q_{reb}	14.70864	MW
$x_{n-butane}$	0.92645	0.01644	R	3.000	
			R_B	2.955	

Problem 2

In the second problem, the iso-butene conversion presents output multiplicity with most inputs. The steady state is the high conversion of three possible steady states for the operating conditions presented in Table 4.3.

Table 4.3: Steady state characteristics. Problem 2

	Stage 1	Stage 17			
T (K)	343.9528	410.9889	D	377.169	mol/s
P (atm)	10.0000	10.1852	B	194.1484	mol/s
$x_{iso-butene}$	0.00703	0.00021	L	2640.181	mol/s
x_{MeOH}	0.05912	0.00004	Q_{reb}	45.3191	MW
$x_{n-butane}$	0.93347	0.00556	R	7.0000	
			R_B	9.3082	

Considered disturbances

Three disturbances were considered during the analysis of the problems: a methanol feed flow change, a C_4 feed flow rate change and a change in composition in the C_4 feed stream. In the analysis, each disturbance was considered separately.

4.4.1 Pre-selection of possible inputs and outputs

This section corresponds to the second step of the proposed methodology. Process knowledge of the problem is used to find the most suitable outputs and inputs.

The primary goals are to maintain both iso-butene conversion and product purity that can be expressed as to keep the iso-butene and MTBE product concentrations.

Assuming that it is not practical to measure such concentrations, the options are either to infer them from temperature and thermodynamic models or to keep certain temperatures, though the last may not be equally convenient when the relationships between concentration and temperature are not simple. For simplicity, to maintain two set point temperatures was selected.

In the first part of the section, the relationship between the conversion and MTBE product purity with temperatures that can be used as outputs is analysed. In the second part, the relationships between the best candidates to be outputs and inputs are analysed. Finally, six control schemes are outlined.

Selection of possible outputs

The temperature selected to be controlled should display a simple and unique relationship with concentration. Moreover, the output should be not far from inputs to avoid time delays.

At the top of the column, the concentration and temperature are almost the same for the three non-reactive stages. The temperature at the first stage, T_1 was selected because it is next to the possible inputs (reflux ratio or reflux flow and distillate flow). Figure 4.1 shows that such a temperature does not greatly vary from a high conversion (low iso-butene concentration) and low conversion (higher iso-butene concentration) for both problems.

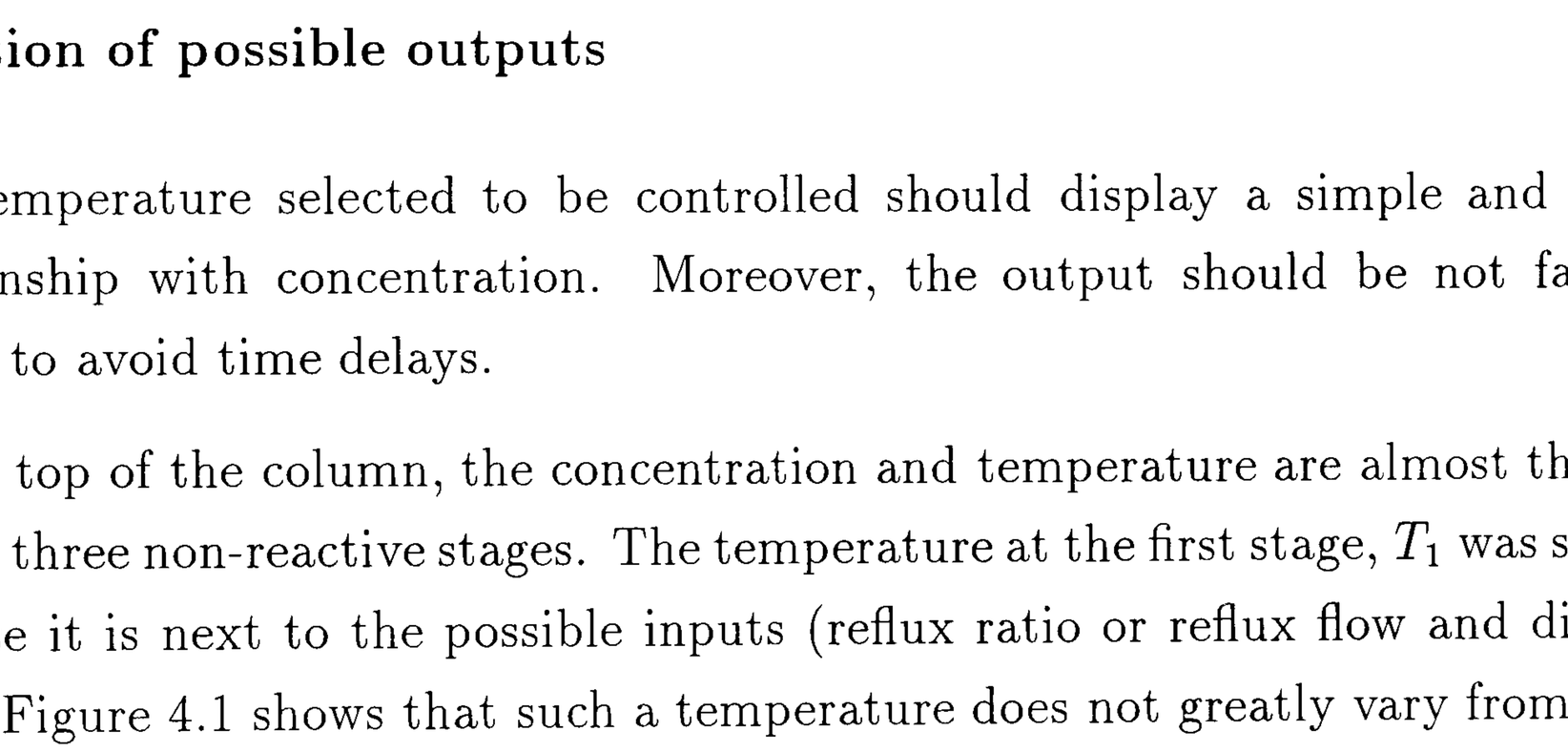

Figure 4.1: iso-butene liquid mole concentration vs. temperature at stage 1

On the other hand, the temperatures at the lower part of the column have complex relationships with the MTBE concentration. Figure 4.2 shows such relationships

for both problems. If T_{12} is used, as suggested by Sneesby *et al.* (1997a). there are two problems. The first is that for high MTBE concentrations, there is a large temperature difference for a very small concentration change. The second problem is that once the maximum concentration has been achieved, the temperature increases relatively slowly for large composition changes. However, the use of T_{12} has one advantage, from the high MTBE concentration to the low concentration that correspond to low iso-butene conversion the relation is unique, though opposite to the displayed at low temperatures. On the other hand, the use of T_{17} is disadvantageous because from the high MTBE concentration to the low concentration related to iso-butene low conversion the relation is not unique (see the curve at high temperatures). However, T_{17} can be advantageous since close to the high MTBE concentration, the MTBE mole fraction changes mean large temperature changes. This last characteristic and the fact that T_{17} is closer to the possible inputs made us to decide that T_{17} could be an appropriate output. Its complex characteristics, make it a good case study as well.

(a)

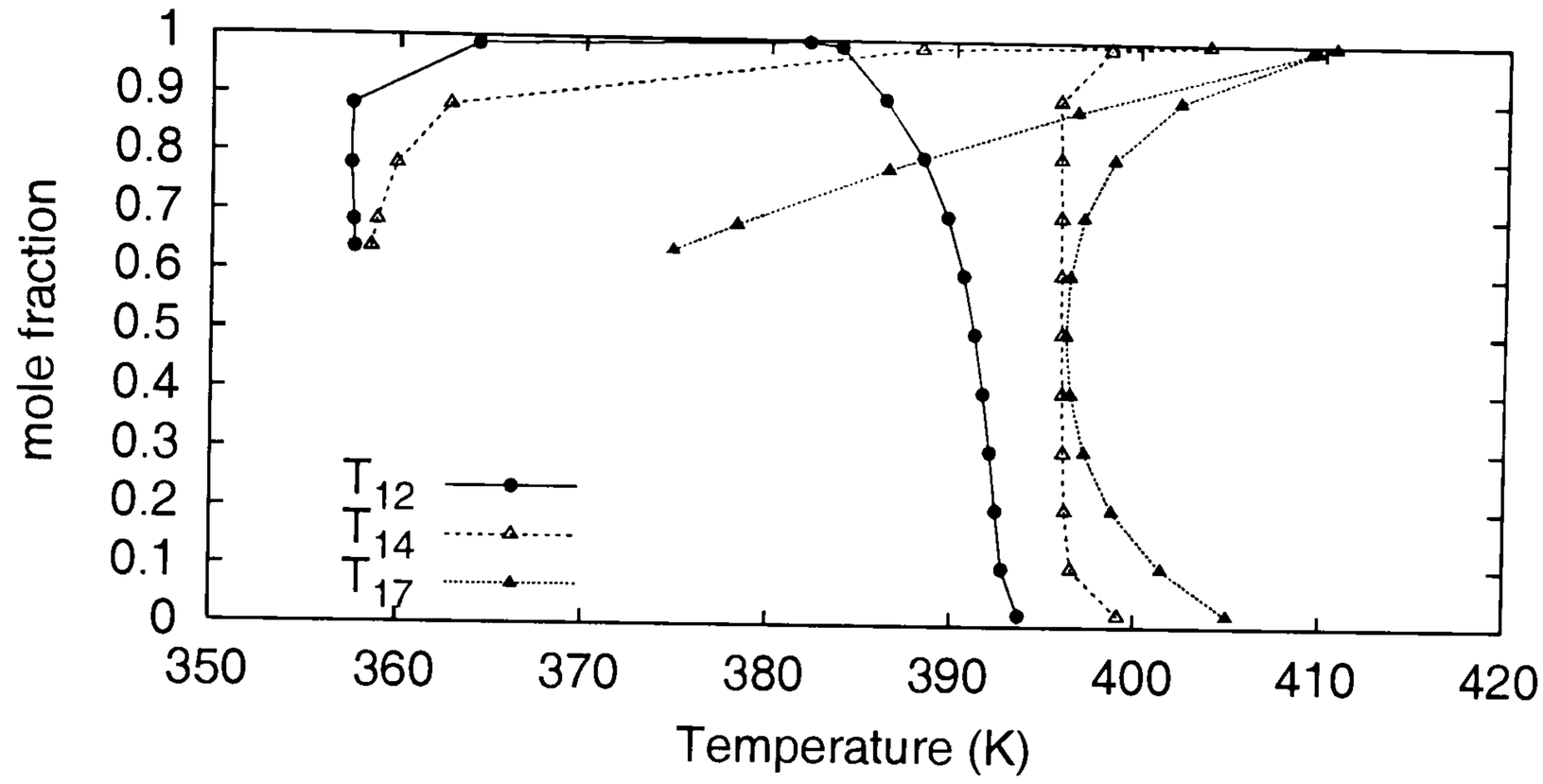

(b)

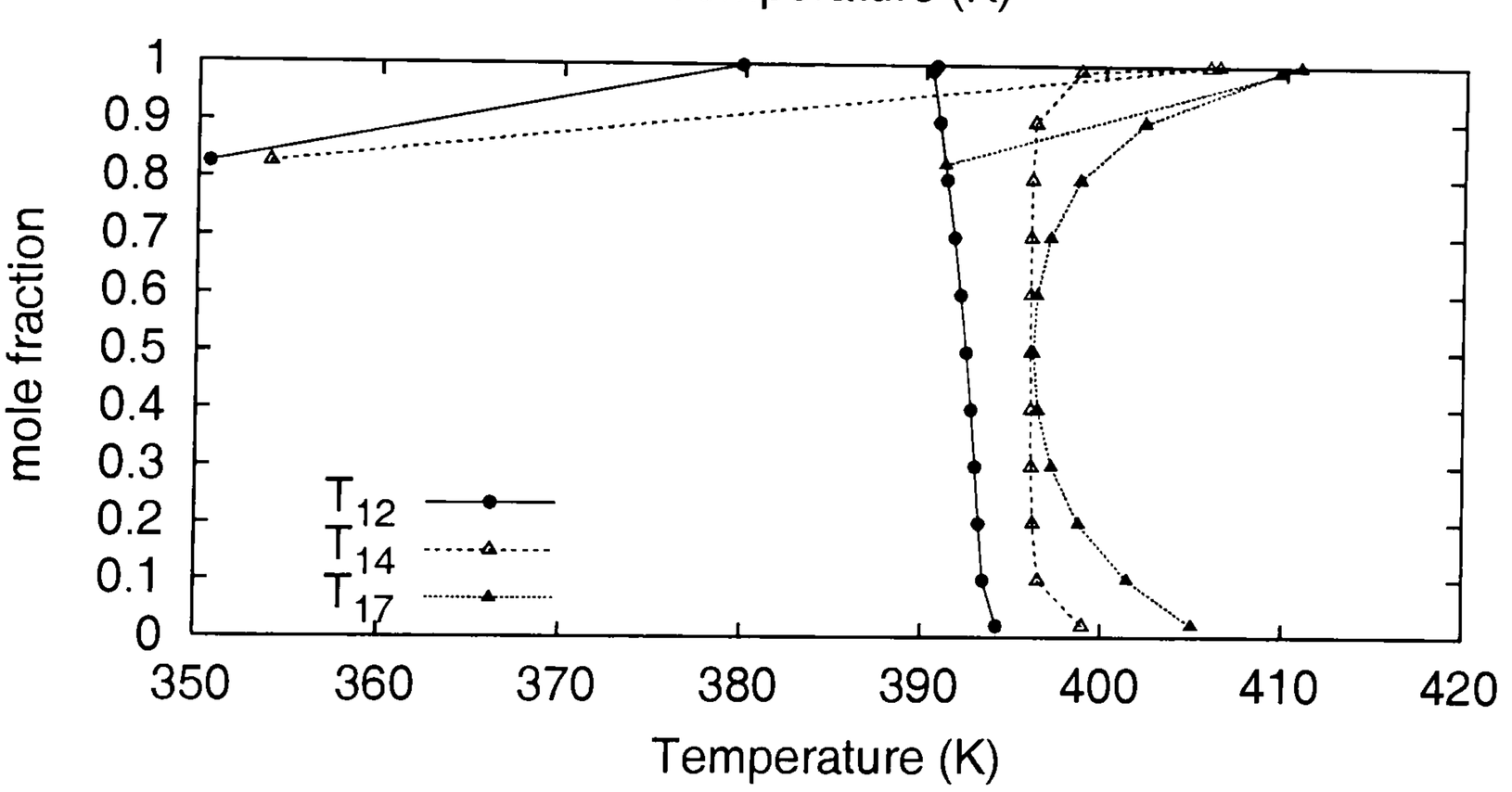

Figure 4.2: Temperature at different non-reactive stages and MTBE product liquid mole fraction (a) Problem 1 (b) Problem 2

Proposed control Schemes

Once T_1 and T_{17} were selected to be controlled, it is necessary to review their performance with the inputs: distillate flow rate D, reflux rate L, reflux ratio R, bottom flow rate B, reboiler heat duty Q_{reb} and reboiler reflux ratio R_B. Table 4.4 shows that the non-multiplicity region if the iso-butene conversion is small. Therefore, the pre-selection of inputs and outputs cannot be based only on avoiding multiplicity.

Table 4.4: Summary of MTBE behaviour under different inputs

Schemes	**Figures**	**Characteristics**	**No-multiplicity**
RB	3.10, 3.17	System more sensitive to R changes. IMSS, OMSS.	$R \leq 3$
RV	3.15	Input multiplicities even for low R. OMSS also present.	$R < 7$
RR_B	3.16	Marked IMSS and OMSS. Maybe difficult to manipulate the ratios	$R < 3$, $R_B < 4$
LV	3.18, 3.19	OMSS in the whole region analysed	
LB	3.20, 3.21	IMSS and OMSS for high internal flow rates	$L < 2000$
RD	3.22	Although the OMSS occurs at high R it may be difficult to control the reflux drum level with V or another variable "far" from it	$R < 9$
DB	3.23, 3.24	No OMSS for low B	$B < 175$
DQ_{reb}	3.25, 3.26	No OMSS, good option if OMSS is to be avoided	
$D_m B_m$	3.27	Difficult to control since OMSS is present in the whole region	
$D_M Q_{reb}$	3.28	OMSS for low Q_{reb}	$Q_{reb} > 50$

As mentioned before, all possible input combinations for controlling a distillation column have advantages and disadvantages. From Skogestad and Morari (1987) study, which was based on RGA analysis, five control schemes were selected. Table 4.5 present the five schemes selected and their main features. The sixth scheme ($D_m Q_{reb}$) is a variation of scheme DQ_{reb} to study the effect of mass based inputs.

Note. In all the schemes where the reflux ratio R was an input, the flow manipulated to change R was the reflux rate L. Similarly, to change the reflux flow rate at the bottom (R_B), the flow used was B.

Table 4.5: Control Schemes analysed

Scheme	Control features
$LQ(LV)$	Bad input uncertainty rejection. Fast response. Good switchbility (from manual to automatic control)
RR_B	Good input uncertainty rejection. Fast response
$RQ(RV)$	Suitable for one composition control
$DQ(DV)$	Good input uncertainty rejection
D_mQ_{reb}	Are the properties similar or different to DQ (DV)?
D_mB_m	Good input uncertainty rejection

4.5 Problem 1: Control structure design

The control structure analysis suggested in Section 4.3 was applied for each scheme. In this section the similarities and main differences found during the process are presented.

4.5.1 Common features shared by all the schemes

For all the schemes analysed, the test of s-controllability and s-observability showed that the system was s-controllable and s-observable. Therefore there were not hidden states. Additionally, all the schemes were functionally controllable. Thus, the outputs can be controlled independently.

The system presented 10 positive poles close to the origin. This is an indication of instability of the steady state selected. However, since the RHP-poles are very close to the origin (see Figure 4.3) compared with the negative ones, it is expected that such an instability is slow.

The last affirmation was confirmed with the open simulation of the scheme RQ_{reb}. Figure 4.4 shows the output T_{17} open loop behaviour at constant R and Q_{reb} when no disturbance was applied. The figure shows that there is a slow decrease of T_{17} over the time.

For the six analysed schemes, the minimum singular value at the steady state and close to the steady state was greater than one. This is a good feature since it means that all the inputs have a significant influence on the outputs. Though, it will be shown later that the system presents control problems when disturbances occur. However, the system is badly conditioned since there are differences of four or five

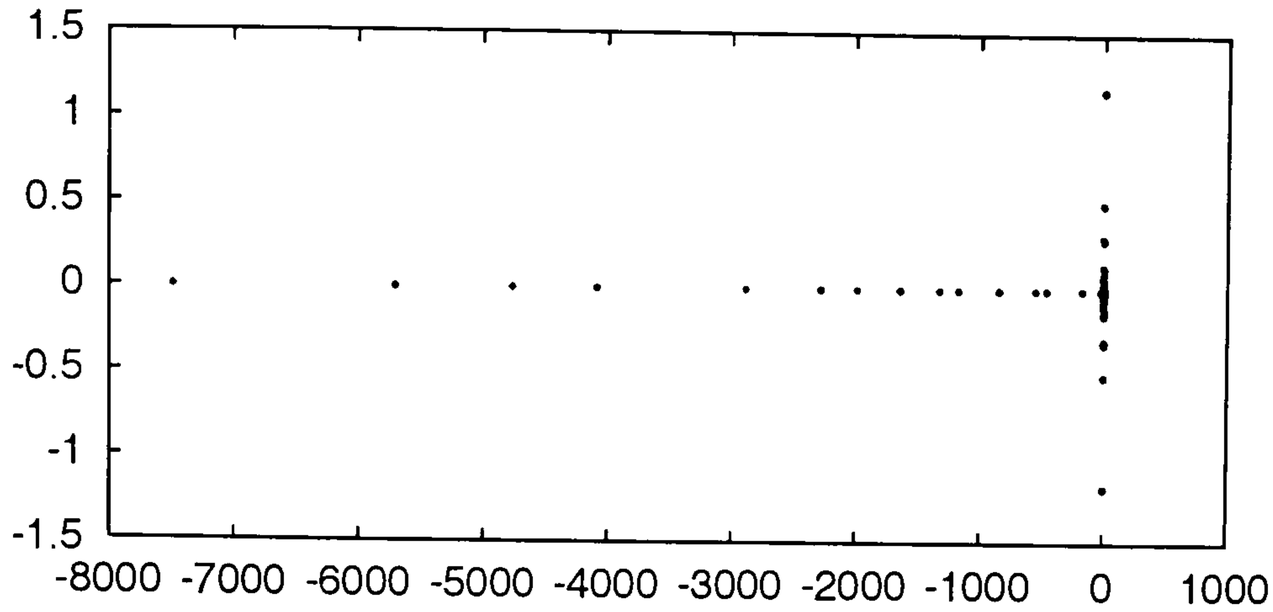

Figure 4.3: Poles for Problem 1.

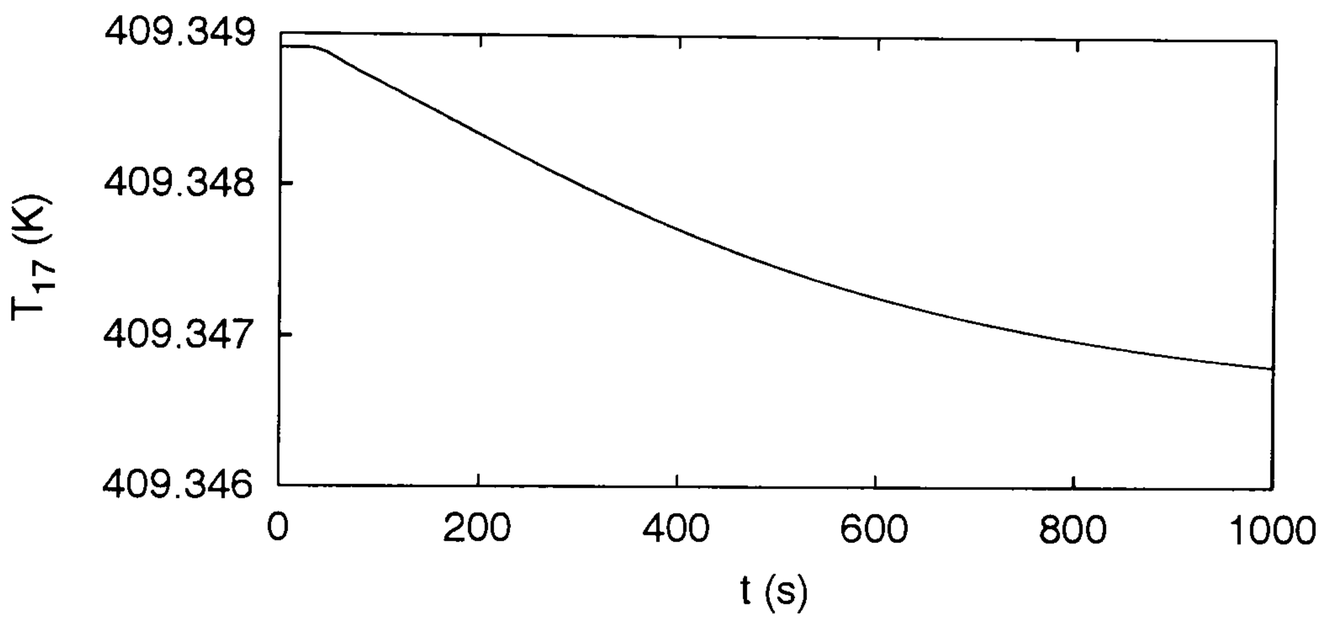

Figure 4.4: T_{17} open loop response. Problem 1, scheme RQ_{reb}

orders magnitude between the maximum and minimum singular values for the six schemes.

Discussion

The presence of positive poles suggested that the steady state selected is unstable. Such an instability is relatively slow. A possible source of the system instability is the role of hydraulics in the model. The state variables of the model are the element hold-up on the stages. The calculation of vapour and liquid flow rates is related to such hold-up. At the same time, the hold-up is related to the liquid and vapour flow rates. Therefore, slight fluctuations in the hold-up calculation (during the integration) result in small fluctuations of the stage pressures, which in return cause vapour flow fluctuations. Those fluctuations are reflected in the calculation of the right hand side of the differential equations. Perhaps, if the hydraulics were ignored and constant vapour flow rates were assumed, the system would be stable.

The other common feature that the analysis suggests, is that although the system

is unstable, it is possible to control it using any of the proposed schemes. This is suggested by the SVD result. However, such a result is without the consideration of the disturbance effects. When disturbances are considered, there are differences between the disturbance rejection capability of the control schemes considered. This is discussed in the next section.

4.5.2 Main differences between control schemes

Disturbances effect

The disturbances were: a methanol feed flow rate change (d_1); a C_4 feed flow rate (d_2) and an iso-butene feed concentration change (d_3). The effect of each disturbance was considered separately. A summary of the disturbance effect is found in Table 4.7.

The analysis of the transfer function at the steady state showed that in general, disturbance d_2, that is the change in the C_4 feed flow, has a strong effect on the system (Table 4.6). If the effect of the inputs could be summed in a way that a maximum combined effect could be obtained, just the $D_m B_m$ scheme would have a combination of the transfer function elements greater than the elements of the disturbance transfer function for such a disturbance.

The same analysis of transfer functions shows that the schemes with the reflux rate as manipulated variable (L) have reduced power against the disturbances.

Another indicator of the disturbance effect is the disturbance condition number. Such a number gives an idea of the alignment between a certain disturbance and the plant. The results for Problem 1 and 2 showed that this indicator offers little relevance for the control system design process. For instance, at the steady state for $D_m B_m$ case the disturbances are aligned to the plant. However, the results in Table 4.6 show that the scheme can overcome disturbances.

More useful is the perfect control criterion (briefly detailed in the methodology, Section 4.3 and Section E.1.1). The results for such a criterion complement the results of the analysis of the transfer function at the steady state because the effect of the inputs is checked for different ω values. Figure 4.5 shows the results for four different schemes. The results show that in some cases, the criterion is met but just very close to the steady state. Note that in case of the $D_m B_m$ scheme, this result corrects the steady state transfer function analysis since there is no perfect

Table 4.6: G and G_d matrices at the steady state. Problem 1

$G_d(0)$		
-1.92E+06	-4.46E+06	1.59E+06
8.00E+02	2.40E+03	-9.00E+02

$G(0)$			u_1 and u_2 combined effect	Disturbance rejected
$Q_{reb}R$	1.12E+05	-2.02E+05	-3.14E+05	none
	1.30E+02	-8.00E+01	2.10E+02	none
LQ_{reb}	-1.91E+05	1.12E+05	-3.03E+05	none
	-8.00E+01	1.30E+02	-2.10E+02	none
DQ_{reb}	3.36E+06	1.12E+05	3.47E+06	d1, d3
	-1.30E+03	1.00E+02	-1.40E+03	d1, d3
RR_b	-2.02E+05	-2.72E+06	-2.92E+06	d1, d3
	-1.00E+02	1.60E+02	-2.60E+02	none
D_mQ_{reb}	3.36E+06	1.12E+05	3.47E+06	d1, d3
	-1.30E+03	1.00E+02	-1.40E+03	d1, d3
D_mB_m	3.36E+06	1.47E+08	1.50E+08	all
	1.32E+03	1.70E+05	1.71E+05	all

control if there is a change in the C_4 feed (disturbance d_2). The perfect control criterion shows that no scheme is perfect though it helps to reject schemes $Q_{reb}R$ and LQ_{reb} because they cannot overcome the disturbances.

It is interesting to observe that the best scheme performance is for D_mB_m which can overcome a change in the methanol feed flow and a change in the C_4 feed composition, but cannot overcome a change in the C_4 feed flow. This scheme is normally not used because it is easy to have problems with the global mass balance. The simulations for this scheme (Case 4.5.5) confirm that the system becomes unstable when C_4 feed flow is reduced. Such simulations show that the scheme can reject a change of the methanol feed flow rate. However, the system becomes unstable when there is a change in the C_4 feed flow.

Table 4.7: Disturbance effect close to the steady state, Problem 2. AC = acceptable control, PC = perfect control

Scheme	d_1	d_2	d_3
$Q_{reb}R$, LQ_{reb}	No PC, No AC	No PC, No AC	No PC, No AC
RR_B	No PC, No AC	No PC, No AC	PC, AC
DQ_{reb},D_mQ_{reb}	PC, AC	No PC, No AC	No PC, No AC
D_mB_m	PC, AC	No PC, No AC	PC, AC

Positive zeros

The location of positive zeros is explained in Section E.5. Perfect control is possible only very close to the steady state due to the presence of small positive zeros. Moreover, the results show that many of the positive zeros are aligned with the disturbances and positive poles.

Table 4.8 shows how many zeros there are and their features. In the cases in which positive zeros are aligned with positive poles, the smallest positive zero is aligned with the smallest positive pole. This could explain why perfect control fails for those schemes. It is possible that a disturbance can bring the system to a point in which it is unstable and difficult to control.

Table 4.8: Number of positive zeros and their characteristics. Problem 1

Scheme	RHP zeros	Smallest RHP zero	Aligned with RHP poles	Aligned with d_1	d_2	d_3
$Q_{reb}R$	9	6.209E-04	3	1	3	3
LQ_{reb}	9	6.209E-04	3	1	3	3
DQ_{reb}	10	2.416E-03	none	9	10	10
RR_b	8	4.615E-02	4	1	1	1
D_mQ_{reb}	10	2.416E-03	none	9	10	10
D_mB_m	10	2.416E-03	none	9	10	10

Singular value decomposition and acceptable control

As mentioned before, the system is not well conditioned. However, there are differences in the condition number of the schemes using the reflux rate and the schemes using the distillate flow rate. When the reflux rate is used, the trend is irregular

(Figure 4.6). The increment of frequency ω brings great fluctuations in the condition number. When the distillate flow rate is used, an ω increment produces a rather steady increment in the condition number until it achieves an almost constant value. Such results suggest that using an external flow is better since the system is better conditioned.

Another important piece of information that can be compared with the minimum and maximum singular values is the acceptable control criterion (Section E.6). The results were similar to the results of the perfect control criterion. That is, the schemes that could not achieve perfect control not even close to the steady state, cannot achieve acceptable control either. As an example of the mentioned behaviour, the reader can compare Figures 4.5 *a* and 4.7. A summary of acceptable control and perfect control for all the schemes analysed is found in Table 4.7.

Frequency response

The frequency response analysis of the six schemes confirmed the instability of the open loop due to the presence of the positive poles for the schemes related to the internal flow rate L. Thus, schemes $Q_{reb}R$, LQ_{reb} and RR_B displayed at low frequencies instability for the pair R or L and T_{17}. That is, those inputs can cause instability to that output (Figure 4.8). Such behaviour indicates that the closed-loop could not be stable.

A pair that displays a critical frequency ($\omega_{180} = 0.042$) is Q_{reb} and T_1. That is, all the schemes that use the reboiler heat duty can make T_1 unstable (Figure 4.10).

On the other hand, T_{17} could display output lead with all the expected inputs except with R_B close to the steady state (Figure 4.11). T_1 could also display output lead with all the schemes using L (Figure 4.9).

RGA

The RGA confirms the expected pairing between the inputs and outputs. For instance, in the case of the scheme $Q_{reb}R - T_1T_{17}$, the RGA diagonal elements are negative. This suggest that the pairing should be $R - T_1$ and $Q_{reb} - T_{17}$ (see Figure 4.12 a). Figure 4.12 also shows that the maximum RGA element for $Q_{reb}R$ and LQ_{reb} is larger than for the cases RR_B, DQ_{reb} (and D_mQ_{reb}) and D_mB_m.

Since a low RGA indicates lower input uncertainty, it would be better to work with schemes RR_B, DQ_{reb} (or D_mQ_{reb}) or D_mB_m.

Discussion

There are more positive poles and zeros aligned for schemes that use the reflux flow rate as input ($Q_{reb}R$, LQ_{reb} and RR_B). Of them, RR_B has the largest of those smallest zeros. In addition, for $Q_{reb}R$, LQ_{reb} more positive zeros are aligned with disturbances than in RR_B case.

There are no aligned positive poles and zeros for the schemes using the distillate flow rate as input. However, they have more positive zeros aligned with the disturbances. On the other hand, the system is better conditioned when the distillate flow rate is used as input than when the reflux flow rate is used as input.

The frequency response showed that for the $Q_{reb}R$, LQ_{reb} and RR_B cases the closed-loop might not be stable. Furthermore, the analysis showed that the useful bandwidth is limited because of the presence of $\omega_{180} = 0.042$.

The RGA analysis showed that schemes $Q_{reb}R$ and LQ_{reb} were more susceptible of presenting input uncertainty, contrary to scheme RR_B that presented the smallest $\lambda_{1,1}$ element for different frequencies. The schemes related to the distillate flow rate presented $\lambda_{1,1}$ almost equal to one for the analysed frequency range.

The analysis of the disturbance effect on the system should be considered. Perfect control was not possible when a change in the C_4 feed flow occurred. Three schemes are supposed to be able to overcome a methanol feed flow change (DQ_{reb}, D_mQ_{reb} and D_mB_m). D_mB_m scheme could also stand a methanol feed flow rate change. RR_B could overcome a C_4 feed composition change. Similar results were got from the acceptable control criterion analysis.

Therefore, although there is no perfect scheme, the analysis suggests that the most advantageous schemes are: DQ_{reb} (or D_mQ_{reb}), RR_B and D_mB_m.

Discriminating the last four schemes is more difficult. If it is true that scheme D_mB_m can overcome two feed changes, it is possible that either the C_4 feed flow rate change or another change can destabilise the column because of the changes in the global mass balance.

We are left then with the two better schemes DQ_{reb} (or D_mQ_{reb}) and RR_B. Perhaps, the main difference between these schemes is in the perfect control criterion. Observing Figure 4.5 *b* and *c* we can see that close to the steady state DQ_{reb} can overcome easily the methanol feed flow change while RR_B can overcome in the same way a C_4 feed composition change. However, RR_B perfect control criterion for

methanol feed flow and C_4 feed flow changes are closer to one than the C_4 composition and feed flow changes for scheme DQ_{reb}. Hence, unless large C_4 composition changes were very likely to occur, RR_B would constitute the best choice.

The analysis shows that it is important to consider the disturbances for the control structure design. For this problem, without the consideration of the disturbances, it would have been difficult to differentiate among the schemes. In the next section, the results of the controllability analysis are tested by rigorous simulation.

(a)

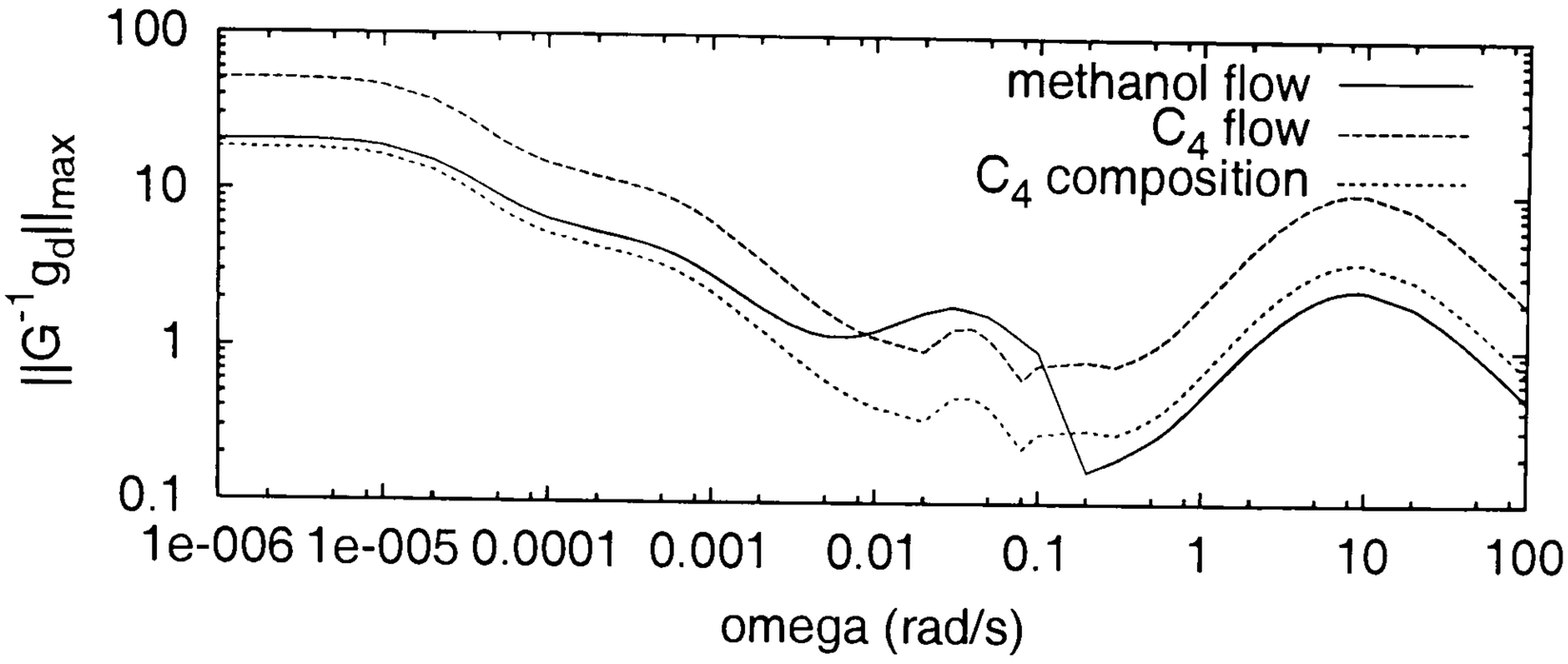

(b)

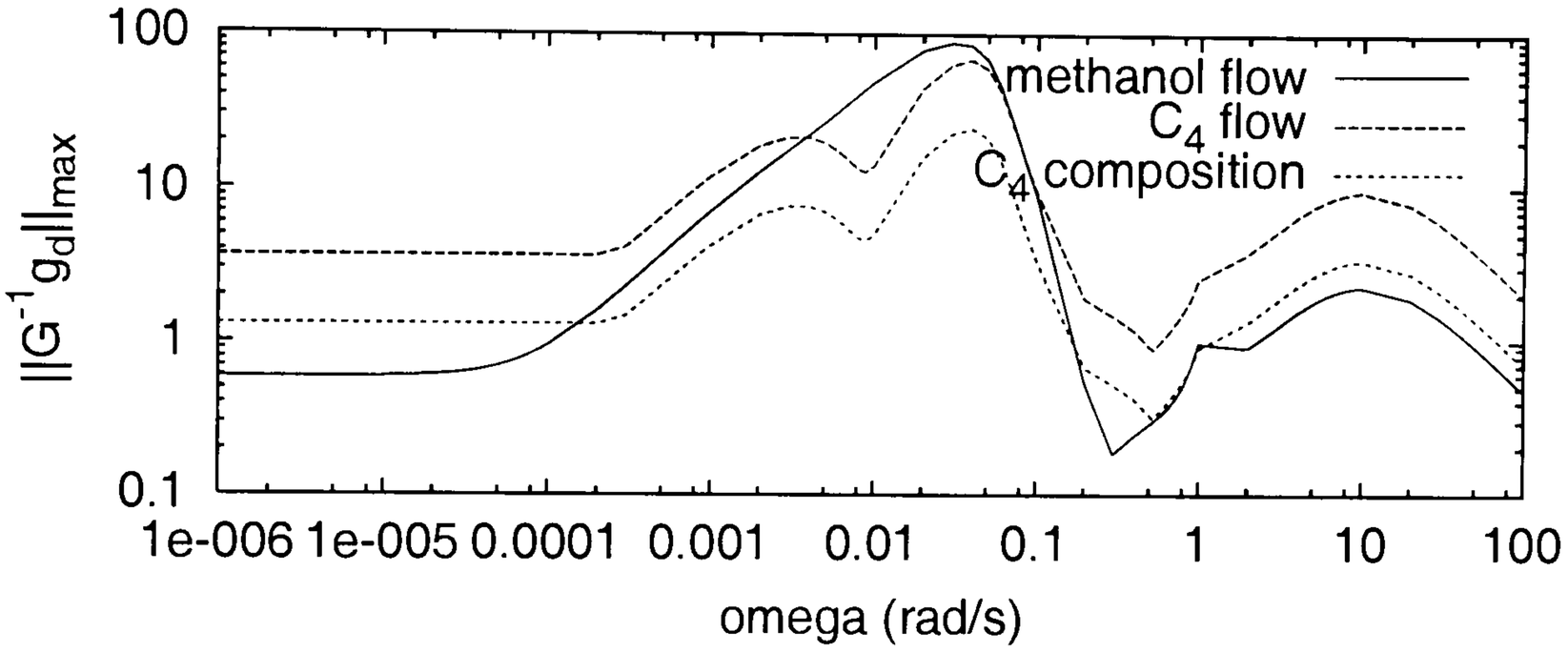

(c)

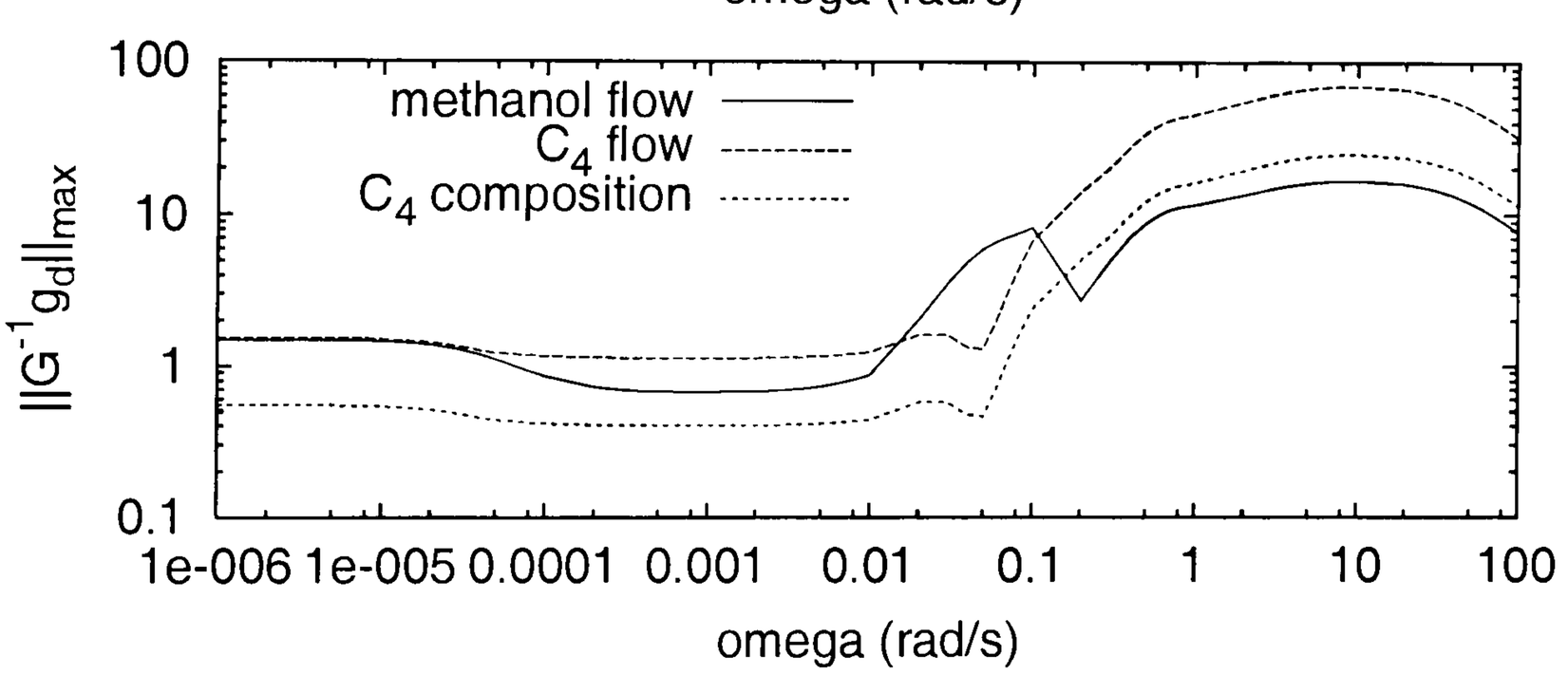

(d)

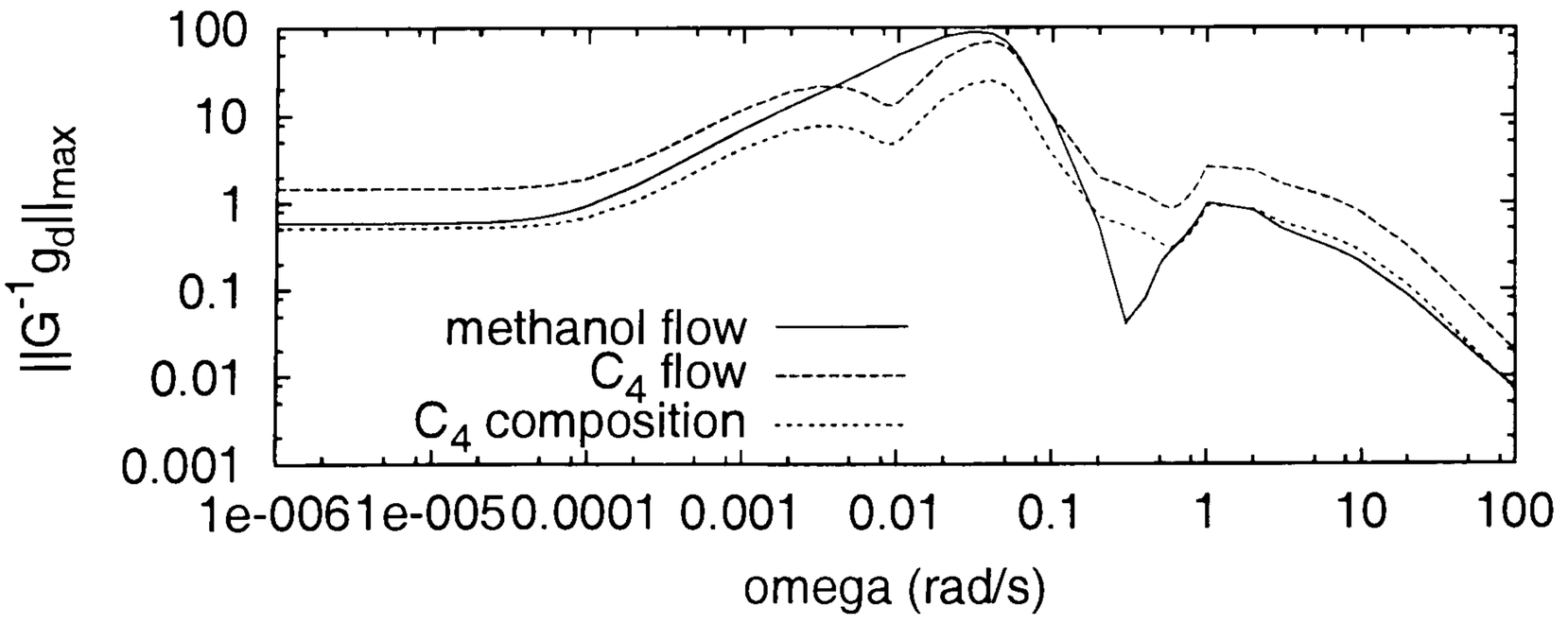

Figure 4.5: Perfect control criterion. Problem 1. (a) Scheme LQ_{reb} (and $Q_{reb}R$), (b) Scheme DQ_{reb} (and D_mQ_{reb}), (c) Scheme RR_B, *(d)* Scheme D_mB_m

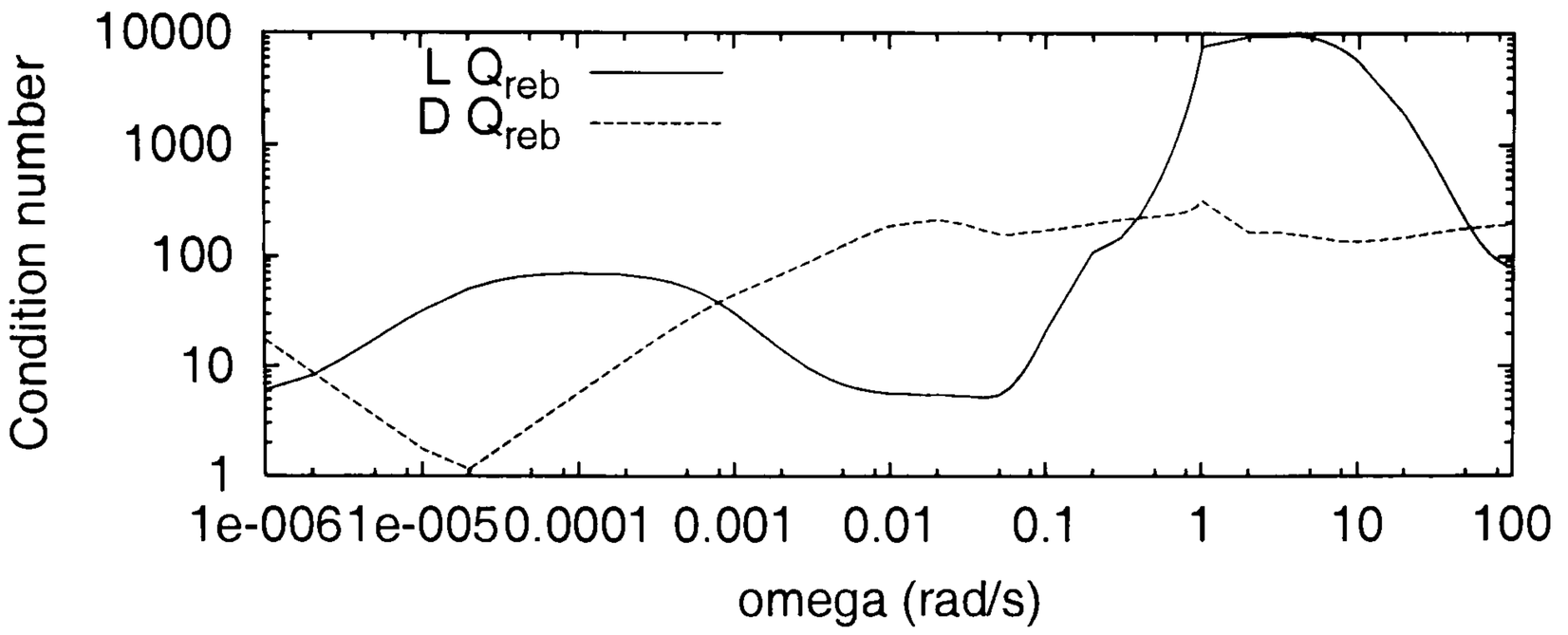

Figure 4.6: Condition number for schemes LQ_{reb} and DQ_{reb}. Problem 1

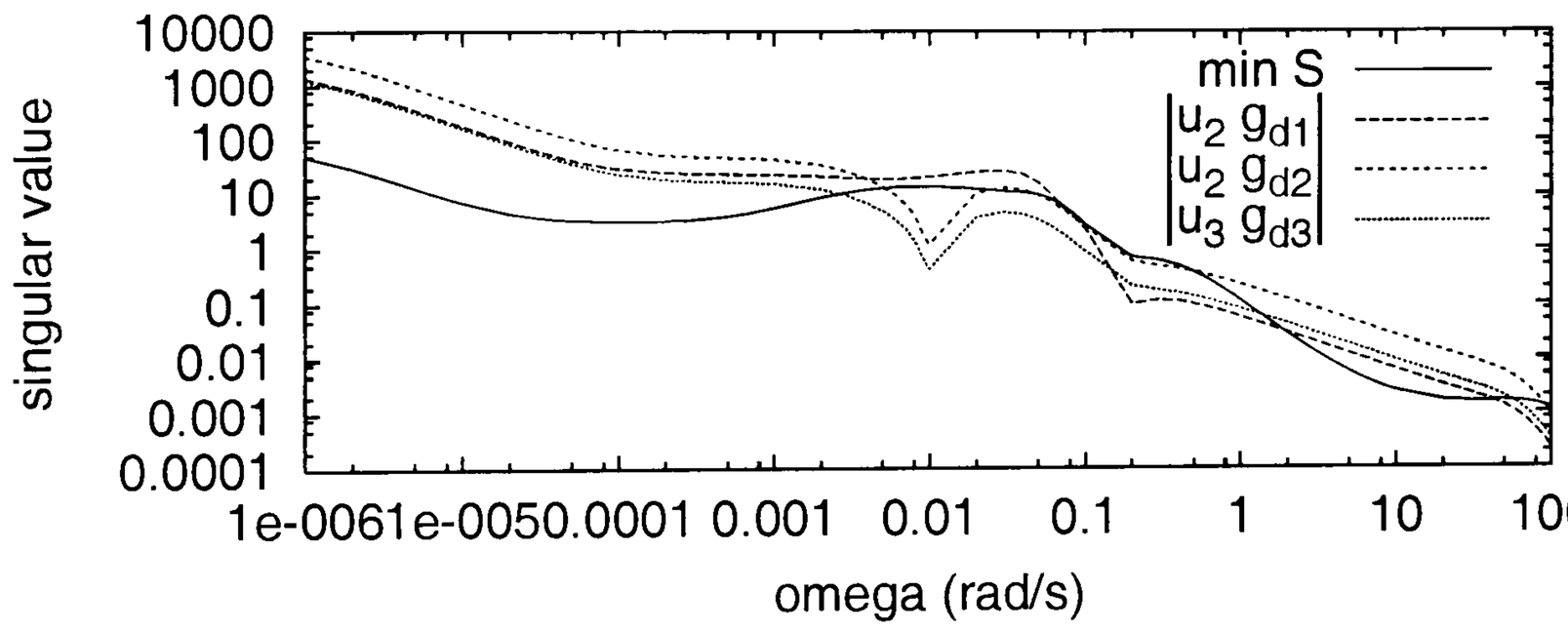

Figure 4.7: Acceptable control criterion for scheme LQ_{reb}. Problem 1

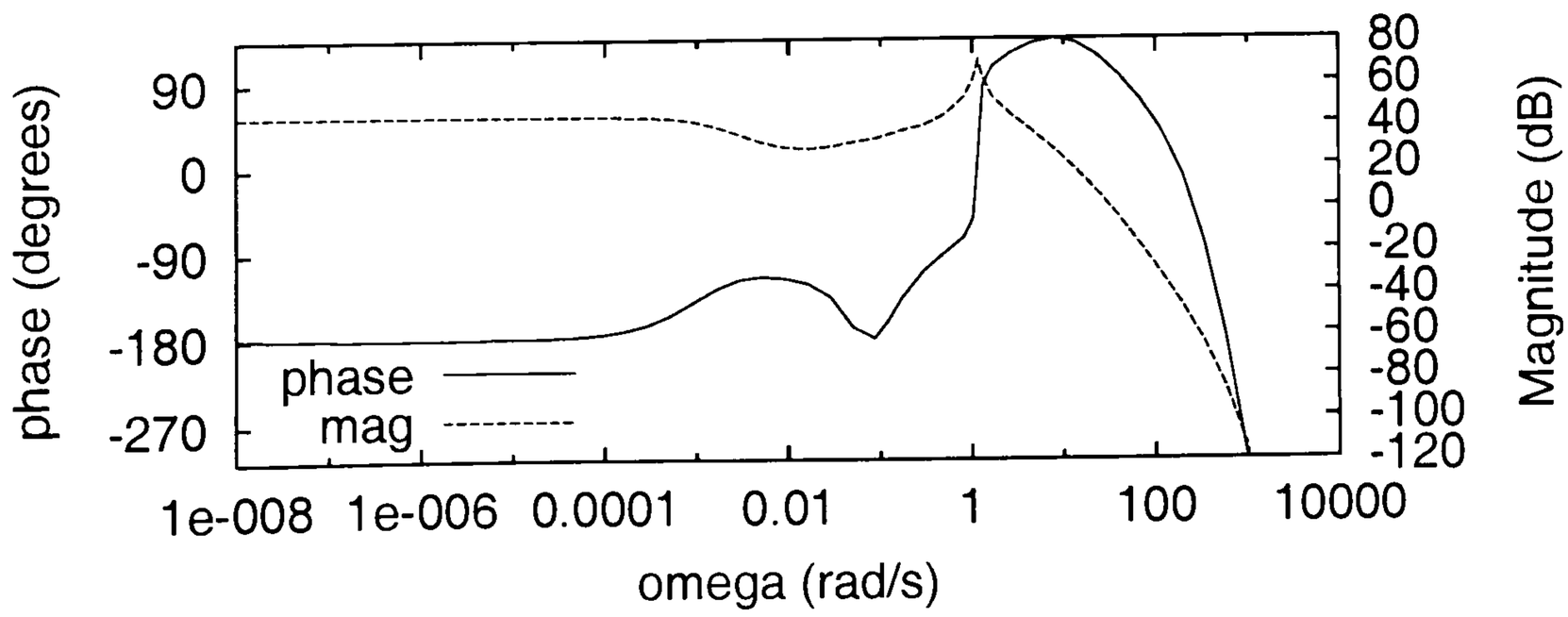

Figure 4.8: Bode plot for pair $L - T_{17}$. Problem 1

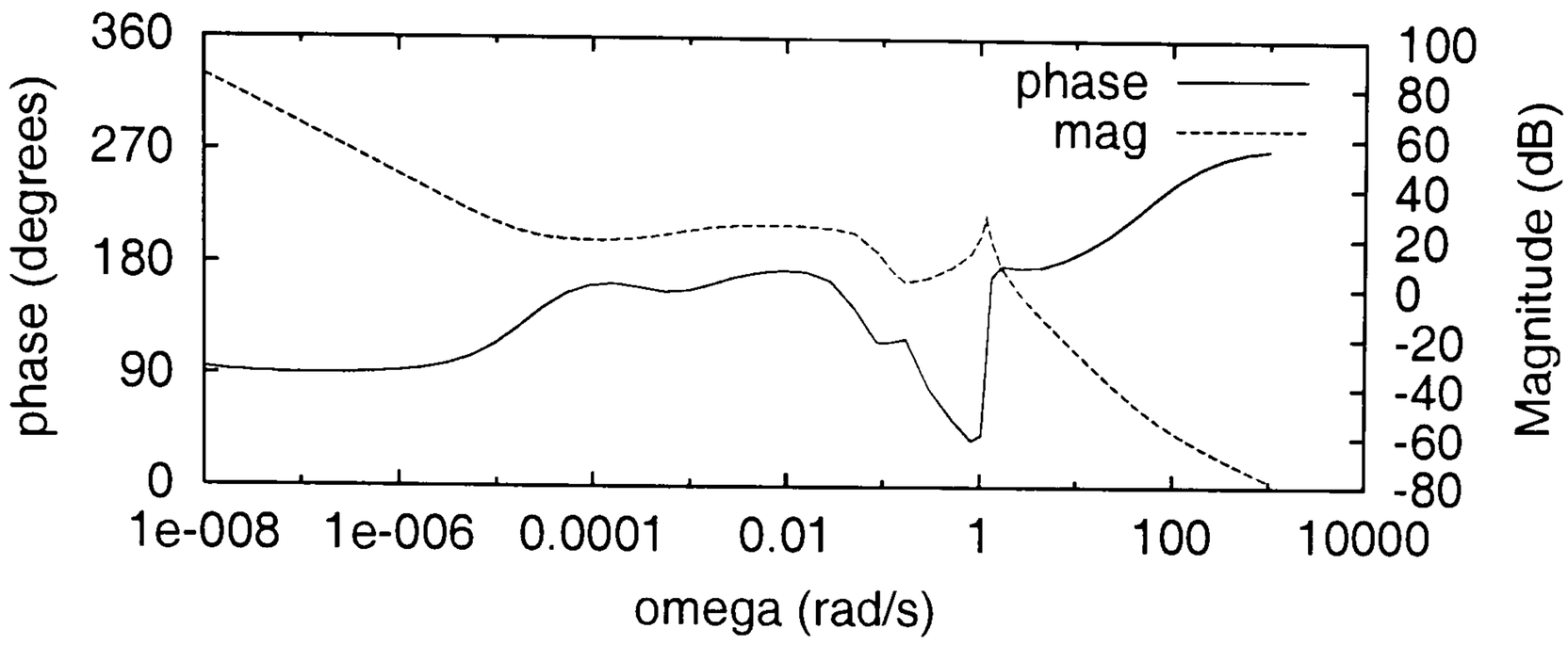

Figure 4.9: Bode plot for pair $L - T_1$. Problem 1

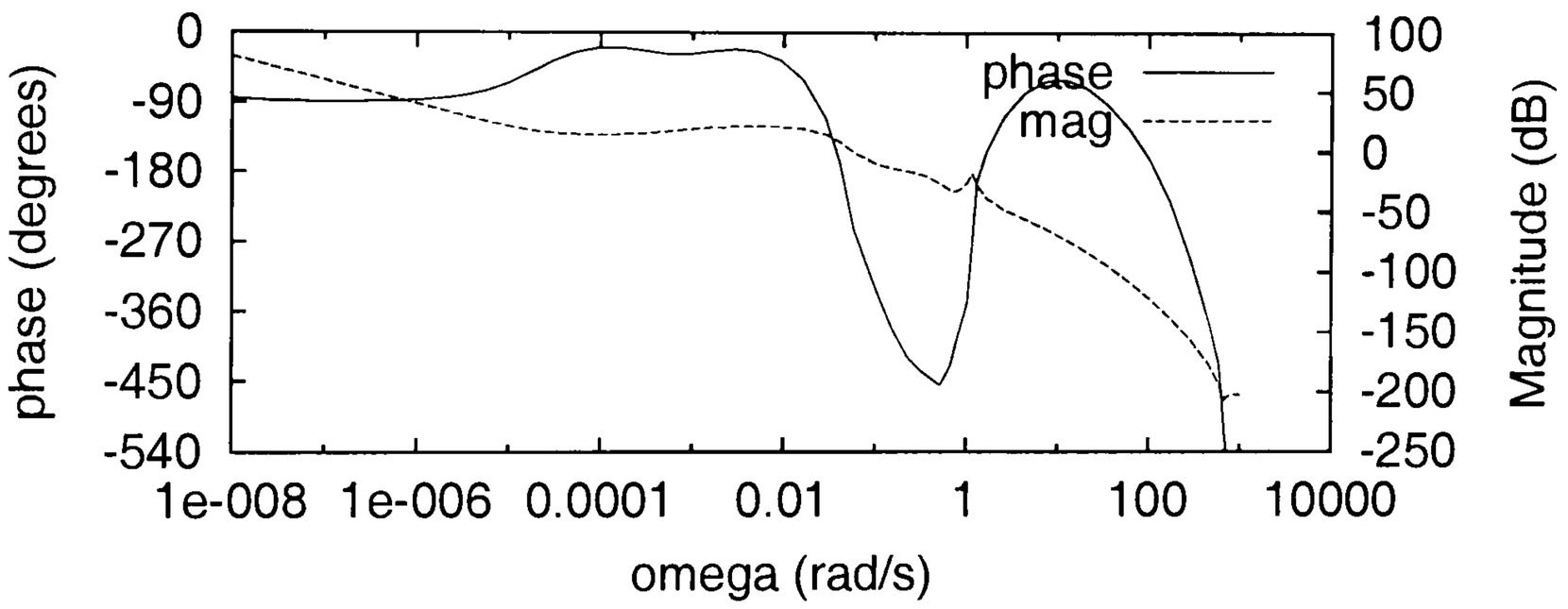

Figure 4.10: Bode plot for pair $Q_{reb} - T_1$. Problem 1

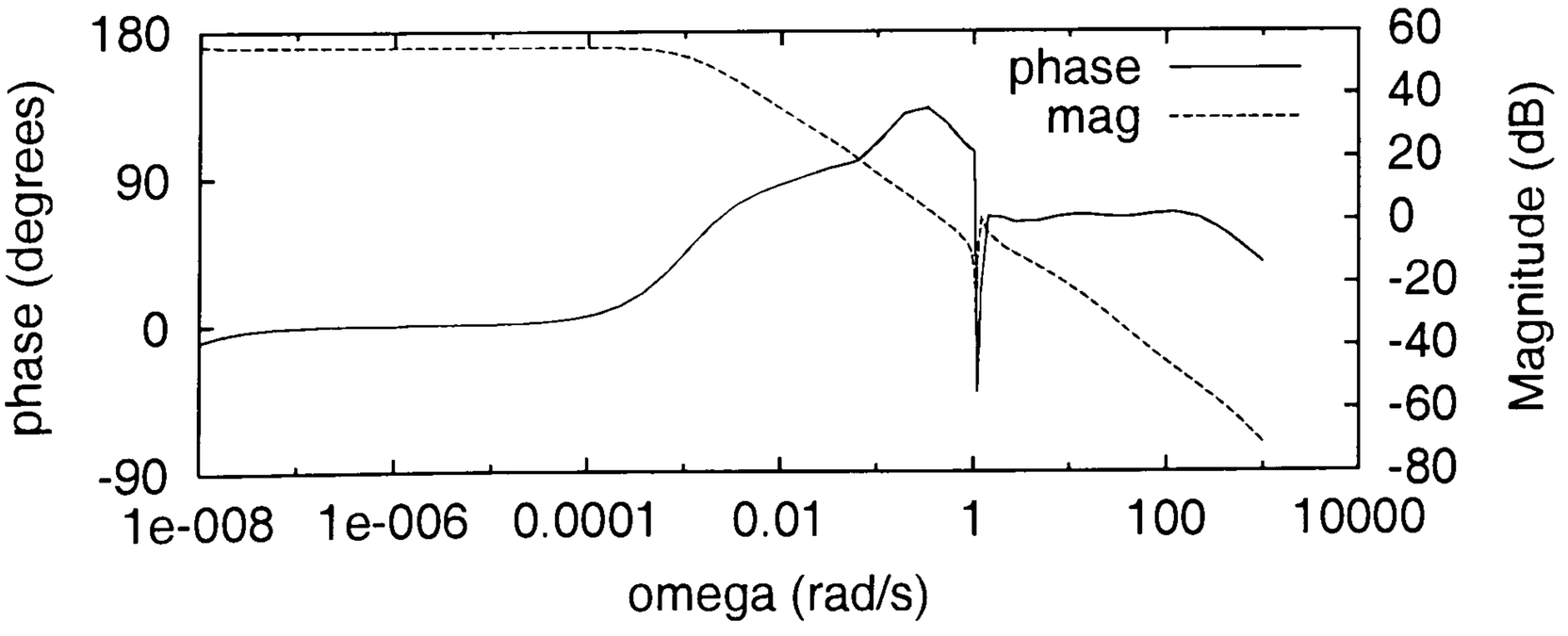

Figure 4.11: Bode plot for pair $R_B - T_{17}$. Problem 1

(a)

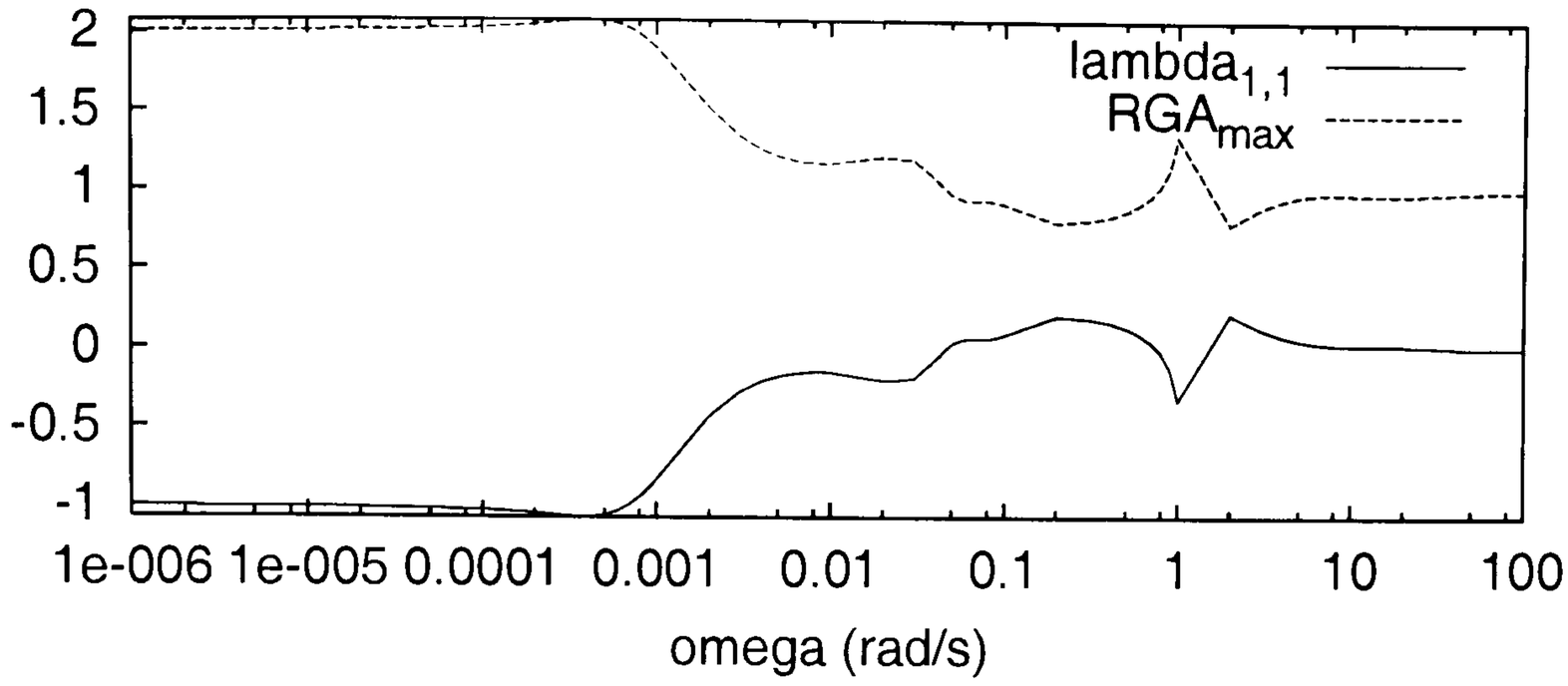

(b)

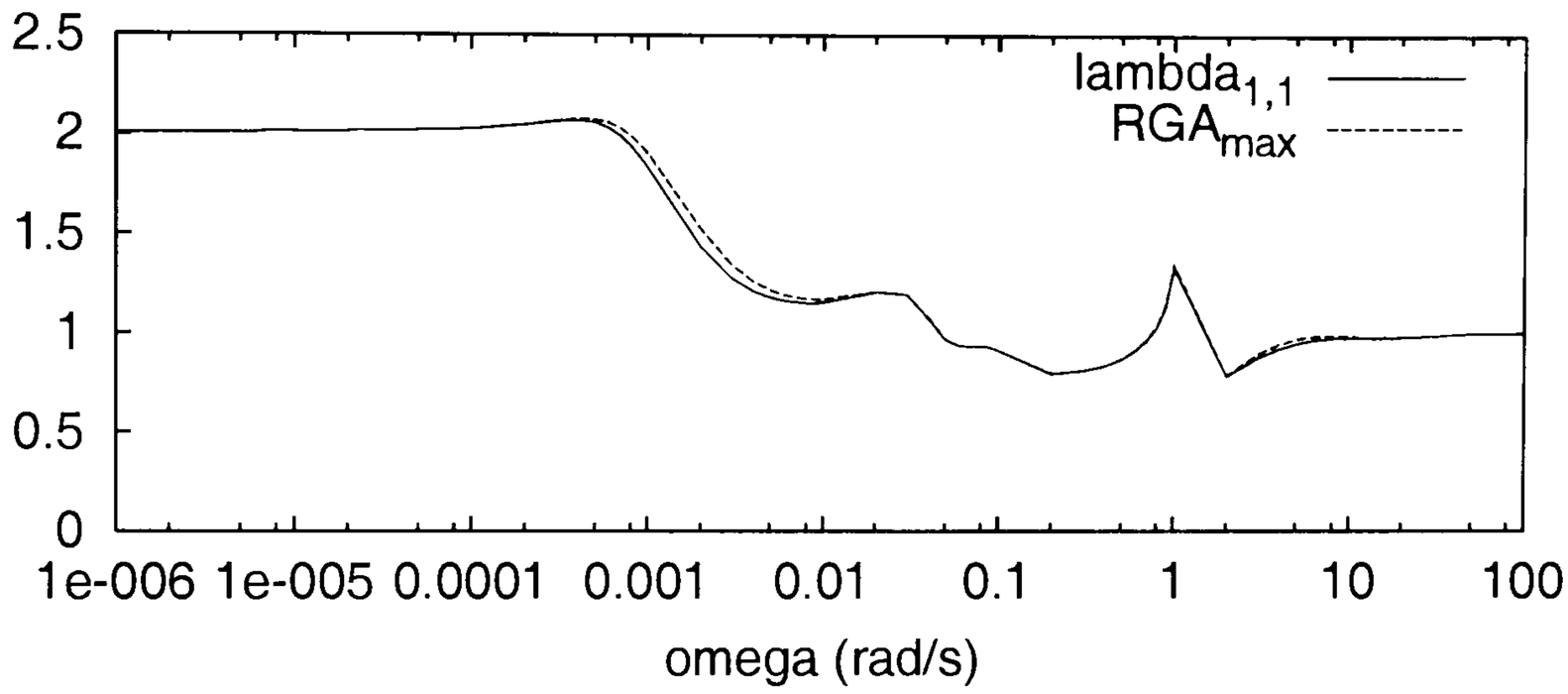

(c)

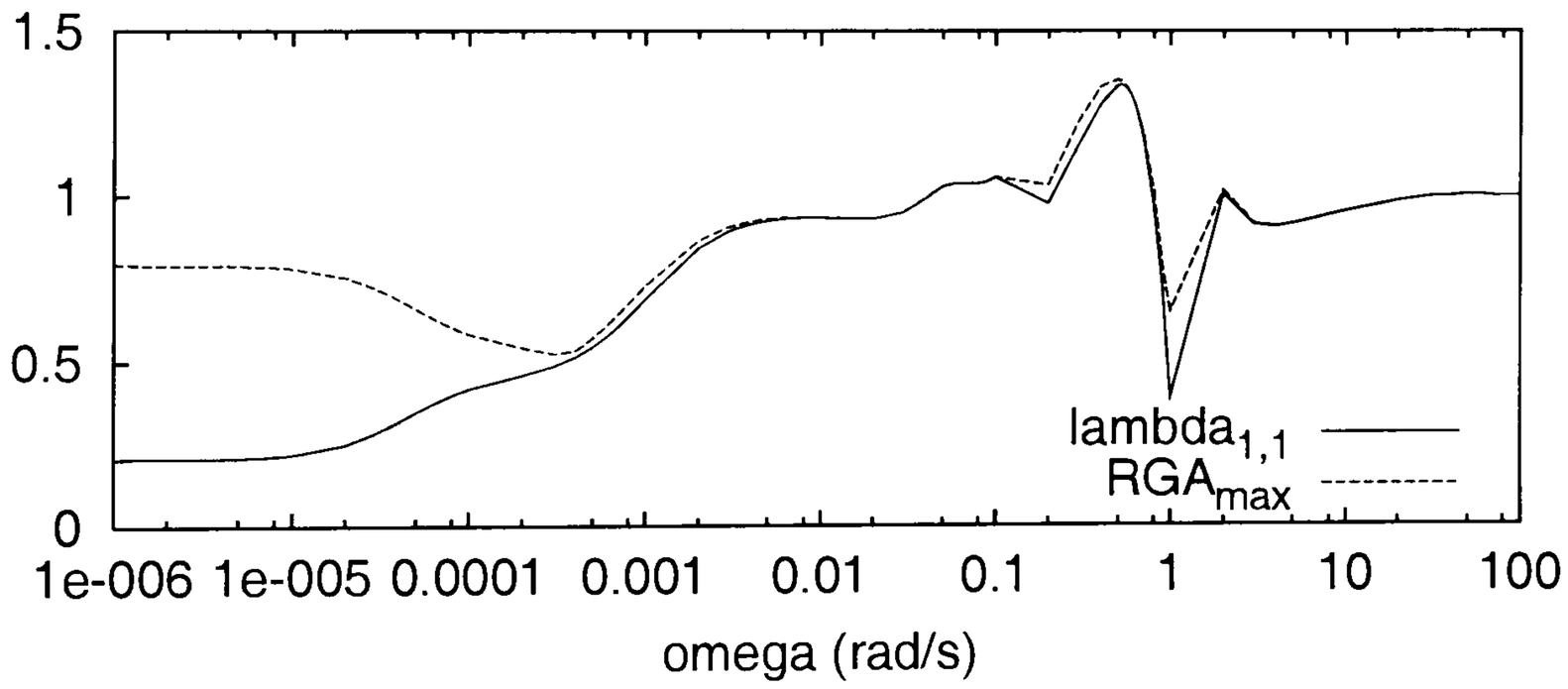

(d)

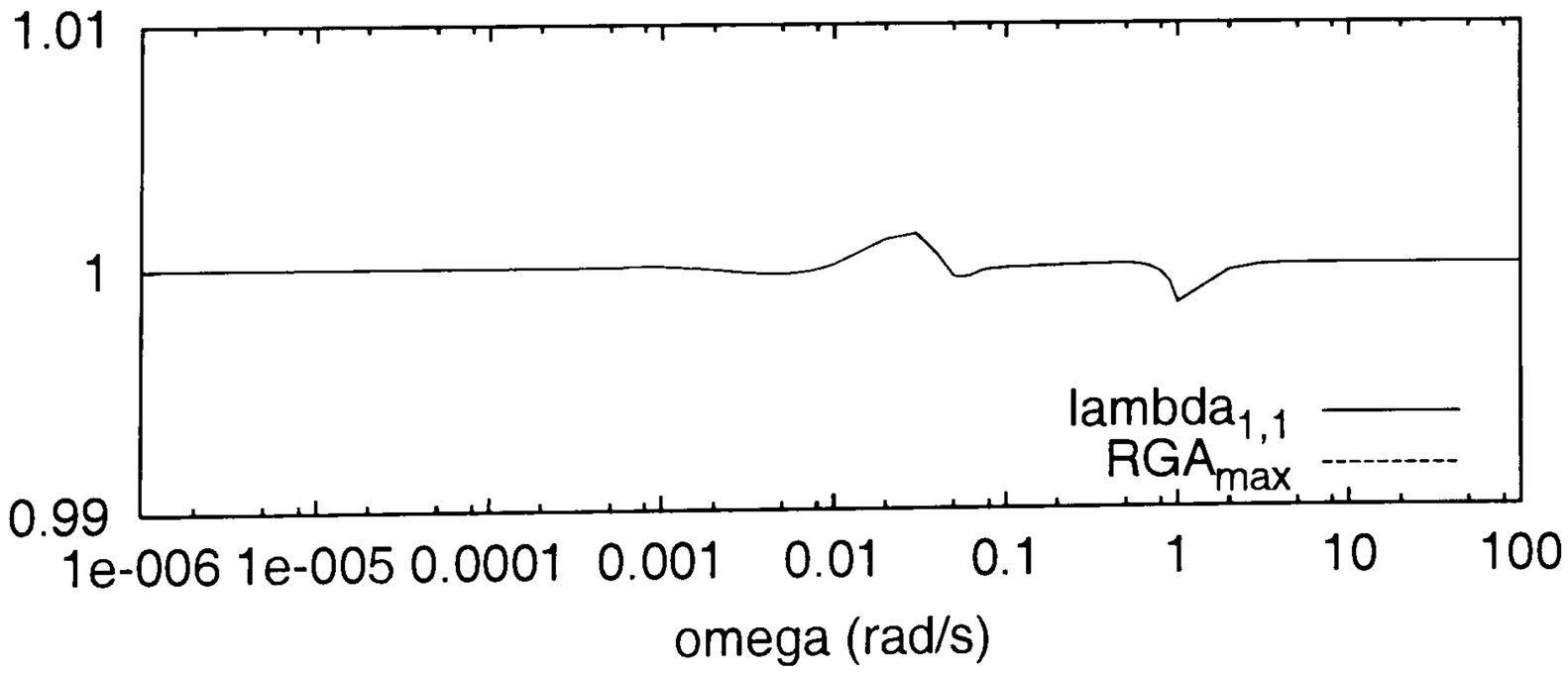

Figure 4.12: RGA first and maximum value elements. Problem 1. (a) Scheme $Q_{reb}R$, (b) Scheme LQ_{reb}, (c) Scheme RR_B, (d) Scheme DQ_{reb} (and D_mQ_{reb}, D_mB_m)

4.5.3 Problem 1 controller design

Controllers design

The column control scheme was divided into 4 independent single input single output (SISO) controllers. Thus, there are a top drum temperature controller. a reboiler temperature controller, a mass controller for the drum and a mass controller for the reboiler. The temperature controllers were selected to be proportional-integral. While the mass (level) controllers were chosen as just proportional.

The implementation of an extra controller to control the pressure at the top of the column was obviated assuming that the column top pressure was perfectly controlled by the condenser heat duty and was assumed equal to 10 atm at all times.

Depending on the scheme, the inputs for temperature and mass control schemes changed. Table 4.9 shows the relationships used for the different schemes. Note, that similarly to the controllability analysis, the reflux ratios were adjusted by manipulating L in the case of R and B in the case of R_B.

Table 4.9: Inputs for the MTBE column controllers

Scheme	T_1	m_1	T_{17}	m_{17}
RQ_{reb}	R	D	Q_{reb}	B
LQ_{reb}	L	D	Q_{reb}	B
DQ_{reb}	D	L	Q_{reb}	B
RR_B	R	D	R_B	Q_{reb}
D_mQ_{reb}	D_m	L_m	Q_{reb}	B_m
D_mB_m	D_m	L_m	B_m	Q_{reb}

The controllers gains and time constants (for the PI-controllers case) were found by trial and error for each scheme. The gain was adjusted from a value that created oscillations to a value in which the oscillations did not occur. The integral time was adjusted as to get a fast response. For each scheme this was performed firstly for the closed-loop simulations in which the methanol feed flow disturbance occurred. The parameters for each scheme were kept for the closed-loop simulation with C_4 feed flow disturbances.

4.5.4 Closed-loop simulations: Problem 1

To test the schemes and compare their performance with the predictions of the controllability analysis, a series of closed-loop simulations with a non-simplified model (Section 2.3.1) was carried out.

The initial conditions were those in Table 4.2. At $t = 10s$ a change in the feed flow started and finished at $t = 1800s$. That change was either a methanol feed flow 10% increase or a 10% C_4 feed flow decrease. In all cases, the controllers acted every $\Delta t = 1s$.

Firstly, the open-loop behaviour is considered for comparison with the closed-loop cases. Secondly, the closed-loop simulations are presented and compared with the control structure analysis results. The closed-loop results are summarised in Table 4.10.

Case 4.5.1 *Open-loop problem*

For this case, there was a 15% step increment in the methanol feed flow. The reflux ratio R and the reboiler heat duty Q_{reb} were constant during the simulation. Nonetheless, the mass controllers were on (Table 4.9).

The mass controllers worked satisfactorily. For the drum there is a total increment of 1%. While, the reboiler mass decreased by 0.1%.

The temperature in the stripping section diminished as a result of the methanol increment and the constant reboiler heat duty. Output T_{17} plummets before arriving to a new steady state value (Figure 4.13 *c*). The cooling within the column results on condensation of light components which results in an concentration increment seen in the stripping section and reboiler (Figure 4.13 *d*). The MTBE production falls by 15%.

Figure 4.13 *a* shows that the temperature at the reflux drum is almost constant, though there is a small decrease that is lower than the maximum error accepted (0.1 K). This behaviour can be explained by the large amount of light components in the drum and by the constant pressure at the condenser (Figure 4.13 *b*). Furthermore, this pattern is repeated for most of the closed loop cases.

Summarising, the methanol feed flow step disturbance can affect the MTBE production in the column. The system arrives to a different steady state provided that the level (mass) controllers work properly.

Table 4.10: Summary of control analysis and simulations for Problem 1

Scheme	Control properties	d_1 Simulations	d_2 Simulations
LQ_{reb}	No well conditioned. $\underline{\sigma}$ decays fast. 3 zeros aligned with poles. d_1: No PC, No AC, aligned with 1 zero. d_2: No PC, No AC, aligned with 3 zeros. Large RGA		T_{17} drops till 388K. When d_1 stops, T_{17} return to its original value. ISE=81018
RR_B	No well conditioned. $\underline{\sigma}$ decays fast. 4 zeros aligned with poles. d_1: No PC, No AC, aligned with 1 zero. d_2: No PC, No AC, aligned with 1 zeros.	T_{17} drops to 406 K. When the disturbance stops, the initial T_{17} value is restored. ISE=27189	T_{17} drops to 405 K. When the disturbance stops, the initial T_{17} value is restored. ISE=26362
DQ_{reb} or D_mQ_{reb}	Better conditioned. $\underline{\sigma}$ high for a large frequency range. d_1: PC, AC, aligned with 9 zeros. d_2: No PC, No AC, aligned with 10 zeros	Control ineffective, T_{17} drops till 402 K. When the disturbance stops, T_{17} arrives to a value slightly higher than the initial one. ISE=70705	Initially T_{17} increases 1 K, but there are interactions between mass and temperature controllers and temperature drops till 400 K. When the disturbance stops, T_{17} arrives to a value slightly higher than the initial one. ISE=48036
D_mQ_{reb}	Similar to DQ_{reb} control scheme	T_{17} decreases till 407 K. When the disturbance stops, T_{17} arrives to a value slightly higher than the initial one. Such a value is the same that the one got with DQ_{reb} scheme. ISE=9540	
D_mB_m	Similar to DQ_{reb} control scheme	T_{17} drops till 407 K, it returns to a slightly higher value than the initial one. ISE=8673	No successful, system become unstable

d_1: MeOH feed flow pulse increment. d_2: C_4 feed flow pulse decrease. PC: Perfect control. AC: Acceptable control. $\underline{\sigma}$: minimum singular value. The table only presents T_{17} results since in most cases T_1 error was below the specified value (0.1K). The mentioned zeros or poles are the positive ones. T_{17} set point was 409.35 K and the allowable error was 2K. ISE: Integral of the square of the error

(a)

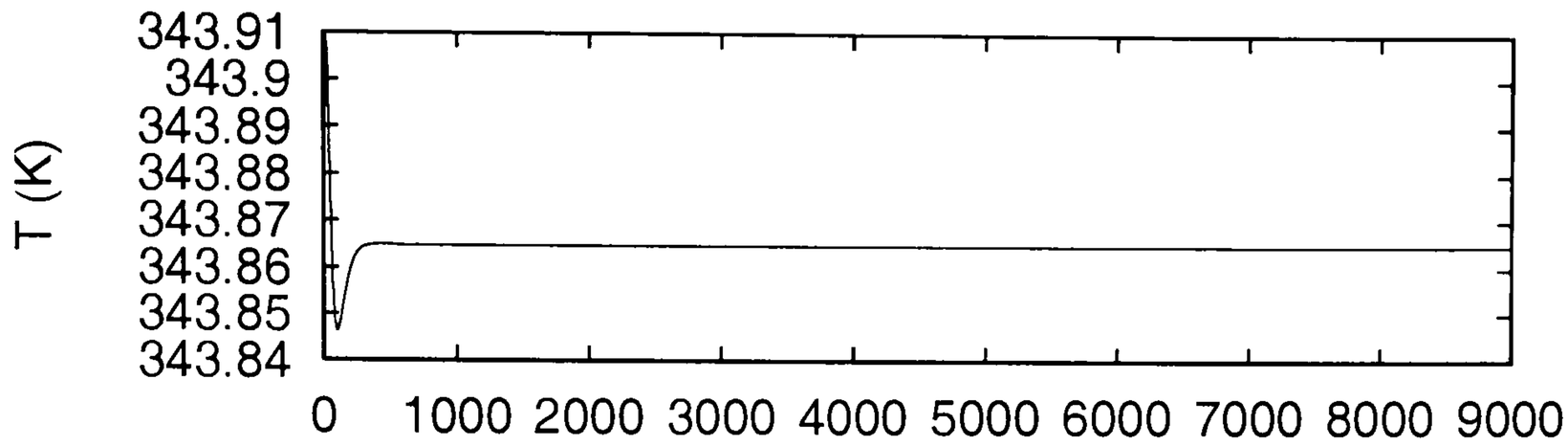

(b)

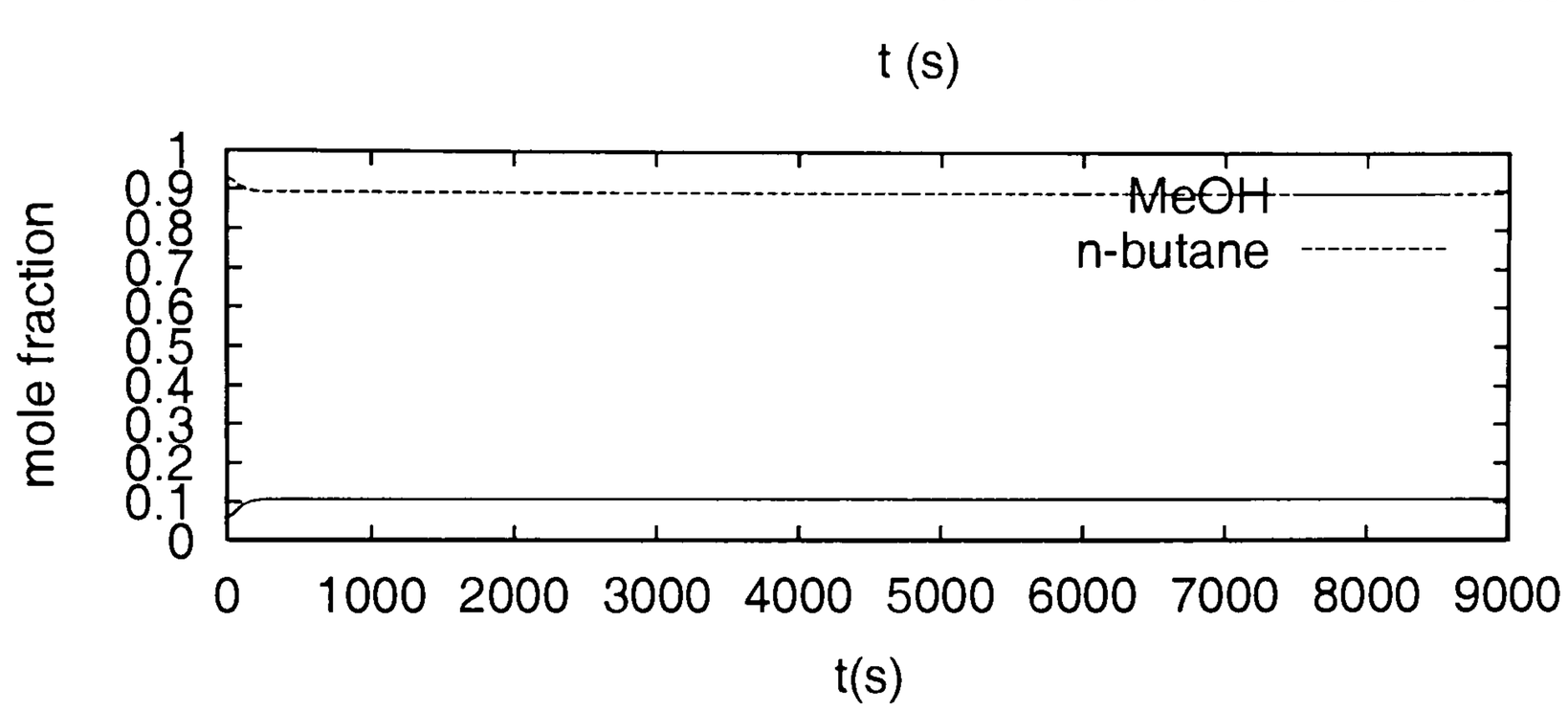

(c)

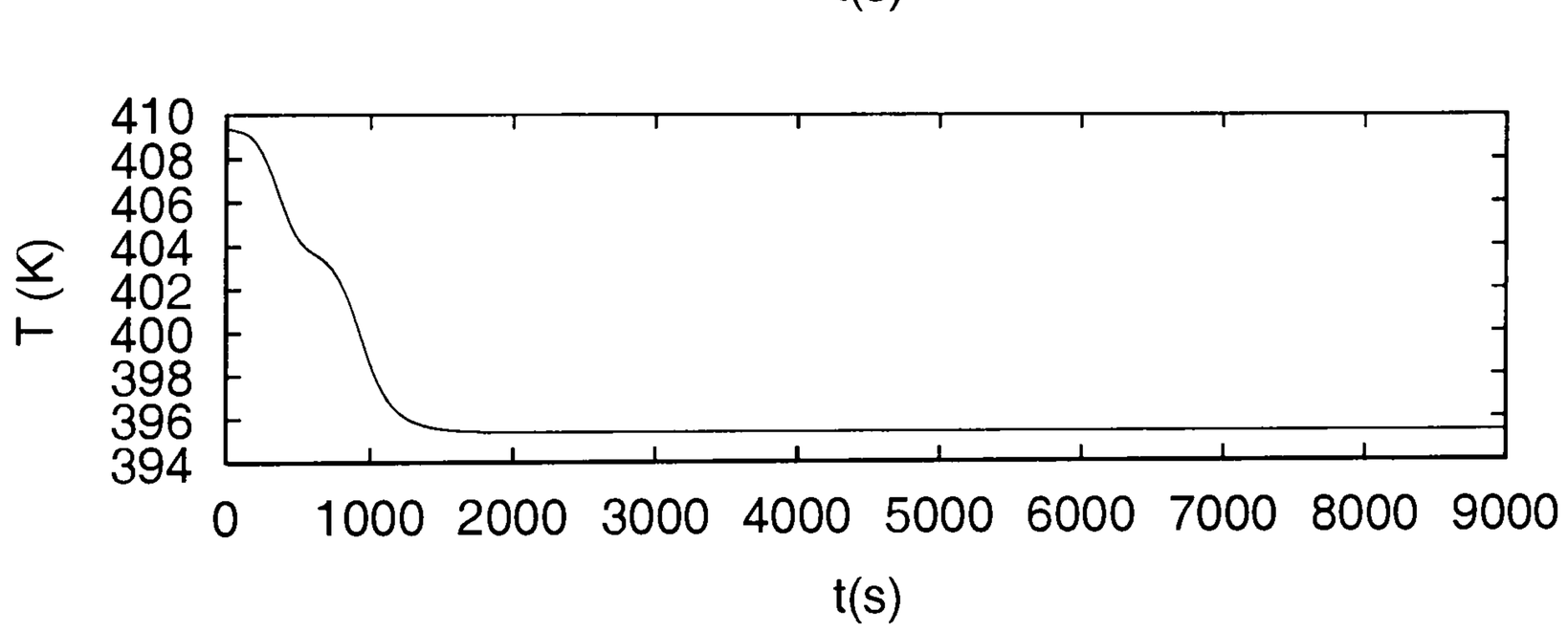

(d)

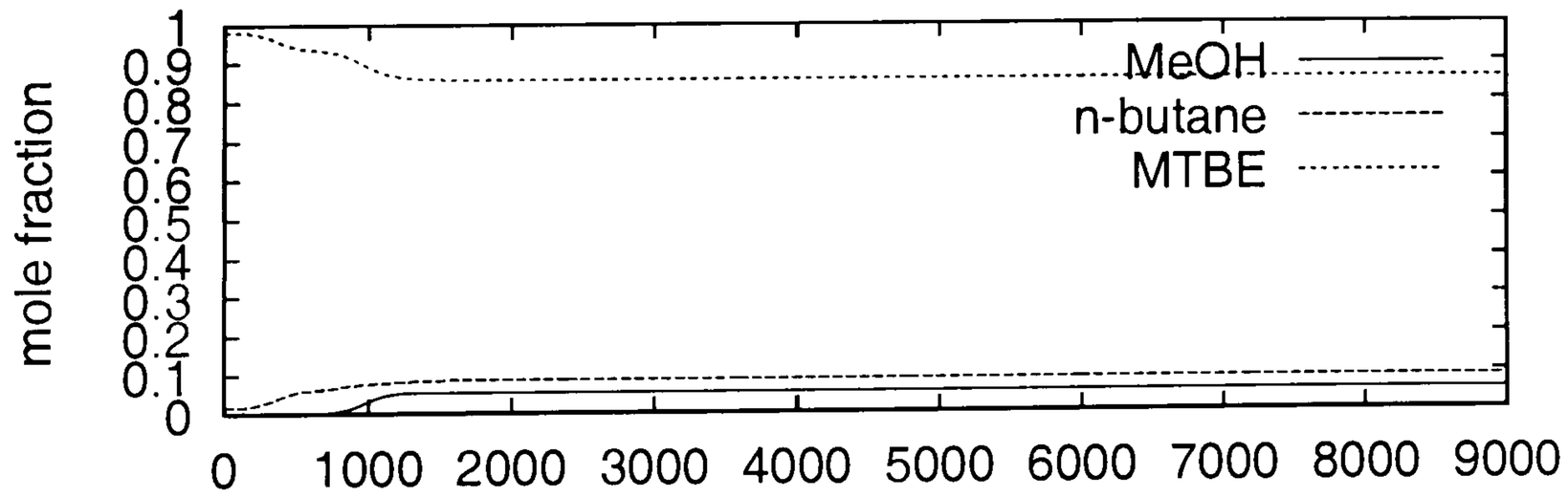

Figure 4.13: Temperature and composition profiles at when a 15% methanol feed flow step is applied and the inputs (reflux ratio R and reboiler heat duty Q_{reb}) are constant. Problem 1. (a) Temperature at the reflux drum, (b) Mole fraction in the liquid phase at the drum($x_{iso-butene}$ and x_{MTBE} are close to zero), (c) Temperature at the reboiler, (d) Mole fraction in the liquid phase at the reboiler ($x_{iso-butene}$ is almost zero)

Case 4.5.2 *$R - R_B$ scheme*

In this case the analysis predicted that neither perfect nor acceptable control would be possible when changes in the methanol or C_4 feed flows occurred. The perfect control criteria were close to one (see Figure 4.5 *c*), so perhaps the controller could at least protect the system against drastic changes. The simulations confirmed this.

In the first experiment, a 10% methanol feed flow increment was applied to at $t = 0s$ and lasted 1800s. There was a 5% increment on the reboiler mass. The use of the reboiler heat duty for controlling the mass at that unit had an effect also on temperature. As predicted, T_{17} surpassed the desired limit (2K) (Figure 4.15), but the results show that T_{17} could have stabilised at 405 K. The same figure shows that once the disturbance ceased, there is a temperature drop due to the fact that the mass is also diminishing and the reboiler heat duty diminishes. The temperature is affected until the effect is contrasted with the R_B change. The excess of the methanol at 320 K cools and the mass increment, provoke condensation of light components. Thus, the amount of MTBE at the reboiler decreases from 98% to 93% during the feed pulse.

The rectifying section of the column is much more stable. Its behaviour is similar to the one presented for the RQ_{reb} example (Case 4.5.1). The temperature and composition return to the original values once the disturbance stops. For instance, Figure 4.14 shows that the temperature T_1 (output) is always kept within the desired error margin (0.1 K) and the reflux ratio R is practically constant.

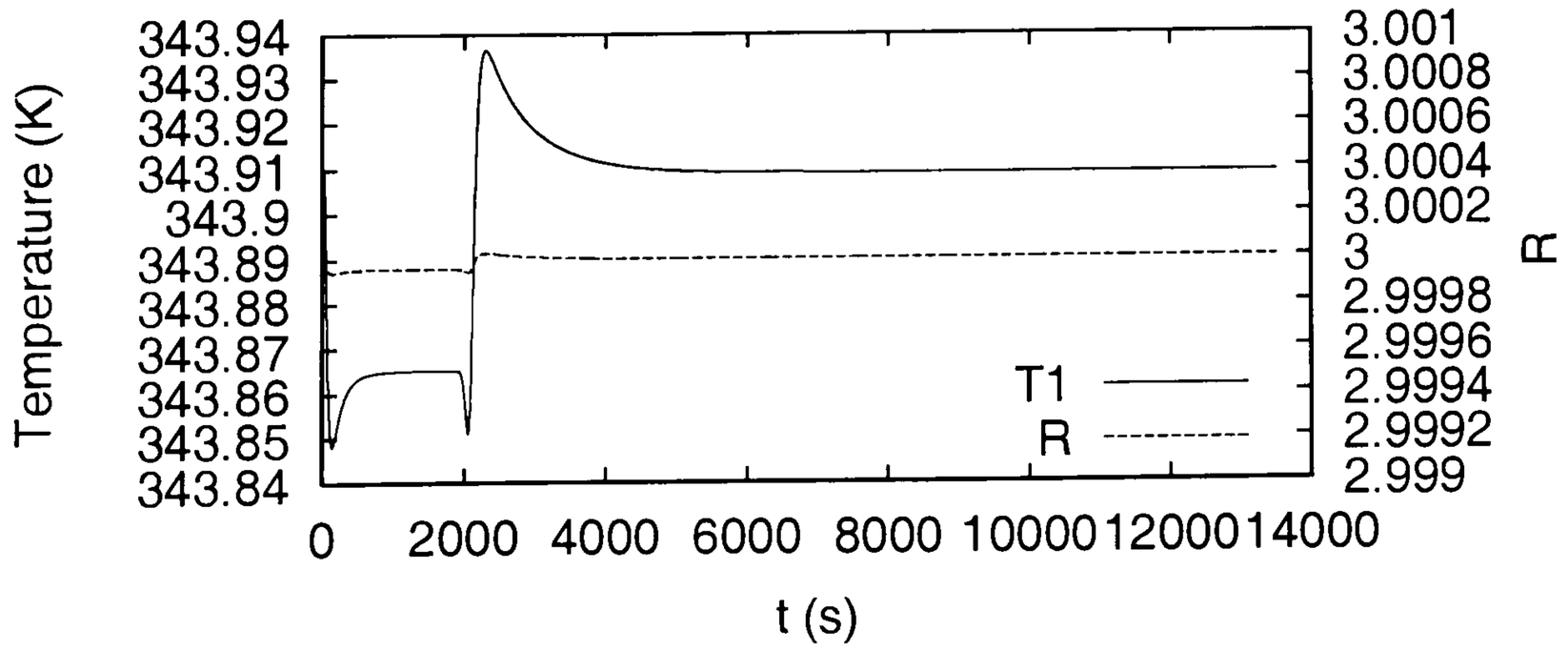

Figure 4.14: Temperature profile and reflux ratio at the drum when a 10% methanol feed flow pulse is applied and scheme RR_B is used. Problem 1

On a second simulation experiment, the system was tested applying a 10% decre-

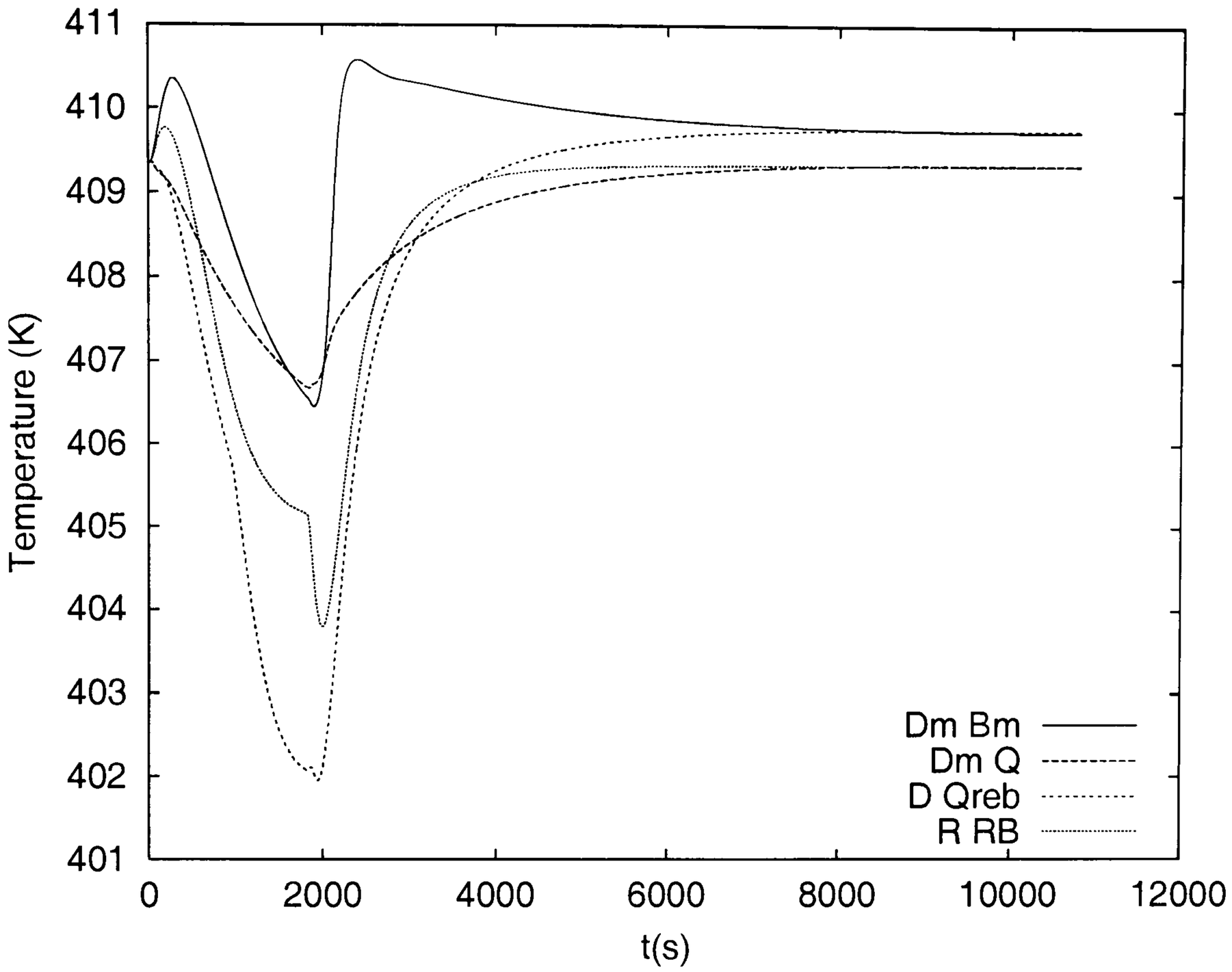

Figure 4.15: Behaviour of output T_{17} for different control schemes when a 10% pulse methanol increment is applied to the MTBE column. Problem 1

ment C_4 feed flow pulse for almost 1800s. In this case, there is strong interaction between the mass and temperature controllers. The mass reduction in the drum reduces the distillate flow rate and since T_1 is almost constant, so R is. Thus, the reflux rate L decreases. This action leads to less mass towards the reboiler where the control response is to decrease the reboiler heat duty. The combination of less heat of reaction, less hot feed and lower reboiler heat duty leads to a general cooling of the column. The control at the reboiler reacts by varying R_B. Nevertheless, T_{17}, decreases till 406 K (Figure 4.16). The error is 1 K beyond the desired value (2 K). There are more interactions when the disturbance elapses, but the system return to the previous steady state.

We can see that in both cases T_{17} surpassed the desired error. However, we can also see that the further error is not large and that the system could be stabilised. This is agreement with the results of the perfect control criterion (Figure 4.5 *c*). and with the fact that positive poles are very close to the origin.

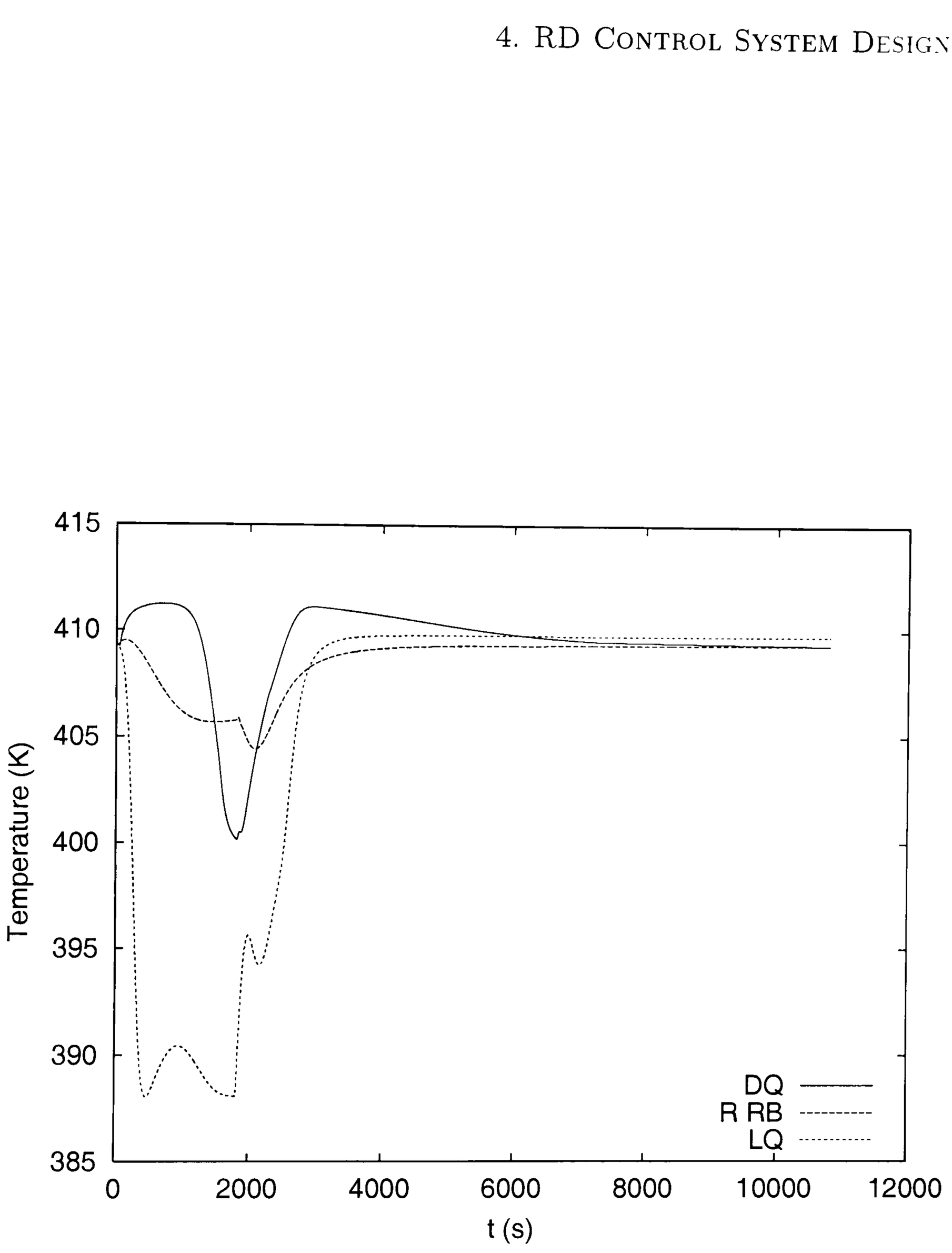

Figure 4.16: Behaviour of output T_{17} for different control schemes when a 10% pulse decrement of the C_4 is applied to the MTBE column. Problem 1

Case 4.5.3 *LQ_{reb} scheme*

The analysis predicted that this scheme would have problems. This was shown by the failure to meet the perfect or acceptable criterion (Figure 4.5 *a* and Figure 4.7), the smallest RHP zero among the schemes and aligned with a RHP pole (Table 4.8), low minimum condition number (Figure 4.6), the instability displayed in the frequency response diagram between input L or R and output T_{17} (Figure 4.8) and the indication that this scheme (and $Q_{reb}R$) is more susceptible to input uncertainty since its RGA elements are larger than the rest of the schemes (Figure 4.12).

Such a result was tested by closed-loop simulation of the MTBE column with a 10% pulse decrement of the C_4 feed that started at $t = 10s$ and finished at $t = 1800s$. The reduction of reactive iso-butene in the column reduces the MTBE production and cools the column. Hence the light components drop into the stripping section and T_{17} plummets to 388 K (Figure 4.16). The changes in the column affect the production. During the disturbance, the MTBE concentration product descends from 98% to 80%.

The simulations results coincide with the analysis results. The LQ_{reb} control scheme is not a good option for the column at the current specifications. It does not control T_{17} and might also destabilise the system.

Case 4.5.4 *DQ_{reb} scheme*

The scheme DQ_{reb} possesses some features that made it a good candidate for control of the MTBE column. Such features are summarised in Table 4.10.

The system was tested with closed-loop simulation: an experiment with the methanol feed flow increase pulse and an experiment with the C_4 feed flow decrease pulse.

In the first experiment, it was not possible to control the second output, T_{17}. Such a temperature drops and the error is 5 K (Figure 4.15). This is in contradiction of the analysis results. However, we must keep in mind that the perfect control criterion and the acceptable control criterion for this case are less than one just very close to the steady state. A possible explanation are the interactions between mass and T that occur in the column in a similar way than for the RR_B control scheme simulations (Case 4.5.2).

When the system is exposed to a C_4 feed flow decrement, the temperature T_{17} controller fails as well (see Figure 4.16). Although there is an initial increment of

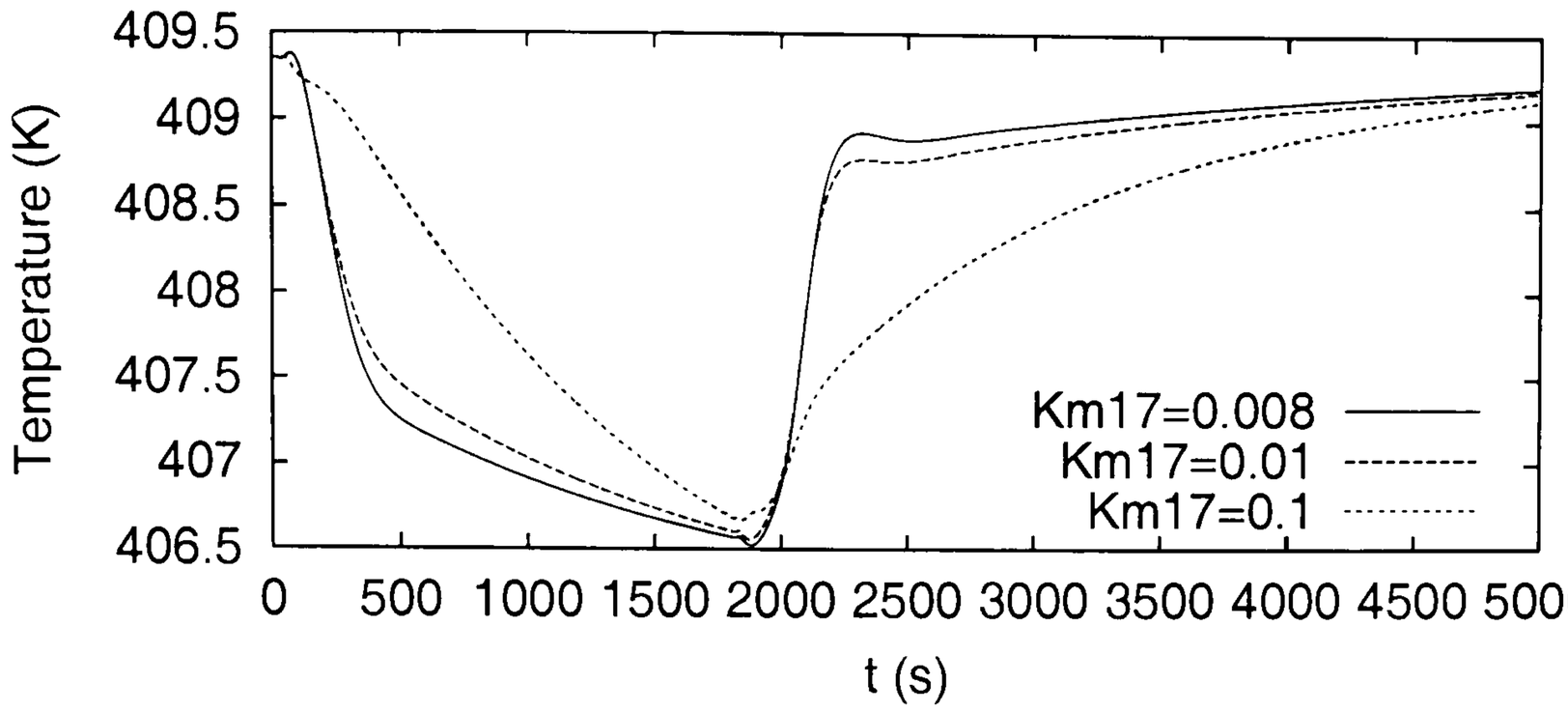

Figure 4.17: Effect of drum mass controller on the reboiler temperature when scheme $D_m Q_{reb}$ is used and the mass drum input is L_m. There is a 10% methanol feed pulse increment from $t = 10s$ to $t = 1800s$. Problem 1

T_{17}, the reactive and the stripping section cool by the lack of reaction. This makes the input to saturate.

We conclude that the temperature control fails. This result does not contradict the analysis because it was predicted that perfect control was possible but just very close to the steady state.

Case 4.5.5 *$D_m Q_{reb}$ scheme*

In the preceding example, it was said that the mass controller (the reflux rate was the input) failed because it interacted with the temperature controller at the reboiler. Such a behaviour is related with the frequency response analysis for the scheme LQ_{reb} (Figure 4.8). The plot shows that there is instability for this pair at low frequencies.

Here the methanol pulse experiment is repeated (in this case all the flow inputs are mass based). Figure 4.17 shows the effect of the reflux rate on T_{17} when different gains are used in the drum mass controller. We can see that when the disturbance applied and small mass controller gains are used, T_{17} could arrive to a new steady state faster than when large mass controller gain was used.

This example shows the importance of considering all the interactions before deciding what the most suitable controller is. Indeed, we should look to control all the process variables. Table 4.11 shows that the error using a tight mass controller for this scheme does not increase significantly the integral square error. Hence, it is preferable to stick to the tight mass controller.

Case 4.5.6 *$D_m B_m$ scheme*

The control properties of this scheme are similar to DQ_{reb} problem. Though the analysis suggested, that close to the steady state this scheme could control the system if there were changes in the methanol feed flow or in the C_4 composition feed, but could no control it if a change in the C_4 feed flow occurred.

The simulation results showed that the controller fails when a methanol pulse increment is applied to the system (Figure 4.15). Though, the slope is less pronounced than for other cases and the error is less than 1K beyond the acceptable error (2K).

Due to the use of the two external flows of the column, it is expected that this column displays problems for the total mass balance (Stichlmair, 1998). That happened when C_4 (gas) feed flow disturbance occured. The system became unstable due to the interactions between the mass and temperature controllers.

Regarding to the C_4 disturbance, the simulations are in agreement with the analysis. The system could not be controlled if there is a change in the C_4 feed flow. However, the simulations did not agree with the analysis regarding methanol disturbance. But we must remember that the analysis results suggest that perfect control would be possible but close to the steady state. Possibly if the methanol had increased less, the scheme could have controlled the system.

Quantitative comparison between scheme performances

To quantitatively compare between the results, the *Integral of the Square of the Error* (ISE) was used. The ISE is defined as follows (Smith and Corripio, 1997):

$$\text{ISE} = \int_0^\infty e^2(t)\mathrm{d}t \tag{4.1}$$

The ISE was used because it puts more weight in the large errors and less in the small ones.

Only the error for T_{17} is considered since it is the largest found. Furthermore, in most cases (the exception being RR_B) the error was not calculated using the temperature set point, but the temperature at the final steady state (see Figures 4.15 and 4.16).

Table 4.11 shows the comparison between the results for the schemes when the methanol and C_4 feed flow pulses were introduced. We can see that the largest ISE

Table 4.11: ISE for T_{17}. Problem 1 simulations

Scheme	ISE	
	MeOH pulse	C_4 pulse
LQ_{reb}	a	810187
RR_B	27189	26362
DQ_{reb}	70705	48036
D_mQ_{reb} $(K_{m1} = 0.008)$	11575	a
D_mQ_{reb} $(K_{m1} = 0.01)$	9383	a
D_mQ_{reb} $(K_{m1} = 0.1)$	9540	a
D_mB_m	8673	b

[a] No experiment. [b] Simulation crashed

correspond to scheme LQ_{reb} and the smallest to D_mB_m. Such results correspond to the analysis prediction. Since it is risky to use D_mB_m scheme, Table 4.11 values suggest that D_mQ_{reb} is a better option.

4.6 Problem 2: Control structure design

The problem characteristics were presented in Section 4.4 (Table 4.3).

The system is functionally controllable. The system is also s-controllable and s-observable, thus, there are not hidden states. There are more positive poles for Problem 2. The total number is 13, though such poles are closer to the origin than for Problem 1. Furthermore, there are more positive complex poles than in the first problem. Possibly that is an indication of higher non-linearity than for the first problem. Figure 4.18 shows the poles for Problem 2. We can see that the negative poles are about three magnitude order larger than the positive poles. Thus, the system should be rather stable.

4.6.1 Main differences between schemes

Disturbances effect

The disturbance effect is summarised in Table 4.12. Similarly to Problem 1, the analysis predicts that those schemes related to the reflux rate ($Q_{reb}R$, LQ_{reb} and RR_B) are unable to overcome the disturbances. The schemes related to the distillate flow rate, can cope with disturbance d_3, that is a change in the C_4 feed

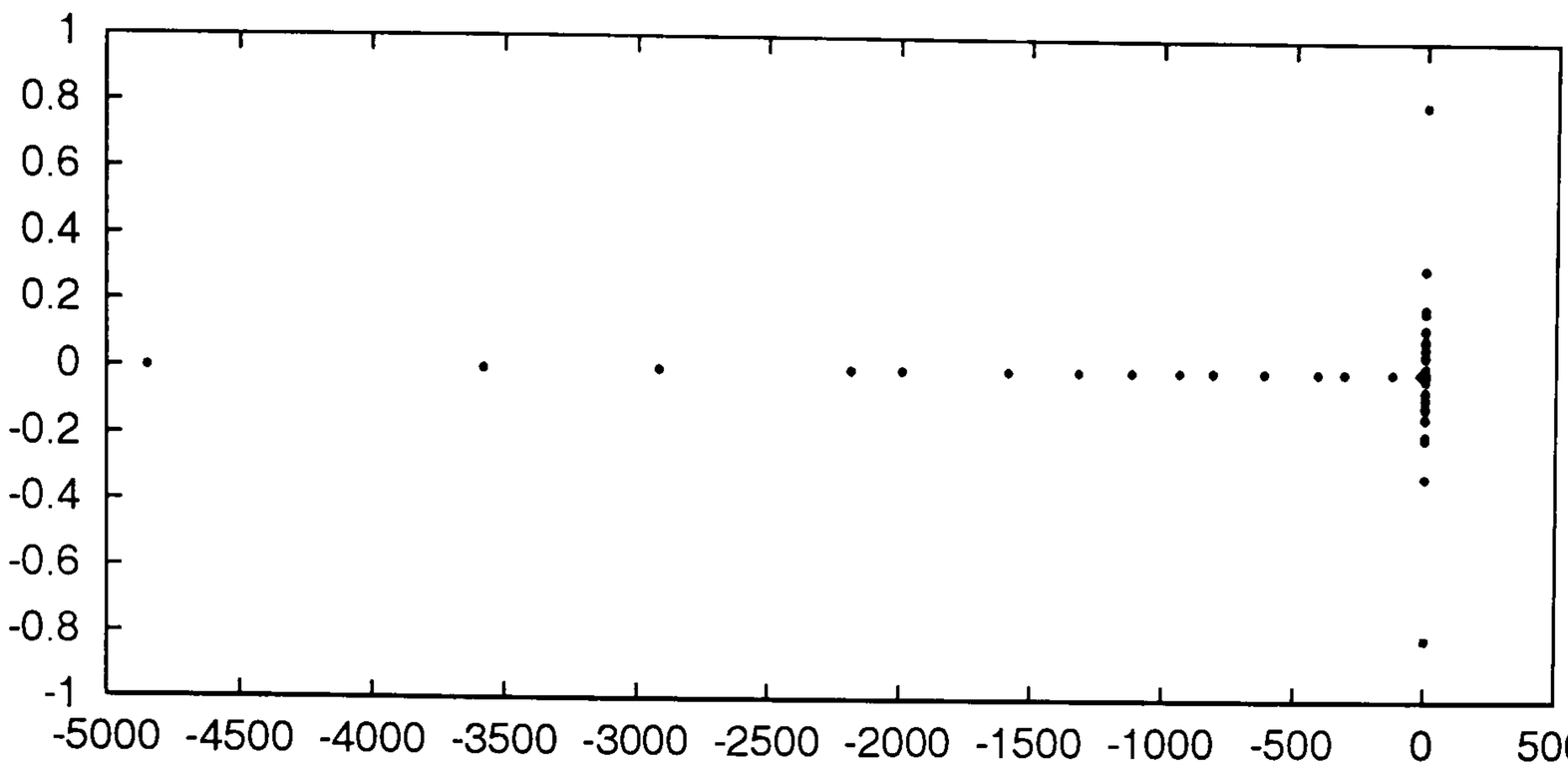

Figure 4.18: Poles. Problem 2

composition. For disturbances d_1 (methanol feed flow change) and d_2 (C_4 feed flow change) the criteria are just above one. Thus, it is possible that schemes DQ_{reb}, D_mQ_{reb} and D_mB_m can overcome the mentioned disturbances. Figure 4.19 shows the described results.

Table 4.12: Disturbance effect close to the steady state, Problem 2. AC = acceptable control, PC = perfect control

Scheme	d_1	d_2	d_3
$Q_{reb}R$, LQ_{reb}	No PC, No AC	No PC, No AC	No PC, No AC
RR_B	PC, almost AC	No PC, No AC	No PC, No AC
DQ_{reb},D_mQ_{reb}	No PC, almost AC	No PC, almost AC	PC, AC
D_mB_m	PC, AC	No PC, AC	PC, AC

Positive zeros

This problem presented more positive zeros than Problem 1, though these are less aligned to positive poles. Table 4.13 shows them and their features.

Note that in this problem RR_B scheme has the smallest RHP zero. This explains why the perfect control criterion deviates greatly from one. This is in contrast with Problem 1 in which this scheme displayed the largest smallest positive zero when compared with the rest of the schemes. Another observation is that the two zeros aligned with positive poles for scheme D_mB_m are not the smallest ones.

Table 4.13 also shows us that the smallest zeros are smaller than for Problem 1.

Table 4.13: Number of positive zeros and their characteristics. Problem 2

Scheme	RHP zeros	Smallest RHP zero	Aligned with RHP poles	Aligned with d_1	d_2	d_3
$Q_{reb}R$	11	4.829E-04	none	8	10	8
LQ_{reb}	11	4.830E-04	none	8	10	8
DQ_{reb}	10	4.502E-04	none	10	10	10
RR_b	11	7.12E-05	1	7	9	7
D_mQ_{reb}	10	4.502E-04	none	10	10	10
D_mB_m	11	3.25E-03	2	11	11	11

This means that it should be more difficult to control Problem 2 because the bandwidth is smaller.

Singular value decomposition and acceptable control

The singular value decomposition results show that in this case, the system is better conditioned when the schemes related to L are used than when the schemes related to D (Figure 4.20) for a longer frequency range. However, close to the steady state, the minimum singular value is higher for D related schemes, though just close to the steady state. However, since the results come from a linearisation of the original model, then we would still prefer the schemes that use D as an input.

The minimum singular values were also compared with the norm of the product of the output direction and the disturbance direction to check whether acceptable control was possible. Figure 4.21 *a* and *c* shows that schemes using L (LQ_{reb} and RQ_{reb}) as an input cannot achieve acceptable control when any of the inputs occur. Though RR_B can achieve acceptable control if there is a change in the C_4 flow. Scheme DQ_{reb} or (D_mQreb can achieve acceptable control when disturbance there are changes in the C_4 feed (flow or composition), though close to the steady state.

An interesting result is that using scheme D_mB_m close to the steady state can achieve acceptable control if any of the disturbances occur. This might be possible because the smallest RHP zero is greater than for other schemes and even though there are two positive zeros aligned with two positive poles, it is not with the smallest one (see Table 4.13).

(a)

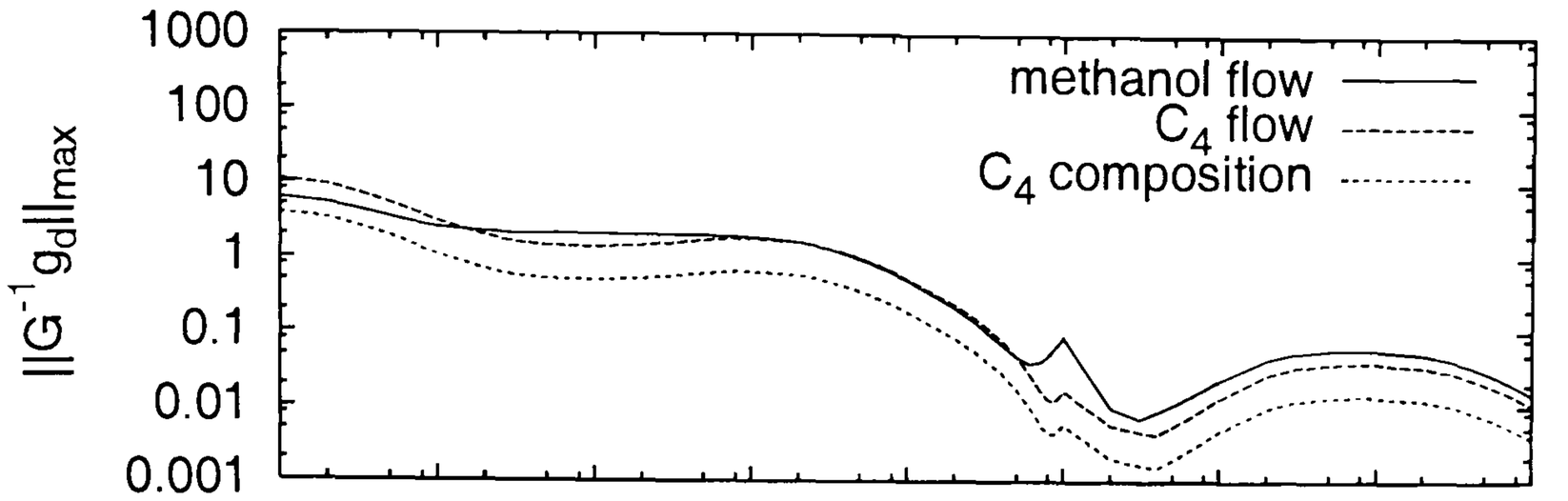

(b)

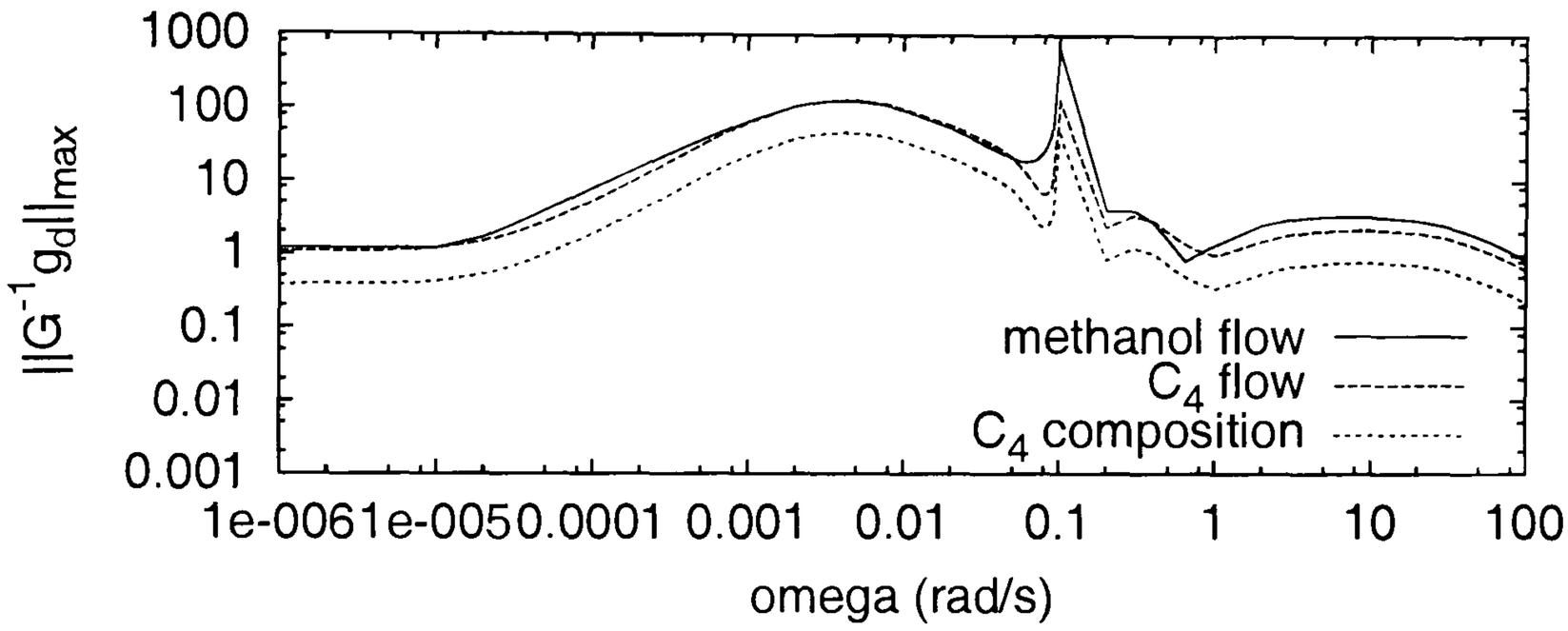

(c)

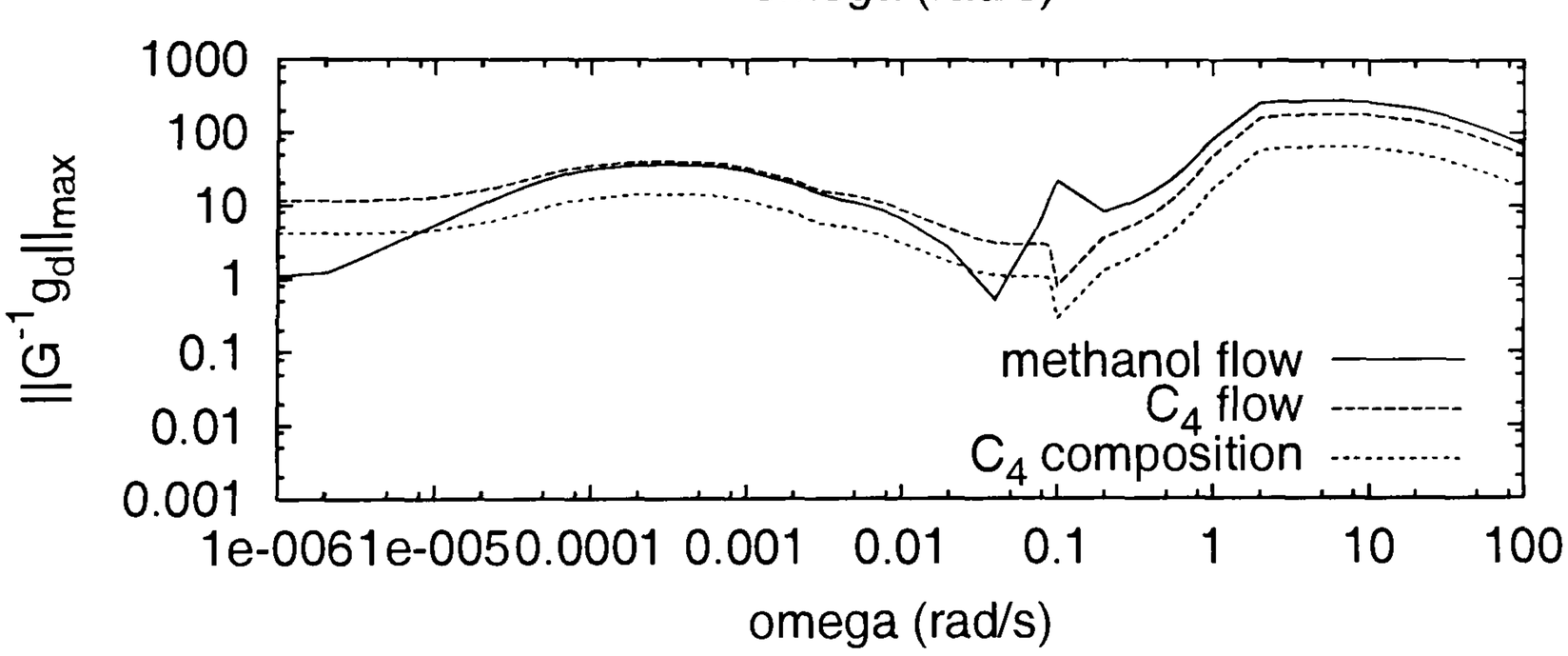

(d)

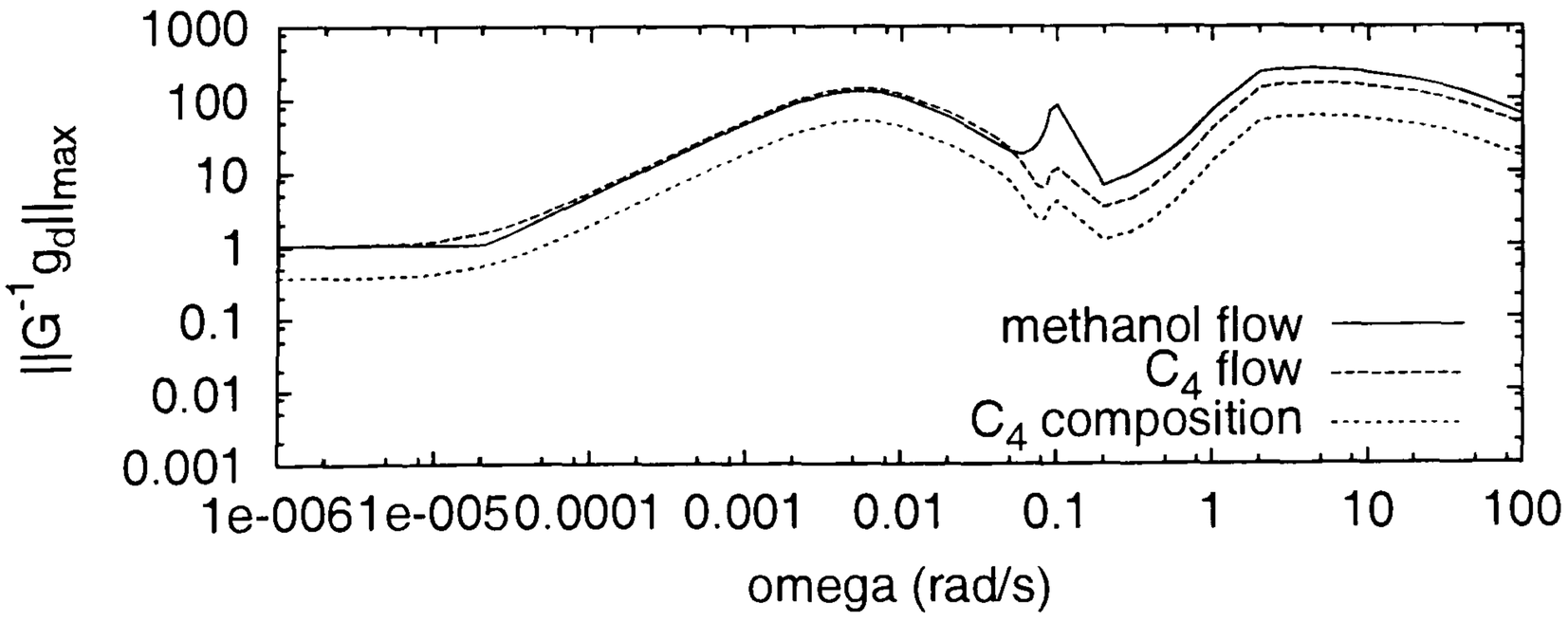

Figure 4.19: Perfect control criterion. Problem 2. (a) Scheme LQ_{reb} (and $Q_{reb}R$), (b) Scheme DQ_{reb} (and D_mQ_{reb}), (c) Scheme RR_B, (d) Scheme D_mB_m

(a)

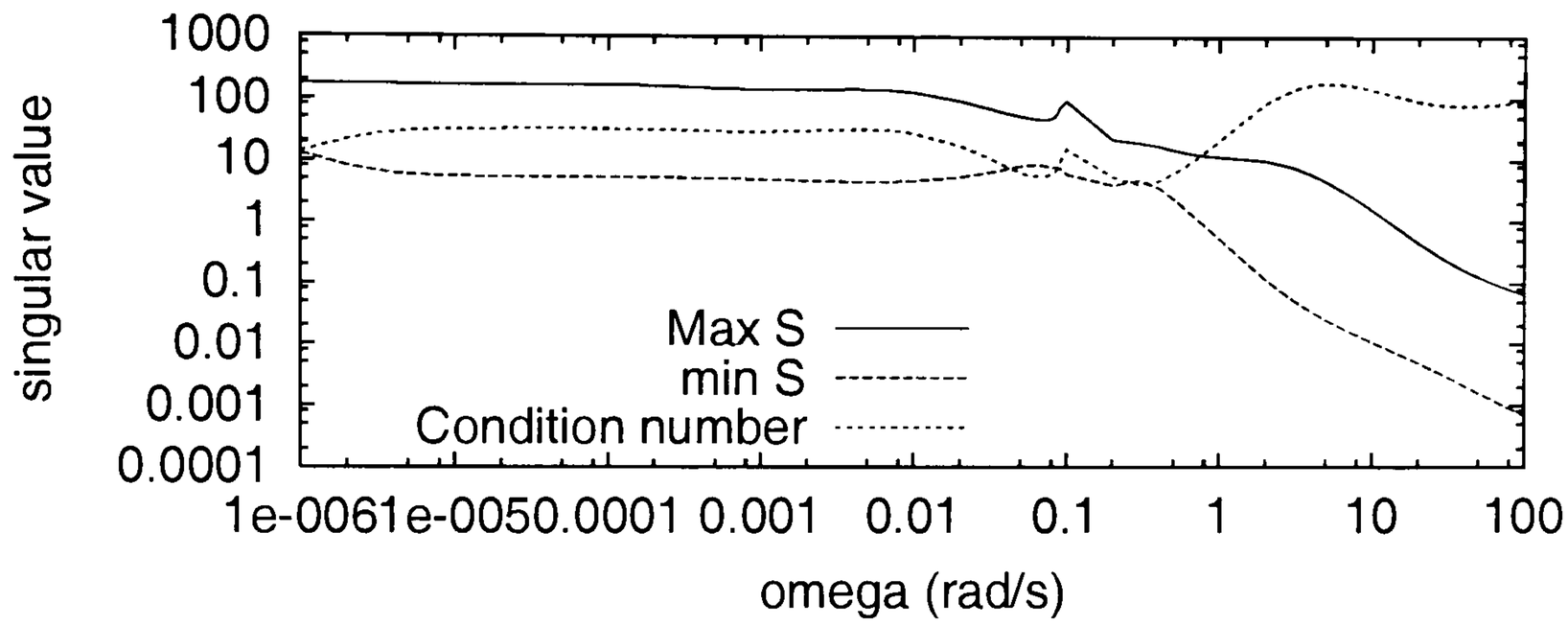

(b)

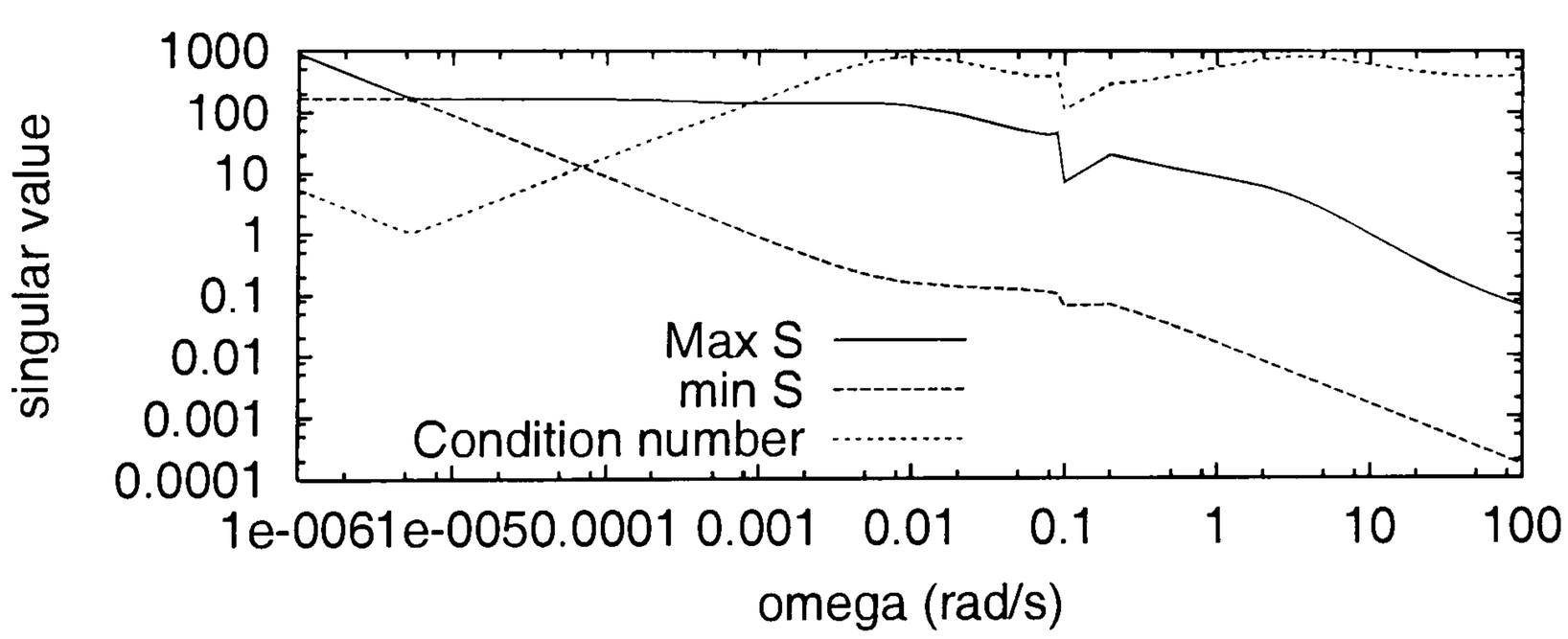

Figure 4.20: Singular value decomposition. Problem 2. (a) Scheme LQ_{reb} (and $Q_{reb}R$), (b) Scheme DQ_{reb} (and D_mQ_{reb}),

(a)

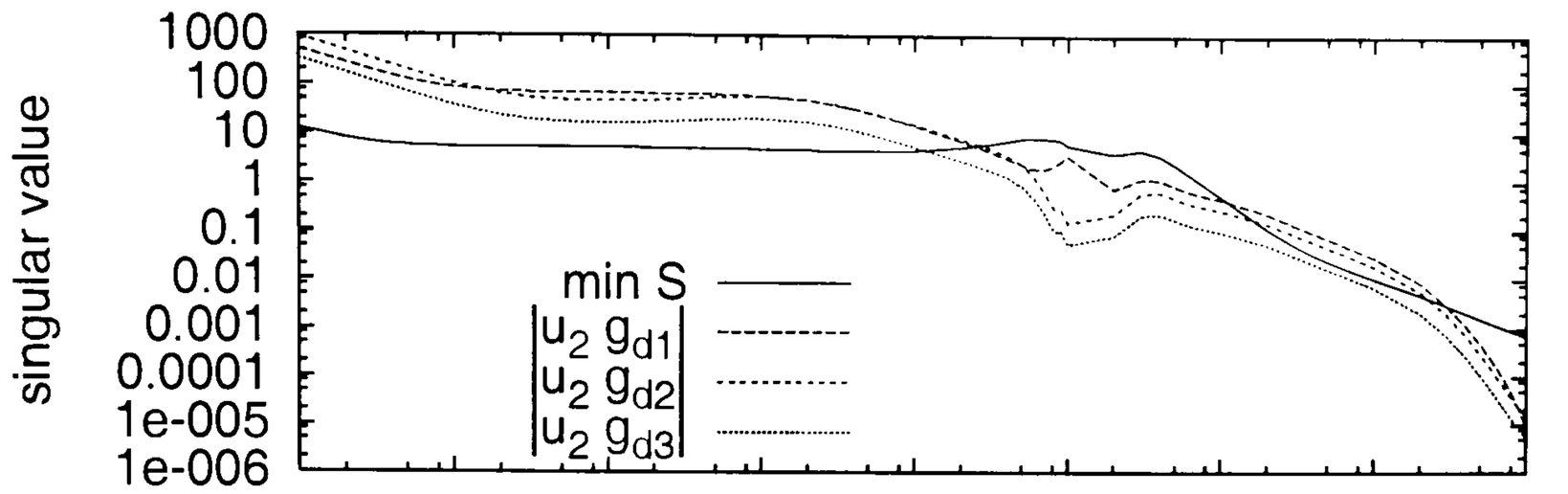

(b)

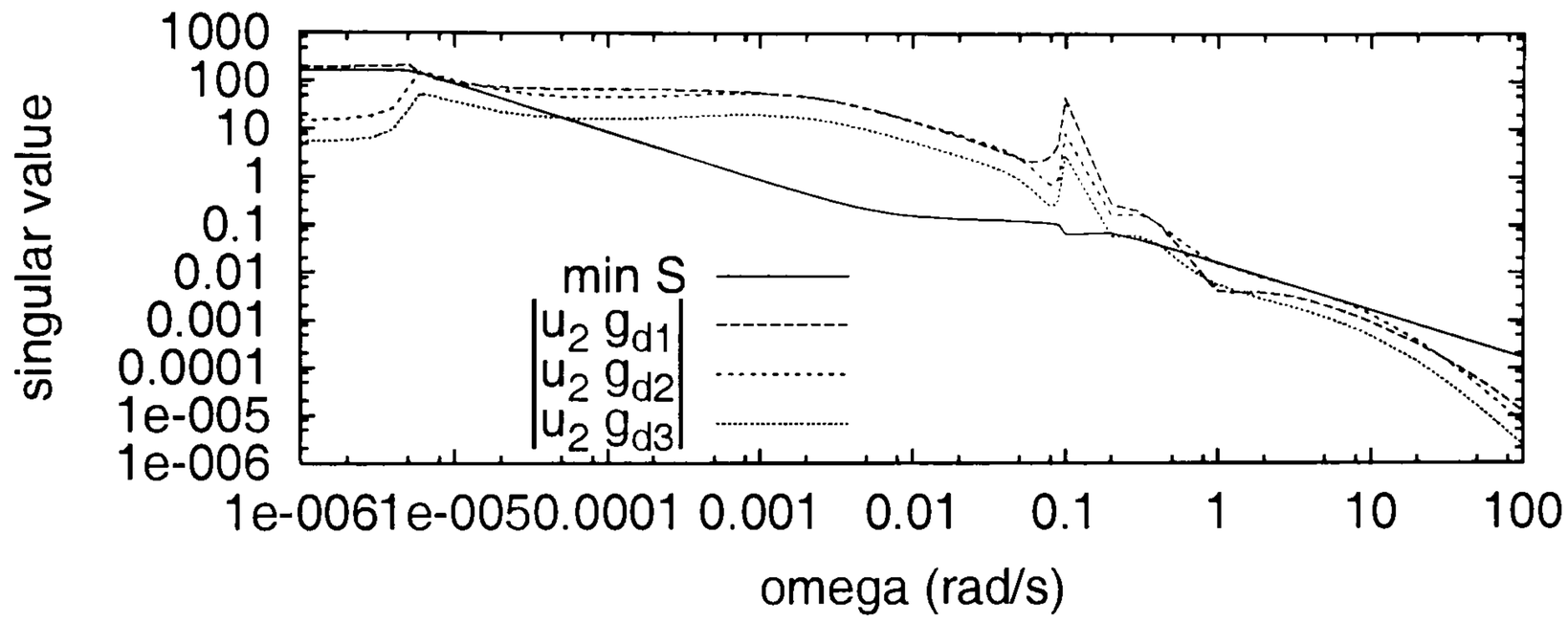

(c)

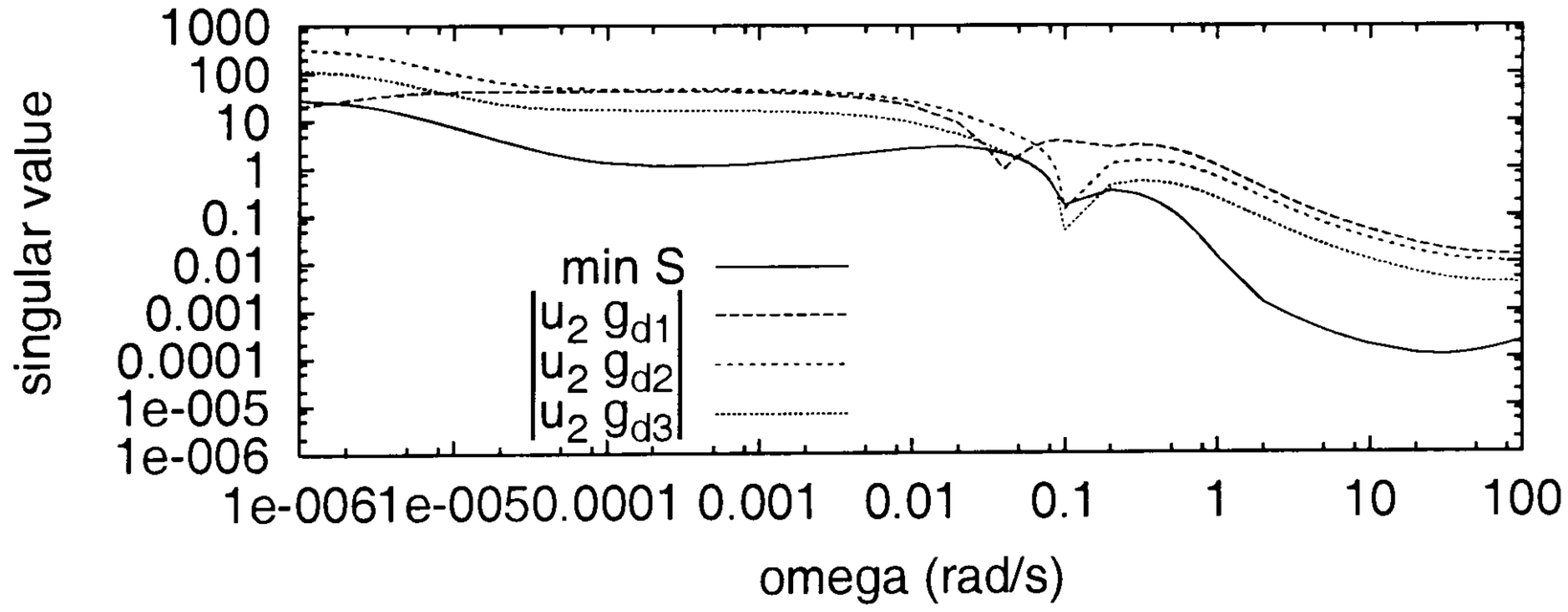

(d)

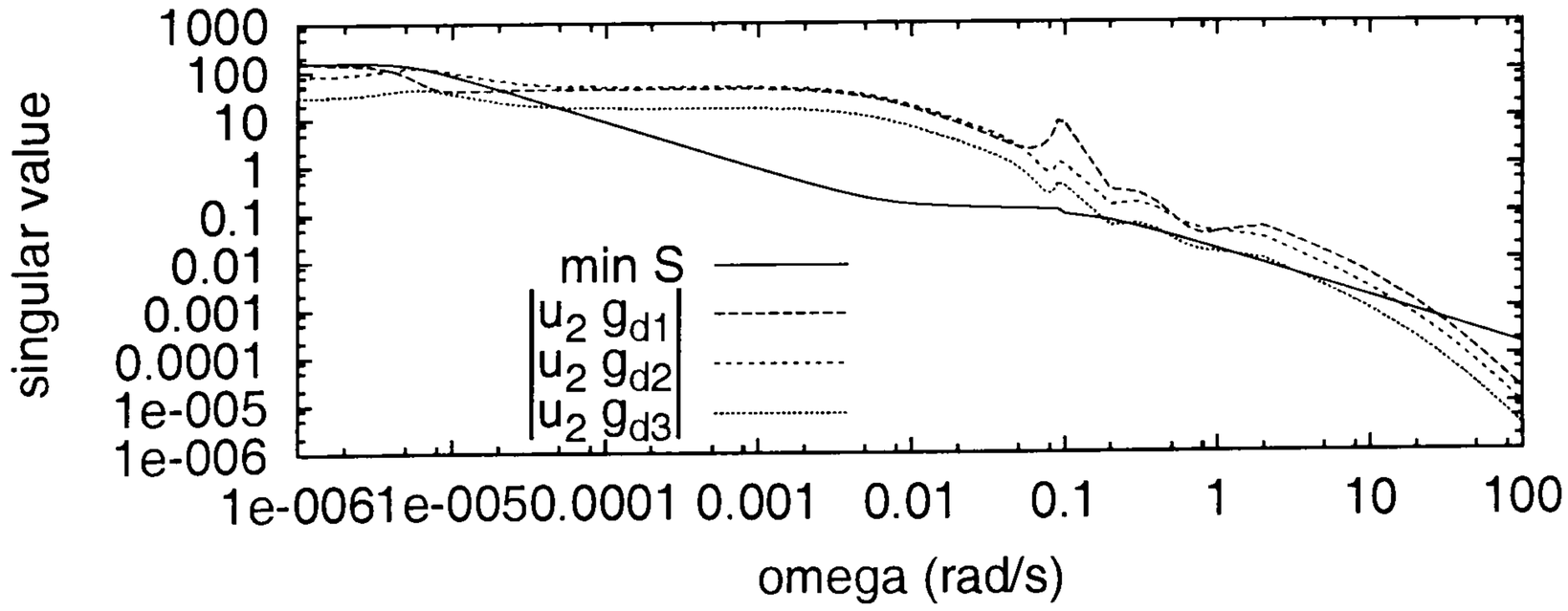

Figure 4.21: Acceptable control criterion. Problem 2. (a) Scheme LQ_{reb} (and $Q_{reb}R$), (b) Scheme DQ_{reb} (and D_mQ_{reb}), (c) Scheme RR_B, (d) Scheme D_mB_m

Frequency response

The frequency response analysis showed similarities between Problem 1 and Problem 2. For instance, in both cases there is a critical frequency ω_{180} that indicates instability problems between Q_{reb} and T_1. A possible explanation for such a behaviour is that although an increment of the reboiler heat duty can evaporate more light components (C_4 compounds), it can also affect the reaction that is occurring within the column if MTBE is also evaporated. On the other hand, Problem 2 did not display any instability close to the steady state.

T_1 displays positive phase when the input is either L or R. When the input is D or D_m the phase was negative (Figure 4.22 and 4.23). Close to the steady state, most of all T_{17}-input relationships displayed a phase close to zero, except with $D_m B_m$ where the phase was positive (Figure 4.24).

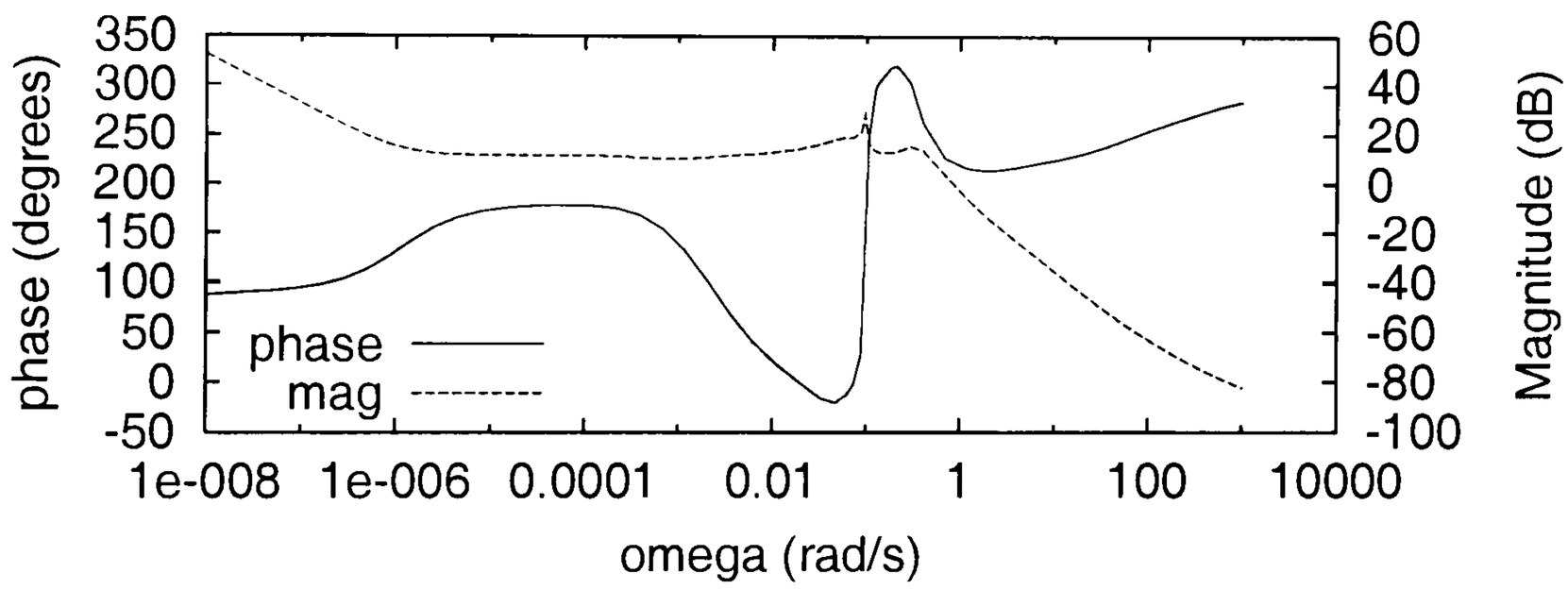

Figure 4.22: Bode plot for pair $R - T_1$. Problem 2

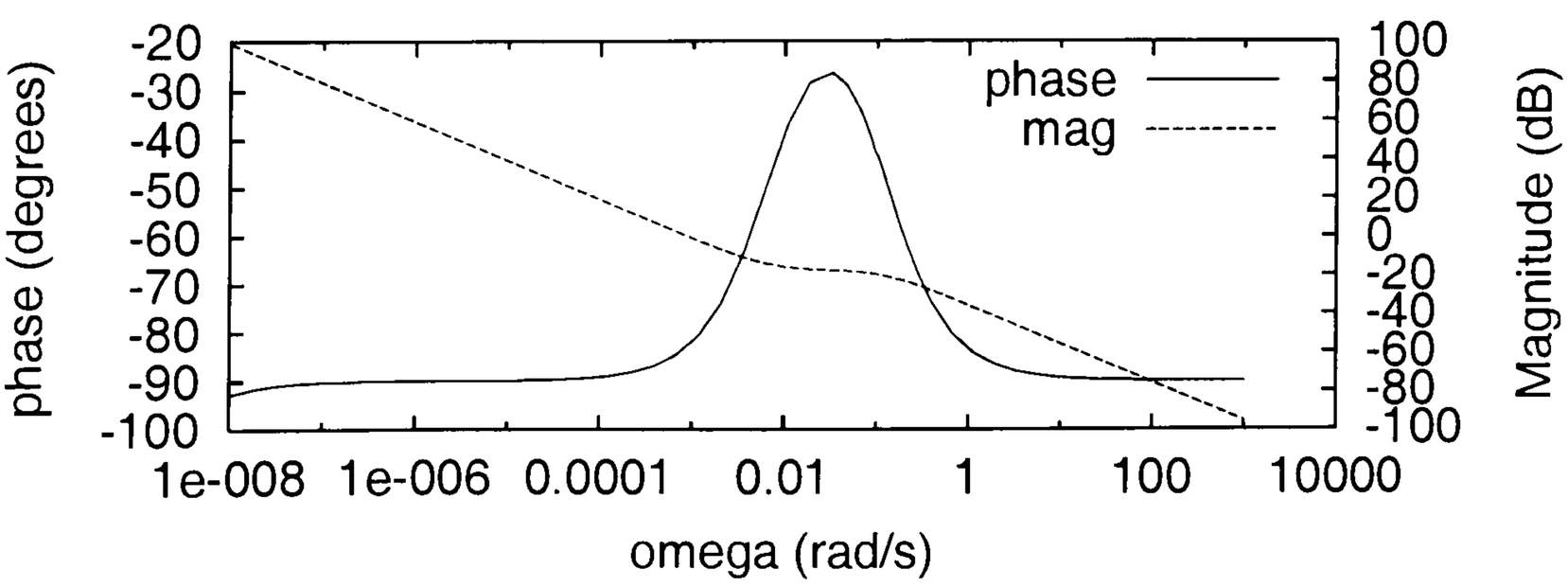

Figure 4.23: Bode plot for pair $D - T_1$. Problem 2

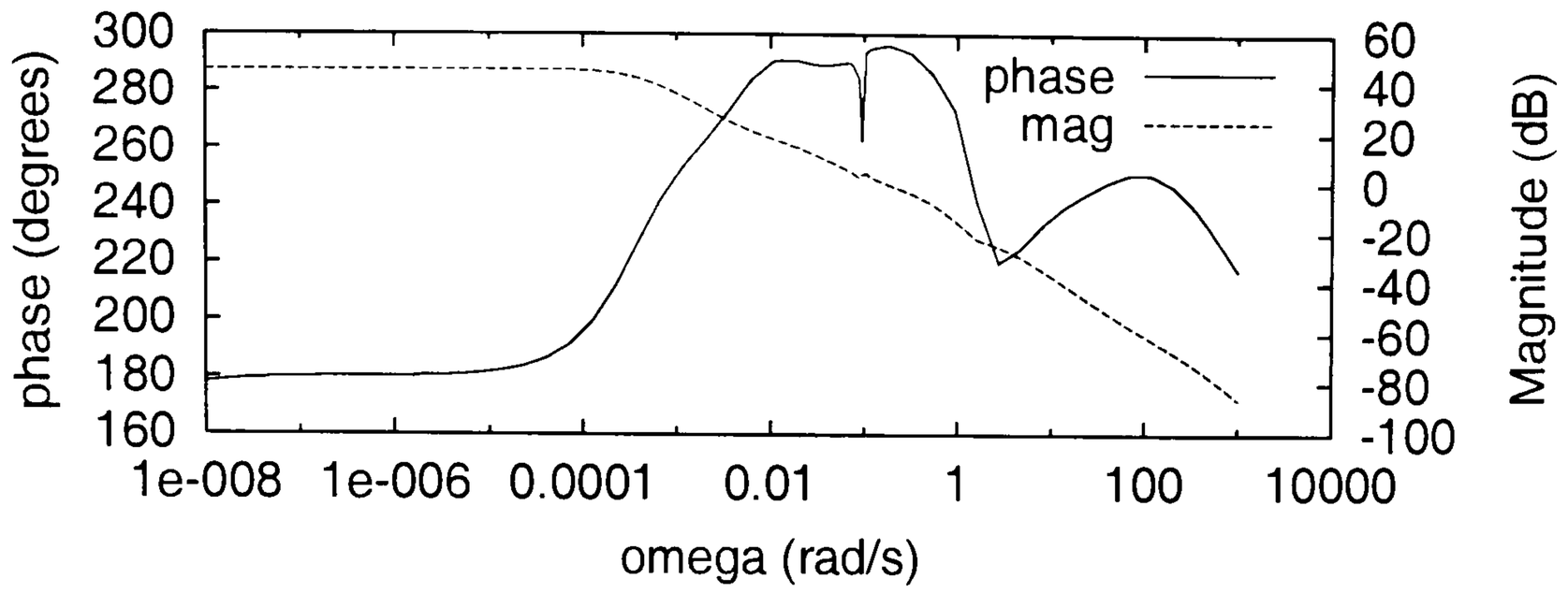

Figure 4.24: Bode plot for pair $B_m - T_1$. Problem 2

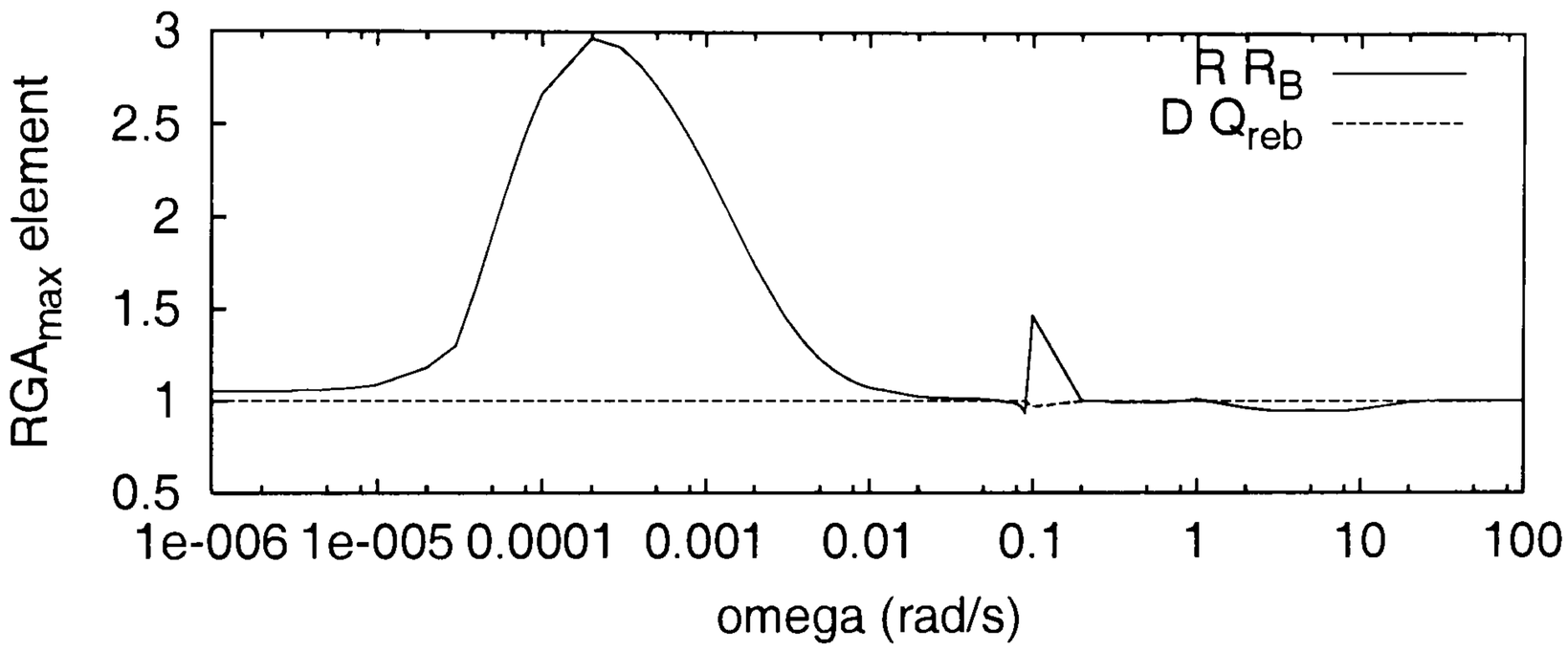

Figure 4.25: Maximum RGA element for schemes RR_B and DQ_{reb}. Problem 2

RGA

All the schemes presented RGA maximum elements close to one. The only different trend was displayed by scheme RR_B in which the RGA increases at higher frequencies. Though, it becomes one afterwards. (Figure 4.25). Since the RGA maximum element is bigger in this case, the scheme must present larger input uncertainty and therefore is disadvantageous.

Discussion

Problem 2 is the high conversion state of a multiplicity point. It is not possible to distinguish such feature with linear control indices. However, there are some indications of the more complex nature of this second problem. For instance, compared with Problem 1, in Problem 2 there are two extra positive poles. Furthermore, there are more complex positive poles in this case. The difficulties of operating on this

state are also seen in smaller positive zeros than in Problem 1. Therefore, it would be expected that Problem 2 is more difficult to control. However, in Problem 2 there are, in general, less positive poles and zeros which are aligned.

On the other hand, comparison of the singular values and the condition number over different frequencies shows that although the system is better conditioned when L or R are used as inputs, it might be better to chose schemes with D as input because the minimum singular value is one order larger close to the steady state.

When the system was tested to know if it could achieve perfect or acceptable control, the results showed that schemes DQ_{reb} (or D_mQ_{reb}) and D_mB_m can reject more disturbances, at least close to the steady state, than the schemes using L (or R) as an input.

Similar to Problem 1, there is a critical frequency for the pair Q_{reb}-T_1. Thus, there is a bandwidth limitation. Also the frequency response analysis show that input B_m creates an output lead for T_{17}. Therefore, neither DQ_{reb} (or D_mQ_{reb}) nor D_mB_m are perfect.

The sum of the results suggest that DQ_{reb} (or D_mQ_{reb}) or D_mB_m can be better options to control the system.

4.6.2 Controller design and closed-loop simulations: Problem 2

In a similar way to Problem 1, the column is exposed to a certain feed disturbance that started at $t = 0s$ and finished at $t = 1800s$. The performance of each scheme is compared with the predicted by the analysis and later compared with the rest of the schemes to reach a conclusion on the benefit of using controllability measures for control system design of reactive distillation. The procedure to design the controllers and tune of them was described in Section 4.5.3. A summary of the analysis and simulation experiments for Problem 2 is presented in Table 4.14.

The same disturbance used to test the system in Problem 1 are used here, both are applied at t=10s and stopped at t=1800s:

1. A 10% methanol feed flow rate increment
2. A 10% C_4 feed flow rate decrease

For all the following examples, the top temperature is very stable and in none of the following cases exceeded the desirable error (0.1 K). Therefore, such results are no presented. Rather, focus is given to the more sensitive output T_{17}.

Case 4.6.1 LQ_{reb}

The analysis suggested that there would be problems controlling the system with this scheme (Table 4.14). Those results suggested that the scheme was unable to control the system when any of the considered disturbances occurred (see Figures 4.19 *a* and 4.20 *a*).

The closed-loop simulations when the methanol pulse was applied produced a large T_{17} decrease(Figure 4.26). The controller is unable to control T_{17} that drops to 399K. In this case, the reflux rate is almost constant since T_1 is also almost constant. This flow plus the extra methanol arrive to the lower parts of the column were the extra reboiler heat duty is unable to increase the temperature. The system is able to return to its previous steady state once the disturbance finished.

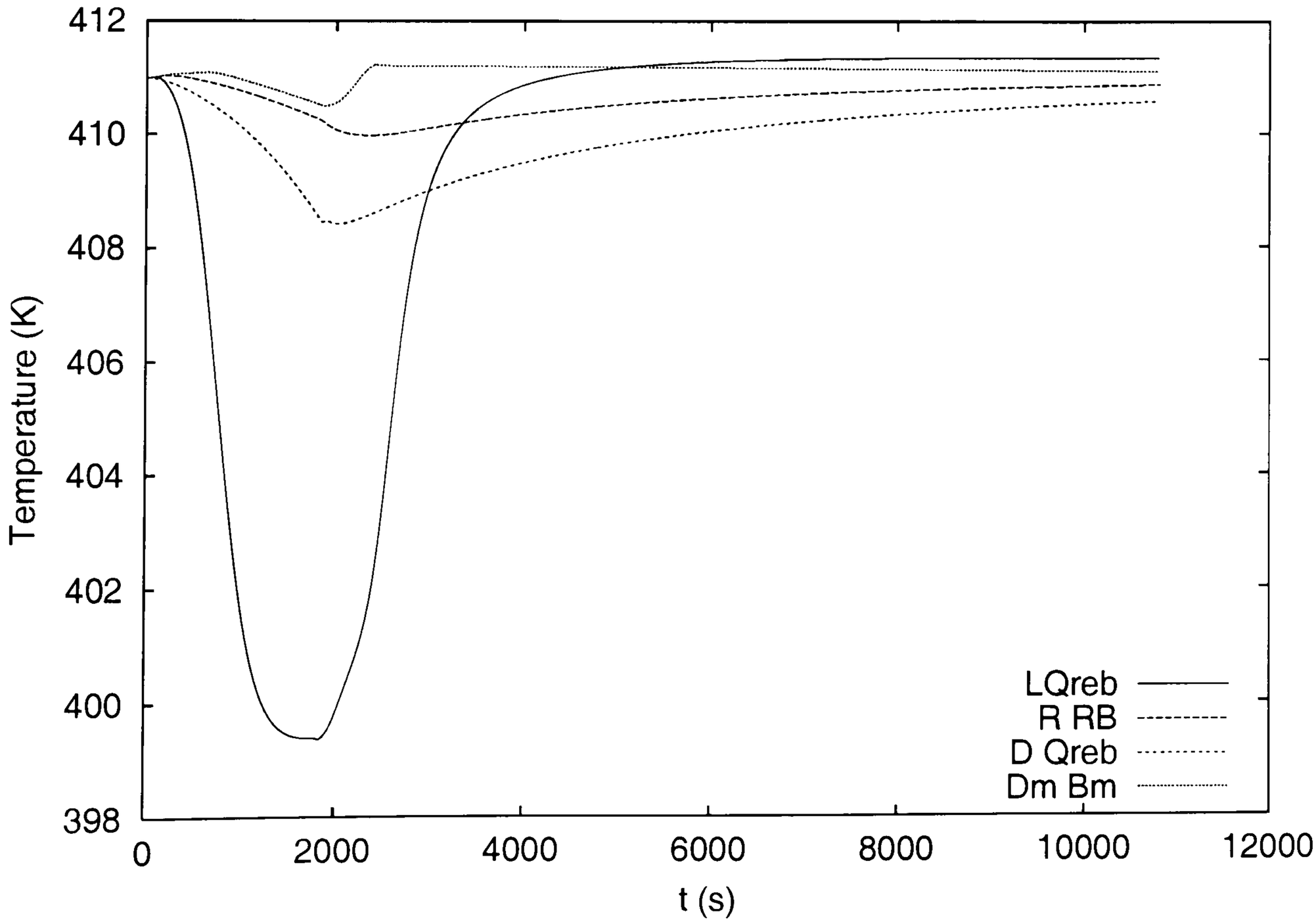

Figure 4.26: Reboiler temperature when a 10% methanol feed flow increment is applied to the system for 1800 s. Problem 2

Table 4.14: Summary of control analysis and simulations for Problem 2

Scheme	Control properties	d_1 Simulations	d_2 Simulations
LQ_{reb}	Well conditioned. $\underline{\sigma}$ remain almost constant for a large frequency range close to the steady state. d_1: No PC, No AC, aligned with 8 zero. d_2: No PC, No AC, aligned with 10 zeros. RGA almost one	T_{17} plummets to 399K. ISE=218782	T_{17} drops till 394 K. ISE=469105
DQ_{reb} or D_mQ_{reb}	Better conditioned. $\underline{\sigma}$ higher than the L cases, but for shorter frequency range. d_1: almost PC, No AC, aligned with 10 zeros. d_2: No PC, AC, aligned with 10 zeros RGA=one	Control ineffective, T_{17} drops till 408 K. ISE=16047	Possible to control T_{17}. ISE=2903
RR_B	Well conditioned. $\underline{\sigma}$ large and almost constant for a large frequency range. A zero aligned with one pole. Close to the steady state RGA=1, though it raises to 3 and returns to 1 at higher frequencies. d_1: No PC, AC, aligned with 7 zeros. d_2: No PC, No AC, aligned with 9 zeros.	T_{17} with small error. Lowest T_{17} equal to 410 K. ISE=2379	Lowest T_{17} equal to 410. ISE=2315
D_mB_m	No so well conditioned compared to DQ_{reb} scheme. $\underline{\sigma}$ greater than one for a relatively large frequency range. 2 zeros aligned with poles. d_1: AC, PC. d_2: PC, AC. Both disturbances aligned with 11 zeros	T_{17} well controlled. T_{17} lowest value is 410.5 K during disturbance. ISE=315	No an experiment

d_1: MeOH feed flow pulse increment. d_2: C_4 feed flow pulse decrease. PC: Perfect control. AC: Acceptable control. $\underline{\sigma}$: minimum singular value. The mentioned zeros or poles are the positive ones. The table only presents T_{17} results since in most cases T_1 error was below the specified value (0.1K). T_{17} set point is 411 K and the allowable error was 2 K

The system response to the C_4 decrease pulse is similar (Figure 4.27). The effect is worse due to the reduction of reaction heat since there is less iso-butene.

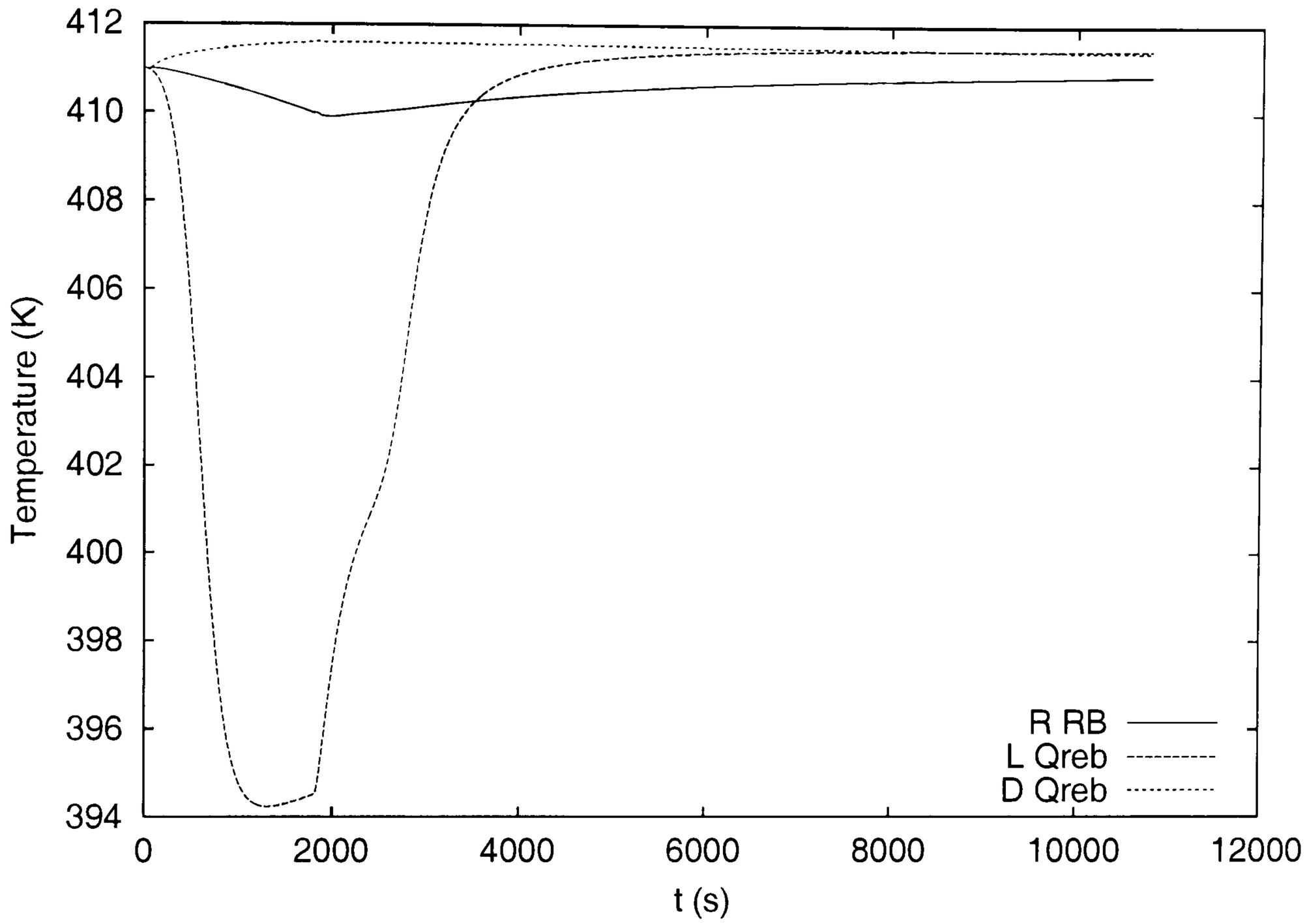

Figure 4.27: Reboiler temperature when a 10% C_4 feed flow decrease is applied to the system for 1800 s. Problem 2

The simulation results agree with the analysis that predict that this particular scheme will present many control problems.

Case 4.6.2 DQ_{reb}

For this case, the analysis predicted that close to the steady state perfect control was possible when changes in the C_4 feed occurred (Figure 4.19 *b*). The analysis also predict that the acceptable control was possible if a methanol feed flow disturbance occured.

The simulations confirm that the system can stand very well the C_4 pulse decrease (Figure 4.27). But when the methanol feed flow pulse occurred, the results are not satisfactory, although it is true that T_{17} does not decrease more than 2K (the allowed error). If we observe Figure 4.26 we can see that the temperature is

plummeting, though slowly. A larger methanol disturbance might result in larger errors.

Case 4.6.3 RR_B

The prediction for this scheme is that close to the steady state it can stand disturbance d_1, that is, the methanol feed flow disturbance. Though it could not overcome a C_4 feed disturbance (see Figure 4.19 *c*). A good feature that this scheme presents is that it is well conditioned and that the minimum singular value is high for a relatively large range close to the steady state.

When the methanol feed pulse disturbance occurred, the controller performs well and the error is below the maximum allowed. The same happens when the C_4 feed flow decrease pulse occurs. These results contradict the analysis results. Apparently, the interaction between mass and temperature controllers is good and this was not considered during the analysis.

Case 4.6.4 $D_m B_m$

The analysis results predicted that close to the steady state the system could achieve acceptable control with this scheme if any of the considered disturbances occured (Figure 4.21 *d*).

Closed-loop simulation of the MTBE column when a methanol feed flow pulse is applied confirms the analysis results. Figure 4.26 shows that the T_{17} error is within the allowable range (2K).

Quantitative comparison between scheme performances

The ISE was calculated for the cases above described using the definition given in equation (4.1). A comparison is presented in Table 4.15.

We can see that, as the analysis predicted, the worst scheme is LQ_{reb} and the best scheme is $D_m B_m$. Analysis results predict that this scheme would control the system if a C_4 disturbance occur. However, since there is a strong relationship with this scheme and the total mass, more tests should be done before choosing it.

DQ_{reb} also performs well, though it is less efficient to control the system when the methanol feed flow pulse occurred. RR_B also performs well. Both schemes would be better options if non-predictable disturbances might occur and using $D_m B_m$ scheme could result risky.

Table 4.15: ISE for T_{17}. Problem 2 simulations

Scheme	ISE	
	MeOH pulse	C_4 pulse
LQ_{reb}	218782	469105
RR_B	2372	2315
DQ_{reb}	16047	2903
$D_m B_m$	315	a

[a] Not an experiment

4.7 Conclusions

The aim of this chapter was the development of a method that incorporated process knowledge, and linear control measures to assist in control system design of reactive distillation. The control system design was based on methods and guidelines given by Stephanopoulos (1982), Seborg, Edgar and Mellicamp (1989) and Skogestad and Postlethwaite (1996) and complemented with process knowledge to give information to develop a control process system design method for reactive distillation. The methodology was tried for a MTBE column.

The operating points selected were the maximum iso-butene conversion with maximum T_{17} temperature for two different reflux ratios ($R = 3$ and $R = 7$). The behaviour of the column at such reflux ratios was studied to determine the most suitable outputs. It was determined that in both cases the distillate product composition was stable and the temperature at the drum could be used as output. On the other hand, the bottom of the column has more complex characteristics that make difficult to select a temperature as an output. The temperature at the reboiler was selected because it displays large changes with composition changes and because it is close to the outputs. In addition, its non-unique relationship with composition makes it an interesting problem to check the capacity of the method to distinguish control difficulties. The process knowledge also showed that all the possible inputs could produce either input or output multiplicity with the outputs.

It was found that the worst control structures in both cases were LQ_{reb} and RQ_{reb} (if L was the varying flow). The analysis also helped to determine that the most convenient schemes were RR_B for Problem 1 and $D_m B_m$, DQ_{reb} (or $D_m Q_{reb}$) and RR_B for Problem 2.

The most helpful indices were the perfect and acceptable control criteria. Those indices helped to reject or accept control schemes. It was found that, although

the disturbance condition number can act as an indicator of how aligned was a disturbance with the system, it could not be used to discriminate between control schemes. This because it gives no indication of the effect magnitude on the system.

Closed-loop simulations following pulses of methanol and C_4 feed flows were used to test the system. In general, the simulations confirm the analysis results.

For Problem 1, the analysis showed that RR_B was better option than DQ_{reb} or D_mQ since using for the last two cases there is strong interaction between the mass and the temperature controllers.

For Problem 2, the simulations confirmed the suggestion that D_mB_m could be the best option. However, due to the implications that this scheme has on the global column mass balance, further analysis and simulations of other disturbances are recommended. As second choice the analysis suggested DQ_{reb} (or D_mQ_{reb}). In the simulations, DQ_{reb} performed well.

There was a contradiction between the analysis and simulations for scheme RR_B. The analysis results suggested that such a scheme cannot reject the C_4 related disturbances. However, the simulations showed that the scheme was able to reject a C_4 decrease feed flow pulse, although it is not possible to say if a larger or periodical disturbance would be rejected.

The results show that the proposed method (that is based on successful application for control system design of conventional distillation) is applicable to reactive distillation. The results also suggest that since there is strong relationship between the mass controllers and the primary output controllers, the mass controllers should be also considered during the analysis.

It is interesting that RR_B scheme that was predicted to achieve good results for an ideal binary distillation column by Skogestad and Jacobsen (1990) can also be a good option for a reactive distillation column. The good interaction between the mass controllers and the outputs controllers that this scheme can achieve might be beneficial for reactive distillation as well.

It is also expected that for a real problem, the pressure controller should be considered during the control design process.

Hence, it is possible that a better option while performing control system design of reactive distillation is to consider a 5×5 controller, though that is beyond the scope of the present work.

An important part of the method are the simulations that give information about the process behaviour and corroborate or correct the analysis results.

Indeed the extent of the simulations and analysis cannot be too large. But rather the schemes and operating points should be based pre-selected on process knowledge. Furthermore, the method relies on a good reactive distillation model and good knowledge of the process.

Chapter 5

Conclusions and Future work

The main interest of the present project was the study of the steady state and dynamics of reactive distillation as well as the operating factors that determine such behaviour.

There were three main objectives: the first one was to develop a model and its solution that properly describe the gross scale behaviour of reactive distillation. The second objective was to study the steady state behaviour of reactive distillation under different operating policies and column designs to determine what conditions triggered multiplicity in this sort of process. The third objective was to develop or modify a method to improve the control system design of reactive distillation. It is hoped that the completion of the mentioned objectives can improve the understanding on the area.

In this chapter the main findings of this project are reviewed and discussed. Some possible directions for future work are also given. The chapter finishes with a summary of the investigation.

5.1 Modeling

The first objective of the present work was to develop a model suitable for the description of the reactive distillation gross behaviour. Such a behaviour can be represented with simple equilibrium models and this was the sort of model developed for the present work.

The model main assumption is that the stages of the column are at chemical and physical equilibrium. The main characteristics of the model are: The hold-up of

liquid is considered more important than vapour, so that only the liquid hold-up is considered. The column hydraulics are part of the model and neither vapour or liquid flow rate is considered as constant. Thus, the model consists of mass and energy balances, equilibrium relationships, expressions that relate the non-reactive and reactive stages, equations to calculate properties, hydraulic equations and control law equations. With simple changes in the information data, it can handle changes such as plate number, feed location, plate and column dimensions. More importantly, it is easy to change the nature of each stage (reactive or non-reactive).

The equilibrium description is based on the element model developed by Pérez-Cisneros *et al.* (1997). In this work such a model is adapted for dynamic simulations.

The advantages of using an element model over a component model are that the number of states is reduced. For instance, for the MTBE column, the 17 stage column had 77 states (60 element hold-ups and 17 energy hold-ups). In comparison, a component model would have had 85. Another advantage is the use of a stoichiometry matrix to describe the reactions which oblige the user to determine the independent reactions, so that it is possible to eliminate unnecessary equilibrium relationships.

The model developed was able to represent the gross behaviour of reactive distillation. When simulation results were compared with experimental ones (Sundmacher and Hoffmann, 1994), the simulations were qualitatively comparable. It was found that among the different parameters needed for the equilibrium calculation, the $\Delta G^{\circ\, ig}_{f\, 298}$ was critical for the correct chemical equilibrium prediction and consequently for the column simulations. Hence, the model can reproduce the gross scale behaviour of reactive distillation if correct thermodynamic models are parameters are used.

The model developed was convenient to reproduce the gross behaviour of reactive distillation. It also has the advantage of reducing the number of states and it is very flexible. Therefore, it was suitable for the development of the main objectives of the project: the study of the steady state and dynamic behaviour of reactive distillation.

5.2 Steady state behaviour study

The second aim of the project was to study how the operating conditions and column design would determine the occurrence of multiple steady states in reactive distillation. To do so, a study of reactive distillation steady state behaviour under different policies and design has been done.

From the literature review, it was found that the output multiplicities commonly found in reactive distillation were inherent to the process due to the reaction and the reaction-separation effects. In this project, it was proposed that such output multiplicities were generated from input multiplicities as a result of the operating conditions.

For a system with large volatility differences, the occurrence of output multiplicity found by other authors (for instance, Schrans *et al.*, 1996) was also found during the present project. However, it was proposed and found that any feed location could produce output multiplicity provided that the internal flow rates were high. Also, it was found that the minimum reflux ratio required to produce multiplicity depended on the feed location. When the reactants feeds were on closer trays, the reflux ratio necessary to produce output multiplicity was lower than for a case in which the feeds are far from each other.

The evolution of a possible pattern of behaviour for output multiplicity for the case study was reproduced. Firstly, the non-reactive distillation of the product of a reactor was simulated. It was found that for the example there was no output multiplicity. Although input multiplicity was not observed, the evidence does not guarantee that it does not exist. When reaction occured in the distillation column input multiplicity appeared for low internal flow rates, while at high internal flow rates, output multiplicity appeared. The greater the internal flow rates were, the larger difference between the high and low conversion stages was.

Following the evolution of a system with input multiplicity revealed that there are critical values in the inputs for which a maximum conversion and production rate is reached. Beyond that point, the balance between reaction and separation effects is broken and further separation affects the reaction since products propagate in the reactive zone.

Another area of exploration was to investigate if further separation (more plates in the stripping section) could make any improvement to avoid output multiplicity. It was found that the extra separation did not have any effect and that the minimum

ratio at which output multiplicity would occur was just above the one found for a column with less stripping stages.

The last study was done to analyse which configurations were more likely to produce multiplicity. To do this, the solution for the case study was developed for different reflux ratios and the composition of one component. The solutions were plotted to show the effect of different input pairs in the conversion. It was found that schemes related to the manipulation of the internal flow rates were more susceptible to possess multiplicity if the internal flow rates were high.

A possible explanation for the above behaviour is that, in a similar way to conventional distillation, changes in the internal flow rates have a strong effect on composition. Furthermore, it is possible that when the internal flow rates are high, the reaction effect is higher because the reactants are better distributed.

The results confirm that for systems in which reaction and separation interact, it is likely that input and output multiplicity will occur. The sources of multiplicity found for conventional distillation (transformation between internal molar flow rates and mass or volumetric external flow rates and the interaction between composition and flows) are combined with the non-linearities originated by reactions, the interaction between separation and reaction, and transport phenomena (not studied here) to make reactive distillation columns very susceptible to multiplicity. This study suggested that output multiplicity occurrence depends on the operating conditions that increase the internal flow rates.

Since the operating conditions are critical for the performance of reactive distillation columns, it was important to study how to improve the control system design of reactive distillation. This is discussed in the following section.

5.3 Reactive distillation control system design

The third aim of the present project was to propose a method to improve control system design for reactive distillation. It is desirable that such a method could find the possible difficulties in controlling a state which has an output multiplicity.

A method, to perform control system design of reactive distillation was developed. The method is based on process knowledge and linear control indices. The method was a combination and extention of methods and guidelines given by Stephanopoulos (1982), Seborg *et al.* (1989) and Skogestad and Postlewaite (1996). The proposed method was applied to two case studies.

Once the primary control objectives are defined, their relationships with possible measurements are studied to propose a number of possible output options. The behaviour of the outputs under different input conditions should be studied as well.

For the case studies, six schemes were chosen because of the characteristics displayed in conventional distillation and for their relationship with the outputs.

When the model is linearised at a steady state point, the system was tested with the following linear control tools: functional controllability, state controllability, state observability, disturbance effect (disturbance condition number, perfect and acceptable control criteria), singular values and frequency response and RGA. From the indices mentioned, it was found that the perfect control criterion and the acceptable control criterion are the most helpful to eliminate or to accept a control scheme.

For the example, the method was able to predict that there were no greater problems controlling the high conversion of a multiple steady state than a maximum conversion of a system without output multiplicity. This was confirmed with simulations which showed that since the internal flow rates were very high, the system was less sensitive to feed changes. In addition, the method was able to predict that schemes which were related to the reflux rate were more likely to display control problems.

Once the most appropriate options were selected, the controllers are designed and simulations with the non-linear model were done to confirm the analysis results.

The method developed is a simple and practical way to assess the control system design of reactive distillation. The use of process knowledge, a linearised method and linear control tools to discriminate between schemes and to study the control configuration properties, generated results that were confirmed with simulations of the non-linear model. Hence, we have confidence in the method's applicability for control system design of reactive distillation.

5.4 Future work

The complexity of reactive distillation deserves attention and it is expected that it will continue attracting the attention of researches for at least the next decade. It is expected that more industrial applications of the process will be implemented

and more research to understand such processes will follow. In this section a series of ideas regarding the design and operation of reactive distillation are proposed.

The first immediate task is to improve the algorithm developed during the present project. An integration method able to better handle stiffness should be added. On the other hand, more options to calculate the activity and the fugacity coefficients should be given to the user. Another possible improvement is the consideration of a possible second liquid phase.

Although the use of linear tools reported satisfactory results for control system design of reactive distillation, it would be interesting to check the performance and utility of non-linear control tools and to compare implementation effort and accuracy for both methodologies.

An interesting issue found during the simulation of the case studies was the interaction between mass and temperature controllers. Thus, it might be interesting to perform the control system design of the case studies relaxing the assumption of perfect level (mass) control during the control system design process of the main control objectives.

It is desirable to contribute more in the operation of reactive distillation investigations. In particular, the research of Scenna *et al.* (1998) and Mohl *et al.* (1999) can be expanded with dynamic simulations to investigate the use of different schemes for better control of start-up operations. Furthermore, simulations can be used to study how start-up times can be minimised and to identify inconvenient start-up policies for reactive distillation.

As a medium term target, it is possible to build an algorithm for optimisation of reactive distillation. Although there has been application of optimisation techniques in the area, for instance Ciric and Gu (1994), there is still room to optimise reactive distillation and its operating policies. In particular, it is desirable to minimise start-up times and the energy required. Since alternative configurations can be easily handled with a matrix of ones and zeros, the model developed here can be used for optimisation purposes.

Since the chemical industry is subject to constant pressure to improve while maintaining product quality but with minimal cost, a long term objective is to automate the integration of the hierarchical tasks of monitoring, optimisation and local control.

5.5 Conclusions

Reactive distillation behaviour (steady state and dynamic) and its relationship with operating conditions and design was the main objective of the project.

For the study of such behaviour, the development of an equilibrium model that considers reaction at equilibrium constituted the first thesis objective. The model developed is based on an appropriate thermodynamic model and its parameters to reproduce correctly the gross scale behaviour of reactive distillation.

It was proposed and found that the output multiplicities of reactive distillation are triggered by operating conditions characterised by large internal flow rates. Although not every reactive distillation process will posses output multiplicity, it is expected that those displaying input multiplicity will develop output multiplicity if the internal flow rates are large.

Due to the relationship between operating conditions and a correct reactive distillation behaviour, the control system design of this sort of unit was analysed. A method to systematise control system design of reactive distillation based on linear control tools and process knowledge was proposed. The method provided a good answer to the design of controllers of reactive distillation. In particular, for a MTBE column, the method was helpful to discriminate between different control configurations. Furthermore, it was possible to determine that the control of the high conversion point of an output multiplicity was easier to control than the maximum conversion of the same system but with only input multiplicity.

The different topics studied here and the results provided should be helpful for a better understanding and design of reactive distillation. Since it is not possible to cover all the interesting subjects regarding reactive distillation, some suggestions for future work were proposed from the results found during the present work and the wide area of investigation that reactive distillation offers.

Appendix A

Nomenclature

Variables

$\mathbf{A}$	stoichiometry matrix	
A	area	m^2
A_{ij}	stoichiometry matrix	
b	amount of element	$moles$
b	flow of element	$moles/s$
B	element hold-up	
B	bottoms flow rate	mol/s
$\mathcal{B}$	bottoms flow rate based on elements	mol/s
C_v	coefficient for the valve calculation	
C_v	discharge coefficient	
C_{valve}	coefficient for the valve calculation	
D	distillate flow rate	mol/s
$\mathcal{D}$	distillate flow rate based on elements	mol/s
$\mathcal{F}$	element feed flow rate	$mole/s$
G	Gibbs free energy	J/mol
h_{ds}	height of the clear liquid over the plate	mm
h_{ow}	height of the crest over weir (clear liquid)	mm
h_{hg}	hydraulic gradient across plate (clear liquid)	mm
h_w	weir height	mm

H	enthalpy	J
$\check{H}$	specific enthalpy based on elements	J/s
$\hat{H}$	specific enthalpy based on components	J/s
k	gain	
$\hat{L}$	Lagrange function	
L	liquid flow rate	mol/s
L	reflux flow rate	mol/s
L_w	weir length	m
$\mathcal{L}$	element liquid flow rate	mol/s
M	number of elements	
n	moles	mol
NC	number of components	
NP	number of phases	
NS	total number of stages	
P	pressure	atm
q	liquid flow rate	m^3/s
Q	heat	J/s
R	reflux ratio	
S	entropy	J/mol
S	side stream flow	mol/s
$\mathcal{S}$	element side stream flow	mol/s
t	time	s
T	temperature	K
U	chemical potential derivative	J/mol^2
U_H	overall heat transfer coefficient	$J/mol\ s\ T\ m^2$
U_s	linear gas velocity through perforations	m/s
$\mathbf{U}$	chemical potential derivative	J/mol^2
v	vapour flow	m^3/s
V	volume	m^3
V	vapour flow rate	mol/s
$\mathcal{V}$	element vapour flow rate	mol/s
x	liquid mole fraction	
y	vapour mole fraction	
z	feed mole fraction	

Greek letters

β	phase	
γ	activity coefficient	
ϵ	advance of reaction	
η	column efficiency	
ϕ	fugacity coefficient	
λ	element chemical potential	
λ	RGA element	
μ	chemical potential	J/mol
ν	stoichiometric coefficient	
ρ	density	
ω	element mole fraction	

Subscripts

A	component or element
c	critic
$cond$	condenser
ext	external
f	feed
i	component
j	element
T	temperature
p	stage
P	pressure
r	reduced
reb	reboiler
T	total
0	initial, set point

Superscripts

E	excess
f	feed
F	feed
ig	ideal gas
L	liquid
NP	number of phases
R	residual
V	vapour

Appendix B

Element model

This appendix contains complementary information for Chapter 2. Here the derivation of the formula matrix **A** is shown. In addition, two examples are included: the first one corresponds to a system with only one reaction and the second one corresponds to a system with several reactions. This appendix is based on Pérez-Cisneros (1997) and Smith and Missen (1982).

B.1 Definitions

Element. An element is a basic unit that can be used to build chemical compounds. It can be a chemical element such as hydrogen, carbon, etc. Otherwise it can be a component of a compound molecule, for instance a radical, an ion, or even a molecule.

Component. A chemical substance constituted by elements.

Formula matrix. Matrix **A** that contains the relationships between components C_1, C_2,..., C_{NC} (columns) and the elements E_1, E_2,..., E_M (rows).

B.2 Conservation of elements

Since the elements can not be divided into simpler species, its number remains constant for a closed system. This can be expressed as follows:

$$\sum_{i=1}^{NC} A_{ji} n_i = b_k \tag{B.1}$$

where $k = 1, \ldots, M$.

B.3 Identification of elements

With the next method, the number of elements is determined. In addition, the elements are also identified and a possible stoichiometry is found.

1. Write a formula matrix $\mathbf{A}^*$ that contains the relationship between the mixture components and the chemical elements.

2. Determine the rank of matrix $\mathbf{A}^*$. The rank of matrix $\mathbf{A}^*$ corresponds to the number of elements (M).

3. Reduce by row operations and columns interchange to get in the upper left corner an identity matrix of rank M. The result is a matrix with the following form:

$$\mathbf{A} = [\mathbf{A}_I : \mathbf{A}_{II}] \tag{B.2}$$

where $\mathbf{A}_I$ is an identity matrix of rank M.

In addition, the maximum number of linearly independent stoichiometric equations is given by:

$$R = NC - M \tag{B.3}$$

4. Identification of elements.

B.3.1 Example 1: MTBE formation

The method outlined above is used to identify the elements for a system constituted by iso-butene, methanol and water. The chemical elements are: carbon (C), hydrogen(H) and oxygen (O). Thus the procedure is as follows:

1. The matrix $\mathbf{A}^*$ is formed:

Elements	Components		
	$i - C_4H_8$	CH_3OH	$C_5H_{12}O$
C	4	1	5
H	8	4	12
O	0	1	1

2. The rank of matrix $\mathbf{A}^*$ is found, $M = 2$.

3. Matrix $\mathbf{A}^*$ is reduced to find matrix $\mathbf{A}$. This was done with row operations and no column exchanges. The final matrix is:

$$\mathbf{A} = \begin{bmatrix} i - C_4H_8 & CH_3OH & C_5H_{12}O \\ 1 & 0 & 1 \\ 0 & 1 & 0 \\ 0 & 0 & 0 \end{bmatrix}$$

4. The upper right corner matrix of $\mathbf{A}$ is an identity matrix of rank equal to the number of elements, in this case two. This matrix also is used to identify that E_1 is iso-butene and E_2 is methanol. Furthermore, the number of independent stoichiometric equations is:

$$NR = NC - M = 3 - 2 = 1$$

.

B.3.2 Esterification of ethyl alcohol

In this example, ethyl alcohol (C_2H_60 reacts with acetic acid (C_2H_6) to form water and ethyl acetate ($C_4H_8O_2$) in a liquid-vapour system. In the vapour phase the dimmer of the acetic acid is produced.

1. The matrix that contains the relationship between the components and the chemical elements is:

	a	b	c	d	e	f	g	h	i
C	0	2	2	4	0	2	2	4	4
H	2	6	4	8	2	6	4	8	8
O	1	1	2	2	1	1	2	2	4

where $a = H_2O(l)$, $b = C_2H_6O(l)$, $c = C_2H_4O_2(l)$, $d = C_4H_8O_2(l)$, $e = H_2O(g)$, $f = C_2H_6O(g)$, $g = C_2H_4O_2(g)$, $h = C_4H_8O_2(g)$ and $i = (C_2H_4O_2)_2(g)$.

2. The rank of matrix $\mathbf{A}^*$ is determined, M=3.

3. Matrix $\mathbf{A}^*$ is reduced to matrix $\mathbf{A}$ after row operations and column exchanges to:

$$\mathbf{A} = \begin{bmatrix} b & a & c & d & e & f & g & h & i \\ 1 & 0 & 0 & 1 & 0 & 1 & 0 & 1 & 0 \\ 0 & 1 & 0 & -1 & 1 & 0 & 0 & -1 & 0 \\ 0 & 0 & 1 & 1 & 0 & 0 & 1 & 1 & 2 \end{bmatrix}$$

4. Observing matrix $\mathbf{A}$ we found that the elements are $C_2H_6O(l)$, $H_2O(l)$ and $C_2H_4O_2(l)$. Furthermore, the number of independent stoichiometric equations is:

$$NR = NC - M = 9 - 3 = 6$$

B.4 Chemical stoichiometry

The last section showed how to get the matrix formula and how to define the elements for a particular system. It was also shown that it is possible to know how many linearly independent stoichiometric equations can be defined. However, it was not shown how these equations can be found from the formula matrix; this is because any one equation can be substituted by a linear combination of any of the equations. In this section, the basic requirement that such equations must follow is presented. That requirement is related to the formula matrix.

The solution for system of M equations (B.1) with NC unknowns (the number of moles) is given by:

$$\mathbf{n} = \mathbf{n}^\circ + \sum_{j=1}^{NR} \nu_j \xi_j \tag{B.4}$$

where $\mathbf{n}^\circ$ is any particular solution of equation B.1 and ξ_j is the extent of the reaction j. The vector ν_j is called the stoichiometric vector. This vector is the solution for the equation $\mathbf{A}\nu_j = \mathbf{0}$. The elements of this vector are real numbers and at least one of the elements of vector ν must be different from zero. Thus, to find the stoichiometry reactions one must solve $\mathbf{A}\nu_j = 0$.

When the NR vectors ν are known, it is possible to build the complete stoichiometric matrix $\mathbf{N}$:

$$\mathbf{N} = (\nu_1, \ldots, \nu_{NR}) \tag{B.5}$$

Thus, the stoichiometry of the system can be determined solving the following

equation:

$$\mathbf{AN} = \mathbf{0} \tag{B.6}$$

B.4.1 Example 1: MTBE formation

The matrix **A** is:

$$\mathbf{A} = \begin{bmatrix} 1 & 0 & 1 \\ 0 & 1 & 0 \\ 0 & 0 & 0 \end{bmatrix}$$

The number of linearly independent reactions was equal to one. Thus, the **N** matrix in this case has only one column. A possible solution is: $\mathbf{N} = [-1, -1, 1]^T$.

B.4.2 Esterification of ethyl alcohol

The matrix **A** for this system is:

$$\mathbf{A} = \begin{bmatrix} 1 & 0 & 0 & 1 & 0 & 1 & 0 & 1 & 0 \\ 0 & 1 & 0 & -1 & 1 & 0 & 0 & -1 & 0 \\ 0 & 0 & 1 & 1 & 0 & 0 & 1 & 1 & 2 \end{bmatrix}$$

The number of linearly independent reactions is equal to six. Therefore, matrix **N** consists of six linearly independent vectors. The complete stoichiometric matrix can be written as:

$$\mathbf{N} = \begin{bmatrix} -1 & 0 & -1 & 0 & -1 & 0 \\ 1 & -1 & 0 & 0 & 1 & 0 \\ -1 & 0 & 0 & -1 & -1 & -2 \\ 1 & 0 & 0 & 0 & 0 & 0 \\ 0 & 1 & 0 & 0 & 0 & 0 \\ 0 & 0 & 1 & 0 & 0 & 0 \\ 0 & 0 & 0 & 1 & 0 & 0 \\ 0 & 0 & 0 & 0 & 1 & 0 \\ 0 & 0 & 0 & 0 & 0 & 1 \end{bmatrix}$$

Appendix C

Calculation of properties

C.1 Overview

This Appendix contains the calculation of properties as performed in the developed codes.

C.2 Basic properties

The vapour pressure $P_{S,i}$ of component i was calculated with the Antoine's equations given by:

$$\ln P_{S,i} = A_i + \frac{B_i}{(T + C_i)} \tag{C.1}$$

where A_i, B_i and C_i are the Antoine's equation constants for component i.

The enthalpy of ideal gas at temperature T is calculated as follows:

$$\Delta H_i^{ig} = \Delta H_{f,i} + a_i(T - T_0) + \frac{b_i}{2}(T^2 - T_0^2) + \frac{c_i}{3}(T^3 - T_0^3) + \frac{d_i}{4}(T^4 - T_0^4) \tag{C.2}$$

where a_i, b_i, c_i and d_i are the constants to calculate the isobaric heat capacity of the ideal gas C_{pi}, with C_{pi} in $J/(molK)$ and T in kelvins.

The evaporation enthalpy is approximated considering ideal gas from the Clausius/Clapeyron equation given by:

$$\Delta H^{lv} = -R\frac{d \ln P_S}{d(1/T)} \tag{C.3}$$

where R is the constants of ideal gas.

Pérez-Cisneros *et al.* (1997) presented a calculation method for the standard state chemical potential of component i is calculated from its relationship with the formation Gibbs free energy of component i at temperature T:

$$\frac{\mu_i^0}{RT} = \frac{\Delta G_{fi}^{ig}(T)}{RT} \tag{C.4}$$

It is possible to relate the formation Gibbs free energy of component i with the change of enthalpy ΔH_i^0 from the reference temperature $T = 298.2K$ to temperature T as follows:

$$\frac{d}{dT}\left(-\frac{\Delta G_{fi}(T)}{RT}\right) = \frac{\Delta H_i^0}{RT^2} \tag{C.5}$$

When equation (C.5) is integrated and substituted in equation (C.4), it is possible to derive the expression for the reference state chemical potential as follows:

$$\frac{\mu_i^0}{RT} = \frac{1}{R}\left[\Gamma_i^{II} - \frac{\Gamma_i^I}{T} + a_i \ln T + \frac{b_i}{2}T + \frac{c_i}{6}T^2 + \frac{d,i}{12}T^3\right] \tag{C.6}$$

where

$$\Gamma_i^{II} = \frac{-\Delta G_{fi(298)}^{ig}}{T_0} - \left[a_i \ln T_0 + \frac{b_i}{2}T_0 + \frac{c_i}{6}T_0^2 + \frac{d_i}{12}T_0^3\right] + \frac{\Gamma_i^I}{T_0}$$

and

$$\Gamma_i^I = \Delta H_{fi(298)}^{ig} - \left[a_i + \frac{b_i}{2}T_0 + \frac{c_i}{3}T_0^2 + \frac{d_i}{4}T_0^3\right] T_0$$

The liquid density of component i was calculated with the Rackett-Spencer-Daniel equation (Perry, 1988) as follows:

$$\rho^{sat} = P_c / RT_c z_{RA}^{[1+(1-T_r)^{2/7}]} \tag{C.7}$$

where the compresibility factor z_{RA} is determined from experimental data. However, in the present work it was equaled to z_c. Perry (1988) affirmed that such substitution would increase the error between 3 or 4 percent.

To calculate the liquid mixture density, the Amagat's law was used:

$$\frac{1}{\rho} = \sum_i 1/\rho_i \tag{C.8}$$

The vapour density was calculated with the residual volume.

C.3 Activity coefficient model

The activity coefficient was calculated with the Wilson equation given by (Sandler. 1989):

$$\frac{G^{ex}}{RT} = -\sum_{i=1}^{NC} x_i \ln\left(\sum_{j=1}^{NC} x_j \Lambda_{ij}\right) \tag{C.9}$$

for which

$$\ln \gamma_i = 1 - \ln\left(\sum_{i=1}^{NC} x_j \Lambda_{ij}\right) - \sum_{j=1}^{NC} \frac{x_j \Lambda_{ji}}{\sum_{k=1}^{NC} x_k \Lambda_{jk}} \tag{C.10}$$

Note that $\Lambda_{ij} \neq \Lambda_{ji}$ and $\Lambda_{ii} = 1$.

The Wilson equation was also used to calculate the excess enthalpy.

C.4 Fugacity coefficient model

The fugacity coefficient of component i and the residual enthalpy were calculated with the Soave-Redlich-Kwong equation:

$$\ln \phi_i = -\ln\left(z - \frac{Pb}{RT}\right) - \frac{2\sqrt{aa_i}}{bRT} \ln\left(1 + \frac{bP}{zRT}\right) + \frac{b_i(z-1)}{b} + \frac{ab_i}{b^2 RT} \ln\left(1 + \frac{bP}{zRT}\right) \tag{C.11}$$

where a_i and b_i are constants for component i while a and b are constants for the mixture. For more details, see Reid *et al.* (1987).

C.5 Enthalpies calculation

The enthalpy of component i during the present work was calculated considering that the reference is the pure substance in the ideal gas state at 1 atm.

C.5.1 Molar specific enthalpy

The enthalpy of component i in the vapor phase $\hat{H}_i^V$ is given by:

$$\hat{H}_i^V = \Delta \hat{H}_i^{ig} + \hat{H}_i^R \tag{C.12}$$

where $\hat{H}_i^R$ is the residual enthalpy of component i.

The enthalpy for the vapour mixture can be calculated as follows:

$$\hat{H}^V = \sum_i^{NC} \hat{H}_i^V y_i \tag{C.13}$$

For component i the liquid phase enthalpy $\hat{H}_i^{ig}$ is calculated as:

$$\hat{H}_i^L = \Delta\hat{H}_i^{ig} + \hat{H}_i^E - \Delta H_i^{lv} \tag{C.14}$$

where $\hat{H}_i^E$ is the excess enthalpy of component i.

Once the component enthalpies are known, the enthalpy of the liquid phase mixture is given by:

$$\hat{H}^L = \sum_i^{NC} \hat{H}_i^L x_i \tag{C.15}$$

C.5.2 Element specific enthalpy

To calculate the element specific enthalpy in the liquid phase, the equation $H^L = \hat{H}^L n_T^L$ is substituted in the element specific enthalpy definition $\check{H}^L = H^L/(n_T^L \sum A_{ji}x_i)$. Thus the element specific enthalpy for the liquid phase is calculated as follows:

$$\check{H}^L = \frac{\hat{H}^L}{\sum_i^{NC} A_{ji}x_i} \tag{C.16}$$

Similarly, the specific enthalpy for the vapour phase is given by:

$$\check{H}^V = \frac{\hat{H}^V}{\sum_i^{NC} A_{ji}y_i} \tag{C.17}$$

Appendix D

Hydraulics and column characteristics

D.1 Column and plate dimensions

The column and its sieve plates were designed with the method presented by Sinnot (1993) considering that there were only liquid and vapour phases present. The mixture characteristics used for the design were from the steady state solution of the problem considered. The column dimensions for the column in Problem 1 and Problem 2 in Chapter 4 are presented in Table D.1 and D.2.

D.2 Column hydraulics

D.2.1 Liquid flow rate calculation

Since the hold-up in the plate is known, it is possible to calculate the height of the clear liquid over the plate h_{ds} with the density. On the other hand, h_{ds} is defined by:

$$h_{ds} = h_w + h_{ow} + h_{hg}/2 \tag{D.1}$$

where h_w is the weir height, h_{ow} is the height of the crest over the weir and h_{hg} is the hydraulic gradient over the weir (equaled to zero during the present work). All these height are equilavent clear liquid in milimeters.

From equation D.1 h_{ow} can be known. The liquid flow rate can be calculated from the Francis formula, for a sieve plate given by:

$$h_{ow} = 664[q/L_w]^{2/3} \tag{D.2}$$

where q is the liquid flow (m^3/s) and L_w is the weir length (m).

D.2.2 Vapour flow rate

To calculate the vapour flow rates, the pressure drop was used. The pressure drop can be expressed in terms of its contributions by:

$$h_t = h_d + (h_w + h_{ow}) + h_{hg}/2 \tag{D.3}$$

where h_d is the pressure drop through the perforations and can be estimated by:

$$h_d = \frac{50.8}{C_v^2}\frac{\rho_g}{\rho_l}U_h^2 \tag{D.4}$$

where U_h^2 is the linear gas velocity through the perforations and C_v^2 is the discharge coefficient and depends on the hole area and active area ratio.

Equation D.4 is used to calculate the vapour flow rate entering the plate.

The vapour flow rate of the second stage is calculated with a valve formula (equation D.5). Constant C_{valve} is calculated from the steady state vapour flow rate at such stage.

$$v = C_{valve}(P_2 - P_{cond})^{1/2} \tag{D.5}$$

Table D.1: Column and plate characteristics for Problem 1

From plate 2 to plate 11	
Column diameter (m)	3.450
Plate thickness (mm)	5.000
Total plate area (sqm)	9.350
Plate active area (sqm)	7.106
Plate perfored area (sqm)	6.326
Downcomer area (sqm)	1.122
Hole area (sqm)	0.711
Hole diameter (mm)	5.000
Weir length (m)	2.553
Weir heigth (mm)	50.000
From plate 12 to plate 16	
Column diameter (m)	2.580
Plate thickness (mm)	5.000
Total plate area (sqm)	5.228
Plate active area (sqm)	3.973
Plate perfored area (sqm)	3.395
Downcomer area (sqm)	0.627
Hole area (sqm)	0.397
Hole diameter (mm)	5.000
Weir length (m)	1.909
Weir heigth (mm)	50.000

Table D.2: Column and plate characteristics for Problem 2

From plate 2 to plate 11	
Column diameter (m)	5.206
Plate thickness (mm)	5.000
Total plate area (sqm)	21.285
Plate active area (sqm)	16.176
Plate perfored area (sqm)	14.981
Downcomer area (sqm)	2.554
Hole area (sqm)	1.618
Hole diameter (mm)	5.000
Weir length (m)	3.956
Weir heigth (mm)	50.000
From plate 12 to plate 16	
Column diameter (m)	4.639
Plate thickness (mm)	5.000
Total plate area (sqm)	16.901
Plate active area (sqm)	11.831
Plate perfored area (sqm)	10.749
Downcomer area (sqm)	2.535
Hole area (sqm)	1.183
Hole diameter (mm)	4.802
Weir length (m)	3.711
Weir heigth (mm)	49.005

Appendix E

Linear control tools

E.1 Transfer function

A linear state space model of a system can be written as follows:

$$\begin{aligned} \dot{x} &= Ax + Bu \\ y &= Cx + Du \end{aligned} \tag{E.1}$$

Such a model can be transformed into a input-output model by using a Laplace transformation. The result is a function named transfer function, $G(s)$ (Skogestad and Postlethwaite, 1996):

$$G(s) = C(sI - A)^{-1}B + D \tag{E.2}$$

The representation of the system with a transfer function allows to "see" the influence of inputs and disturbances on the outputs as follows:

$$y(s) = G(s)u + G_d(s)d \tag{E.3}$$

where y represents the outputs, u represents the inputs and d represents the disturbances. $G(s)$ contains the information referent to the influence of inputs on outputs and $G_d(s)$ contains the information relative to the influence of disturbances on outputs.

When the state-space model is nonlinear like in equation (E.4), it is possible to linearise it at a certain steady state with a Taylor's series.

$$\begin{aligned} \frac{dx}{dt} &= f(x,u) \\ y &= g(x,u) \end{aligned} \tag{E.4}$$

The procedure involves three basic steps. The first one is to re-write the non-linear model using only the first two terms of a Taylor series evaluated at a certain steady state. The second step is to introduce deviation variables (equation E.5) and substitute them in the linearised model as follows:

$$\delta x(t) = x(t) - x^* \tag{E.5}$$

where the star denotes the steady state value of x.

The third step is to eliminate all the terms that involve only steady state quantities. The resulting linearised model is:

$$\frac{d\delta x(t)}{dt} = \left(\frac{\partial f}{\partial x}\right)^* \delta x(t) + \left(\frac{\partial f}{\partial u}\right)^* \delta u(t) \tag{E.6}$$

The derivatives can be renamed as $\left(\frac{\partial f}{\partial x}\right)^* = A$ and $\left(\frac{\partial f}{\partial u}\right)^* = B$. The same procedure is followed for the output y non linear function. The resulted model has a similar form to equation (E.1).

Note that when x, y and f are vectors, A, B, C and D are matrices.

Finally, for analysis purposes is recommended to scale the transfer function and the variables.

Details of this procedure can be found in many Process Control books such as Skogestad and Postlethwaite (1996) and Stephanopoulos (1984).

E.1.1 Disturbance transfer function

It is necessary to investigate how large can be the effect of the disturbance(s) in the system and whether the control can cope with it.

A first attempt to study the disturbance influence is by examination of the disturbance transfer function G_d. If the elements of the disturbance transfer function at frequency ω are greater than one, the disturbance should be considered as important.

A concept that will be later useful to examine the disturbance influence is the *disturbance output direction* that can be found with the following definition:

$$y_d = \frac{1}{||g_d||_2} g_d \tag{E.7}$$

Disturbance condition number

The disturbance condition number $\gamma_d(G)$ can tell us the magnitude of the control action required to reject the actual disturbance compared with the control action required to reject the same disturbance but in the best direction (the direction associated with the smallest singular value of the transfer function G) (Agamennoni *et al.* 1994). The definition that Skogestad and Postlethwaite provided is the following:

$$\gamma_d(G) = \overline{\sigma}(G)\,\overline{\sigma}(G^{-1} y_d) \tag{E.8}$$

The disturbance condition number does not provide information about the magnitude of the control action required to reject the disturbance. Therefore, it would be difficult to use it as a discriminatory reason of control schemes. This is due to the fact that it does not say how good or bad is the best direction.

For instance, if the disturbance condition number is equal to one, it is telling us that the disturbance is in the direction of the smallest singular value and that it harms the minimum (it is said that the disturbance is not aligned to the plant). However, it does not say how bad is that minimum.

On the other hand, if the disturbance condition number is close to the plant condition number ($\gamma(G) = \overline{\sigma}(G)\overline{\sigma}(G^{-1})$), it is said that the disturbance is in the worst direction (the disturbance is aligned to the plant). But again, it does not say if the scheme can overcome the disturbance or not.

Hence, to judge if a control scheme would be effective to reject a disturbance, there are certain criteria that a control scheme should satisfy. For instance, a requirement

for perfect control was given by Skogestad and Postlethwaite (1996). It is based on the concept of inverse control and its effectiveness in the presence of a disturbance d.

$$||G^{-1}g_d||_{max} \leq 1 \; \forall \, \omega \tag{E.9}$$

where g_d is the disturbance transfer function of disturbance d.

E.2 State controllability and state observability

To check the s-controllability and s-observability of the system is important because when all the states included in the model are state observable and state controllable, the model is a *minimal realization* of the system. This ensures that there are not hidden states in the system.

When a process is state-controllable, this process can be brought from an initial state to any final state by the use of certain inputs (Skogestad and Postlethwaite, 1996).

Note, that the definition includes no measure of controllability and says nothing about how to bring the system from the initial state to the final state.

There are different alternatives to check the s-controllability of a system. They involve the rank evaluation of a certain matrix. If the rank of the matrix is equal to the number n of states, then the system is s-controllable.

The first alternative is to find the rank of the controllability matrix in equation E.10 (Skogestad and Postlethwaite, 1996).

$$rank[\mathbf{B} \quad \mathbf{AB} \quad \mathbf{A}^2\mathbf{B} \ldots \mathbf{A}^{n-1}\mathbf{B}] = n \tag{E.10}$$

The criterion defined in equation (E.10) may present numerical problems when it involves several matrix multiplications.

An alternative to check the s-controllability of a system is to find the rank of another matrix (Kaczorek, 1992). The system is s-controllable if it satisfy:

$$rank[\mathbf{I}s - \mathbf{A}, \mathbf{B}] = n \quad \text{for all} \quad s \quad \epsilon \quad \mathrm{C} \tag{E.11}$$

Similarly, a dynamic system is state observable if the initial condition of the states can be determined when the history of the inputs and outputs is known in the interval $[0, t]$.

To find if a system is s-observable, the criteria are similar to the s-observability ones. The system is s-observable if a the rank of a certain matrix is equal to the states number n.

The first test (equation E.12) was included by Skogestad and Postlethwaite, 1996. This test may present numerical problems also. It may be more convenient to use the test included by Kaczorek (1992).

$$rank \begin{bmatrix} \mathbf{CA} \\ \vdots \\ \mathbf{CA}^{n-1} \end{bmatrix} = n \tag{E.12}$$

$$rank \begin{bmatrix} \mathbf{I}s - \mathbf{A} \\ \mathbf{C} \end{bmatrix} = n \tag{E.13}$$

E.3 Functional controllability

One of the essential requirements for a control is that the inputs must influence the outputs. When this requirement is met, the system is *Functionally controllable*

Such a requirement can be divided into two. The first step is that there must be at least as many inputs as outputs. The second one is that the normal rank of the transfer function must be equal to the number of outputs.

If the rank of a transfer function is lower than the number of outputs, there are inputs that do not influence the outputs. This condition is not achieved for the zeros of $G(s)$.

The functional controllability can be also addressed by the singular value decomposition of the transfer function. If the minimum singular value of $G(j\omega)$ for all ω is zero (except at possible $j\omega$ axis zeros) it means that the proposed scheme will not influence all the outputs.

In addition, if matrix D is zero for the linear model (equation E.6) the system is functionally uncontrollable when the rank of matrices $\mathbf{B}$, $\mathbf{C}$ or $(s\mathbf{I} - \mathbf{A})$ is lower than the number of outputs.

E.4 Poles location

A pole can be defined as a finite value of the independent variable s where the transfer function is infinite, this is, in which the transfer function has a singularity (Skogestad and Postlethwaite, 1996).

When the dynamic behaviour of a system on the state-space can be described with equations (E.1), the poles p_i of the system can be defined as the eigenvalues of matrix A. Thus the poles of the system can be defined as the roots of the characteristic equation (Skogestad and Postlethwaite, 1996):

$$\phi(s) \triangleq \det(sI - A) = 0 \tag{E.14}$$

The dynamical response of the linear model in equation E.1 is written as a sum of exponential terms of the eigenvalues λ_i and time t, this is $e^{\lambda_i(A)t}$. Hence if the real part of the eigenvalue λ_i is positive, the system is unstable since it is not bounded when $t \to \infty$. Thus, the system is stable if and only if all the poles are located in the left-hand plane, LHP (Skogestad and Postlethwaite, 1996).

When the imaginary part of a pole is not zero, the output of the system will oscillate. Such an oscillation will grow or decay if the real part is positive or negative respectively. If the real part is equal to zero, the oscillations keep a sustained amplitude (Stephanopoulos, 1984).

Therefore, if there are poles with positive real part, the system will require a controller to maintain stability. Not every control configuration can be used for this purpose, since we need a good response of the system with the application of certain inputs. Therefore we should ask that the minimum singular value (see Section E.7) of the closed-loop transfer function T is larger than one.

E.5 Zeros location

There are certain points in the Laplace space where the transfer function $G(s)$ is equal to zero. Physically, this means that the output will be zero even though the inputs are not.

The mathematical definition of system zeros is based on the fact that matrix $G(z_i)$ loses rank for $s = z_i$.

Since normally the transfer function is written in terms of a polynomial ratio. the zeros of the system can also be found by solving the numerator equation $Q(s)$ of the transfer function (Stephanopoulos, 1984):

$$G(s) = \frac{Q(s)}{P(s)} \tag{E.15}$$

If the transfer function is inverted for control purposes, zeros with positive real part would lead to an unstable controlled system. Thus, perfect control is no possible in such a case and inverse control should not be used.

Hence, it is desirable to have a control configuration with no positive zeros. However, positive zeros are common in *multiple inputs-multiple outputs* (MIMO) systems. A MIMO system can have positive zeros and still be controllable due to the fact that the direction of the *right hand plane* (RHP) zero may have no effect in a particular output.

Although it is difficult to be conclusive with respect to the harmfulness degree of a RHP zero without the output direction information, the information given from zeros location can still be useful for control system design purposes.

First, if control is needed close to the steady state, then there should not be positive zeros close to the origin. Second, if control is required at high frequencies, then there should not be positive zeros close to the closed-loop bandwidth. Some specific examples can be seen in (Skogestad and Postlethwaite, Section 6.5).

As mentioned before, the directions of RHP zeros are important for control system design and they can be moved to reduce their harm to a specific output. Thus, zeros direction is important while considering inputs-outputs interconnections and controller design.

Another event that can occur is the presence of RHP poles and zeros and a possible pairing between them. This is particularly undesirable since the system would be unstable and difficult to control at that point. However, for the complete problem to be so bad, the pole and zero must have the same direction.

During the present project, the parallelism of matching positive poles and zeros was checked with the next definition (Curtis, 1979):

Definition E.1 *If A and B are vectors in $V_n(R)$, different to zero, they are parallel if $A = tB$ for a scalar t different to zero.*

E.5.1 RHP zeros and disturbances

The disturbance effect can worsen in the presence of a positive zero (a value where the control performance will be imperfect) if both are aligned. Since, it is necessary to avoid such a circumstance, we would prefer a control scheme in which this problem does not exist.

The minimum requirement to proof that the last described situation is avoided, is related with the necessary condition for acceptable performance as follows:

$$||Sg_d||_\infty \geq |y_z^H g_d(z)| = |y_z^H y_d| \cdot ||g_d(z)||_2 \tag{E.16}$$

We need to satisfy $||Sg_d||_\infty < 1$. Thus the requirement for acceptable control is that the inner product of the RHP zero direction y_z and the disturbance vector g_d is lower than one:

$$|y_z^H g_d(z)| < 1 \tag{E.17}$$

However, it is possible a proposed scheme presents the mentioned problem, which might be fixed during the controller design process.

E.6 Disturbances and input saturation

A basic requirement for acceptable control is disturbance rejection. It is necessary that a control structure rejects a disturbance but without getting too close to its limits. That is, it is necessary to avoid input saturation. If all elements of $G^{-1}G_d$ are less than 1, we know that the system is far from input saturation. Such a condition should be achieved for all frequencies within the bandwidth.

If the last condition is not met at a certain frequency within the bandwidth, we should test whether acceptable control is still possible. Skogestad and Postlethwaite provided a requirement for acceptable control based on SVD. For acceptable control is required that each of the singular values of G must satisfy:

$$\sigma_i(G) \geq |u_i^H g_d| - 1 \tag{E.18}$$

E.7 Singular value decomposition

Singular Value Decomposition (SVD) is a matrix factorisation (like the LU factorisation) that can be also used for input-output decisions.

Before defining SVD it is necessary to define the unitary matrix.

Consider matrix $\mathbf{U}$ where some elements u_{ij} are complex. Thus, the complex conjugate matrix of $\mathbf{U}$ is $\overline{\mathbf{U}} = \overline{u}_{ij}$. Let's define the Hermitian transpose matrix of $\mathbf{U}$ as:

$$\mathbf{U}^H \equiv \left(\overline{\mathbf{U}}\right)^T \tag{E.19}$$

If the columns of $\mathbf{U}$ conform an orthogonal base and

$$\mathbf{U}^H\mathbf{U} = \mathbf{I} \tag{E.20}$$

$\mathbf{U}$ is called a unitary matrix.

In addition, if $\mathbf{U}$ is unitary, then its eigenvalues have an absolute value equal to one. Moreover the determinant of $\mathbf{U}$ is equal to one. A further explanation and proof can be found in (Goldberg, 1991).

Suppose $\mathbf{A}$ is a $m \times n$ matrix. $\mathbf{A}$ can be decomposed into unitary matrices $\mathbf{U}_{m\times m}$ and $\mathbf{V}_{m\times m}$ as follows:

$$\mathbf{A} = \mathbf{USV}^H \tag{E.21}$$

In equation (E.21) $\mathbf{S}$ is a $m \times n$ matrix that contains the singular values of A along its diagonal and zeros elsewhere (Goldberg, 1991).

The singular values σ_i of $\mathbf{A}$ are the positive eigenvalues of $(\mathbf{A}^H\mathbf{A})^{1/2}$. Furthermore, σ^2 is an eigenvalue of $\mathbf{A}^H\mathbf{A}$ and of $\mathbf{AA}^H$.

The $m \times m$ matrix $\mathbf{U}$ is the matrix of eigenvectors of $\mathbf{AA}^H$ while the $n \times n$ matrix $\mathbf{V}$ is the matrix of eigenvectors of $\mathbf{A}^H\mathbf{A}$ (Skogestad and Postlethwaite, 1996).

Matrix $\mathbf{U}$ contains vectors (columns) associated with the outputs direction change. Similarly, $\mathbf{V}$ contains vectors (columns) associated with the possible input directions. For instance, if the first column of matrix $\mathbf{V}$ had only positive elements.

it would indicate that changing the inputs in the same direction would change σ_i times the outputs. The change direction of the outputs would be indicated by the first column of matrix **U**. For instance, if the elements of such a column were of different signs, the mentioned input change would increase or decrease the value of the outputs.

The minimum singular value $\underline{\sigma}(G)$ has important implications for control structure design. If $\underline{\sigma}(G)$ is too low, it means that the inputs have little influence on the associated output direction. Hence, we would prefer control schemes with $\underline{\sigma}(G)$ larger than one.

Note that the singular values are note constant, but change when the frequency changes. Thus, the SVD of the plant should be made not only at the steady state value, but also at frequencies within the closed bandwidth of interest.

E.7.1 Condition number

Associated with the SVD of matrix G(s), there is another parameter useful for control system design: the condition number.

The condition number is the ratio between the maximum and the minimum singular value of matrix **A**.

$$\gamma(G) \triangleq \frac{\overline{\sigma}(G)}{\underline{\sigma}(G)} \tag{E.22}$$

When the condition number of a matrix is much larger than one, it is said that the matrix is ill-conditioned (Skogestad and Postlethwaite, 1996).

Among the control characteristics that the condition number can reveal are:

- A large condition number may indicate sensitivity to input uncertainty.
- A small condition number indicates that the system is no very sensitive to input uncertainty.
- When the reason of a large condition number is a small minimum singular value, it indicates that the gain will be small and control action poor. As mentioned before, this is an undesirable situation. Thus, schemes presenting large condition number and small $\underline{\sigma}(G)$ within the frequency bounds of interest would be rejected.

E.8 Relative Gain Array (RGA)

The relative gain array (RGA) of matrix $\mathbf{G}$ is defined as follows (Skogestad and Postlethwaite, 1996):

$$\mathrm{RGA(G)} = \Lambda(\mathbf{G}) \triangleq \mathbf{G} \times (\mathbf{G}^{-1})^T \tag{E.23}$$

The product in equation (E.23) is an element by element product.

Among the most important algebraic properties of the RGA are: It is independent of input and output scaling; the row and columns sum one; the sum-norm of RGA is approximately equal to the minimised minimum singular value; if $\mathbf{G}$ triangular then RGA is an identity matrix.

The RGA of the transfer function at the steady state has been widely used to select input-output pairs (Stephanopoulos, 1984). The λ_{ij} of the RGA matrix can be seen as a measure of the interaction between an input and an output:

Let's consider a system with two outputs y_1 and y_2. Consider now that the outputs are controlled by m_1 and m_2 respectively.

The open-loop gain on output y_1 when output m_1 is changed while output m_2 is constant is:

$$\left(\frac{\delta y_1}{\delta m_1}\right)_{m_2}$$

If m_1 changes, it affects directly to y_1, but it also affects indirectly to y_2. Thus, is this output changes, m_2 also changes. The change of m_2 affects indirectly to y_1. This gain is calculated as:

$$\left(\frac{\delta y_1'}{\delta m_1}\right)_{y_2}$$

Such open-loop ratios define the relative gain between input y_1 and output m_1:

$$\lambda_{11} = \frac{(\delta y_1'/\delta m_1)_{y_2}}{(\delta y_1'/\delta m_1)_{y_2}} \tag{E.24}$$

Depending on the values of the relative gain, it is possible to say how y_1 is affected by m_1 and m_2. For instance, if the relative gain is equal to zero, it means that input m_1 does not affect y_1. Moreover, if the relative gain is negative, it means that input m_2 affects y_1 in a different direction in which it affects y_2. Thus, we can now how the control schemes can perform at the steady state.

The definition given in equation (E.24) can be extended to MIMO as follows:

$$\lambda_{ij} = \frac{(\delta y_i'/\delta m_j)_m}{(\delta y_i'/\delta m_j)_y} \tag{E.25}$$

RGA can provide information of the controller possible performance not only at the steady state, but also close to the crossover frequency (Skogestad and Postlethwaite, 1996).

When at the crossover frequency the RGA elements are large, it is an indication of possible difficulties to control due to input uncertainty. The effect is exaggerated by inverse control.

If there is change of sign in any of the RGA elements when the s moves from zero to infinity, it is an indication of a RHP-zero in $\mathbf{G}$.

Skogestad and Postlethwaite provided the next two rules for pairing inputs and outputs. A proof can be found in Skogestad and Postlethwaite book (Section 10.8.2).

1. Systems with RGA elements close to one at the crossover frequency present less instability due to interactions.

   Regarding to distillation, Skogestad and Morari (1987) pointed out that the last behaviour is expected for columns with high purity both in the distillate and bottom products.

2. At low frequencies, pairs that result in negative relative gain should be avoided. The reason above explained, negative relative gain is an indication that one input is affecting two outputs in different directions.

Another conclusion from Skogestad and Postlethwaite is that a plant with large RGA elements is no robust to input uncertainty and is difficult to control.

Bibliography

[Agamennoni *et al.*(1994)] Agamennoni, O., Figueroa, J., Barton, G., and Romagnoli, J. (1994). Advancer controller design for a distillation column. *Int. J. Control*, **59**(3), 817–839.

[Agreda and Partin(1984)] Agreda, V. and Partin, L. (1984). Reactive distillation process for the production of methyl acetate. US patent No. 4,435,595.

[Agreda *et al.*(1990)] Agreda, V. H., Partin, L. R., and Heise, W. H. (1990). High-purity methyl acetate via reactive distillation. *Chem. Engng. Progress*, **86**(2), 40–46.

[Al-Arfaj and Luyben(2000)] Al-Arfaj, M. and Luyben, W. (2000). Comparison of alternative control structures for an ideal two-product reactive distillation column. *Ind. Eng. Chem. Res.*, **39**(9), 3298–3307.

[Alejski and Duprat(1996)] Alejski, K. and Duprat, F. (1996). Dynamic simulation of the multicomponent reactive distillation. *Chem. Engng. Sci.*, **51**(18), 4237–4252.

[Backhaus(1921)] Backhaus, A. (1921). Continuous processes for the manufacture of esters. USpatent 1403224.

[Barbosa and Doherty(1987)] Barbosa, D. and Doherty, M. (1987). A new set of composition variables for the representation of reactive-phase diagrams. *Proc. R. Soc. Lond.*, **A 413**, 459–464.

[Barbosa and Doherty(1988a)] Barbosa, D. and Doherty, M. (1988a). Design and minimum-reflux calculations for single-feed multicomponent reactive distillation columns. *Chem. Engng. Sci.*, **43**(7), 1523–1537.

[Barbosa and Doherty(1988b)] Barbosa, D. and Doherty, M. (1988b). The simple distillation of homogeneous reactive mixtures. *Chem. Engng. Sci.*, **43**(3), 541–550.

[Baur *et al.*(2001)] Baur, R., Taylor, R., and Krishna, R. (2001). Influence of column hardware on the performance of reactive distillation columns. *Catal. Today*, **66**, 225–232.

[Bekiaris *et al.*(1996)] Bekiaris, N., Meski, G., and Morari, G. (1996). Multiple steady states in heterogeneous azeotropic distillation. *Ind. Eng. Chem. Res.*, **35**(1), 207–227.

[Bessling *et al.*(1997)] Bessling, B., Schembecker, G., and Simmorock, K. (1997). Design of processes with reactive distillation line diagrams. *Ind. Eng. Chem. Res.*, **36**, 3032–3042.

[Bisowarno and Tadé(2000)] Bisowarno, B. and Tadé, M. (2000). Dynamic simulation of startup in ethyl tert-butyl ether reactive distillation with input multiplicity. *Ind. Eng. Chem. Res.*, **39**, 1950–1954.

[Blagov *et al.*(2000)] Blagov, S., Bessling, B., Schoemakers, H., and Hasse, H. (2000). Feasibility and multiplicity in reaction-distillation processes for systems with competing irreversible reactions. *Chem. Engng. Sci.*, **55**, 5421–5436.

[Boyd and Barratt(1991)] Boyd, S. and Barratt, C. (1991). *Linear controller design: limits of performance.* P T R Prentice Hall, USA.

[Cardoso *et al.*(2000)] Cardoso, M., Salcedo, R., de Azevedo, S., and Barbosa, D. (2000). Optimisation of reactive distillation processes with simulated annealing. *Chem. Engng. Sci.*, **55**(21), 5059–5078.

[Carney(1937)] Carney, S. (1937). Process and apparatus for conducting chemical reactions. US patent No. 2,081,322.

[Chang and Seader(1988)] Chang, Y. and Seader, J. (1988). Simulation of continuous reactive distillation by a homotopy-continuation method. *Comp. Chem. Engng.*, **12**(12), 1243–1255.

[Ciric and Gu(1994)] Ciric, A. and Gu, D. (1994). Synthesis of nonequilibrium reactive distillation processes by MINLP. *AICHE J.*, **40**(9), 1479–1487.

[Ciric and Miao(1994)] Ciric, A. and Miao, P. (1994). Steady state multiplicities in an ethylene glycol reactive distillation column. *Ind. Eng. Chem. Res.*, **33**. 2738–1748.

[Colombo *et al.*(1983)] Colombo, F., Dalloro, L., and Delogu, P. (1983). Equilibrium constant for the methyl tert-butyl ether liquid phase synthesis by use of UNIFAC. *Ind. Eng. Chem. Fund.*, **22**, 219–223.

[Curtis(1979)] Curtis, P. C. (1979). *Cálculo de varias variables con álgebra lineal.* Editorial Limusa, Mexico.

[DeGarmo *et al.*(1992)] DeGarmo, J., Parulekar, V., and Pinjala, V. (1992). Consider reactive distillation. *Chem. Engng. Progress*, **3**, 43–50.

[Doherty and Buzad(1992)] Doherty, M. and Buzad, G. (1992). Reactive distillation by design. *IChemE Symposium series*, **1**(128), A51–A68.

[Ellenberger and Krishna(1999)] Ellenberger, J. and Krishna, R. (1999). Countercurrent operation of structured catalytically packed distillation columns: pressure drop, hold-up and mixing. *Chem. Engng. Sci.*, **54**, 1339–1345.

[Espinosa *et al.*(1993)] Espinosa, J., Scenna, N., and Pérez, G. (1993). Graphical procedure for reactive distillation systems. *Chem. Engng. Comm.*, **119**, 109–124.

[Espinosa *et al.*(1995)] Espinosa, J., Aguirre, P., and Gérez (1995). Some aspects in the design of multicomponent reactive distillation columns including nonreactive species. *Chem. Engng. Sci.*, **50**(3), 469–484.

[Estrada-Villagrana *et al.*(1999a)] Estrada-Villagrana, A., Bogle, I., Fraga, E., and Gani, R. (1999a). Analysis of input-output controllability in reactive distillation using the element model. *European Symposium on Computer Aided Process Engineering-10*, pages 157–162.

[Estrada-Villagrana *et al.*(1999b)] Estrada-Villagrana, A., Bogle, I., Pérez-Cisneros, E., and Gani, R. (1999b). Exploring the interaction between flows and composition in reactive distillation. *Comp. Chem. Engng.*, **23 Supplement**, 339–342.

[Fenwick *et al.*(1975)] Fenwick, J., Harrop, D., and Head, J. (1975). Thermodynamic properties of organic oxygen compounds 41. enthalpies of formation of eight ethers. *J. Chem. Thermodynamics*, **7**, 943–954.

[Fernholz *et al.*(2001)] Fernholz, G., Friedrich, M., Güner, S., Mohl, K., Kienle, A., and Gilles, E. (2001). Linear mimo controller design for an industrial reactive distillation column. In *DYCOPS-6*, pages 137–142. preprints.

[Gani *et al.*(1998)] Gani, R., Jepsen, T., and Pérez-Cisneros, E. (1998). A generalized reactive separation unit model, modelling and simulation aspects. *Comp. Chem. Engng.*, **22**(Supplement), s363–s370.

[Giessler *et al.*(1998)] Giessler, S., Danilov, R., Pisarenko, R., Serafimov, L., Hasebe, S., and Hashimoto, I. (1998). Feasibility study of reactive distillation using the analysis of the statics. *Ind. Eng. Chem. Res.*, **37**, 4375–4382.

[Goldberg(1991)] Goldberg, J. (1991). *Matrix theory with applications*. International series in pure and applied mathematics. McGraw-Hill Inc., U.S.A. Chapter used: 2.

[Grosser *et al.*(1987)] Grosser, J., Doherty, M., and Malone, M. (1987). Modeling of reactive distillation systems. *Ind. Eng. Chem. Res.*, **26**, 983–989.

[Güttinger and Morari(1999a)] Güttinger, T. and Morari, M. (1999a). Predicting multiple steady states in equilibrium reactive distillation. 1. Analysis of nonhybrid systems. *Ind. Eng. Chem. Res.*, **38**, 1633–1648.

[Güttinger and Morari(1999b)] Güttinger, T. and Morari, M. (1999b). Predicting multiple steady states in equilibrium reactive distillation. 2. Analysis of hybrid systems. *Ind. Eng. Chem. Res.*, **38**, 1649–1665.

[Han *et al.*(1997)] Han, S., Jin, Y., and Yu, Z. (1997). Application of a fluidized reaction-distillation column for hydrolysis of methyl acetate. *Chemical Engineering Journal*, **66**, 227–230.

[Hansen *et al.*(1998)] Hansen, J., Jørgensen, S., J.Heath, and Perkins, J. (1998). Control structure selection for energy integrated distillation column. *Journal of Process Control*, **8**(3), 185–195.

[Harding and Floudas(2000)] Harding, S. and Floudas, C. (2000). Locating all heterogeneous and reactive azeotropes in multicomponent mixtures. *Ind. Eng. Chem. Res.*, **39**, 1576–1595.

[Hauan *et al.*(1995)] Hauan, S., Hertzberg, T., and Lien, K. (1995). Multiplicity in reactive distillation of MTBE. *Comp. Chem. Engng.*, **19**(Supplement), S327–S332.

[Hauan *et al.*(1997)] Hauan, S., Schrans, S., and Lien, K. (1997). Dynamic evidence of the multiplicity mechanism in methyl tert-butyl ether reactive distillation. *Ind. Eng. Chem. Res.*, **36**, 3995–3998.

[Higler *et al.*(1998)] Higler, A., Taylor, R., and Krishna, R. (1998). Modeling of a reactive separation process using a nonequilibrium stage model. *Comp. Chem. Engng.*, **22**(Supplement), s111–s118.

[Higler *et al.*(1999)] Higler, A., Taylor, R., and Krishna, R. (1999). Nonequilibrium modelling of reactive distillation: multiple steady states in MTBE synthesis. *Chem. Engng. Sci.*, **54**, 1389–1395.

[Higler *et al.*(2000)] Higler, A., Krishna, R., and Taylor, R. (2000). Nonequilibrium modeling of reactive distillation: A dusty fluid model for heterogeneously catalyzed processes. *Ind. Eng. Chem. Res.*, **39**, 1596–1607.

[Hoffmann(1958)] Hoffmann, H. (1958). Berechnung von reaktoren für gemischtphase-reaktionen. *Chem. Engng. Sci.*, **8**, 113–122.

[Holland(1975)] Holland, C. (1975). *Fundamentals and modelling of separation processes.* Prentice Hall, U.S.A. 430p.

[Isla and Irazoqui(1996)] Isla, M. and Irazoqui, H. (1996). Modeling, analysis, and simulation of a methyl tert-butyl ether reactive distillation. *Ind. Eng. Chem. Res.*, **35**, 2696–2708.

[Ismail *et al.*(2000)] Ismail, S., Proios, P., and Pistikopoulos, E. (2000). Modular synthesis framework for combined separation/reaction systems. *AICHE J.*, **47**(3), 629–649.

[Izarraraz *et al.*(1980)] Izarraraz, A., Bentzen, G., Anthony, R., and Holland, C. (1980). Solve more distillation problems, part 9–when chemical reactions occur. *Hydro. Proc.*, **59**(4), 195–203.

[Jacobs and Krishna(1993)] Jacobs, R. and Krishna, R. (1993). Multiple solutions in reactive distillation for methyl-tert butyl ether synthesis. *Ind. Eng. Chem. Res.*, **32**, 1706–1709.

[Jacobsen and Skogestad(1991)] Jacobsen, E. and Skogestad, S. (1991). Multiple steady-states in ideal 2-product distillation. *AICHE J.*, **37**(4), 499–511.

[Jacobsen and Skogestad(1994)] Jacobsen, E. and Skogestad, S. (1994). Instability of distillation columns. *AICHE J.*, **40**(9), 1466–1478.

[Jiménez *et al.*(2001)] Jiménez, L., Wanhschafft, O., and Julka, V. (2001). Analysis of residue curve maps of reactive and extractive distillation units. *Comp. Chem. Engng.*, **25**, 635–642.

[Jr.(1981)] Jr., L. S. (1981). Catalytic distillation process. US patent 4,307.254.

[Kaczorek(1992)] Kaczorek, T. (1992). *Linear Control Systems: analysis of multivariable systems*, volume 1. Research Studies Press, U.K. section 2.15.

[Keyes(1932)] Keyes, D. (1932). Esterification processes and equipment. *Ind. Engng. Chem.*, **24**, 1096–1103.

[Kister(1992)] Kister, H. Z. (1992). *Distillation Design.* McGraw-Hill, U.S.A.

[Kołodziej *et al.*(2001)] Kołodziej, A., M. Jaroszński, A. H., and Górak, A. (2001). Determination of catalytic packing characteristics for reactive distillation. *Catal. Today*, **69**, 75–85.

[Komatsu(1977)] Komatsu, H. (1977). Application of the relaxation method for solving reacting distillation problems. *J. Chem. Engng. Japan*, **10**(3), 200–205.

[Komatsu and Holland(1977)] Komatsu, H. and Holland, C. (1977). A new method of convergence for solving reacting distillation problems. *J. Chem. Engng. Japan*, **10**, 292–297.

[Kreul *et al.*(1998)] Kreul, L., Górak, A., Dittich, C., and Barton, P. (1998). Dynamic catalytic distillation: Advanced simulation and experimental validation. *Comp. Chem. Engng., Supplement*, **22**, S371–S378.

[Kumar and Daoutidis(1999)] Kumar, A. and Daoutidis, P. (1999). Modeling, analysis and control of ethylene glycol reactive distillation column. *AICHE J.*, **45**(1), 51–68.

[Lambert(1991)] Lambert, J. (1991). *Numerical Methods for Ordinary Differential Equations.* Wiley, U.K.

[Lebens *et al.*(1999)] Lebens, P., Kapteijn, F., Sie, S., and Moulijn, J. (1999). Potentials of internally finned monoliths as a packing for multifunctional reactors. *Chem. Engng. Sci.*, **54**, 1359–1365.

[Lee and Dudukovic(1998)] Lee, J. and Dudukovic, M. (1998). A comparison of the equilibrium and nonequilibrium models for a multicomponent reactive distillation column. *Comp. Chem. Engng.*, **23**(1), 159–172.

[Lee *et al.*(2000)] Lee, J., Hauan, W., and Westerberg, A. (2000). Reaction distribution in a reactive distillation column by graphical methods. *AICHE J.*, **46**, 1218–1233.

[Leversund *et al.*(1994)] Leversund, E. S., Macchieto, S., Stuart, G., and Skogestad, S. (1994). Optimal control and on-line operation of reactive batch distillation. *Comp. Chem. Engng.*, **18**(Supplement), S391–S395.

[Leyes and Othmer(1945)] Leyes, C. and Othmer, D. (1945). Continuous esterification of butanol and acetic acid. *Ind. and Engng. Chem.*, **37**, 968–977.

[Luyben and Floudas(1994)] Luyben, M. and Floudas, C. (1994). Analyzing the interaction of design and control .1. A multiobjective framework and application to binary distillation synthesis. *Comp. Chem. Engng.*, **18**(10), 933–969.

[Luyben(pore)] Luyben, W. (Singapore). *Process modeling, simulation and control for chemical engineers.* McGraw-Hill, Singapore, second edition.

[Malanowski and Anderko(1992)] Malanowski, S. and Anderko, A. (1992). *Modelling phase equilibria: thermodynamic background and practical tools.* Wiley series in Chemical Engineering. John Wiley & Sons, Inc, New York.

[Michelsen(1995)] Michelsen, M. (1995). Chemical models for reactive phase equilibrium. Institut for Kemiteknik publication.

[Mohl *et al.*(1998)] Mohl, K., Kienle, A., and Gilles, E. (1998). Multiple steady states in a reactive distillation column for the production of the fuel ether TAME. i. theoretical analysis. *Chem. Engng. Technol.*, **21**(2), 133–136.

[Mohl *et al.*(1999)] Mohl, K., Kienle, A., Gilles, E., Rapmund, P., Sundmacher, K., and Hoffmann, U. (1999). Steady-state multiplicities in reactive distillation columns for the production of fuel ethers MTBE and TAME: theoretical analysis and experimental verification. *Chem. Engng. Sci.*, **54**, 1029–1043.

[Monroy-Loperena *et al.*(1999)] Monroy-Loperena, R., Pérez-Cisneros, E., and Alvarez-Ramírez, J. (1999). Nonlinear PI control of an ethylene glycol reactive distillation column. *Comp. Chem. Engng.*, **supplement**, S.

[Monroy-Loperena *et al.*(2000)] Monroy-Loperena, R., Pérez-Cisneros, E., and Alvarez-Ramírez, J. (2000). A robust PI control configuration for a high-purity ethylene glycol reactive distillation column. *Chem. Eng. Sci.*, **55**, 4925–4937.

[Moritz and Hasse(1999)] Moritz, P. and Hasse, H. (1999). Fluid dynamics in reactive distillation packing katapak-s. *Chem. Engng. Sci.*, **54**, 1367–1374.

[Mościński and Ogonowski(1995)] Mościński, J. and Ogonowski, Z. (1995). *Advanced control with MATLAB and SIMULINK*. Ellis Horwood, U.K.

[Naphtali and Sandholm(1971)] Naphtali, L. and Sandholm, D. (1971). Multicomponent separation calculations by linearisation. *AICHE. J.*, **17**(1), 148–153.

[Nijhuis *et al.*(1993)] Nijhuis, S., Kerkhof, F., and Mak, A. (1993). Multiple steady states during reactive distillation of methyl-tert-butyl-ether. *Ind. Eng. Chem. Res.*, **32**, 2767–2774.

[Okasinski and Doherty(1998)] Okasinski, M. and Doherty, M. (1998). Design method for kinetically, staged reactive distillation columns. *Ind. Eng. Chem. Res.*, **76**, 2821–2834.

[Oudshoorn *et al.*(1999)] Oudshoorn, O., Janissen, M., van Kooten, W., Jansen, J., van Bekkum, H., van den Bleek, C., and Calis, H. (1999). A novel structured catalyst packing for catalytic distillation of etbe. *Chem. Engng. Sci.*, **54**, 1413–1418.

[Parra *et al.*(1994)] Parra, D., Tejero, J., Cunill, F., Iborra, M., and Izquierdo, J. (1994). Kinetic-study of MTBE liquid-phase synthesis using C-4 olefinic cut. *Chem. Engng. Sci.*, **49**, 4563–4578.

[Pekkanen(1995)] Pekkanen, M. (1995). A local optimisation method for the design of reactive distillation. *Comp. Chem. Engng.*, **19**(Supplement), S235–S240.

[Pérez-Cisneros *et al.*(1996)] Pérez-Cisneros, E., Schenk, M., Gani, R., and Pilavachi, P. (1996). Aspects of simulation, design and analysis of reactive distillation operation. *Comp. Chem. Engng.*, **20**(Supplement), S267–S272.

[Pérez-Cisneros *et al.*(1997)] Pérez-Cisneros, E., Gani, R., and Michelsen, M. (1997). Reactive separation systems. Part i: computation of physical and chemical equilibrium. *Chem. Engng. Sci.*, **52**, 527–543.

[Perry *et al.*(1988)] Perry, R., Green, D., and Maloney, J. (1988). *Perry's chemical engineers' handbook*. McGraw-Hill, Japan, sixth edition.

[Pilavachi *et al.*(1997)] Pilavachi, P., Schenk, M., Pérez-Cisneros, E., and Gani, R. (1997). Modeling and simulation of reactive distillation operations. *Ind. Eng. Chem. Res.*, **36**, 3188–3197.

[Press *et al.*(1996)] Press, W., Teukolsy, S., Vetterling, W., and Flannery, B. (1996). *Numerical recipes in Fortran 77, the art of scientific computing*, volume 1. Cambridge University Press, U.S.A., 2nd. edition. 933.

[Rademaker *et al.*(1975)] Rademaker, O., Rijnsdorp, J., and Maarleveld, A. (1975). *Dynamics and control of continuous distillation units*. Elsevier scientific publishing company, The Netherlands.

[Rehfinger and Hoffmann(1990)] Rehfinger, A. and Hoffmann, U. (1990). Kinetics of methyl tertiary butyl ether liquid phase synthesis catalyzed by ion exchange resin-i. intrinsic rate expression in liquid phase activities. *Chem. Engng. Sci.*, **45**, 1605–1617.

[Reid *et al.*(1977)] Reid, R., Prausnitz, J., and Poling, B. (1977). *The properties of gases and liquids*. McGraw-Hill book Company, U.S.A, third edition.

[Reid *et al.*(1987)] Reid, R., Prausnitz, J., and Poling, B. (1987). *The properties of gases and liquids*. McGraw-Hill book Company, U.S.A, fourth edition.

[Rojey(1994)] Rojey, A. (1994). Optimal use of energy in separation processes for refining and natural-gas treatment. *Rev. Inst. Franc. Petrol.*, **49**(6), 627–637.

[Ruiz *et al.*(1995)] Ruiz, C., Basualdo, M., and Scenna, N. (1995). Reactive distillation dynamic simulation. *Chem. Engng. Res. Des.-Trans. IChemE. Part A*, **73**, 363–378.

[S. Güner *et al.*(2001)] S. Güner, K. M., Kienle, A., Gilles, E., Fernholz, G., and Friedrich, M. (2001). Nonlinear control of an industrial reactive distillation column. In *DYCOPS-6*, pages 125–130. preprints.

[Sågfors and Waller(1998)] Sågfors, M. and Waller, K. (1998). Multivariable control of ill-conditioned distillation columns utilising process knowledge. *J. Proc. Cont.*, **8**(3), 197–208.

[Saito *et al.*(1971)] Saito, S., Michishita, T., and Maeda, S. (1971). Separation of meta- and para-xylene mixture by distillation accompanied by chemical reactions. *J. Chem. Engng. Japan*, **4**, 37–43.

[Sandler(1989)] Sandler, S. (1989). *Chemical and engineering thermodynamics*. Wiley, U.S.A., second edition.

[Scenna *et al.*(1998a)] Scenna, N., Muñoz, M., and Benz, S. (1998a). Dynamic simulation for start-up operations of distillation columns with multiple steady states. *Latin Amer. Appl. Res.*, **28**, 257–263.

[Scenna *et al.*(1998b)] Scenna, N., Ruiz, C., and Benz, S. (1998b). Dynamic simulation of start-up procedures of reactive distillation columns. *Comp. Chem. Engng.*, **22**(Supplement), S719–S722.

[Schenk *et al.*(1999)] Schenk, M., Gani, R., Bogle, D., and Pistikopoulos, E. (1999). A hybrid modeling approach for separation systems involving distillation. *Chem. Engng. Res. Des.*, **77**(A6), 519–534.

[Schneider *et al.*(2001)] Schneider, R., Noeres, C., Kreul, L., and Górak, A. (2001). Dynamic modeling and simulation of reactive batch distillation. *Comp. Chem. Engng.*, **25**, 169–176.

[Schrans *et al.*(1996)] Schrans, S., de Wolf, S., and Baur, R. (1996). Dynamic simulation of mtbe reactive distillation. *Comp. Chem. Engng.*, **20 supplement**, S1619–S1624.

[Seborg *et al.*(1989)] Seborg, D., Edgar, T., and Mellichamp, D. (1989). *Process dynamics and control.* Wiley series in Chemical Engineering. John Wiley and Sons, U.S.A. Chapter 1.

[Seferlis and Grievnink(2001)] Seferlis, P. and Grievnink, J. (2001). Optimal design and sensitivity analysis of reactive distillation units using collocation models. *Ind. Eng. Chem. Res.*, **40**(7), 1673–1685.

[Sennewald *et al.*(1971)] Sennewald, K., Gehrmann, K., and Schafer, S. (1971). Column for carrying out organic chemical reactions in contact with fine particulate catalyst. U.S. Patent 3,579,309.

[Sharma(1985)] Sharma, M. (1985). Separations through reactions. *J. Separ. Proc. Technol.*, **6**, 9–16.

[Shinskey(1984)] Shinskey, F. (1984). *Distillation control.* McGraw-Hill, U.S.A.. second edition.

[Shoemaker and Jones(1987)] Shoemaker, J. and Jones, E. (1987). Cumene by catalytic distillation. *Hydro. Proc.*, **66**(6), 57–58.

[Sinnot(1993)] Sinnot, R. (1993). *Coulson and Richardson's chemical engineering. design*, volume 6. Pergamon, U.K., second edition.

[Skogestad and Morari(1987)] Skogestad, S. and Morari, M. (1987). Control configuration selection for distillation columns. *AICHE J.*, **33**(10), 1620–1635.

[Skogestad and Postlethwaite(1996)] Skogestad, S. and Postlethwaite, I. (1996). *Multivariable feedback control, analysis and design.* John Wiley and Sons Ltd., U.K.

[Skogestad *et al.*(1990a)] Skogestad, S., Jacobsen, E., and Lundström, P. (1990a). Modelling requirements for robust control of distillation columns. *IFAC 11th Triennial World Congress, USSR 1990*, pages 191–197.

[Skogestad *et al.*(1990b)] Skogestad, S., Lundström, P., and Jacobsen, E. (1990b). Selecting the best distillation control configuration. *AICHE J.*, pages 753–764.

[Smith and Corripio(1997)] Smith, C. and Corripio, A. (1997). *Principles and practice of automatic process control.* John Wiley and Sons, Inc., USA, second edition. Chapter 7.

[Smith and Van Ness(1987)] Smith, J. and Van Ness, H. (1987). *Introduction to Chemical Engineering Thermodynamics.* Chemical Engineering Series. McGraw-Hill, Singapore, fourth edition.

[Smith and Missen(1982)] Smith, W. and Missen, R. (1982). *Chemical Reaction Equilibrium Analysis.* John Wiley and Sons, U.S.A.

[Sneesby *et al.*(1997a)] Sneesby, M., Tadé, M., Datta, R., and Smith, T. (1997a). ETBE synthesis via reactive distillation. 2. Dynamic simulation and control aspects. *Ind. Eng. Chem. Res.*, **36**, 1870–1881.

[Sneesby *et al.*(1997b)] Sneesby, M., Tadé, M., Datta, R., and Smith, T. (1997b). Implications of steady-state multiplicity for operation and control of etherification columns. *Proceedings of the 1997 Symposium Distillation and Absorption. IChemEng Symposiym Series*, **1**, 205–216.

[Sneesby *et al.*(1998a)] Sneesby, M., Tadé, M., Datta, R., and Smith, T. (1998a). Detrimental influence of excessive fractionation on reactive distillation. *AICHE J.*, **44**, 388–393.

[Sneesby *et al.*(1998b)] Sneesby, M., Tadé, M., and Smith, T. (1998b). Mechanistic interpretation of multiplicity in hybrid reactive distillation: physically realizable cases. *Ind. Eng. Chem. Res.*, **37**, 4424–4433.

[Sneesby *et al.*(1998c)] Sneesby, M., Tadé, M., and Smith, T. (1998c). Multiplicity and pseudo-multiplicity in MTBE and ETBE reactive distillation. *Trans IChemE*, **76A**, 525–531.

[Sneesby *et al.*(1998d)] Sneesby, M., Tadé, M., and Smith, T. (1998d). Steady-state transitions in the reactive distillation of MTBE. *Comp. Chem. Engng.*, **22**(7-8), 879–892.

[Sørensen and Skogestad(1994)] Sørensen, E. and Skogestad, S. (1994). Control strategies for reactive batch distillation. *J. Proc. Cont.*, **4**(4), 205–217.

[Sørensen *et al.*(1996)] Sørensen, E., Macchietto, S., Stuart, G., and Skogestad, S. (1996). Optimal control and on-line operation of reactive batch distillation. *Comp. Chem. Engng.*, **20**(12), 1491–1498.

[Stephanopoulos(1984)] Stephanopoulos, G. (1984). *Chemical process control, an introduction to theory and practice.* P T R Prentice Hall, USA.

[Stichlmair and Frey(1999)] Stichlmair, J. and Frey, T. (1999). Reactive distillation processes. *Chem. Engng. Technol.*, **22**(2), 95–103.

[Stichlmair and Fair(1998)] Stichlmair, J. G. and Fair, J. R. (1998). *Distillation, principles and practice.* Wiley-VCH, USA.

[Subawalla *et al.*(1997)] Subawalla, H., González, J., Seibert, A., and Fair, J. (1997). Capacity and efficiency of reactive distillation bale packing: modeling and experimental validation. *Ind. Eng. Chem. Res.*, **36**(9), 3821–3832.

[Sundmacher and Hoffmann(1992)] Sundmacher, K. and Hoffmann, U. (1992). Importance of irreversible thermodynamics for liquid phase ion exchange catalyst: experimental verification for MTBE-synthesis. *Chem. Engng. Sci.*, **47**, 2733–2738.

[Sundmacher and Hoffmann(1993)] Sundmacher, K. and Hoffmann, U. (1993). Activity evaluation of a catalytic distillation packing for MTBE production. *Chemical Engineering and Technology*, **16**, 279–289.

[Sundmacher and Hoffmann(1994)] Sundmacher, K. and Hoffmann, U. (1994). Multicomponent mass and energy transport on different length scales in a packed reactive distillation column for heterogeneously catalyzed fuel ether production. *Chem. Engng. Sci.*, **49**(24A), 4443–4664.

[Sundmacher and Hoffmann(1995)] Sundmacher, K. and Hoffmann, U. (1995). Oscillatory vapor-liquid transport phenomena in a packed reactive distillation column for fuel ether production. *Chem. Engng. J.*, **57**, 219–228.

[Sundmacher and Hoffmann(1996)] Sundmacher, K. and Hoffmann, U. (1996). Development of a new catalytic distillation process for fuel ethers via a detailed nonequilibrium model. *Chem. Engng. Sci.*, **51**(10), 2359–2368.

[Taylor and Krishna(2000)] Taylor, R. and Krishna, R. (2000). Modelling reactive distillation. *Chem. Engng. Sci.*, **55**, 5183–5229.

[Thiel *et al.*(1997)] Thiel, C., Sundmacher, K., and Hoffmann, U. (1997). Residue curve maps for heterogeneously catalyzed reactive distillation of fuel ethers MTBE and TAME. *Chem. Engng. Sci.*, **52**(6), 993–1005.

[Tuchlenski *et al.*(2001)] Tuchlenski, A., Beckmann, A., Reusch, D., Weidlich, U., and Janowsky, R. (2001). Reactive distillation: industrial applications, process design and scale-up. *Chem. Engng. Sci.*, **56**, 387–394.

[Ung and Doherty(1995)] Ung, S. and Doherty, M. (1995). Synthesis of reactive distillation systems with multiple equilibrium chemical reactions. *Ind. Eng. Chem. Res.*, **34**, 2555–2565.

[Unger *et al.*(1995)] Unger, J., Köner, A., and Marquardt, W. (1995). Structural analysis of differential-algebraic equation systems - theory and applications. *Computers Chem. Engng.*, **19**(8), 867–882.

[Unknown(1991)] Unknown (1991). AICHE Design Institute for Physical Property Data Series. Technical Report 1, American Institute of Chemical Engineers, U.S.A.

[van Baten *et al.*(2001)] van Baten, J., Ellenberger, J., and Krishna, R. (2001). Hydrodynamics of reactive distillation tray column with catalyst containing envelopes: experiments vs. CFD simulations. *Catal. Today*, **66**, 233–240.

[van Winkle(1967)] van Winkle, M. (1967). *Distillation*. McGraw-Hill, U.S.A.

[Venimadhavan *et al.*(1999)] Venimadhavan, G., Malone, M., and Doherty, M. (1999). A novel distillate policy for batch reactive distillation with application to the production of butyl acetate. *Ind. Eng. Chem. Res.*, **38**, 714–722.

[Venkataraman *et al.*(1990)] Venkataraman, S., Chan, W., and Boston, J. (1990). Reactive distillation using Aspen plus. *Chem. Engng. Progress*, **86**(4), 45–54.

[von Scala *et al.*(1999)] von Scala, C., Wehrli, M., and Gaiser, G. (1999). Heat transfer measurements and simulation of katapak-m catalyst support. *Chem. Engng. Sci.*, **54**, 1375–1381.

[Vora and Daoutidis(2001)] Vora, N. and Daoutidis, P. (2001). Dynamics and control of an ethyl acetate reactive distillation column. *Ind. Eng. Chem. Res.*, **40**, 833–849.

[Wang and Henke(1966)] Wang, J. and Henke, G. (1966). Tridiagonal matrix for distillation. *Hydro. Proc.*, **45**(8), 155–163.

[Xu and Duduković(1999)] Xu, Z. and Duduković, M. (1999). Modeling and simulation of semi-batch photo reactive distillation. *Chem. Engng. Sci.*, **54**, 1397–1403.

[Yu *et al.*(1997)] Yu, S., Zhou, A., and Tan, Q. (1997). Simulation of multistage catalytic stripping with a nonequilibrium stage model. *Comp. Chem. Engng.*, **21**(4), 409–415.